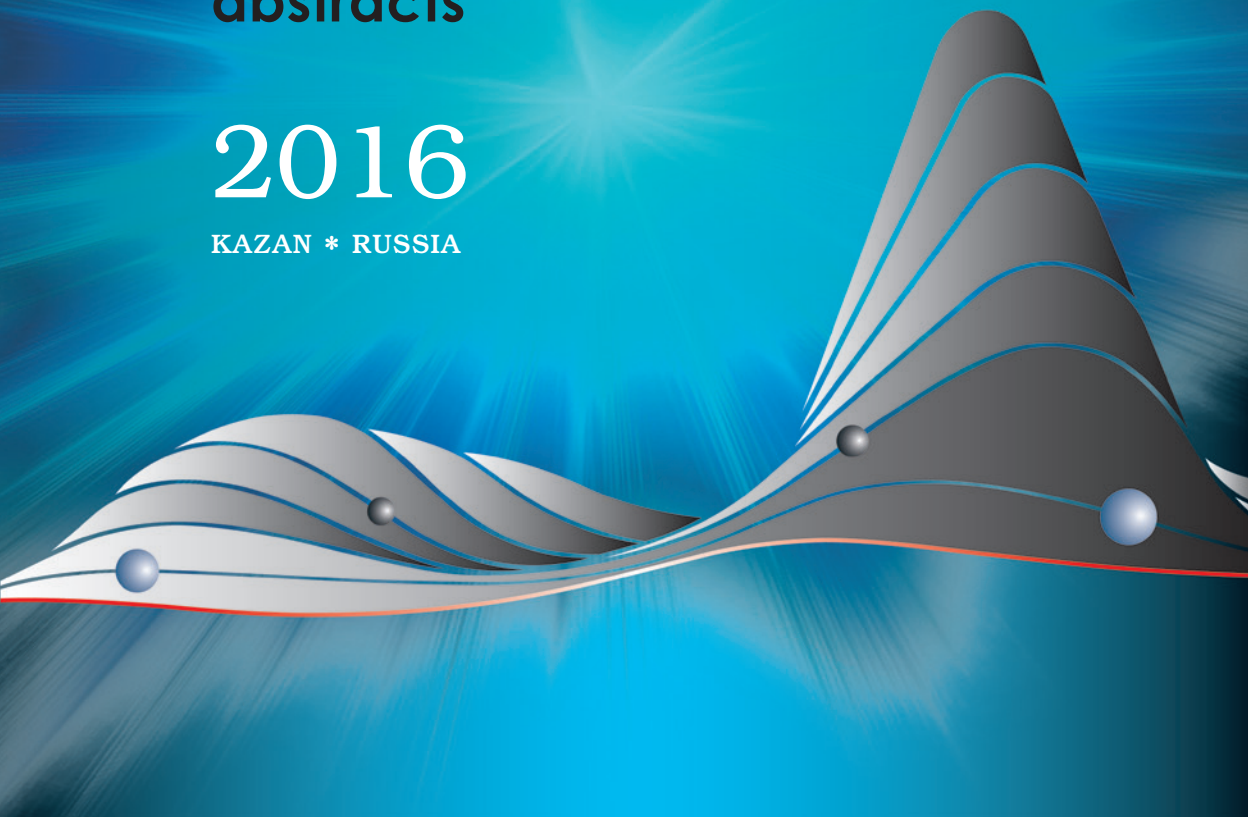


# MODERN DEVELOPMENT OF MAGNETIC RESONANCE

**abstracts**

**2016**

KAZAN \* RUSSIA









# MODERN DEVELOPMENT OF MAGNETIC RESONANCE

ABSTRACTS OF THE  
INTERNATIONAL CONFERENCE

Editor:  
KEV M. SALIKHOV

KAZAN, OCTOBER 31 – NOVEMBER 4, 2016

This work is subject to copyright.

All rights are reserved, whether the whole or part of the material is concerned, specifically those of translation, reprinting, re-use of illustrations, broadcasting, reproduction by photocopying machines or similar means, and storage in data banks.

© 2016 Kazan E. K. Zavoisky Physical-Technical Institute, Kazan

© 2016 Igor A. Aksenov, graphic design

Printed in the Russian Federation

Published by Kazan E. K. Zavoisky Physical-Technical Institute, Kazan

[www.kfti.knc.ru](http://www.kfti.knc.ru)

**CHAIR**

Alexey A. Kalachev

**PROGRAM COMMITTEE**

Albert Aganov (Russia)  
Vadim Atsarkin (Russia)  
Pavel Baranov (Russia)  
Bernhard Blümich (Germany)  
Michael Bowman (USA)  
Sabine Van Doorslaer (Belgium)  
Rushana Eremina (Russia)  
Jack Freed (USA)  
Ilgiz Garifullin (Russia)  
Alexey Kalachev (Russia)  
Wolfgang Lubitz (Germany)  
Klaus Möbius (Germany)  
Hitoshi Ohta (Japan)  
Igor Ovchinnikov (Russia)  
Kev Salikhov (Russia)  
Vladimir Skirda (Russia)  
Murat Tagirov (Russia)  
Takeji Takui (Japan)  
Valery Tarasov (Russia)  
Yurii Tsvetkov (Russia)  
Violeta Voronkova (Russia)

## **LOCAL ORGANIZING COMMITTEE**

Kalachev A.A., chairman  
Mamin R.F., vice-chairman  
Adzhaliev Yu.A.  
Akhmin S.M.  
Chuclanov A.P.  
Falin M.L.  
Fazlizhanov I.I.  
Galeev R.T.  
Goleneva V.M.  
Gubaidulina A.Z.  
Guseva R.R.  
Kupriyanova O.O.

Kurkina N.G.  
Latypov V.A.  
Mosina L.V.  
Salikhov K.M.  
Siafetdinova A.Z.  
Tarasov V.F.  
Voronkova V.K.  
Voronova L.V.  
Yanduganova O.B.  
Yurtaeva S.V.  
Ziganshina S.A.

## **SCIENTIFIC SECRETARIAT**

Violeta K. Voronkova  
Laila V. Mosina  
Vlad A. Latypov  
Sufia A. Ziganshina

The conference is organized under the auspices of the AMPERE Society

## **ORGANIZERS**

Kazan E. K. Zavoisky Physical-Technical Institute  
The Academy of Sciences of the Republic of Tatarstan  
Kazan Federal University

## **SUPPORTED BY**

The Government of the Republic of Tatarstan  
The Russian Foundation for Basic Research  
Bruker BioSpin Moscow

## **CONFERENCE LOCATION**

The Academy of Sciences of the Republic of Tatarstan  
Kazan, ul. Baumana 20



---

## CONTENTS

### ZAVOISKY AWARD LECTURES

- Electron Transport and Energy Transduction: Lessons From Proteins  
M. K. Bowman 2
- Practical Aspects of Multi-Frequency (from S Band to D Band)  
Pulsed EPR/ENDOR Spectroscopies for Biological Applications:  
Structure of Metalloenzymes, Characterization of MRI Contrast Agents,  
Distance Measurements with Gd(III) Tags and More...  
A. Raitsimring 3

### PLENARY LECTURES

- Electron Spin Resonance on the Border between  
Para- and Ferromagnetism: Quantum *versus* Classical  
V. A. Atsarkin 6
- Molecular Spin Technology for Quantum Computers and Quantum  
Information Processing  
K. Sato, S. Yamamoto, T. Shibata, E. Hosseini, N. Mori, T. Yamane,  
T. Nakagawa, S. Sawada, K. Sugisaki, S. Nakazawa, K. Maruyama,  
K. Toyota, D. Shiomi, Y. Morita, S. Nishida, S. Suzuki,  
K. Okada, T. Takui 7
- Overcoming Insufficient Signal Strength in ESR  
M. Srivastava, E. R. Georgieva, B. Dzikovski, J. H. Freed 8
- Multi-Extreme THz ESR: Recent Developments and Future  
H. Ohta, S. Okubo, E. Ohmichi, T. Sakurai, S. Hara, H. Takahashi 10
- New Porphyrin Molecules with Möbius-Strip Topology as Studied by  
Modern Magnetic Resonance Methods  
K. Möbius 11
- Why EPR Will Save the World?  
K. Salikhov 12

SECTION 1  
CHEMICAL AND BIOLOGICAL SYSTEMS

- ESR-Spectroscopy in Ionic Liquids: High Pressure Investigations on the Dynamics and Kinetics of Organic Radicals  
*G. Grampp, B. Mladenova, K. Rasmussen, D. Kattinig* 14
- Application of Trytil Radicals in Biology and Materials Science  
*E. Bagryanskaya* 16
- ELDOR-Detected NMR: a Powerful EPR Technique for Hyperfine and Polarization Transfer Studies  
*A. Savitsky* 17
- Intramolecular Hydrogen Bonding and Solvent Effect in  $\beta$ -Phosphorylated Nitroxides  
*G. Audran, P. Brémond, S. Marque* 18
- Ionic and Molecular Transport in Ion Exchange Systems Studied by NMR  
*V. I. Volkov* 19

SECTION 2  
STRONGLY CORRELATED ELECTRON SYSTEMS.  
MAGNETIC RESONANCE INSTRUMENTATION

- Complex Electronic Order in Fe-Based Superconductors Studied by Nuclear Probe Spectroscopy  
*H.-H. Klauss* 24
- Magnetic Resonance Anisotropy in  $CeB_6$   
*S. V. Demishev, A. V. Semeno, M. I. Gilmanov, A. V. Bogach, V. V. Glushkov, V. N. Krasnorussky, A. N. Samarin, N. A. Samarin, N. E. Sluchanko, N. Yu. Shitsevalova, V. B. Filipov* 25
- Anomalous ESR Behavior of Lanthanum Doped  $CeB_6$   
*A. V. Semeno, M. I. Gilmanov, V. N. Krasnorusski, N. Yu. Shitsevalova, V. B. Filipov, A. N. Samarin, S. V Demishev* 26
- NMR Investigation of Ir-Based Double Perovskites  
*M. Iakovleva, E. Vavilova, H.-J. Grafe, V. Kataev, M. Kaustuv, M. Vogl, T. Dey, S. Wurmehl, B. Büchner* 27

SECTION 3  
THEORY OF MAGNETIC RESONANCE

- Impurity Spin in Normal Stochastic Field: Basic Model of Magnetic Resonance  
*F. S. Dzheparov, D. V. Lvov* 30
- Relaxation and Coherence Transfer in Radicals in Liquids  
*A. G. Maryasov, M. K. Bowman* 31

## SECTION 4

MODERN METHODS OF MAGNETIC RESONANCE.  
RELATED PHENOMENA

|   |    |
|---|----|
| Recent Advances in NMR Diffusometry<br><i>F. Zong, N. Spindler, L. R. Ancelet, I. F. Hermans, P. Galvosas</i>   | 34 |
| Novel Applications of MRI: Structural and Functional<br>Connectivity in Brain. Can MRI Contribute to the Understanding of<br>Mental Disorders?<br><i>U. Eichhoff</i>  | 36 |
| Graphical Methods for Spectral Simulation<br><i>K. A. Earle</i>   | 37 |
| Capability of Modern X-EPR Spectroscopy in Determining<br>Characteristics of Rotational Mobility of Nitroxide Radicals<br><i>N. A. Chumakova, A. Kh. Vorobiev, D. A. Pomogailo,<br/>N. A. Paramonov, S. V. Kuzin</i>  | 38 |
| The Quantum Dynamical Basis of a Classical Kinetic Scheme Describing<br>Coherent and Incoherent Regimes of Radical Pair Recombination<br><i>N. N. Lukzen, J. H. Klein, C. Lambert, U. E. Steiner</i>  | 39 |
| Nonlinear Spin Dynamics in Highly Polarised Liquids<br><i>V. V. Kuzmin, G. Tastevin, P.-J. Nacher</i>   | 40 |
| Operando NMR Studies of Electrochemical Systems<br><i>W. Münchgesang, V. Koroteev, T. Zakharchenko, D. Itkis, D. C. Meyer,<br/>A. Vyalikh</i>   | 41 |
| Effect of Dry Trehalose Glassy Matrix on the Forward Electron<br>Transfer in Photosystem I from Cyanobacteria<br><i>Synechocystis sp. PCC 6803</i><br><i>A. Semenov, I. Shelaev, M. Gorka, A. Savitsky, V. Kurashov,<br/>F. Gostev, V. Nadtochenko, K. Möbius, J. Golbeck</i> | 42 |
| Bruker BioSpin Latest EPR Developments:<br>Rapid Scan Unit and Fitting Software Anisotropic-SpinFit<br><i>R. Weber, I. Gromov, P. Carl, M. Mokeev</i>   | 43 |

## SECTION 5

## SPIN-BASED INFORMATION PROCESSING

|  |    |
|--|----|
| Magnetic Resonance at the Quantum Limit and Beyond<br><i>A. Bienfait, J. J. Pla, X. Zhou, C. C. Lo, C. D. Weis, T. Schenkel,<br/>D. Vion, D. Esteve, J. J. L. Morton, K. Mølmer, P. Bertet</i> | 46 |
| Spin Qubits Based on Donors in Silicon<br><i>J. J. L. Morton, S. Nur, P. Ross, H. Lim</i>  | 47 |

|  |    |
|--|----|
| Hybrid Quantum Systems – Coupling Color Centers to Superconducting Cavities<br><i>J. Majer</i>   | 48 |
| High-Q and Novel Cavity Structures for Photon-Spin Strong Coupling<br><i>M. Tobar</i>  | 49 |
| Electron Spin Decoherence of J-Coupled Donor Dimers in Two-Dimensional $\delta$ -Layers, 50 nm below Surface in Silicon<br><i>A. M. Tyryshkin, E. S. Petersen, A. J. Sigillito, J. Jhaveri, J. C. Sturm, S. A. Lyon, M. House, M. Simmons, C. C. Lo, J. J. L. Morton</i> | 50 |
| Optically Detected Magnetic Resonance in Diamond NV-Centers under Resonant Optical Excitation at Cryogenic Temperatures<br><i>R. A. Akhmedzhanov, L. A. Gushchin, N. A. Nizov, V. A. Nizov, D. A. Sobgayda, I. V. Zelensky</i>   | 51 |
| Spins as Qubits: Quantum Information Processing by Magnetic Resonance<br><i>D. Suter</i>   | 52 |
| Optical Quantum Memory in Isotopically Pure Crystals Doped by Rare-Earth Ions<br><i>R. Akhmedzhanov, L. Gushchin, A. Kalachev, S. Korableva, D. Sobgayda, I. Zelensky</i>  | 53 |
| Impedance-Matched Bragg-Type Microwave Quantum Memory<br><i>S. A. Moiseev, F. F. Gubaidullin, R. S. Kirillov, R. R. Latypov, N. S. Perminov, K. V. Petrovnin, O. N. Sherstyukov</i>  | 54 |
| Microwave and Optical Coherence of Erbium Doped Crystals below 1 K<br><i>P. Bushev</i>   | 56 |
| Investigations of $Y_2SiO_5:Nd^{143}$ Isotopically Pure Impurity Crystals for Quantum Memory by ESR Method<br><i>R. Eremina, T. Gavrilova, I. Yatsyk, I. Fazlizhanov, R. Likerov, V. Shustov, Yu. Zavartsev, A. Zagumennyi, S. Kutovoi</i>                               | 57 |
| Dipolar Relaxation of Multiple Quantum Coherences of One-Dimensional Systems in Multiple Quantum NMR<br><i>G. A. Bochkin, E. B. Fel'dman, S. G. Vasil'ev</i>   | 59 |
| Microwave Pulses Storage by Using Spin-Frequency Comb Protocol Combined with Gradient Pulses of Magnetic Field<br><i>K. I. Gerasimov, S. A. Moiseev, V. I. Morozov, R. B. Zaripov</i>  | 60 |

## SECTION 6

## ELECTRON SPIN BASED METHODS FOR ELECTRONIC AND SPATIAL STRUCTURE DETERMINATION IN PHYSICS, CHEMISTRY AND BIOLOGY

|  |    |
|--|----|
| Spin Interactions and Structure in the Condensed Phase<br><i>M. K. Bowman</i>  | 62 |
| EPR Studies of Doped TiO <sub>2</sub> Photocatalysts: Structures, Properties and Dynamics of Paramagnetic Centers in the Lattice and on the Surface<br><i>A. I. Kokorin, A. I. Kulak</i>   | 63 |
| EPR Spectroscopy for Studying the Structure and Dynamics of Supercritical Fluids<br><i>E. Golubeva</i>   | 65 |
| The Development of Nitroxide Spin Probe Technique for Determination of Molecular Orientation Distribution Function<br><i>A. Kh. Vorobiev, N. A. Chumakova</i>  | 66 |
| Determining the Structure and Magnetic Properties of Ytterbium Impurity Centers in Synthetic Forsterite by X-band EPR Spectroscopy<br><i>V. Tarasov, A. Sukhanov, E. Zharikov</i>  | 68 |
| Spins of Current Carriers as a Probe of Physical and Chemical Transformations in Conductors<br><i>A. M. Ziatdinov</i>  | 69 |
| SECTION 7  |    |
| LOW-DIMENSIONAL SYSTEMS AND NANO-SYSTEMS   |    |
| Level-Anticrossing Spectroscopy of Excited States in Semiconductors and Semiconductor Nanostructures<br><i>N. G. Romanov, A. N. Anisimov, V. A. Soltamov, P. G. Baranov</i>  | 72 |
| Magnetic Investigation of One-Dimensional Organic Conductors, (TMTTF) <sub>2</sub> X<br><i>M. Asada, T. Nakamura</i>   | 73 |
| ESR Reveals Doping-Induced Change of Spin Structure in a “Triangular” Antiferromagnet<br><i>A. I. Smirnov, T. A. Soldatov, T. Kida, A. Takata, M. Hagiwara, O. Petrenko, M. Zhitomirsky</i>  | 75 |
| Unusual Magnetic Excitations in a Weakly Ordered Spin-1/2 Chain Antiferromagnet Sr <sub>2</sub> CuO <sub>3</sub> : Possible Evidence for the Goldstone-Higgs Interaction<br><i>S. S. Sosin, E. G. Sergeicheva, I. A. Zaliznyak</i> | 76 |
| Ferromagnetic Resonance of Localized Nonuniform States in Magnetic Nanostructures<br><i>R. V. Gorev, M. V. Sapozhnikov, E. V. Skorohodov, V. L. Mironov</i>  | 77 |

|   |    |
|---|----|
| Ferromagnetic Resonance in Exchange-Related Ferromagnet-Paramagnet Multilayer Structures<br><i>A. A. Fraerman, E. V. Skorohodov, S. N. Vdovichev, R. V. Gorev, E. S. Demidov</i>  | 79 |
| ESR Study of Electron States in Ge/Si Heterostructures with Nanodisc Shaped Quantum Dots<br><i>A. F. Zinovieva, V. A. Zinovyev, A. V. Nenashev, L. V. Kulik, A. V. Dvurechenskii</i>  | 80 |
| Spin-1/2 Chain Magnet BaAg <sub>2</sub> Cu[VO <sub>4</sub> ] <sub>2</sub> Studied by Magnetic Resonance Technique<br><i>E. Vavilova, Y. Krupskaya, M. Schäpers, A. U. B. Wolter, H.-J. Grafe, A. Möller, B. Büchner, V. Kataev</i>      | 82 |
| Application of Ferromagnetic Resonance for Investigation of Magnetic Properties of Strained Permalloy Microparticles<br><i>D. A. Biziyayev, A. A. Bukharaev, Yu. E. Kandrashkin, T. F. Khanipov, L. V. Mingalieva, N. I. Nurgazizov</i> | 83 |
| <br>SECTION 8<br>OTHER APPLICATIONS OF MAGNETIC RESONANCE   |    |
| Nanoscale Magnetic Resonance Microscopy<br><i>A. Volodin</i>  | 86 |
| Recent Developments in Microwave & Magnetic Resonance Detection of Explosive/Illicit Materials<br><i>B. Z. Rameev, B. Çolak, İ. S. Ünver, G. V. Mozzhukhin</i>  | 88 |
| Advantages of SLASH (Slow Low Angle SHot) Sequence in Low-Field MRI of Hyperpolarised Gases<br><i>K. Safiullin, P.-J. Nacher, C. Talbot</i>   | 89 |
| Double NMR-NQR for Studies of N-14 Nuclei<br><i>G. V. Mozzhukhin, D. A. Shulgin, I. G. Mershiev, B. Z. Rameev</i>   | 90 |
| EPR Study of Special Cases of the Jahn-Teller Effect Realized in the Fluorite Type Crystals with d-Ion Dopants<br><i>V. A. Ulanov</i>   | 92 |
| Proton NMR Dipolar-Correlation Effect as a Method for Investigating Segmental Diffusion in Polymer Melts<br><i>A. Lozovoi, C. Mattea, N. Fatkullin, S. Stapf</i>  | 94 |
| Electron Transfer Pathways in Molecular Triads Centered by Aluminum Porphyrin<br><i>Yu. E. Kandrashkin, P. K. Poddutoori, A. van der Est</i>  | 96 |
| Beating of Light During Photon Echo. Observation and Application<br><i>V. N. Lisin, A. M. Shegeda, V. V. Samartsev</i>  | 97 |

---

|   |     |
|---|-----|
| Conversions and Transformations: Deformation-Induced Chemical Bonding in Pharmaceutics<br><i>D. S. Rybin, G. N. Konygin, V. E. Porsev, D. R. Sharafutdinova, G. G. Gumarov, V. Yu. Petukhov, I. P. Arsentyeva, V. V. Boldyrev</i> | 99  |
| SECTION 9   |     |
| PERSPECTIVES OF MAGNETIC RESONANCE IN SCIENCE AND SPIN-TECHNOLOGY. THEORY OF MAGNETIC RESONANCE   |     |
| Advanced Pulse EPR Studies of the Water Oxidation Cycle in Photosynthesis<br><i>W. Lubitz</i>   | 102 |
| Perspectives of Hyperpolarization and its Role in Structural Biology<br><i>R. Kaptein</i>   | 104 |
| Gd(III) Based Markers for Pulsed Dipolar Spectroscopy: Features, Theory, Instrumentation and Optimization of Measurements<br><i>A. Raitsimring</i>  | 105 |
| Can Spin Chemistry Explain all Effects of Electromagnetic Fields on Living Organisms?<br><i>G. I. Likhtenshtein</i>   | 106 |
| EPR Spectroscopy of Pulse Double Electron-Electron Resonance (PELDOR). Some Results and Prospects<br><i>Yu. D. Tsvetkov</i>   | 107 |
| Revealing Structures of Immobilized Catalysts by Solid State NMR<br><i>G. Buntkowsky</i>  | 108 |
| Supramolecular Organization: What Can We Learn from Magnetic Resonance<br><i>H. W. Spiess</i>   | 109 |
| Unexpected Changes in EPR Spectra of Liquid Solutions of Nitroxide Biradicals<br><i>A. I. Kokorin</i>   | 110 |
| POSTERS   |     |
| NMR Investigation of Conformational Changes in Calcium Gluconate<br><i>M. M. Akhmetov, G. G. Gumarov, V. Yu. Petukhov, G. N. Konygin, D. S. Rybin, A. B. Konov</i>  | 114 |
| Analysis of Manifestations of the Spin Coherence Transfer in EPR Spectra of Nitroxyl Radicals in Liquids<br><i>M. M. Bakirov, K. M. Salikhov, R. T. Galeev</i>  | 116 |
| First-Principles Solid-State Calculations and Pulsed EPR Measurements: a Study of Ionic Substitutions in Hydroxyapatite<br><i>T. Biktagirov, M. Gafurov, G. Mamin, S. Orlinskii</i>   | 118 |

---

|  |     |
|--|-----|
| Compare Acetonitrile and Solid-Phase Extractions for Sample Preparation of Plasma at Metabolom Study by NMR<br><i>A. Bogaychuk, M. Dambieva, G. Kupriyanova, S. Babak</i>  | 119 |
| Orientation Order and Rotation Mobility of Nitroxide Biradicals Determined by Quantitative Simulation of EPR Spectra<br><i>A. V. Bogdanov, A. Kh. Vorobiev</i>   | 121 |
| Chemical Exchange in Water<br><i>P. Dvořák, J. Lang</i>  | 123 |
| ESR Study of Mn-Heterovalent Ludwigite $Mn_{3-x}Cu_xBO_5$<br><i>R. M. Eremina, I. V. Yatsyk, E. M. Moshkina, M. V. Rautskii, L. N. Bezmaternykh, H.-A. Krug von Nidda, A. Liodl</i>  | 124 |
| Electron Paramagnetic Resonance of $Ce^{3+}$ Ion in $Rb_2NaYF_6$ Single Crystal: Experiment and Theoretical Calculations of the Optical Spectra<br><i>M. L. Falin, V. A. Latypov, A. M. Leushin, S. L. Korableva</i>   | 126 |
| EPR and Optical Spectroscopy of $Yb^{3+}$ in Hexagonal Perovskite $RbMgF_3$ Single Crystal<br><i>M. L. Falin, V. A. Latypov, G. M. Safullin, A. M. Leushin, S. V. Petrov</i>   | 128 |
| Spin Dynamics in the Vicinity of Levels Anticrossing<br><i>R. T. Galeev</i>  | 129 |
| Effect of Activation and Inhibition of $K_{ATP}^+$ -Channels on the NO Production in the Blood of Rats with Ischemic Stroke<br><i>S. A. Gavrilova, O. G. Deryagin, Kh. L. Gainutdinov, V. V. Andrianov, A. V. Golubeva, G. G. Yafarova, V. S. Iyudin, A. V. Buravkov, V. B. Koshelev</i> | 130 |
| Magnetic Resonance Investigations of Core-Shell Composites Based on $CaCu_3Ti_4O_{12}$<br><i>T. Gavrilova, I. Yatsyk, R. Eremina, I. Gilmutdinov, Y. Kabirov, J. Nikitina</i>  | 132 |
| Measurement of ESR Oscillating Magnetization Value in Strongly-Correlated Metals<br><i>M. I. Gilmanov, A. V. Semeno, A. N. Samarin, S. V. Demishev</i>   | 135 |
| EPR Investigation of the Radiation-Induced Transformation in Calcium Gluconate<br><i>I. A. Goenko, V. Yu. Petukhov, I. V. Yatzyk, G. N. Konygin, D. S. Rybin, I. N. Andreeva, A. V. Anisimov, D. R. Sharafutdinova</i>   | 136 |
| Electron Spin Resonance on $Eu^{2+}$ Impurities in 3D Topological Semimetal<br><i>Yu. V. Goryunov, A. N. Nateprov</i>  | 138 |



---

|  |     |
|--|-----|
| Correlation of EPR and Biochemical Results of Iron Metabolism Study in Serum of Professional Athletes<br><i>M. I. Ibragimova, A. I. Chushnikov, G. V. Cherepnev, V. Yu. Petukhov</i>   | 140 |
| Magnetic Susceptibility of an Antiferromagnetic System with Disorder: Griffiths Phase and Phases with an Intermediate Magnetic Order<br><i>T. V. Ischenko, A. N. Samarin, S. V. Demishev</i>   | 142 |
| Determination of Magnetic Anisotropies Parameters and Miscut Angles for Epitaxial Thin Films Grown on Vicinal (111) Substrates Using Ferromagnetic Resonance<br><i>A. V. Izotov, B. A. Belyaev, P. N. Solovev</i>  | 143 |
| Influence of the Outer-Sphere Anion on Electronic and Magnetic Properties of $[\text{Fe}(\text{3-CH}_3\text{O-Qsal})_2]\text{Y} \cdot n$ Solvent ( $n = 0, 1$ ) Complexes<br><i>T. A. Ivanova, I. V. Ovchinnikov, O. A. Turanova, L. V. Mingalieva, I. F. Gilmutdinov, V. A. Shustov</i> | 145 |
| Elucidating Mechanisms of Intramolecular Exchange Interaction in Substituted N,N'-Dioxy-2,6-Diazaadamantane Biradicals<br><i>O. N. Kadkin, N. R. Khafizov, T. I. Madzhidov, I. S. Antipin</i>  | 146 |
| Modeling of the Temperature Dependence of the EPR Spectra of Fullerene C60 Nitroxide Derivatives in Liquid<br><i>I. T. Khairuzhdinov, R. B. Zaripov, K. M. Salikhov, V. P. Gubskaya, I. A. Nuretdinov</i>  | 148 |
| Cloud Project for Storage and Processing of Medical Images Obtained by MRI of Zavoisky Kazan Physical Technical Institute<br><i>R. Khabipov, I. Sitdikov, Ya. Fattakhov</i>  | 149 |
| High Temperature Fast Field Cycling Study of Crude Oil<br><i>A. Lozovoi, M. Hurlimann, R. Kausik, S. Stapf, C. Mattea</i>  | 151 |
| Manipulating Electron Spin Hyper-Polarization by Means of Adiabatic Switching of a Spin-Locking MW Field<br><i>N. N. Lukzen, K. L. Ivanov</i>  | 153 |
| Hyperfine Structure of $\text{Er}^{3+}$ Ion in Bulk Copper<br><i>S. Lvov, E. Kukovitsky</i>  | 154 |
| NQR Relaxation Times Distribution of 5-Aminotetrazole Monohydrate<br><i>S. Mamadazizov, G. Kupriyanova</i>   | 155 |
| Investigation of Influence Conformations of Nitroxyl Radicals on EPR Parameters by DFT Method<br><i>A. Mamatova, L. Savostina</i>  | 158 |
| Development of Permanent Magnet System for Time-Domain NMR<br><i>A. Maraşlı, M. Maksutoğlu, Y. Öztürk, B. Z. Rameev</i>  | 159 |

|   |     |
|---|-----|
| Molecular Mobility of n-Hexane in Silicailte-1 by 2D NMR Relaxo- and Diffusometry<br><i>D. L. Melnikova, T. V. Shipunov, M. N. Makarov, H. Zhou, B. I. Gizatullin</i>   | 160 |
| Complex Downhole Apparatus for Magnetic Resonance Logging<br><i>V. Murzakaev, A. Bragin, D. Kirgizov, D. Nurgaliev, A. Alexandrov, A. Ivanov, M. Doroginitcky, V. Skirda, Ya. Fattakhov, V. Shagalov, A. Fakhrutdinov, R. Khabipov, A. Anikin</i> | 162 |
| EPR Investigation of Some Complexes of Fe(III) with Pentadentate Ligand<br><i>I. Ovchinnikov, T. Ivanova, A. Suhanov, E. Frolova, O. Turanova, L. Mingalieva, L. Gafiyatullin</i>   | 164 |
| Development of New Approaches to NMR Data Processing in Time-Domain NMR<br><i>O. V. Petrov, S. Stapf</i>  | 165 |
| Effects of Femtosecond Magnetooptics Based on Photon Echo and Practical Significance<br><i>I. Popov, N. Vashurin, A. Bahodurov</i>  | 166 |
| Consistent Paradigm of the Spectra Decomposition into Independent Resonance Lines<br><i>K. M. Salikhov</i>  | 167 |
| Influence of Non-Stoichiometry on the Frustrated Honeycomb System $\text{Li}_3\text{Ni}_2\text{SbO}_6$<br><i>T. Salikhov, E. Klysheva, M. Iakovleva, E. Zvereva, I. Shukaev, V. Nalbandyan, B. Medvedev, E. Vavilova</i>                          | 168 |
| High-Frequency EPR Spectroscopy of YAG: Fe, Ce<br><i>G. S. Shakurov, G. R. Asatryan, K. L. Hovhannesyan, A. G. Petrosyan</i>  | 169 |
| Synthesis and Characterization of $\text{Gd}_{1-x}\text{Sr}_x\text{MnO}_3$<br>( $x = 0.5, 0.6, 0.7, 0.8$ )<br><i>A. K. Shukla, T. Maiti, R. M. Eremina, I. V. Yatsyk, H.-A. Krug von Nidda</i>  | 170 |
| Dysprosium Containing Clusters: Some Features of EPR of the Polycrystalline Samples<br><i>A. Sukhanov, R. Galeev, V. Voronkova, A. Baniodeh, A. Powell</i>  | 172 |
| Investigation Magnetic Properties of the Mercury Chalcogenides<br><i>A. V. Shestakov, I. I. Fazlizhanov, I. V. Yatsyk, M. I. Ibragimova, V. A. Shustov, R. M. Eremina</i>   | 174 |
| Photoinduced Spin States of Copper Porphyrin Dimers<br><i>A. A. Sukhanov, V. K. Voronkova, V. S. Tyurin</i>   | 177 |
| High Frequency Zero Field EPR Spectroscopy of Thulium Impurity Centers in Synthetic Forsterite<br><i>V. Tarasov, N. Solovarov, E. Zharikov</i>  | 179 |

---

|  |     |
|--|-----|
| Ethanol Clusters in Gasoline-Ethanol Blends<br><i>A. Turanov, A. K. Khitrin</i>  | 180 |
| New Protocol of Experiments for Determining the Rate of the Spin<br>Coherence Transfer in a Course of the Spectral Diffusion when<br>Spectra Have Resolved Multicomponent Structure<br><i>M. Yu. Volkov, M. M. Bakirov, R. T. Galeev, A. A. Sukhanov,<br/>K. M. Salikhov</i> | 182 |
| Orientation-Dependent EMR Signals in Biological Tissues.<br>Characteristics and Interpretation<br><i>S. V. Yurtaeva, V. N. Efimov, V. V. Salnikov, A. A. Rodionov,<br/>I. V. Yatsyk</i>  | 183 |
| EPR Study of the BaF <sub>2</sub> Crystals Activated by Nb <sup>4+</sup> Ions<br><i>E. R. Zhiteitsev, R. B. Zaripov, V. A. Ulanov</i>  | 186 |
| The Concentration Dependence of the Wings of a Dipolar-Broadened<br>Line of Magnetic Resonance in a Magnetically Dilute Lattice of Spins<br><i>V. E. Zobov, M. M. Kucherov</i>   | 187 |
| EMR Searching of Quantum Behavior of Superparamagnetic $\gamma$ -Fe <sub>2</sub> O <sub>3</sub><br>Nanoparticles Fabricated in Dendrimeric Matrix<br><i>N. E. Domracheva, V. E. Vorobeva, M. S. Gruzdev</i>  | 188 |
| Counterion Effect on the Spin-Transition Properties of<br>the Second Generation Iron(III) Dendrimeric Complexes<br><i>N. E. Domracheva, V. E. Vorobeva, V. I. Ovcharenko, A. S. Bogomyakov,<br/>E. M. Zueva, M. S. Gruzdev, U. V. Chervonova, A. M. Kolker</i>               | 190 |
| AUTHOR INDEX   | 191 |

---

---

## ZAVOISKY AWARD LECTURES

## **Electron Transport and Energy Transduction: Lessons From Proteins**

**M. K. Bowman**

Department of Chemistry, The University of Alabama, Tuscaloosa, Alabama 35486, USA

Living cells have several systems to generate and store energy. One system is based on the transport of electrons. Another on the absorption of light energy, and yet another on chemical transformations. All three systems have specific points at which one form of energy can be converted into another form, so the energy can be utilized for work or can be stored for future needs. One of the most fascinating of these energy transduction points is the cytochrome bc<sub>1</sub> protein complex where electron transfers are used to generate chemical energy for storage or immediate use. This protein complex uses a variety of unexpected tactics to achieve high efficiency and stability. These tactics include recycling unused electrons, using insulating barriers, not following the easiest path and taking one step at a time.

---

## **Practical Aspects of Multi-Frequency (from S Band to D Band) Pulsed EPR/ENDOR Spectroscopies for Biological Applications: Structure of Metalloenzymes, Characterization of MRI Contrast Agents, Distance Measurements with Gd(III) Tags and More...**

### **A. Raitsimring**

Department of Chemistry and Biochemistry, University of Arizona, Tucson, Arizona 85721-0041, USA,  
arnold@u.arizona.edu.

(i) The customary way to resolve the close structure of metalloenzymes *in vitro* is to measure hyperfine (hfi) and quadrupole interactions of nuclei (nqi) in the vicinity of the metal ion and relate them to the structure. In this lecture, I discuss the importance of operational frequencies and pulse techniques to unambiguously determine the hfi and nqi parameters of various nuclei (H,  $^{17}\text{O}$ ,  $^{33}\text{S}$ ,  $^{31}\text{P}$ , D,  $^{35}\text{Cl}$ ), taking as an example the Mo(V) based enzyme and model systems. I will also discuss the essentials of pulsed EPR spectrometers necessary for efficient performance.

(ii) The efficiency of Gd(III) based contrast agents depends on the number of water molecules directly ligated to Gd(III). I discuss the procedures and operational frequencies to correctly determine the number and geometry of water molecule ligation to Gd (III) using 1D and 2D varieties of  $^{17}\text{O}$ ,  $^{13}\text{C}$ , H and D pulsed ENDOR.

(iii) I will discuss the *pro et contra* of traditional nitroxide labels vs recently introduced Gd(III) tags for the measurements distance variation and distance distribution between attachment sites in biological objects by pulsed dipolar spectroscopy (PDS) as well as feasible venues to further decrease the acquisition time, increase the sensitivity and range of the distance when the latter are used.

---



---

## PLENARY LECTURES

## Electron Spin Resonance on the Border between Para- and Ferromagnetism: Quantum *versus* Classical

**V. A. Atsarkin**

Kotel'nikov Institute of Radio Engineering and Electronics of RAS, Moscow 125009,  
Russian Federation, atsarkin@cplire.ru

Electron spin resonance of individual paramagnetic centers and small exchange clusters is commonly interpreted on the basis of spin Hamiltonian, whereas the classical (Landau-Lifshits) description is adopted for description of ferromagnetic resonance (FMR) in macroscopic ferromagnetic objects. In this report, we present and discuss interesting examples of intermediate behavior on the border between para- and ferromagnetism.

First we consider magnetic nanoparticles (MNPs) containing hundreds or thousands of exchange coupled spins. It is found that the resonance spectra of MNPs demonstrate peculiarities which cannot be described by classical FMR and calls for quantum approach typical of the EPR spectroscopy. The giant spin approximation is suggested and used to fit quantitatively the shape and evolution of the spin-resonance spectra of MNPs with changing the particle size and temperature [1].

Another example is the evolution of magnetic resonance spectrum with growing the spin value in an anisotropic system under conditions of level anti-crossing. It is shown that a giant narrow peak of the r.f. absorption (“pseudoresonance”) arises here in the high-spin limit. Both the experimental data obtained at thin ferromagnetic films [2] and theoretical description of this phenomenon are presented.

Finally, several resonance spin-charge phenomena in thin films and nanostructures are considered in the intermediate region between ferro- and paramagnetic states around the Curie point [3].

1. Noginova N., Bates B., Atsarkin V.A.: Appl. Magn. Reson. (2016); DOI: 10.1007/s00723-016-0804-6
2. Atsarkin V.A., Demidov V.V., Mefed A.E., Nagorkin V.Yu.: Appl. Magn. Reson. **45**, 809 (2014)
3. Atsarkin V. A., Sorokin B.V., Borisenko I.V., Demidov V.V., Ovsyannikov G.A.: J. Phys. D: Appl. Phys. **49**, 125003 (2016)

## Molecular Spin Technology for Quantum Computers and Quantum Information Processing

**K. Sato<sup>1</sup>, S. Yamamoto<sup>1</sup>, T. Shibata<sup>1</sup>, E. Hosseini<sup>1</sup>, N. Mori<sup>1</sup>, T. Yamane<sup>1</sup>, T. Nakagawa<sup>1</sup>, S. Sawada<sup>1</sup>, K. Sugisaki<sup>1</sup>, S. Nakazawa<sup>1</sup>, K. Maruyama<sup>1</sup>, K. Toyota<sup>1</sup>, D. Shiomi<sup>1</sup>, Y. Morita<sup>2</sup>, S. Nishida<sup>2</sup>, S. Suzuki<sup>1</sup>, K. Okada<sup>1</sup>, and T. Takui<sup>1</sup>**

<sup>1</sup> Department of Chemistry and Molecular Materials Science, Graduate School of Science, Osaka City University, Osaka 558-8585, Japan

<sup>2</sup> Department of Applied Chemistry, Faculty of Engineering, Aichi Institute of Technology, Aichi 470-0392, Japan, takui@sci.osaka-cu.ac.jp

The field of quantum computing/quantum information processing (QC/QIP) has emerged into a new phase since 2012 Nobel Prize for Physics was awarded to two pioneers who first have manipulated, independently, a single atom/ion or photon with its quantum nature maintained. These techniques are essential to implement QC/QIP technology, illustrating physical realization of qubits (quantum bits). In recent development of QC/QIP, all the relevant physical qubits are facing the problems of the scalability of qubits in addition to decoherence intrinsic to their quantum nature. Among candidates for physically realized qubits, molecular spin qubits are the latest arrival [1], but have their own right [2, 3].

We introduce the latest achievements based on molecular spin qubits in ensemble and discuss their advantages and disadvantages in terms of quantum spin technology [4]. Attempts to apply molecular spins to the implementation of QC/QIP have been underlain by enormous efforts by organic chemist to synthesize stable molecular spins which fulfil the requirements of spin qubits for QC gate operations. In terms of the gate operations, we utilize weakly exchange-coupled multi-partite electron spin systems because of the limitations of current pulse microwave technology enabling us to manipulate or control matter spin qubits. In order to implement practical QC/QIP systems, a large number of quantum memory elements are required as well. We illustrate that open shell chemistry plays an important role to afford the memory elements for the architecture of scalable superconducting flux qubits or microwave photons.

Molecular spin qubits, properly designed, can also give a testing ground for “Adiabatic Quantum Computing”, which is different from the circuit model of quantum computing and thus an alternative approach to QC/QIP.

1. (a) Rahimi R., Sato K., Takui T. *et al.*: *Int. J. Quantum Inf.* **3**, 197–204 (2005); (b) Sato K., Takui T. *et al.*: *Physica E* **40**, 363–366 (2007); (c) Sato K., Morita Y., Takui T. *et al.*: *J. Mater. Chem.* **19**, 3739–3754 (2009)
2. Special issue, Molecular Spintronics and Quantum Computing, *J. Mater. Chem.* **19**, 1670–1766 (2009)
3. Troiani F., Bellini V., Candini A., Lorusso G., Affronte M.: *Nanotechnology* **21**, 274009 (2010)
4. Nakazawa S., Nishida S., Morita Y., Takui T. *et al.*: *Angew. Chem. Int. Ed.* **51**, 9860–9864 (2012)

## Overcoming Insufficient Signal Strength in ESR

M. Srivastava<sup>1,2</sup>, E. R. Georgieva<sup>2,3</sup>, B. Dzikovski<sup>2,3</sup>, and J. H. Freed<sup>1,2,3</sup>

<sup>1</sup> Nancy E. and Peter C. Meinig School of Biomedical Engineering, Cornell University, Ithaca, NY

<sup>2</sup> National Biomedical Center for Advanced ESR Technology (ACERT), Cornell University, Ithaca, NY

<sup>3</sup> Department of Chemistry and Chemical Biology, Cornell University, Ithaca, NY

Pulsed Dipolar Spectroscopy (PDS) ESR is currently used to obtain structural information on biological systems, whereas cw-ESR is frequently applied to study the dynamics. These are a difficult challenge, since samples of spin labeled proteins are small and dilute and exhibit short electron-spin relaxation times, which result in a low Signal to Noise Ratio (SNR), thereby complicating the analysis. To obtain sufficient SNR, substantial signal averaging is needed. Addressing the challenge of noise removal in a PDS signal in order to obtain reliable distance distributions, we developed a new wavelet denoising method and a novel approach to remove/reduce noise. Our wavelet denoising method improves the stability and reliability of the reconstruction of the distance distributions, and it can reduce the required signal acquisition time by as much as a factor of 10 (cf. Fig. 1). Similarly, for cw-ESR we developed another related wavelet denoising method, which also substantially reduces the needed signal averaging (cf. Fig.

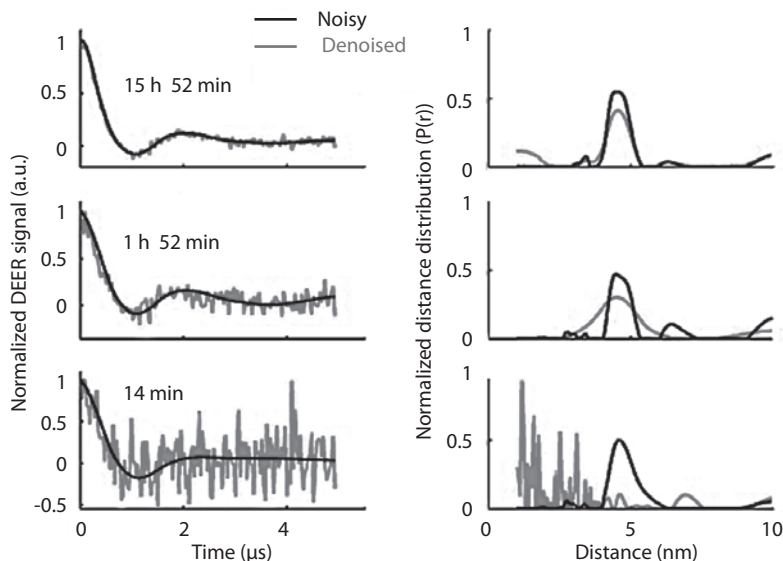


Fig. 1.

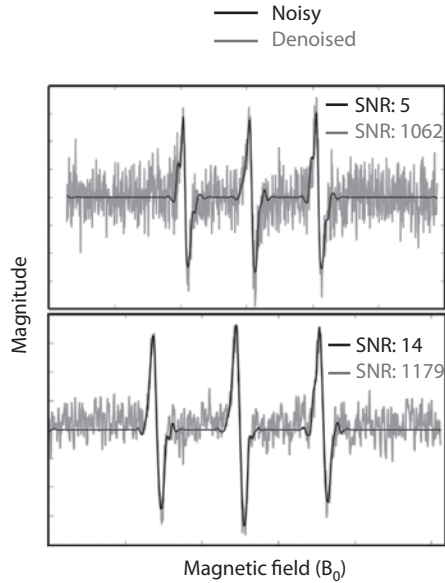


Fig. 2.

2). At various SNR's for both model and experimental signals, we show that our method can effectively remove, or at least substantially reduce noise without distorting the signal, unlike other standard denoising methods. Our method is able to identify and eliminate noise at and near the peaks of the signal spectrum, which has been a major concern in recovering the original spectrum.

## Multi-Extreme THz ESR: Recent Developments and Future

**H. Ohta<sup>1</sup>, S. Okubo<sup>1</sup>, E. Ohmichi<sup>2</sup>, T. Sakurai<sup>3</sup>, S. Hara<sup>3</sup>,  
and H. Takahashi<sup>4</sup>**

<sup>1</sup> Molecular Photoscience Research Center, Kobe University, Kobe 657-8501, Japan,  
hohta@kobe-u.ac.jp

<sup>2</sup> Graduate School of Science, Kobe University, Kobe 657-8501, Japan

<sup>3</sup> Center for Support to Research and Education Activities, Kobe University, Kobe 657-8501, Japan

<sup>4</sup> Organization of Advanced Science and Technology, Kobe University, Kobe 657-8501, Japan

Recent developments and future perspectives of multi-extreme THz ESR in Kobe will be presented. Our multi-extreme THz ESR can cover the frequency region between 0.03 and 7 THz [1], the temperature region between 1.8 and 300 K [1], the magnetic field region up to 55 T [1], and the pressure region up to 1.5 GPa [2] simultaneously. Recently we have developed the hybrid-type pressure cell, which consists of the NiCrAl alloy inner cell, the Cu-Be alloy outer cell and the ceramic piston parts, and achieved 2.7 GPa [3]. Our micro-cantilever ESR [4], which reached 1.1 THz recently [5], and SQUID ESR [6] will be also presented.

1. Ohta H. *et al.*: J. Low Temp. Phys. **170**, 511 (2013)
2. Sakurai T. *et al.*: Rev. Sci. Instr. **78**, 065107 (2007); Sakurai T.: J. Phys.: Conf. Series **215**, 012184 (2010)
3. Fujimoto K. *et al.*: Appl. Mag. Res. **44**, 893 (2013); Ohta H. *et al.*: J. Phys. Chem. B **119**, 13755 (2015); Sakurai T. *et al.*: J. Mag. Res. **259**, 108 (2015)
4. Ohta H. *et al.*: AIP Conf. Proceedings **850**, 1643 (2006); Ohmichi E. *et al.*: Rev. Sci. Instrum. **79**, 103903 (2008); Ohmichi E. *et al.*: Rev. Sci. Instrum. **80**, 013904 (2009); Ohta H., Ohmichi E.: Appl. Mag. Res. **37**, 881 (2010); Ohmichi E. *et al.*: J. Low Temp. Phys. **159**, 276 (2010); Tokuda Y. *et al.*: J. Phys.: Conf. Series **400**, 032103 (2012); Ohmichi E. *et al.*: J. Mag. Res. **227**, 9 (2013)
5. Takahashi H., Ohmichi E., Ohta H.: Appl. Phys. Lett. **107**, 182405 (2015)
6. Sakurai T. *et al.*: J. Phys.: Conf. Series **334**, 012058 (2011); Sakurai T. *et al.*: J. Mag. Res. **223**, 41 (2012); Sakurai T. *et al.*: J. Magnetism **18**, 168 (2013)

## New Porphyrin Molecules with Möbius-Strip Topology as Studied by Modern Magnetic Resonance Methods

**K. Möbius**<sup>1,2</sup>

<sup>1</sup> Dept. of Physics, Free University, Berlin 14195, Germany, moebius@physik.fu-berlin.de

<sup>2</sup> Max Planck Institute for Chemical Energy Conversion, Mülheim (Ruhr) 45470, Germany

The one-sided Möbius band topology with its characteristic 180° twist has inspired artists and scientists since a long time. On the molecular level, the Möbius band symmetry exists only seldom in Nature, but recently spectacular discoveries of remarkably stable small ring-shaped proteins of Möbius topology from plants, the Cyclotides, have been reported. They have a potential for drug design with stable protein templates. Only in the last 13 years a few organic chemistry groups succeeded to synthesize novel compounds with Möbius symmetry by means of theory-based molecular design and ingenious chemical synthesis strategies. In 2007, the group of L. Latos-Grażyński [1] in Wrocław successfully synthesized an expanded free base porphyrin, [28]hexaphyrin, which can be dynamically switched between Hückel and Möbius  $\pi$ -conjugation via polarity or temperature changes of the matrix solvent.

The present EPR, ENDOR and DFT work [2] on the radical cation state of free base [28]hexaphyrin is the first study of a ground-state open-shell system that exhibits a temperature-controlled Hückel-Möbius topology switch, similar to what was observed earlier by NMR for the closed-shell precursor molecule [1]. Our work has now been extended to the open-shell photo-excited triplet state of [28]hexaphyrin [3]. State-of-the art DFT theory studies come to the conclusion that, besides hyperfine couplings, the zero-field splitting interaction between the two unpaired electron spins is a viable sensor for electronic-structure changes upon Hückel  $\leftrightarrow$  Möbius topology switching. Among the most promising applications of such novel expanded porphyrin molecules with Möbius-Hückel topological switching are their high non-linear optical properties (NLOP).

1. Stępień M., Latos-Grażyński L., Sprutta N., Chwalisz P., Szterenberg L.: *Angew. Chem. Int. Ed.* **46**, 7869 (2007)
2. Möbius K., Plato M., Klihm G., Laurich S., Savitsky W., Lubitz W., Szyszko B., Stępień M., Latos-Grażyński L.: *Phys. Chem. Chem. Phys.* **17**, 6644 (2015)
3. Möbius K., Savitsky A., Lubitz W., Plato M.: *Appl. Magn. Reson.* **47**, 757 (2016)

## Why EPR Will Save the World?

**K. Salikhov**

Zavoisky Physical-Technical Institute, Russian Academy of Sciences, Kazan 420029,  
Russian Federation

- Science as one of the basic resource to save world: Potential of the electron paramagnetic resonance methodology.
- Examples of the key problems of our world where EPR is of real help to solve.
- How does EPR contribute to solving those key problems.
- How should we do our fundamental research work to serve better for our mission?:
  - to make things as simple as possible, but not simpler,
  - to make scientific results available for public judging.
- About competition, cooperation and solidarity.



---

## SECTION 1

# CHEMICAL AND BIOLOGICAL SYSTEMS

## ESR-Spectroscopy in Ionic Liquids: High Pressure Investigations on the Dynamics and Kinetics of Organic Radicals

**G. Grampp<sup>1</sup>, B. Mladenova<sup>1</sup>, K. Rasmussen<sup>1</sup>,  
and D. Kattnig<sup>2</sup>**

<sup>1</sup> Institute of Physical & Theoretical Chemistry, Graz University of Technology,  
Graz A-8010, Austria, grampp@tugraz.at.

<sup>2</sup> Physical and Theoretical Chemistry Laboratory, University of Oxford,  
Oxford OX1 3QZ, UK, daniel.kattnig@chem.ox.ac.uk.

Ionic liquids (ILs) are molten salts of mainly organic cations and inorganic or organic anions, liquid at room temperature. They are of interest, not only from scientific point of view but also for chemical industrial productions. Environmental friendly industrial productions based on so-called “Green Chemistry” principles mainly use ionic liquids as solvent to avoid classical toxic organic solvents. But, only a few reports exist on ESR-spectroscopic investigations using ionic liquids as solvents. We would like to report on ESR-measurements using the ionic liquids: 1-butyl-3-methylimidazolium hexafluorophosphate 1-butyl-3-imidazolium fluoroborate and 1-ethyl-imidazolium ethylsulfate.

At our labs we have constructed a high-pressure system for use in electron spin resonance (ESR) spectroscopy. The apparatus allows the application of pressures of up to 100 MPa to solutions and with several key solvent properties (viscosity, dielectric constant, relaxation times, refractive index) being pressure dependent, reaction kinetics may be probed via pressure variations.

*Rotational correlation times  $\tau_{\text{rot}}$ .* Using the high viscosity of ionic liquids, the rotational correlation times,  $\tau_{\text{rot}}$ , of uncharged TEMPO derivatives and of charged Fremy’s salt are measured as a function of temperature and high pressure. The rotation correlation times vary between 54 and 1470 ps at 300 K. Within a temperature range of 280–380 K, the rotational tumbling is well described by the extended Debye-Stokes-Einstein law. This study is distinguished from similar studies by the fact that proton super-hyperfine coupling constants could be resolved for all nitroxides in the ionic liquids by carefully optimizing the experimental protocol. As a consequence, many rotational correlation times reported here are smaller than those found previously. Furthermore, the temperature dependence of the nitrogen ESR coupling constants is reported and discussed in detail [1–3].

*Electron-self exchange reactions.* Electron-self exchange rates of various organic redox-couples like,  $MV^+/MV^{2+}$  (methylviologene),  $TCNE^-/TCNE$  (tetracyanoethylene),  $TCNQ^-/TCNQ$  (tetracyanoquinoninedimethane),  $TMPPD^{+}/TMPPD$  ( $N,N,N',N'$ -tetramethyl-p-phenylenediamine) and  $TEMPO^{\bullet}/TEMPO^{+}$  have been measured in ILs. From ESR-line-broadening experiments rate constants corrected for diffusion vary between  $8.2 \cdot 10^7 \text{ M}^{-1}\text{s}^{-1}$  and  $1.2 \cdot 10^9 \text{ M}^{-1}\text{s}^{-1}$ , depending on the ionic liquid used. The activation energies range from  $\Delta G^{\ddagger} = 27.4\text{--}42.1 \text{ kJ/mol}$ . These results will be compared with measurements obtained

in different common classical organic solvents. The solvent dependent outer-sphere reorganization energy is discussed in the sense of Marcus-Theory. This theory is not applicable to ionic liquids [4–8].

1. Kundu K., Kattnig D.R., Mladenova B., Grampp G., Das R.: *J. Phys. Chem. B* **119**, 3200 (2015)
2. Mladenova B., Chumakova N., Pergushov V.I., Kokorin A.I., Grampp G., Kattnig D.R.: *J. Phys. Chem. B* **116**, 12295 (2012)
3. Mladenova B., Kattnig D.R., Grampp G.: *J. Phys. Chem. B* **115**, 8183 (2011)
4. Sudy B., Rasmussen K., Grampp G.: *Mol. Phys.* **113**, 1378 (2015)
5. Grampp G., Rasmussen K.: *Phys. Chem. Chem. Phys.* **4**, 5546 (2002)
6. Rasmussen K., Hussain T., Landgraf S., Grampp G.: *J. Phys. Chem. A* **116**, 193 (2012)
7. Grampp G., Kattnig D.R., Mladenova B.: *Spectrochim. Acta A* **63**, 821 (2006)
8. Choto P., Rasmussen K., Grampp G.: *Phys. Chem. Chem. Phys.* **17**, 3415 (2015)
9. Mladenova B., Kattnig D.R., Sudy B., Choto P., Grampp G.: *Phys. Chem. Chem. Phys.* **18**, 14442 (2016)

## Application of Trytil Radicals in Biology and Materials Science

**E. Bagryanskaya**

N. N. Vorozhtsov Novosibirsk Institute of Organic Chemistry SB RAS, Novosibirsk 630090,  
Russian Federation, egbagryanskaya@nioch.nsc.ru

During the last 30 years, tetrathiatriarylmethyl (TAM) radicals have been widely used as spin probes for oxymetry in electron paramagnetic resonance (EPR) spectroscopy and EPR tomography because of the narrow EPR linewidth and high stability in living systems. Recently, some researchers proposed to use TAMs as spin labels for studies on the structure of proteins and nucleic acids using site-directed spin labeling (SDSL) and pulsed dipolar EPR spectroscopy. In this presentation, the peculiarities of applying TAMs as spin labels, including approaches to TAM spin labeling of proteins and nucleic acids, the methods for distance measurement using TAM spin labels, electron spin relaxation time, room temperature measurements, and advantages of orthogonal spin labeling are reviewed. Examples of applications of TAMs to research on the structure and functions of biopolymers are presented from recently published papers [1–7], in particular room-temperature distance measurement in trityl-labeled immobilized DNA duplexes. The peculiarities of different approaches for the immobilization procedure (nucleosil@DMA, trehalose, sucroza, etc.) will be discussed. Remarkably, room-temperature electron spin dephasing time of triarylmethyl-labeled DNA in trehalose is noticeably longer compared to previously used immobilizers, thus providing a broader range of available distances. Therefore, saccharides, and especially trehalose, can be efficiently used as immobilizers of nucleic acids, mimicking native conditions and allowing wide range of structural EPR studies at room temperatures. The results of EPR measurements at room temperatures were compared with 2D NMR study for the same duplex in solution [6]. It is shown that distance measurements at physiological temperatures by the DQC method allow researchers to obtain valid structural information on an unperturbed DNA duplex using terminal TAM spin labels.

In addition the possibilities of TAM application in controlled radical polymerization will be shown [8].

This work is supported by Russian Scientific Fund (no. 14-14-00922).

1. Bagryanskaya E.G. *et al.*: *Methods in Enzymology* **563**, 36 (2015)
2. Kuzhelev A. *et al.*: *J. Phys. Chem. B* **119**, 13630 (2015)
3. Shevelev G. *et al.*: *J. Phys. Chem. B* **119**, 13641 (2015)
4. Shevelev G. Yu. *et al.*: *J. Amer. Chem. Soc.* **136**, 9874(2014)
5. Kuzhelev A. *et al.*: *J. Phys. Chem. Lett.* **7**, 2544 (2016)
6. Lomzov A. *et al.*: *J. Phys. Chem. B* **120**, 5125 (2016)
7. Kuzhelev A.A. *et al.*: *J. Magn. Reson.* **266**, 1 (2016)
8. Audran G. *et al.*: *Inorganic Chemistry Frontiers* (2016) accepted

## ELDOR-Detected NMR: a Powerful EPR Technique for Hyperfine and Polarization Transfer Studies

**A. Savitsky**

Max-Planck-Institut für Chemische Energiekonversion, Mülheim and der Ruhr, Germany,  
anton.savitsky@cec.mpg.de

Electron-electron Double Resonance (ELDOR)-detected NMR (EDNMR) is growing in popularity as a means to characterize the hyperfine structure of complex chemical systems. First developed in the Schweiger laboratory [1] it uses selective microwave pulses which simultaneously pump EPR and NMR transitions of the spin manifold, so called spin-forbidden transitions, where both the electron and nuclear spins change their projection direction ( $\Delta m_s = \pm 1$ ,  $\Delta m_I = \pm 1, \pm 2$ ). As compared to conventional ENDOR techniques it has a much higher sensitivity and does not exhibit nucleus-dependent or pulse-dependent spectral artifacts and does not require additional radio-frequency hardware. Historically, the wide spread adoption of EDNMR has been hampered by what is termed the central blind spot. Spin-forbidden transitions that are sufficiently close in absolute frequency to the allowed EPR transition are masked due to the simultaneous pumping of this allowed transition, i.e. transitions within 5–10 MHz. This problem can, however, be solved by performing experiments at high magnetic fields and, thus, higher nuclear Larmor frequencies.

In this presentation the EDNMR technique is introduced. Its general applicability for hyperfine studies is discussed. Several examples are given which include the experimental results on nitroxide radicals [2, 3] and transition-metal containing systems [4, 5]. Advantages and disadvantages of the method as compared to conventional ENDOR technique are pointed out. Additionally, selected examples of EDNMR application to electron-nuclear polarization transfer studies are presented using molecular systems containing Mn(II) and Gd(III) tags.

1. Schosseler P., Wacker T., Schweiger A.: *Chem. Phys. Lett.* **224**, 319–324 (1994)
2. Nalepa A., Möbius K., Lubitz W., Savitsky A.: *J. Magn. Reson.* **242**, 203–213 (2014)
3. Cox N., Nalepa A., Pandelia M.-E., Lubitz W., Savitsky A. in: *Methods in Enzymology* (Peter Z.Q., Kurt W., eds.), vol. 563, pp. 211–249. Academic Press, 2015.
4. Rapatskiy L., Ames W.M., Perez-Navarro M., Savitsky A., Griese J.J., Weyhermueller T., Shafaat H.S., Hogbom M., Neese F., Pantazis D.A., Cox N.: *J. Phys. Chem. B* **119**, 13904–13921 (2015)
5. Cox N., Lubitz W., Savitsky A.: *Mol. Phys.* **111**, 2788–2808 (2013)

## Intramolecular Hydrogen Bonding and Solvent Effect in $\beta$ -Phosphorylated Nitroxides

G. Audran<sup>1</sup>, P. Brémond<sup>2</sup>, and S. Marque<sup>1,2</sup>

<sup>1</sup> Aix-Marseille Université, Marseille 13297, France, sylvain.marque@univ-amu.fr

<sup>2</sup> Novosibirsk Institute of Organic Chemistry SB RAS, Novosibirsk 630090, Russian Federation

Recently, we reported a dramatic solvent effect on the phosphorus hyperfine coupling constant  $a_p$  of  $\beta$ -phosphorylated 6-membered ring nitroxides, ca. 25 G of difference in  $a_p$  from *n*-hexane to water [1]. Here, the report on the effect of Intramolecular Hydrogen Bonding (IHB) – 3 nitroxides exhibiting IHB between the hydroxyl and diethylphosphoryl groups and one exhibiting IHB between the hydroxyl group and the nitroxyl moiety. It is observed that for the first three nitroxides  $a_p$  increases with increasing polarity/polarizability and Hydrogen Bond Donor properties of the solvent ( $\pi^*$  and  $\alpha$ , respectively) – in sharp contrast to the data reported in the literature – and for the last one  $a_p$  decreases with  $\pi^*$  and  $\alpha$ . In fact, the occurrence of IHB induces a large strain whose suppression by Hydrogen Bond Acceptor (HBA) solvents affords an increase in  $a_p$ .

1. Audran G., Bosco L., Brémond P., Butscher T., Marque S.R.A.: *Org. Biomol. Chem.* **14**, 1228–1292 (2016)

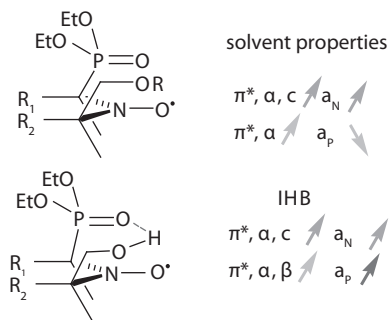


Fig. 1.

## Ionic and Molecular Transport in Ion Exchange Systems Studied by NMR

**V. I. Volkov<sup>1,2</sup>**

<sup>1</sup> Institute of Problems of Chemical Physics RAS Acad., Chernogolovka 142432, Russian Federation

<sup>2</sup> Science Center in Chernogolovka RAS, Moscow Region, Chernogolovka 142432,  
Russian Federation, vitwolf@mail.ru

The mass and charge transfer mechanism investigation in polymeric electrolytes may be realized on the basis of mutual NMR spectroscopy, NMR spin-relaxation and pulsed field gradient NMR (PFG NMR) unique techniques for direct structural and dynamic studies.

Two types of polymeric systems applied to electrochemical energy sources are viewed: ion-exchange membranes (fuel cells application), gel and solid polymeric electrolytes for lithium battery.

The perfluorinated cation-exchange membranes are the membranes of number one for electrochemical applications

The potential of NMR methods in studying the formation of transport channels, the mechanisms of ion polymer matrix interaction, the mobility and diffusion of ions and molecules in polymer ion exchangers are analyzed and generalized.

The self-diffusion measurement especially the techniques using the pulsed field gradient NMR (PFG NMR) following by Fourier transforms is the unique methods for direct structural and dynamic studies in systems with the fast ionic and molecular transport.

This presentation is mainly devoted to investigations of ionic and water transport in ion exchange membranes. The results were obtained at the Labora-

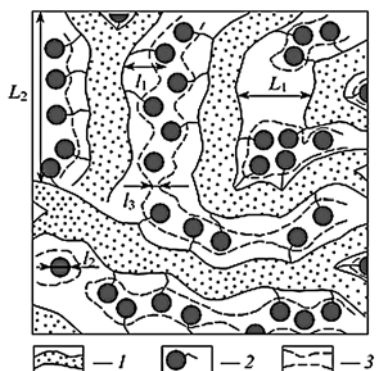


**Fig. 1.** Structure of the amorphous part of a perfluorinated sulfonate cation-exchange membrane. Polymer backbone; (2) hydrated counter-ions and functional groups at a low moisture content; (3) transport channels for ions and water molecules at a high moisture content;  $L_1 = 4$  nm according to low-angle X-ray scattering data;  $L_2 = 10$  nm according to Mössbauer spectroscopy;  $l_1 = l_2 = 1$  nm according to ENDOR and relaxation NMR data;  $l_3 = 1.5$  nm according to standard porosimetry and ENDOR methods.

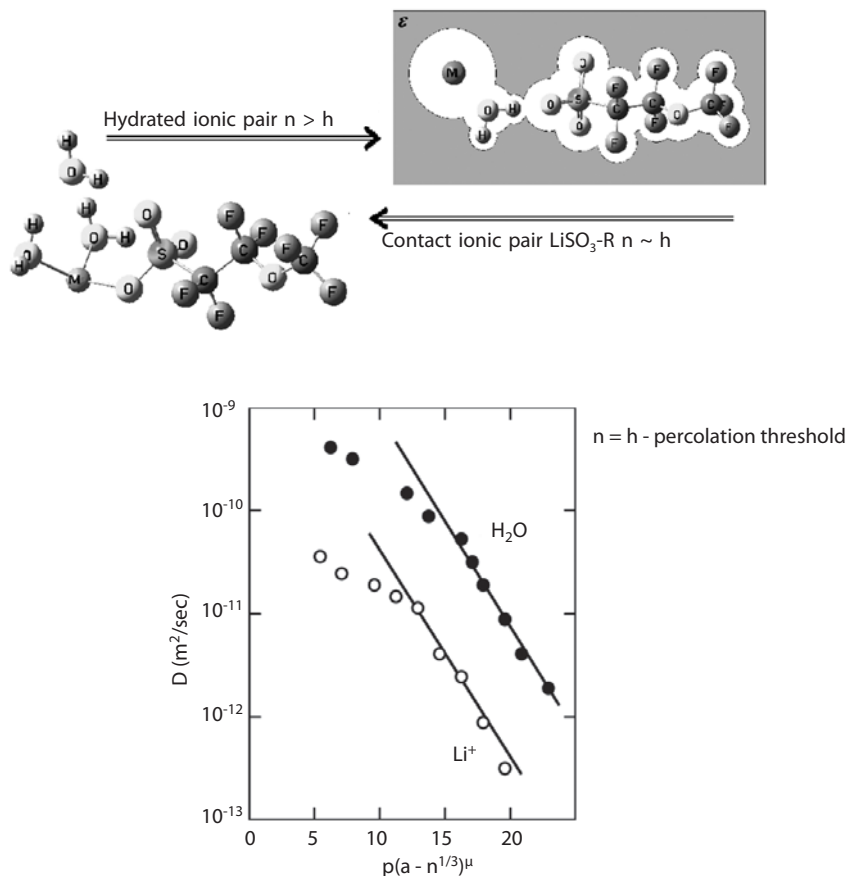


**Fig. 2.** Self-diffusion coefficients water molecules and Li<sup>+</sup> cation dependences on water content in perfluorinated sulfonation membranes on PFG NMR data. The lines are Eq. 1 approximation.

tory of Membrane Processes, Karpov Institute of Physical Chemistry, Moscow, Russia, Laboratory of NMR, Institute of Problems of Chemical Physics, Russian Academy of Sciences, Chernogolovka, Moscow Region.

Cation exchange membranes with polymer matrix of various chemical types are considered.

The translation mobility of ions measured by pulsed field gradient NMR is compared with the data on ionic conductivity acquired by impedance spectroscopy methods.

Attention is focused on the possibilities of NMR methods in studying the state of ions and molecules in polymeric electrolytes and also their diffusion mobility on different spatial scales.

Based on the NMR data, the mechanisms of ion transport in ion exchange perfluorinated membranes are proposed [1]. The detailed diffusion channels structure in different spatial scales shown in Fig. 1 was understood.



The dependence of water molecules and lithium cations self-diffusion coefficients on water content was analyzed (Fig. 2). The structure of hydrated cation complexes  $M(\text{H}_2\text{O})_h^+$  was determined from  $^1\text{H}$ ,  $^7\text{Li}$ ,  $^{23}\text{Na}$ ,  $^{133}\text{Cs}$  NMR spectra. Conditions for separated hydrated and contact ionic pairs forming were obtained.

The theoretical description of ionic and water transport was done on the basis of percolation theory from Eq. 1:

$$D = D_0 \exp(p(a - n^{1/3})^\mu), \quad (1)$$

где  $p$ ,  $a$ ,  $\mu$  – parameters characterize hydrated complexes structure,  $n$  – the number of water molecules per sulfonate group,  $h$  – hydration number.

The detailed mechanism of alkaline ions and water molecules transport was understood on the basis of these NMR experimental results.

I. Volkov V.I., Marinin A.A.: Russian Chemical Reviews **82**, no. 3, 248–272 (2013)

---

---

## SECTION 2

STRONGLY CORRELATED ELECTRON SYSTEMS.  
MAGNETIC RESONANCE INSTRUMENTATION

## Complex Electronic Order in Fe-Based Superconductors Studied by Nuclear Probe Spectroscopy

**H.-H. Klauss**

TU Dresden, Institute of Solid State Physics, Dresden, Germany

The interplay of itinerant magnetism, electronic nematic order and unconventional superconductivity in Fe based superconductors and other intermetallic systems with complex Fermi surfaces is a fascinating topic in contemporary correlated electron physics.

In my talk I will discuss Mössbauer spectroscopy and muon spin relaxation experiments on several series of hole doped 122 pnictides like  $\text{Ba}_{1-x}\text{K}_x\text{Fe}_2\text{As}_2$  [1, 2] and  $\text{Ca}_{1-x}\text{Na}_x\text{Fe}_2\text{As}_2$ . The parent compound  $\text{CaFe}_2\text{As}_2$  shows a spin density wave order below  $T_N = 165$  K [2]. Our microscopic study proves that with increasing Na-substitution level, the magnetic order parameter as well as the magneto-structural phase transition is suppressed. For  $x = 0.50$  we find a microscopic coexistence of magnetic and superconducting phases accompanied by a reduction of the magnetic order parameter below the superconducting transition temperature  $T_C$ . A systematic comparison with other 122 pnictides reveals a linear correlation between the magnetic order parameter reduction and the ratio of the transition temperatures,  $T_C/T_N$ , which can be understood in the framework of a Landau-theory. In the optimally doped specimen with  $T_C \approx 34$  K, the temperature dependence of the penetration depth and superfluid density were obtained, which proves the presence of two superconducting s-wave gaps.

I will also discuss multigap superconductivity with broken time reversal symmetry in locally non-centrosymmetric SrPtAs.  $\mu\text{SR}$  experiments prove the development of a small static spontaneous internal field just below  $T_C$ , evidencing the time reversal symmetry (TRS) breaking SrPtAs [4].  $^{75}\text{As}$ -NMR and -NQR investigations clearly reveal a two step behaviour in the spin-lattice relaxation rate evidencing multigap superconductivity with very weak inter-band coupling and constraints for the possible pairing symmetries. Unconventional chiral d-wave or f-wave order parameters are consistent with our data [5].

1. Wiesenmayer E. *et al.*: Phys. Rev. Lett. **107**, 237001 (2011)
2. Goltz T. *et al.*: Phys. Rev. B **89**, 144511 (2014)
3. Materne Ph. *et al.*: Phys. Rev. B **92**, 134511 (2015)
4. Biswas P.K. *et al.*: Phys. Rev. B **87**, 180503 (2013)
5. Brückner F. *et al.*: Phys. Rev. B **90**, 220503 (2014)

## Magnetic Resonance Anisotropy in CeB<sub>6</sub>

**S. V. Demishev<sup>1,2,3</sup>, A. V. Semeno<sup>1,2</sup>, M. I. Gilmanov<sup>2</sup>, A. V. Bogach<sup>1</sup>,  
V. V. Glushkov<sup>1,2,3</sup>, V. N. Krasnorussky<sup>1</sup>, A. N. Samarin<sup>2</sup>, N. A. Samarin<sup>1</sup>,  
N. E. Sluchanko<sup>1,2</sup>, N. Yu. Shitsevalova<sup>4</sup>, and V. B. Filipov<sup>4</sup>**

<sup>1</sup> Prokhorov General Physics Institute of RAS, Moscow 119991, Russian Federation,  
demis@lt.gpi.ru

<sup>2</sup> Moscow Institute of Physics and Technology, Dolgoprudny 141700, Moscow region,  
Russian Federation

<sup>3</sup> National Research University Higher School of Economics, Moscow 101000, Russian Federation

<sup>4</sup> Institute for Problems of Materials Science of NASU, Kiev 03680, Ukraine

Electron spin resonance (ESR) in strongly correlated metals is an exciting phenomenon, as strong spin fluctuations in this class of materials broaden extremely the absorption line below the detection limit. In this respect the ESR observation in CeB<sub>6</sub> provides a unique chance to inspect Ce<sup>3+</sup> magnetic state in the antiferroquadrupole (AFQ) phase. Although the magnetic resonance in CeB<sub>6</sub> was discovered more than decade ago, the anisotropy of the ESR characteristics has not been investigated so far. In the present work, we apply the original high frequency (60 GHz) experimental technique to extract the temperature and angular dependences of  $g$ -factor, line width and oscillating magnetization. Experimental data show unambiguously that the modern ESR theory in the AFQ phase considering the  $\Gamma_8$  ground state of Ce<sup>3+</sup> ion fails to predict both  $g$ -factor magnitude and its angular dependence. A strong (more than twofold) broadening of ESR line width is induced by external magnetic field aligned along [100] axis that results also in the anomalous temperature dependences of the  $g$ -factor and oscillating magnetization. Surprisingly the latter parameter exceeds total static magnetization by 20% at  $T^* \sim 2.5$  K. We argue that the unusual physical picture of ESR in CeB<sub>6</sub> arises due to the mixing of the  $\Gamma_7$  doublet and  $\Gamma_8$  quartet in the ground state of CeB<sub>6</sub>, which is strongly affected by spin fluctuations and dynamic spin-polaron effects predominantly pronounced in [100] direction.

This work was supported by programmes of Russian Academy of Sciences “Electron spin resonance, spin-dependent electronic effects and spin technologies”, “Electron correlations in strongly interacting systems” and by RFBR grant no. 14-02-00800.

## Anomalous ESR Behavior of Lanthanum Doped CeB<sub>6</sub>

**A. V. Semeno<sup>1</sup>, M. I. Gilmanov<sup>1,2</sup>, V. N. Krasnorusski<sup>1</sup>,  
N. Yu. Shitsevalova<sup>3</sup>, V. B. Filipov<sup>3</sup>,  
A. N. Samarin<sup>1,2</sup>, and S. V. Demishev<sup>1,2,4</sup>**

<sup>1</sup> Prokhorov General Physics Institute of RAS, Moscow 119991, Russian Federation, semeno@lt.gpi.ru

<sup>2</sup> Moscow Institute of Physics and Technology, Dolgoprudny 141700, Moscow region, Russian Federation

<sup>3</sup> Frantsevich Institute for Problems of Materials Science NASU, Kiev, Ukraine

<sup>4</sup> National Research University "Higher School of Economics", Moscow 101000, Russian Federation

Electron spin resonance (ESR) is the intriguing feature of heavy fermion compound CeB<sub>6</sub> found in its antiferroquadrupolar (AFQ) phase [1]. Here we study the influence of lanthanum doping on the resonance behavior by measuring high-frequency ( $f = 60$  GHz) ESR on the set of Ce<sub>1-x</sub>La<sub>x</sub>B<sub>6</sub> single crystals with  $x = 0.03, 0.1, 0.2, 0.3$  for  $H$  [110]. Special attention was given to samples surfaces preparation in order to reach the identity of skin layer and bulk material properties. Comparative analysis of the microwave magneto-absorption and the resistivity data allowed deriving the resonance spectra in units of magnetic permeability [2] and obtaining the resonance parameters:  $g$ -factor, linewidth  $\Delta H$  and oscillating magnetization  $M_0$ . The dependencies  $M_0(T)$  confirm the intimate relation of the ESR onset and growth with the development of AFQ state. We found that doping with La leads to strong ESR lines broadening (from  $\Delta H = 1.7$  kOe for  $x = 0$  to  $\Delta H = 4.5$  kOe for  $x = 0.1$  and  $\Delta H = 10.6$  kOe for  $x = 0.2$  at  $T = 1.8$  K) so that the resonance line becomes unobservable at  $x = 0.3$ . The value of  $g$ -factor remains constant  $g \approx 1.6$  at all temperatures for all  $x$  in spite large variation of  $\Delta H$ . The observed behavior is inconsistent with standard models of ESR of magnetic ions in metals emphasizing the unusual character of this phenomenon in AFQ phase of Ce<sub>1-x</sub>La<sub>x</sub>B<sub>6</sub>.

This work was supported by Programs of RAS "Electron spin resonance, spin-dependent electronic effects and spin technologies", "Electron correlations in strongly interacting systems" and by the grant RFBR no. 14-02-00800.

1. Demishev S.V. *et al.*: Phys. Status Solidi B **242**, R27 (2004)
2. Demishev S.V. *et al.*: Phys. Rev. B **80**, 245106 (2009)
3. Barnes S.E.: Advances in Physics **30**, 801 (1981)

## NMR Investigation of Ir-Based Double Perovskites

**M. Iakovleva<sup>1,2</sup>, E. Vavilova<sup>2</sup>, H.-J. Grafe<sup>1</sup>, V. Kataev<sup>1</sup>, M. Kaustuv<sup>1</sup>,  
M. Vogl<sup>1</sup>, T. Dey<sup>3</sup>, S. Wurmehl<sup>1</sup>, and B. Büchner<sup>1</sup>**

<sup>1</sup> Institute for Solid State Research, IFW Dresden, Dresden 01069, Germany

<sup>2</sup> Zavoisky Physical-Technical Institute, Russian Academy of Sciences, Kazan 420029,  
Russian Federation

<sup>3</sup> Institute of Physics, Universität Augsburg, Augsburg 86159, Germany

Iridium based double perovskites are unique materials where strong spin-orbit coupling, Coulomb repulsion, exchange interaction and crystal field have comparable energy scales. The interplay between all of these interactions and correlations may lead to the emergence of novel electronic and magnetic states. In the present work we report the  $^{139}\text{La}$  nuclear magnetic resonance (NMR) results on the double perovskite compounds  $\text{La}_2\text{M}\text{IrO}_6$  with magnetic and nonmagnetic ions at M position (M = Co, Cu, Zn). The magnetic Co ( $S = 3/2$ ) and Cu ( $S = 1/2$ ) spins are strongly coupled to Ir ( $J_{\text{eff}} = 1/2$ ) sublattice and exhibit non-collinear antiferromagnetic phase transitions at 90 K and 74 K, correspondingly [1, 2]. In contrast to this materials the  $\text{La}_2\text{ZnIrO}_6$  indicates a paramagnetic to ferromagnetic transition at  $T \sim 10$  K [3].

Nuclear relaxation rate  $T_1^{-1}$  measurements in  $\text{La}_2\text{CuIrO}_6$  shows the peak at  $T \sim 74$  K that is the signature of a magnetic transition. Moreover with further decreasing the temperature the  $T$ -dependence of  $T_1^{-1}$  shows the shoulder at  $T \sim 60$  K that can be associated with a cooperative ordering of the transverse moments. In case of  $\text{La}_2\text{CoIrO}_6$  the  $T_1^{-1}$  measurements do not show any anomalies at  $T$  below the ordering temperature.

Our investigation has revealed complex magnetic interactions in the compound where strongly spin-orbit coupled 5d transition metal ions coexist with strongly correlated spin-only 3d (Co, Cu) and non-magnetic Zn ions.

1. Kolchinskaya A. *et al.*: Phys. Rev. B **85**, 224422 (2012)
2. Kaustuv Manna. *et al.*: arXiv:1608.07513 [cond-mat.str-el] (2016)
3. Zhu W.K. *et al.*: Phys. Rev. B **91**, 144408 (2015)

---



---

## SECTION 3

# THEORY OF MAGNETIC RESONANCE

## Impurity Spin in Normal Stochastic Field: Basic Model of Magnetic Resonance

**F. S. Dzheparov and D. V. Lvov**

Institute for Theoretical and Experimental Physics, Moscow 117258, Russian Federation,  
dzheparov@itep.ru, lvov@itep.ru

Spin system with the Hamiltonian (written in rotating frame)

$$H = H_0(t) + H_1, \quad H_1 = \omega_1 I_x, \quad H_0(t) = (\Delta + \omega_l(t)) I_z = H_l + H_l(t)$$

is one of most important basic models for studies in spin dynamics. Here  $I_\alpha$  is spin operator,  $\Delta$  is the detuning from the resonance,  $\omega_1$  represents magnitude of the rotating field, and  $\omega_l(t)$  corresponds to time dependent local field, produced by surrounding substance. Famous Anderson-Weis-Kubo model [1] considers  $\omega_l(t)$  as a normal stochastic process with the correlation function  $\langle \omega_l(t) \omega_l(t_1) \rangle_n = M_2 \kappa(|t - t_1|)$ ,  $M_2 = \langle \omega_l^2 \rangle_n$ .

The model was created to explain the “narrowing of the resonance line by motion”, but it was successful for explaining of the line shape of impurity beta-active nuclei and it was adopted to describe two- and multi-spin transitions [2] and spin dynamics in magnetically diluted systems [3]. An important application of the model consists in derivation of the applicability conditions for perturbation theory in calculation of longitudinal correlation function  $F(t) = \langle I_z I_z(t) \rangle / \langle I_z^2 \rangle$  for small  $\omega_1$ . The advantage of the model is the realistic smooth time dependence of local field contrary to known exactly solvable models with hopping evolution of  $\omega_l(t)$ . If  $\Delta = 0$ , then the simplest conditions  $\varepsilon_1 = RT_2 \ll 1$  and  $\varepsilon_2 = R\tau_c \ll 1$ , where  $R = \omega_1^2 T_2$ ,  $T_2 = \int_0^\infty dt \exp(-M_2 \int_0^t d\tau (t - \tau) \kappa(\tau))$ ,  $\tau_c = \int_0^\infty dt \kappa(t)$ , produce  $F(t) = \exp(-Rt)$ , but nothing was known for slow motion, when  $R\tau_c \gg 1$ .

Here we present the solution valid in the main order in  $\varepsilon_1 = \omega_1^2 T_2^2 \ll 1$  and  $\varepsilon_s = (\omega_1 \tau')^{-2} \ll 1$ , where  $\tau' = |\partial^2 \kappa(t=0) / \partial t^2|^{-1} \sim \tau_c$ . It has the form  $F(t) = (2/\pi) \text{arcsink}(t)$ .

1. Abragam A.: Principles of Nuclear Magnetism. Oxford University Press, Oxford, 1961.
2. Abov Yu.G., Gul'ko A.D., Dzheparov F.S. *et al.*: Phys. Part. Nucl. **26**, 692 (1995)
3. Dzheparov F.S., Lvov D.V., Veretennikov M.A.: JETP Lett. **98**, 484 (2013)

## Relaxation and Coherence Transfer in Radicals in Liquids

**A. G. Maryasov<sup>1</sup> and M. K. Bowman<sup>2</sup>**

<sup>1</sup> Institute of Chemical Kinetics & Combustion, Novosibirsk 630090, Russian Federation,  
maryasov@kinetics.nsc.ru

<sup>2</sup> The University of Alabama, Tuscaloosa AL 35405-0336, USA,  
mkbowman@ua.edu

Fast rotational movement of paramagnetic molecule in liquids averages anisotropy of the system spin Hamiltonian and induces paramagnetic relaxation in the system [1]. The secular approximation is used to describe relaxation processes, it uses the interaction presentation (sometimes this is reduced to use of the rotating frame) for the system density matrix and omits oscillating terms in the presentation chosen. When considering relaxation in the lab frame, there are no oscillating terms and the terms traditionally omitted provide coherence transfer between transitions having different frequencies and also couple populations and coherences [2–3]. Accounting for coherence transfer caused by molecular collisions was successfully applied to the analysis of dipole and exchange interactions manifested in EPR spectra of radicals in non-viscous liquids [2, 4].

Here spectroscopic manifestations of coherence transfer process induced by rotation of radicals in liquids in high magnetic field are analysed for model system with  $S = I = 1/2$ . Relaxation couples all single quantum transitions: two allowed and two forbidden; thus causing the appearance of an additional low-intensity doublet with a splitting approximately equal to twice the nuclear Zeeman frequency. Manifestations of the process in pulse EPR and in dynamic nuclear polarization are analysed.

This work was supported by: the National Science Foundation (grant no. 1416238) and the Russian Foundation for Basic Research (grant no. 14-03-93180).

1. Ernst R.R., Bodenhausen G., Wokaun A.: Principles of Nuclear Magnetic Resonance in One and Two Dimensions. Oxford: Clarendon Press 1987.
2. Salikhov K.M., Semenov A.G., Tsvetkov Yu.D.: Electron Spin Echo and Its Applications, Chapter 4. Novosibirsk: Nauka 1976.
3. Salikhov K.M.: Editor's note at p. 77 of the Russian edition of Ref. [1], 1990.
4. Salikhov K.M.: Appl. Magn. Reson. **38**, 237 (2010)

---

---

## SECTION 4

### MODERN METHODS OF MAGNETIC RESONANCE. RELATED PHENOMENA

## Recent Advances in NMR Diffusometry

F. Zong<sup>1</sup>, N. Spindler<sup>2,3</sup>, L. R. Ancelet<sup>4,5</sup>, I. F. Hermans<sup>4,5,6</sup>,  
and P. Galvosas<sup>1</sup>

<sup>1</sup> MacDiarmid Institute for Advanced Materials and Nanotechnology, School of Chemical and Physical Sciences, Victoria University of Wellington, Wellington, New Zealand

<sup>2</sup> Tecan Schweiz AG, Männedorf 8708, Switzerland

<sup>3</sup> Forschungszentrum Jülich, Institute of Bio- and Geosciences-Agrosphere, Jülich 52425, Germany

<sup>4</sup> Malaghan Institute of Medical Research, Wellington, New Zealand

<sup>5</sup> Maurice Wilkins Centre, Auckland, New Zealand

<sup>6</sup> School of Biological Sciences, Victoria University of Wellington, Wellington, New Zealand

Multidimensional Inverse Laplace Transform (ILT) NMR methods have established themselves over the last two decades in material science, engineering, medical research and industry [1]. Here we report on **two variants** of the two-dimensional (2D) Diffusion-Diffusion Correlation Spectroscopy (DDCOSY) [2, 3]. This method is a so called double Pulsed Gradient Spin Echo (dPGSE) experiment which performs two NMR diffusion experiments in close succession but different spatial directions. This allows for the correlation of molecular displacements associated with the two directions, thus sampling local mobility and confinement. Identical displacements in the two subsequent measurements indicate isotropic diffusion. In contrast, different displacements in the two directions are a signature for local diffusion anisotropy which may manifest itself as off-diagonal features in 2D correlation maps.

The **first variant** aims to measure Fractional Anisotropy (FA) averaged over the whole sample. FA is commonly derived from the diffusion tensor (DT) measured via Diffusion Tensor Imaging (DTI) [4]. The core idea of DTI is to sample diffusion in at least six independent spatial directions which is sufficient to reconstruct the DT. Transferring the approach of sampling six spatially independent directions to DDCOSY results in the acquisition of at least three independent DDCOSY experiments, thus sampling diffusion along a particular choice of gradient directions and obtaining corresponding 2D correlation maps [5]. Sample averaged FA can be extracted subsequently from the DDCOSY results [5]. We will demonstrate that this method is robust and returns averaged FA values for a number of biological samples which are consistent with DTI measurements. We will further discuss the potential of sample averaged FA values for the discrimination of healthy and cancerous biological tissue [5].

The **second variant** concerns a shortened version of the DDCOSY (sDDCOSY) experiment for which gradients in the two different directions are applied at the same time but incremented independently [6]. This pulse sequence structure is a single PGSE (more akin to DTI) and fundamentally different from the dPGSE scheme used for DDCOSY. The particular focus is on the additional attenuation of the echo signal. This attenuation occurs for sDDCOSY due to cross terms between the two gradients applied in different directions. In the case of conventional DDCOSY the echo signal is affected by the displacement

correlation tensor [7] which is typical for dPGSE experiments in general. We will demonstrate that sDDCOSY is able to return results consistent with simulations and DDCOSY experiments if contributions arising from the cross terms are compensated. This shortened DDCOSY version may prove indispensable for samples with short  $T_2$  relaxation times. Furthermore, true correlation is sampled with sDDCOSY since displacements in different directions are traced simultaneously. sDDCOSY may also provide further insight into diffusion mechanisms in anisotropic porous materials because it should allow to extract and study the off-diagonal elements in the 2D correlation maps alone.

1. Galvosas P., Callaghan P.T.: *C. R. Physique* **11** 172–180 (2010)
2. Callaghan P.T., Godefroy S., Ryland B.N.: *Magn. Reson. Imaging* **21**, 243–248 (2003)
3. Callaghan P.T., Furo I.: *J. Chem. Phys.* **120**, 4032–4038 (2004)
4. Basser P.J., Mattiello J., LeBihan D.: *Biophys. J.* **66**, 259–67 (1994)
5. Zong F., Ancelet L.R., Hermans I.F., Galvosas P.: *Magn. Reson. Chem.*, DOI: 10.1002/mrc.4492 (2016)
6. Spindler N.: *Diffusion and Flow Investigations in Natural Porous Media by Nuclear Magnetic Resonance*, RWTH Aachen University, 2011.
7. Jespersen S.N., Buhl N.: *J. Magn. Reson.* **208**, 34–43 (2011)

## **Novel Applications of MRI: Structural and Functional Connectivity in Brain. Can MRI Contribute to the Understanding of Mental Disorders?**

**U. Eichhoff**

Bruker BioSpin GmbH (retired), Barbara.use@t-online.de

MRI is the most universal imaging modality and applied in clinical practice in almost any anatomical locations. Furthermore *in vivo* spectroscopy allows the investigation of metabolic defects and molecular and cellular MRI, especially in transgenic animals contribute to the understanding of diseases on the molecular and cellular level.

But there are still diseases, where all imaging methods fail to deliver reproducible meaning full information, These are the mental diseases. I will try to give an overview of the possibilities of MRI in this field.

The nowadays most accepted hypothesis of the origin of such diseases is an impaired connectivity between various brain areas. Modern MRI methods allow the investigation of these connectivities. Diffusion Tensor Imaging (DTI) and MR-tractography reveals structural connectivities through neuronal fibers between brain areas. Functional Imaging in the Resting State (rs-fMRI) allows to visualize functional connectivities. In this method the time course of rapidly repeated MRI scans is evaluated through the Blood Oxygen Level Dependent (BOLD) contrast. Even in complete rest the brain is active and oxygen is extracted from blood and fresh blood is supplied. The detection of the small signal changes needs highest sensitivity and the MRI scans must be repeated as fast as possible. Statistical evaluation and cross-correlation of the signals in all voxels show synchrony of signal level fluctuations even in remote brain areas. This allows to establish networks in the brain. The most important are the Default Mode Network (DMN), the Salience Network (SN) and the Centre Executive Network (CEN). Applications to Schizophrenia and Depression will be discussed. In Deep Brain Stimulation (DBS) the excitation, currently used for therapy of Parkinsons disease, is now introduced for therapy of Major Depressive Disorder (MDD) and can be taylorred to the necessary brain location.



---

## Graphical Methods for Spectral Simulation

K. A. Earle

University at Albany, State University of New York, Physics Department, NY 12222, USA

I present recent work on graphical methods for evaluating the matrix elements that arise in the simulation of spectra using the Stochastic Liouville Equation. These graphical methods are generic and are relevant to many calculations besides those specific to magnetic resonance. For the magnetic resonance lineshape problem, these methods allow spin and spatial degrees of freedom to be treated on an equal footing. Using these methods, I show how the matrix elements of the Stochastic Liouville operator factorize into a form consistent with the Wigner-Eckart theorem, where a factor proportional to a Wigner  $3j$  symbol encoding the details of the system preparation and observation, and a factor which encodes the structure of the relevant spin(s) or spatial degrees of freedom may be separated out. This factorization also facilitates the computation of spectral derivatives with respect to model parameters. Such derivatives are important for assessing parameter sensitivity for error analysis, for example. These spectral derivatives are also important for quantifying the geometry of parameter space for a particular spin Hamiltonian. I will present examples of how this formalism may be applied to ESR, NMR, and NQR lineshape calculations. The modular nature of these graphical techniques suggests that they may be incorporated into a graphical interface for arbitrary spin systems with automatic code generation capabilities. Some proof of principle examples using the Vision platform will be shown.

## Capability of Modern X-EPR Spectroscopy in Determining Characteristics of Rotational Mobility of Nitroxide Radicals

**N. A. Chumakova, A. Kh. Vorobiev, D. A. Pomogailo,  
N. A. Paramonov, and S. V. Kuzin**

Chemistry Department, Moscow State University, Moscow, Russian Federation,  
harmonic2011@yandex.ru

It is well known that shape of EPR spectra of nitroxide radicals is very sensitive to rotational mobility of paramagnetic molecules. To date a number of methods are worked out for numerical analysis of EPR spectra to determine parameters of rotation. Usually such analysis is carried out in the model of Brownian rotational diffusion assuming that all paramagnetic molecules have similar rotational characteristics. Present report is devoted to analysis of EPR spectra of nitroxide radicals in liquid crystals, polymeric matrices and at the surface of graphite oxide. It is shown that chemically identical paramagnetic molecules in structured media can have different localization and therefore possess different movability. Moreover, rotational mobility of radicals in such systems is complicated and cannot be described in the model of anisotropic Brownian diffusion. It is demonstrated that computer modeling of X-EPR spectra permits to establish parameters of rotational mobility of radicals with different localization. It is shown that analysis of spectrum of stochastically ordered (isotropic) sample is insufficient for adequate characterization of radicals' rotation in liquid crystal matrices. For determination of rotational parameters in such case it is necessary to perform joint simulation of series of spectra recorded at different positions of macroscopically ordered sample in magnetic field of spectrometer.

As illustration the result of simulation of EPR spectrum of stable nitroxide radical in liquid crystal H-115 (p-hexyloxyphenyl ester of p-decyloxybenzoic acid) is presented in Fig. 1.

Work supported by Russian Fund of Basic Research (grant no. 14-03-00323).

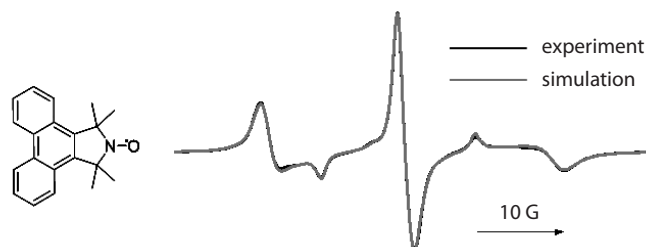


Fig. 1.

## The Quantum Dynamical Basis of a Classical Kinetic Scheme Describing Coherent and Incoherent Regimes of Radical Pair Recombination

N. N. Lukzen<sup>1</sup>, J. H. Klein<sup>2</sup>, C. Lambert<sup>2</sup>, and U. E. Steiner<sup>3</sup>

<sup>1</sup> International Tomography Center, Novosibirsk 630090, Russian Federation, luk@tomo.nsc.ru

<sup>2</sup> Institut für Organische Chemie, Wilhelm Conrad Röntgen Research Center for Complex Material Systems, Center for Nanosystems Chemistry, Universität Würzburg, Würzburg 97074, Germany

<sup>3</sup> Fachbereich Chemie, Universität Konstanz, Konstanz 78457, Germany

In recent work J. H. Klein et al. (J. Am. Chem. Soc. **137**, 11011 (2015)), the magnetic field dependent charge recombination kinetics in donor/Ir-complex/acceptor triads has been determined with outstanding accuracy and reproducibility. The field-dependent kinetics has been analyzed in terms of a classical reaction scheme including the field-independent rate parameters of singlet recombination (rate constant  $k_s$ ) and S/T<sub>0</sub> mixing (rate constant  $k_{ST_0}$ ) and the field-dependent rate constant  $k_{\pm}(B)$  connecting central and outer Zeeman levels. In the present work, the extraction of  $k_{\pm}$  from the experimental data is more precisely defined and the appearance of a “coherent” and “incoherent” regime of spin motion in a double log plot of  $k_{\pm}$  vs.  $B$  is confirmed. The experimental decay curves have been reproduced by a full quantum dynamical model based on the stochastic Liouville equation, which was solved numerically, taking into account isotropic hyperfine coupling with five nuclear spins (1 N on donor radical, 4 H on acceptor radical) and anisotropic hyperfine coupling with the nitrogen nucleus at the donor radical. The results of the quantum calculations serve as a rigorous basis of interpreting the classical parameter  $k_{\pm}$ . Furthermore, it is demonstrated that the incoherent part of spin motion is essential for a full understanding of the charge recombination kinetics even in the “coherent” regime.

## Nonlinear Spin Dynamics in Highly Polarised Liquids

V. V. Kuzmin<sup>1,2</sup>, G. Tastevin<sup>2</sup>, and P.-J. Nacher<sup>2</sup>

<sup>1</sup> Kazan Federal University, Kazan 420008, Russian Federation, slava625@yandex.ru

<sup>2</sup> Laboratoire Kastler Brossel, ENS-CNRS-UPMC-Collège de France, Paris 75005, France, nacher@lkb.ens.fr

Hyperpolarisation (HP) methods and using the high-Q probes provide high sensitivity in liquid-state NMR, but also give rise to enhanced contributions of radiation damping (RD) and long-range magnetic interactions (the distant dipolar field: DDF). This leads to ill-controlled non-linear dynamics either due to DDF only (precession instability or spectral clustering, when large flip-angle or small flip probe pulse is applied, respectively) or due to both RD and DDF (bizarre signals and cross-peaks, spatio-temporal chaos, multiple maser emissions: MMEs) [1].

We have performed in-depth studies of precession instabilities, with and without RD at low field (3 mT) with condensed laser-polarised <sup>3</sup>He-<sup>4</sup>He dilute mixtures (0.3–5% of <sup>3</sup>He, with ~10% polarisation at 1 K), using an active feedback scheme to control RD.

In this report I will focus on investigations of DDF-induced (without RD) precession instabilities after 90° RF flipping pulses, associated to the development of unstable magnetization patterns. We have developed MRI-based techniques to probe the evolution of these magnetization patterns and we have been able to observe parametric amplification of the initially imprinted patterns, as well as spatial harmonic generation, in experiments and in numerical simulations alike.

This work directly probes the sample size and shape effects that have previously only been inferred from multiple spin echoes features in HP <sup>129</sup>Xe and <sup>3</sup>He [2] and are expected to be important whenever strong DDFs are encountered.

This work was supported in part by the ANR grant IMAGINE and by the FPGG (Pierre-Gilles de Gennes) foundation.

1. Desvaux H.: Prog. Nucl. Magn. Reson. Spectrosc. **70**, 50 (2013)
2. Morgan S.W., Baudin E., Huber G., Berthault P., Tastevin G., Goldman M., Nacher P.-J., Desvaux H.: Eur. Phys. J. D **67**, 29 (2013)

## Operando NMR Studies of Electrochemical Systems

W. Münchgesang<sup>1</sup>, V. Koroteev<sup>2</sup>, T. Zakharchenko<sup>3</sup>, D. Itkis<sup>4</sup>,  
D. C. Meyer<sup>1</sup>, and A. Vyalikh<sup>1</sup>

<sup>1</sup> Institut für Experimentelle Physik, Technische Universität Bergakademie Freiberg,  
Freiberg D-09599, Germany, Anastasia.Vyalikh@physik.tu-freiberg.de

<sup>2</sup> Nikolaev Institute of Inorganic Chemistry, Novosibirsk 630090,  
Russian Federation

<sup>3</sup> Department of Material Science, Moscow State University, Moscow 119991, Russian Federation

<sup>4</sup> Department of Chemistry, Moscow State University, Moscow 119991, Russian Federation

Current research efforts in the field of energy storage are directed towards improving cost and performance of lithium ion batteries as well as evaluating post Li ion concepts. Applying *ex-situ* analysis to the studies of battery materials leads to the loss of the important information and hinders the development of novel technologies, as the intermediates and electrochemical reaction products often cannot be “quenched” for post process analysis. [1, 2] Therefore deep understanding of the electrochemical processes on a molecular level often requires a large set of data to be recorded *in operando* with temporal and spectral resolution. Whereas a high-resolution advantage afforded by magic angle spinning (MAS) of the sample is currently limited to *ex-situ* analysis, we show here that the spectral information can also be available from static NMR, due to the fact that the chemical transformations during the battery cycling are associated with changes in the electronic environment around the nucleus, which result in strong shifts in the NMR spectra and therefore in diverse NMR chemical shifts parameters.

Our *in operando* NMR set-up comprises an NMR cell, which allows an appropriate electrochemical functioning and a measurement quality, an external battery cyler synchronized with the NMR experiment and an Automatic Tuning Matching Cyler [3] designed for automated “on-the-fly” recalibration of the NMR circuit and the frequency sweep experiments. Applying this set-up to the electrochemical cell composed of <sup>13</sup>C enriched pyrolytic graphite as anode we were able to follow formation of stable electrolyte interface (SEI) and surface microstructures in the operating cell. Using the Automatic Tuning Matching Cyler enabled the detection of a strongly shifted very broad <sup>51</sup>V signal in the electrochemical cell containing V<sub>2</sub>O<sub>5</sub>-graphene composite cathode, when the cell was discharged to 2V. A large negative Knight shift and significant broadening are assumed to result from delocalisation of spin density in a new structural phase of lithiated vanadium oxide.

1. Itkis D.M., Velasco-Velez J.J., Knop-Gericke A., Vyalikh A., Avdeev M.V., Yashina L.V.: *ChemElectro-Chem* **2**, 1427 (2015)
2. Pecher O., Vyalikh A., Grey C.P.: *AIP Conference Proceedings* **1765**, 20011 (2016)
3. Pecher O., Liu H., Grey C.P.: *Z. Anorg. Allg. Chem.* **640**, 2339 (2014)

## Effect of Dry Trehalose Glassy Matrix on the Forward Electron Transfer in Photosystem I from Cyanobacteria *Synechocystis* sp. PCC 6803

**A. Semenov<sup>1,2</sup>, I. Shelaev<sup>2</sup>, M. Gorka<sup>3</sup>, A. Savitsky<sup>4</sup>, V. Kurashov<sup>3</sup>,  
F. Gostev<sup>2</sup>, V. Nadtochenko<sup>2</sup>, K. Möbius<sup>4</sup>, and J. Golbeck<sup>3</sup>**

<sup>1</sup>A. N. Belozersky Institute of Physical-Chemical Biology, Moscow State University, Moscow, Russian Federation

<sup>2</sup>N. N. Semenov Institute of Chemical Physics, Russian Academy of Sciences, Moscow, Russian Federation

<sup>3</sup>Dept. Biochem. & Molec. Biol., Dept. Chemistry, The Pennsylvania State University, University Park, USA

<sup>4</sup>Max-Planck-Institut für Chemische Energiekonversion, Mülheim (Ruhr), Germany

The effect of dehydration on the kinetics of forward electron transfer has been studied in cyanobacterial Photosystem I (PS I) complexes in a trehalose glassy matrix by time-resolved optical and EPR spectroscopies. The kinetics of the flash-induced absorption changes in the subnanosecond time domain, which are due to primary and secondary charge separation steps, were monitored by pump-probe laser spectroscopy with 20-fs low-energy pump pulses. The back-reaction kinetics of the PS I primary donor P700 were measured by high-field time-resolved EPR spectroscopy. The forward kinetics from the phylloquinone primary acceptor  $A_1^-$  to the iron-sulfur cluster FX were measured by time-resolved optical spectroscopy at 480 nm. The kinetics of the primary electron transfer reactions to form the primary  $P_{700}^+A_0^-$  and the secondary  $P_{700}^+A_1^-$  ion radical pairs were not affected by dehydration in the trehalose matrix, while the yield of the  $P_{700}^+A_1^-$  was decreased by ~20%. Forward electron transfer from the phylloquinone molecules in the  $A_{1A}^-$  and  $A_{1B}^-$  sites of the A and B branches of the cofactors to the iron-sulfur cluster FX slowed from ~200 ns and ~20 ns in solution to ~13  $\mu$ s and ~80 ns, respectively. However, as shown by EPR spectroscopy, the ~14  $\mu$ s kinetic phase also contains a small contribution from the recombination between  $A_{1B}^-$  and  $P_{700}^+$ . These data reveal that the initial electron transfer reactions from the excited  $P_{700}^*$  to  $A_1$  remain unaffected whereas electron transfer beyond  $A_{1A}$  and  $A_{1B}$  is slowed or prevented by constrained protein dynamics due to the dry trehalose glassy matrix. The kinetics of forward electron transfer between  $A_1$  and  $F_X$  in dry trehalose glass generally mimicked the kinetics of PS I in water-glycerol at the temperature of the protein-glass transition (Agalarov and Brettel: BBA **1604**, 7–12 (2003)).

This work was supported by grants from the Russian Science Foundation and the Russian Foundation for Basic Research (14-14-00789 and 15-04-04252 to A.Y.S. and V.N.), the U.S. National Science Foundation (1021725 to J.G.) and the Max Planck Society (A.S. and K.M.).

## Bruker BioSpin Latest EPR Developments: Rapid Scan Unit and Fitting Software Anisotropic-SpinFit

R. Weber<sup>1</sup>, I. Gromov<sup>2</sup>, P. Carl<sup>2</sup>, and M. Mokeev<sup>3</sup>

<sup>1</sup> Bruker BioSpin Corp, Billerica MA 01821, USA

<sup>2</sup> Bruker BioSpin GmbH, Rheinstetten 76287, Germany

<sup>3</sup> Bruker Ltd., Moscow 119017, Russian Federation,  
maxim.mokeev@bruker.com

Bruker BioSpin has developed a functional model of the new X-band Rapid Scan unit. Unlike the classical Continuous Wave EPR technique the Rapid Scan (RS) mode utilizes direct detection and fast field scans with scan widths up to 150 G and scan rates up to 10 MG/s. The RS accessory comprises the following newly designed elements: RS coils for standard Bruker's 10" magnet; RS power supply; RS unit with scan generator (AWG), X-band I/Q-detector and dual channel digitizer; transparent RS resonator compatible with standard VT units (He and N<sub>2</sub>) and acquisition & reconstruction software. The following specifications have currently been achieved:

- Maximum scan frequency: 100 kHz
- Maximum scan rate:  $\geq 10$  MG/s
- Maximum scan width:  $\geq 150$  G at 20 kHz (segments joining is possible)
- Magnetic field homogeneity: 0.1–0.2% in sample volume  $L = 15$  mm,  $D = 4$  mm.

Along with the possibility to easily detect short-lived radicals and EPR lines with short relaxation times, in many cases RS spectra demonstrate several times signal-to-noise ratio improvement compared to CW spectra measured in the same amount of time. This effect is largely a consequence of the being able to measure at higher microwave power without saturation.

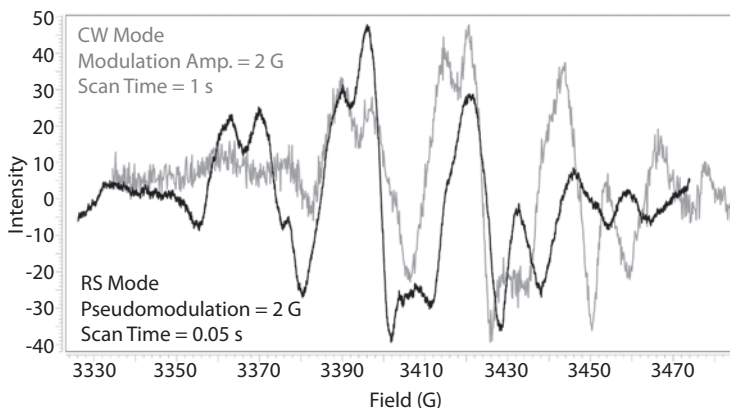


**Fig. 1.** EPR spectrum of Alanine measured in CW-mode and RS-mode (with pseudo-modulation post-processing applied). X-axis shift is due to the fast field scans in CW-mode.

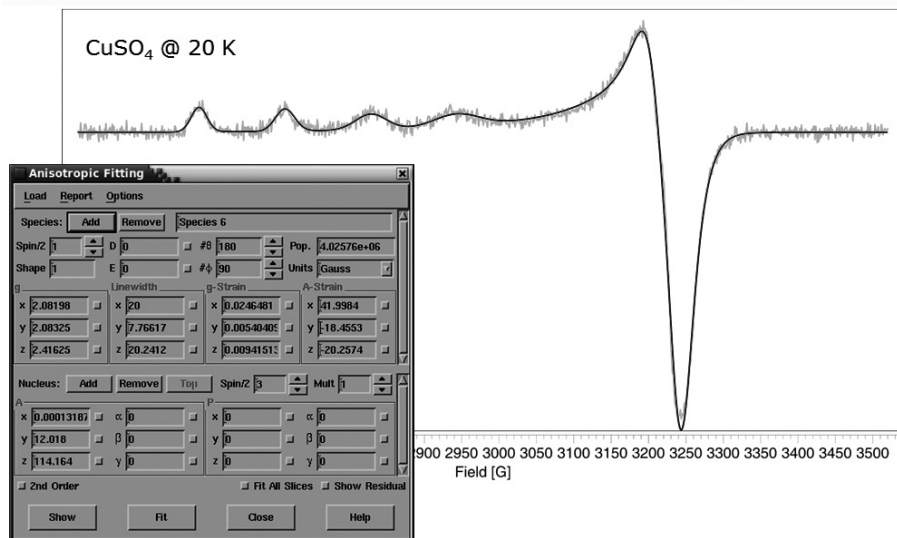


**Fig. 2.** Anisotropic-SpinFit user interface and example of correctly fitted EPR spectrum of copper sulfate powder with significant anisotropy and strain for both  $g$ -factor and hyperfine constant  $A$ .

Serial product release is scheduled at the end of 2017 and will be compatible with Bruker EPR spectrometers of the ELEXSYS E500/E580 series.

Bruker BioSpin also presents a new version of the SpinFit software which is the part of Bruker's research-class EPR software Xenon/Xepr. The new Anisotropic-SpinFit algorithm uses 2<sup>nd</sup> order perturbation theory and allows fitting and simulation of anisotropic EPR spectra of multiple EPR species with  $A$ - and  $g$ -strain. Fit parameters include  $g$ -factor, hyperfine splitting, quadrupole splitting, strain, zero field and population for each species. Every parameter can optionally be included or excluded from the fitting process. Simulation parameters also include line shape and powder average angles.

Anisotropic-SpinFit is applicable for all microwave frequency bands and supplied with simulation library which can be enlarged by user. Easy data transfer to SpinCount procedure allows improving accuracy of quantitative analysis for noisy EPR spectra.



---

## SECTION 5

### SPIN-BASED INFORMATION PROCESSING

## Magnetic Resonance at the Quantum Limit and Beyond

A. Bienfait<sup>1</sup>, J. J. Pla<sup>2,3</sup>, X. Zhou<sup>1,4</sup>, C. C. Lo<sup>2</sup>, C. D. Weis<sup>5</sup>, T. Schenkel<sup>5</sup>,  
D. Vion<sup>1</sup>, D. Esteve<sup>1</sup>, J. J. L. Morton<sup>2</sup>, K. Mølmer<sup>6</sup>, and P. Bertet<sup>1</sup>

<sup>1</sup> Quantronics Group, SPEC, CEA, CNRS, Université Paris-Saclay, CEA-Saclay,  
Gif-sur-Yvette 91191, France

<sup>2</sup> London Centre for Nanotechnology, University College London, London WC1H 0AH, UK

<sup>3</sup> School of Electrical Engineering & Telecommunications, University of New South Wales, Sydney,  
New South Wales 2052, Australia

<sup>4</sup> Institute of Electronics Microelectronics and Nanotechnology, CNRS UMR 8520, ISEN Department,  
Villeneuve d'Ascq Cedex 59652, France

<sup>5</sup> Accelerator Technology and Applied Physics Division, Lawrence Berkeley National Laboratory,  
Berkeley, California 94720, USA

<sup>6</sup> Department of Physics and Astronomy, Aarhus University, Aarhus C DK-8000, Denmark

The detection and characterization of paramagnetic species by electron-spin resonance (ESR) spectroscopy has numerous applications in chemistry, biology, and materials science [1]. Most ESR spectrometers rely on the inductive detection of the small microwave signals emitted by the spins during their Larmor precession into a microwave resonator in which they are embedded. Using the tools offered by circuit Quantum Electrodynamics (QED), namely high quality factor superconducting micro-resonators and Josephson parametric amplifiers that operate at the quantum limit when cooled at 20 mK [2], we report an increase of the sensitivity of inductively detected ESR by 4 orders of magnitude over the state-of-the-art, enabling the detection of 1700 Bismuth donor spins in silicon with a signal-to-noise ratio of 1 in a single echo [3]. We also demonstrate that the energy relaxation time of the spins is limited by spontaneous emission of microwave photons into the measurement line via the resonator [4], which opens the way to on-demand spin initialization via the Purcell effect. Finally, we show that the sensitivity can be enhanced beyond the quantum limit by using quantum squeezed states of the microwave field [5].

1. Schweiger A., Jeschke G.: Principles of Pulse Electron Magnetic Resonance. Oxford University Press, 2001.
2. Zhou X. *et al.*: Physical Review B **89**, 214517 (2014)
3. Bienfait A. *et al.*: Nature Nanotechnology **11**(3), 253–257 (2015)
4. Bienfait A. *et al.*: Nature **531**, 74 (2016)
5. Bienfait A. *et al.*: in preparation

## Spin Qubits Based on Donors in Silicon

**J. J. L. Morton, S. Nur, P. Ross, and H. Lim**

London Centre for Nanotechnology, UCL, London WC1H 0AH, UK

The electron and nuclear spins of (Group V) donors in silicon have been proposed as potential quantum bits, or qubits, and the past few years have seen several breakthroughs towards this goal, including: the measurement of donor electron spin coherence times exceeding seconds, donor nuclear spin coherence times ranging from minutes to hours, and the measurement of the spins of single donor atoms, with high fidelity, in nanoelectronic devices. In this talk I will discuss recent progress in three areas of relevance to donor spin qubits:

i) The effect of strain [1] and electric fields [2] on the electron and nuclear spins of donors – this is essential if they are to be used in nanoelectronic devices where electric fields sufficient to ionize dopants and where strain arises from the fabrication process and different thermal expansion coefficients of the materials involved;

ii) The coherence times of  $^{29}\text{Si}$  nuclear spins in the vicinity of donors [3] – this supports an understanding of the nature of the  $^{29}\text{Si}$  nuclear spins as a decohering bath [4], and allows an assessment of their suitability as ancilla qubits for donor spins; and, finally,

iii) The use of the donor bound exciton transition to enable the initialization and measurement of small ensembles of donor spins [5] – this can either be performed purely optically (for example, it is possible to detect photons from  $\sim 1000$  phosphorus donors in 1 minute, and using photonic crystal cavities with  $Q \sim 10,000$  we anticipate being able to approach the single donor limit), or electrically, by detecting the change in conductivity arising from the Auger recombination (so far, this has enabled measurements down to  $\sim 10^5$  donors in devices  $\sim 10$  microns in size, and we expect the method to extend to smaller numbers).

1. Pla J.J., Bienfait A., Pica G., Mohiyaddin F.A., Morello A., Schenkel T., Lovett B.W., Morton J.J.L., Bertet P.: arXiv:1608.07346 (2016)
2. Wolfowicz G., Urdampilleta M., Thewalt M.L.W., Riemann H., Abrosimov N.V., Becker P., Pohl H.-J., Morton J.J.L.: Phys. Rev. Lett. **113**, 157601 (2014)
3. Wolfowicz G., Mortemousque P.A., Guichard R., Simmons S., Thewalt M.L.W., Itoh K.M., Morton J.J.L.: New J. Phys. **18**, 023021 (2016)
4. Ma W.L., Wolfowicz G., Li S.S., Morton J.J.L., Liu R.-B.: Phys. Rev. B **92**, 161403 (2015)
5. Lo C.C., Urdampilleta M., Ross P., Gonzalez-Zalba M.F., Mansir J., Lyon S.A., Thewalt M.L.W., Morton J.J.L.: Nature Materials **14**, 490 (2015)

## Hybrid Quantum Systems – Coupling Color Centers to Superconducting Cavities

**J. Majer**

Atominsttitut, TU Vienna, Vienna, Austria

Hybrid quantum systems based on spin-ensembles coupled to superconducting microwave cavities are promising candidates for robust experiments in cavity quantum electrodynamics (QED) and for future technologies employing quantum mechanical effects. In particular the electron spins hosted by nitrogen-vacancy centers in diamond. The main source of decoherence in this systems is inhomogeneous dipolar spin broadening and a full understanding of the complex dynamics is essential and has not been addressed in recent studies yet. We investigate the influence of a non-Lorentzian spectral spin distribution in the strong coupling regime of cavity QED. We show experimentally how the so-called cavity protection effect influences the decay rate of coherent Rabi oscillation by varying the coupling strength in our experiment. We then demonstrate how the Rabi oscillation amplitude can be enhanced by two orders of magnitude by pulsing the strongly coupled system matching a special resonance condition. Furthermore, we show that by burning narrow spectral holes into a spin ensemble we create long-lived collective dark states. We observe long-lived Rabi oscillations with high visibility and a decay rate that is a factor of forty smaller than the spin ensemble linewidth and thereby more than a factor of three below the pure cavity dissipation rate.

---

## High-Q and Novel Cavity Structures for Photon-Spin Strong Coupling

**M. Tobar**

ARC Centre of Excellence for Engineered Quantum Systems, University of Western Australia,  
Crawley WA 6009, Australia

Strong coupling between microwave photons and spins at millikelvin temperatures is necessary to realise quantum information processing. We will present our most recent results in coupling strongly to a variety of cavity and spin systems. Novel cavity systems include whispering gallery modes, 3D lumped element meta-structures based on the reentrant cavity and dielectric TE modes. Spin systems include paramagnetic iron group and rare-earth impurities doped in low-loss crystalline materials (such as YSO, YAP and Silicon), P1 centers in diamond and magnons in ferrimagnetic YIG.

In particular we will focus on new cavities, which couple photons and magnons in YIG spheres in a super- and ultra-strong way at around 20 mK in temperature. Few/Single photon couplings (or normal mode splitting, 2g) of more than 7 GHz at microwave frequencies are obtained for a 15.5 GHz mode. Types of cavities include multiple post reentrant cavities, which co-couple photons at different frequencies with a coupling greater than the free spectral range, as well as spherical loaded dielectric cavity resonators. In such cavities we show that the bare dielectric properties can be obtained by polarizing all ferromagnetic effects and magnon spin wave modes to high energy using a 7 Tesla magnet. We also show that at zero-field, collective effects of the spins significantly perturb the photon modes. Other effects like time-reversal symmetry breaking are observed.

## Electron Spin Decoherence of J-Coupled Donor Dimers in Two-Dimensional $\delta$ -Layers, 50 nm below Surface in Silicon

**A. M. Tyryshkin<sup>1</sup>, E. S. Petersen<sup>1</sup>, A. J. Sigillito<sup>1</sup>, J. Jhaveri<sup>1</sup>,  
J. C. Sturm<sup>1</sup>, S. A. Lyon<sup>1</sup>, M. House<sup>2</sup>, M. Simmons<sup>2</sup>,  
C. C. Lo<sup>3</sup>, and J. J. L. Morton<sup>3</sup>**

<sup>1</sup> Princeton University, Princeton, USA

<sup>2</sup> University of New South Wales, Australia

<sup>3</sup> University College London, London, UK

To date, electron spin coherence studies of donors and exchange-coupled (J-coupled) donor dimers in silicon have been focused on bulk silicon crystals. Long coherence times have been demonstrated and the limiting spin decoherence mechanisms have now been well understood in bulk silicon. Here, we report the spin coherence measurements for <sup>31</sup>P donors and J-coupled donor dimers in 2D  $\delta$ -layers at 50 nm depth below silicon surface. The donors in the  $\delta$ -layers are randomly “seeded” by exposing a Si [100] surface to a low dose of phosphene gas in an ultra-high vacuum environment. The 2D density of phosphorus atoms is estimated using scanning tunneling microscopy and a 50 nm thick capping silicon layer is then overgrown on top by solid source molecular beam epitaxy. In addition, the surface is passivated with 4 nm amorphous TiO<sub>2</sub> layer formed by chemical deposition and low-temperature anneal. At donor densities of  $2 \cdot 10^{11} \text{ cm}^{-2}$  in our  $\delta$ -layers, only 25% of donors stay as isolated donors and all other donors form J-coupled dimers or higher-order clusters with a random distribution of J-couplings. We focus our coherence measurements on J-coupled donor dimers since their ESR signal sits separately from all other donor-related signals. The spin coherence times for donor dimers in our  $\delta$ -layers ( $T_2 = 70\text{--}140 \mu\text{s}$ ) are substantially shorter than 600  $\mu\text{s}$  measured earlier for donor dimers in bulk natural silicon (4.7% of <sup>29</sup>Si). The decoherence decays are non-exponential and show substantial dependence on magnetic field orientation. We find that the main decoherence mechanism for donor dimers in the  $\delta$ -layers is related to dangling-bond ( $P_{b0}$ ) defects at the silicon surface 50 nm away. The decoherence mechanism is similar to a known instantaneous diffusion mechanism, however here the microwave pulses that excite the dimer spins also excite the overlapping signal from the  $P_{b0}$  spins. Overlapping of the donor dimer signal with the  $P_{b0}$  signal depends on magnetic field orientation and this explains the observed orientation dependence in dimer’s  $T_2$ .

---

## Optically Detected Magnetic Resonance in Diamond NV-Centers under Resonant Optical Excitation at Cryogenic Temperatures

**R. A. Akhmedzhanov<sup>1</sup>, L. A. Gushchin<sup>1</sup>, N. A. Nizov<sup>1</sup>, V. A. Nizov<sup>1</sup>,  
D. A. Sobgayda<sup>1</sup>, and I. V. Zelensky<sup>1</sup>**

<sup>1</sup> Institute of Applied Physics of the RAS, Nizhny Novgorod 603950,  
rinat@appl.sci-nnov.ru

We study optically detected magnetic resonance (ODMR) in diamond NV-centers at cryogenic temperatures. We find that when we use resonant optical excitation at the zero phonon line wavelength, turning on microwave radiation leads to an increase in fluorescence intensity. This is different from the conventional case of nonresonant optical pumping where the resonant MW radiation instead leads to a dip in the fluorescence level. In addition, we observe a significant increase in contrast compared to the nonresonant ODMR which can be beneficial for NV-based magnetometry. To explain the new effect, we propose a theoretical model based on the interaction of resonant optical radiation with different groups from the inhomogeneously broadened ensemble of NV-centers. We find that the effect is temperature dependent and can only be observed at temperatures below 35 K.

## Spins as Qubits: Quantum Information Processing by Magnetic Resonance

**D. Suter**

Fakultät Physik, TU Dortmund, Dortmund 44221, Germany, Dieter.Suter@tu-dortmund.de

The “Digital Revolution” that transformed our lives and our economy is based on the ubiquity of information-processing devices whose processing power increased exponentially, following Moore’s law. As this trend is approaching fundamental physical limits, new directions are explored for even more powerful computational devices based on quantum mechanical systems [1]. Such devices can solve problems that will remain out of reach for conventional computers. Qubits as the basic units of quantum information can be implemented directly in nuclear or electronic spins and magnetic resonance represents an ideal tool for processing this information. For many demonstration experiments, liquid-state nuclear magnetic resonance is well suited. For other tasks, including the targeted initialization of the spins into the ground state, the nitrogen-vacancy (NV) center of diamond allows experiments with single spins at room temperature. The main difficulty for the realization of the potential of quantum information processing is the fragility of information stored in coherent superpositions of quantum mechanical eigenstates. Techniques for overcoming these obstacles include quantum error correction as well as active and passive techniques for protecting quantum states against environmental noise [2]. Initial demonstration experiments of quantum computing by magnetic resonance focused on problems like factoring and database search. Perhaps more appealing for the physics community is the field of quantum simulations, where special-purpose quantum information processing devices simulate physical problems for which conventional computers do not provide sufficient computational power [3]. Many other applications are currently being explored, including image processing, where quantum devices may improve the storage capacity and the processing speed or provide confidentiality for transmission and processing.

1. Stolze J., Suter D.: Quantum Computing: A Short Course from Theory to Experiment. Berlin: Wiley-VCH, 2008.
2. Suter D., Álvarez G.A.: Colloquium: Protecting quantum information against environmental noise. *Rev. Mod. Phys.*, in print (2016)
3. Álvarez G.A., Suter D., Kaiser R.: *Science* **349**, 846 (2015)



## Optical Quantum Memory in Isotopically Pure Crystals Doped by Rare-Earth Ions

R. Akhmedzhanov<sup>1,2</sup>, L. Gushchin<sup>1,2</sup>, A. Kalachev<sup>2</sup>, S. Korableva<sup>3</sup>,  
D. Sobgayda<sup>1,2</sup>, and I. Zelensky<sup>1,2</sup>

<sup>1</sup> Institute of Applied Physics of the Russian Academy of Science,  
Nizhny Novgorod 603950, Russian Federation

<sup>2</sup> Zavoisky Physical-Technical Institute, Russian Academy of Sciences, Kazan 420029,  
Russian Federation, a.a.kalachev@mail.ru

<sup>3</sup> Kazan Federal University, Kazan 420008, Russian Federation

Quantum memories are of crucial importance for developing quantum information technologies and form a platform for creating scalable linear optical quantum computers, realizing long-distance quantum communication, making deterministic single-photon and multiphoton sources, and some other applications. The most commonly discussed materials for quantum storage are rare-earth-ion-doped solids, in which the phase relaxation time at cryogenic temperatures may be as long as several hours. Among them, isotopically pure crystals are of particular interest since they can demonstrate very small inhomogeneous broadening of optical transitions, which allows implementing memory protocols based on off-resonant Raman interaction.

In this work we report experimental results obtained recently on the way to realization of such off-resonant Raman schemes [1, 2]. In particular, atomic frequency comb protocols were implemented in the  $^{143}\text{Nd}^{3+}:\text{Y}^7\text{LiF}_4$  crystal, where inhomogeneous broadening of optical transitions was found to be 70–90 MHz, both in free space [1] and in a cavity [2]. Ideal lambda-structures of optical transitions were identified and signal-to-noise ratio was studied theoretically.

The work was supported by Russian Science Foundation (grant no. 14-12-00806).

1. Akhmedzhanov R.A., Gushchin L.A., Kalachev A.A., Korableva S.L., Sobgayda D.A., Zelensky I.V.: *Laser Phys. Lett.* **13**, 015202 (2016)
2. Akhmedzhanov R.A., Gushchin L.A., Kalachev A.A., Nizov N.A., Nizov V.A., Sobgayda D.A., Zelensky I.V.: *Laser Phys. Lett.* (2016), accepted.

## Impedance-Matched Bragg-Type Microwave Quantum Memory

**S. A. Moiseev<sup>1,2</sup>, F. F. Gubaidullin<sup>2</sup>, R. S. Kirillov<sup>3</sup>, R. R. Latypov<sup>3</sup>,  
N. S. Perminov<sup>1</sup>, K. V. Petrov<sup>3</sup>, and O. N. Sherstyukov<sup>3</sup>**

<sup>1</sup> Kazan Quantum Center, Kazan National Research Technical University, Russia

<sup>2</sup> Zavoisky Physical-Technical Institute, Russian Academy of Sciences, Kazan 420029,  
Russian Federation

<sup>3</sup> Kazan Federal University, Kazan 420008, Russian Federation

Control and manipulation of electromagnetic fields play a basic role in quantum technologies [1]. These problems attracted a large interest to a quantum storage of single photon fields used as a carrier of quantum information. The main stream of current studies focuses on the quantum memory (QM) using the atomic/spin ensembles as a keeper of quantum information. Herein, the photon echo effect [2] in the atomic/spin ensemble located in a single mode resonator [3, 4] is considered most promising for multi-mode microwave QM [5, 6].

In this report, we propose a new approach for broadband impedance matching microwave QM. Instead of the atomic/spin ensembles, we use an array of high-Q single mode microresonators located at a distance of a whole number of half wavelengths from each other and coupled to the common broadband microwave waveguide. Microresonator frequencies form a periodic structure of narrow lines ( $\omega_n = \omega_0 + n\Delta$ , where  $n$  is an integer) which cover a wide frequency range similar to AFC protocol [7].

We have found that point-like spatial Bragg-type location of the microresonators (i.e. its coupling with the waveguide) can provide a broadband QM for microwave fields. Herein, the perfect (100%) storage occurs only at certain optimal parameters of the microresonators. The parameters are determined by a single new impedance matching condition (Fig. 1) for the interaction strength of

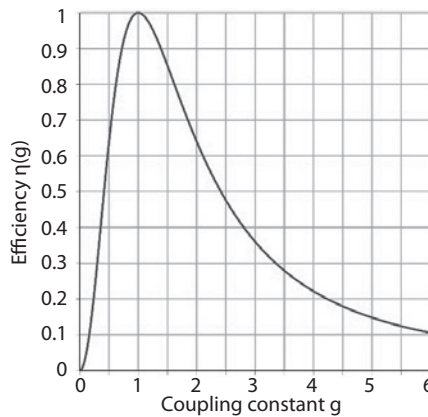


**Fig. 1.** Quantum efficiency vs dimension-less coupling constant  $g = (1/\pi)\sqrt{c\Delta}$ .

propagating microwave fields with microresonators. The broadband character and presence of many interacting local quantum subsystems in these schemes seem to be also interesting for generation and studying the entanglement states in the multi-particle quantum systems. Experimental implementation of the proposed QM scheme is under consideration.

1. Kurizki G., Bertet P., Kubo Y., Mølmer K., Petrosyan D., Rabl P., Schmiedmayer J.: Proceedings of the National Academy of Sciences **112**, 3866 (2015)
2. Moiseev S.A., Kroll S.: Phys. Rev. Lett. **87**, 173601 (2001)
3. Moiseev S.A., Andrianov S.N., Gubaidullin F.F.: Phys. Rev. A **82**, 022311 (2010)
4. Afzelius M., Simon C.: Phys. Rev. A **82**, 022310 (2010)
5. Grezes C., Julsgaard B., Kubo Y. *et al.*: Phys. Rev. X **4**, 021049 (2014)
6. Gerasimov K.I., Moiseev S.A., Morosov V.I., Zaripov R.B.: Phys. Rev. A. **90**, 042306 (2014)
7. de Riedmatten H., Afzelius M., Staudt M.U., Simon C., Gisin N.: Nature (London) **456**, 773 (2008)

## Microwave and Optical Coherence of Erbium Doped Crystals below 1 K

**P. Bushev**

Saarland University, Saarbrücken, Germany, pavel.bushev@physik.uni-saarland.de

Quantum communication networks are considered to distribute entangled states over a large scale computing architecture. The core elements of future quantum networks, i.e., quantum repeaters as well as network nodes, can be realized by using qubits and quantum memories of diverse physical nature. Solid-state systems such as superconducting quantum circuits, nanomechanical devices, and spin doped solids potentially offer larger scalability and faster operation time compared to systems based on the single atom approach. However, such solid-state devices operate at microwave and rf's, which are less suitable for long-range quantum communication than optical channels due to losses in cables and the high noise temperature of antennas. To establish a fiber-optical link between them, one has to use quantum media converter, i.e., a device which coherently interfaces matter and photonic qubits.

One of the promising ways towards implementation of such a converter relies on using optically active spin ensembles in a hybrid quantum architecture. Among these, rare-earth (RE) ion doped crystals are very attractive for application in hybrid systems due to their high spin tuning rate and long optical and spin coherence time. Erbium ions offer a unique opportunity of a coherent conversion of microwave photons into the telecom C band at 1.54  $\mu\text{m}$ , which is used for long distance fiber-optical communication.

Crucial step towards the development of quantum media converter requires highly efficient reversible mapping of temporal modes into the rare-earth doped crystal at power level corresponding to a single microwave photon. The resolution of a microwave photon at 5 GHz frequency requires the cooling of the system below 0.25 K. So far, the most experiments with erbium doped crystals have been limited to temperatures above 2 K. Microwave and optical coherence properties of rare-earth doped crystals have not been studied below 1 K. In my talk we will shortly overview our experimental studying of microwave and optical coherence of different crystals at millikelvin temperature range. We show that for some crystals optical coherence starts to appear below 1 K.

1. Probst S. *et al.*: Phys. Rev. Lett. **110**, 157001 (2013)
2. Probst S. *et al.*: Phys. Rev. B **92**, 014421 (2015)

## Investigations of $Y_2SiO_5:Nd^{143}$ Isotopically Pure Impurity Crystals for Quantum Memory by ESR Method

**R. Eremina<sup>1,2</sup>, T. Gavrilova<sup>1,2</sup>, I. Yatsyk<sup>1,2</sup>, I. Fazlizhanov<sup>1,2</sup>,  
R. Likierov<sup>2</sup>, V. Shustov<sup>1</sup>, Yu. Zavartsev<sup>3</sup>,  
A. Zagumennyi<sup>3</sup>, and S. Kutovoi<sup>3</sup>**

<sup>1</sup> Zavoisky Physical-Technical Institute, Russian Academy of Sciences, Kazan 420029, Russian Federation, REremina@yandex.ru

<sup>2</sup> Kazan Federal University, Kazan 420008, Russian Federation

<sup>3</sup> Prokhorov General Physics Institute of the RAS, Moscow, 119991 Russian Federation

One of the research areas in the field of advanced materials and their applications modern information technologies of processing and transmission of information through a quantum memory modules is the study of dielectric crystals activated by rare-earth ions. To create high-performance modules can be used the group of crystals, to which  $Y_2SiO_5 \cdot ^{143}Nd^{3+}$  belongs. These crystals have properties, required to create highly efficient optical quantum memory, namely, large optical density, and large phase relaxation times, the presence of long-lived hyperfine states [1]. The aim of this work was to study the paramagnetic centers of neodymium ion doped by  $Nd^{3+}$  in the  $Y_2SiO_5$  single crystals by ESR method.

The X-ray analysis of the  $Y_2SiO_5$  monocrystal showed that the compound is in single-phase state and its structure belongs to the space group  $C2/c$ , lattice parameters are  $a = 10.410 \text{ \AA}$ ;  $b = 6.721 \text{ \AA}$ ;  $c = 12.490 \text{ \AA}$ ,  $\alpha = \gamma = 90^\circ$ ,  $\beta = 102.65^\circ$ , and in agreement with literature data [2]. Yttrium ions in the unit cell are located in two positions in Y(1) and Y(2) substituted by  $Nd^{3+}$  (see Fig. 1a and 1b).

The observed ESR spectrum  $Nd^{3+}$  in  $Y_2SiO_5$  exhibits two groups of eight lines, which represent the hyperfine structure (HFS) components due to the odd neodymium isotope  $^{143}Nd$  for two structurally nonequivalent positions; the line from the even isotope is absent. The positions of observed ESR lines does not demonstrate the temperature dependence in the temperature range  $5 \text{ K} < T < 20 \text{ K}$ . Fig. 2 presents angular dependencies of HFS lines recorded in  $(a^*c)$  and  $(a^*b)$ -planes,

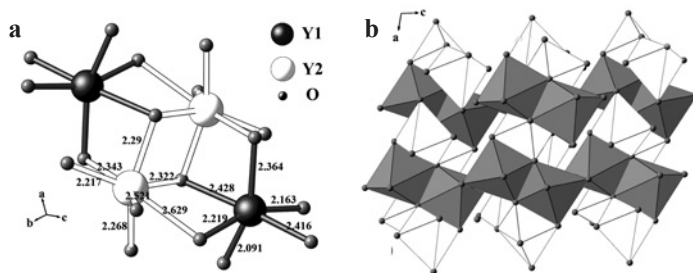


**Fig. 1.** Crystal structure of  $Y_2SiO_5$ : **a** two structurally nonequivalent positions of Y ions, which substituted by  $Nd^{3+}$  ions; distances are given in  $\text{\AA}$ ; **b** pairs of distorted octahedrons  $YO_6$  in  $(ac)$ -plane; nonequivalent octahedrons are shown by white and grey, respectively to **(a)**; the distance  $2.629 \text{ \AA}$  for Y(2) in **(b)** is not shown.

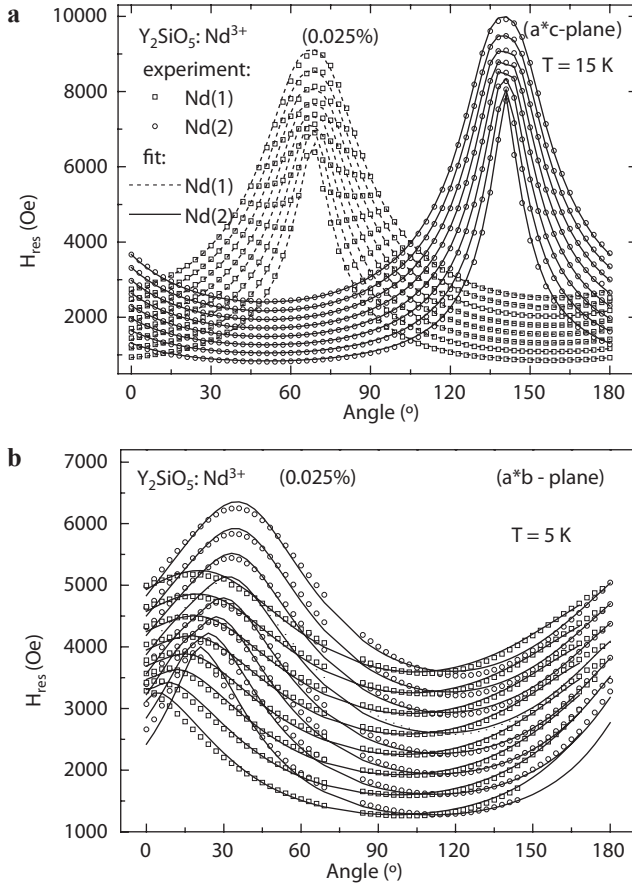


**Fig. 2.** Angular dependencies of ESR lines in  $Y_2SiO_5:^{143}Nd^{3+}$  (0.025%): **a** ( $a^*c$ )-plane at  $T = 15$  K; **b** ( $a^*b$ )-plane at  $T = 5$  K.

respectively. To fit the experimental data we used the effective electron spin  $S = 1/2$  and the nuclear spin  $I = 7/2$  for  $^{143}Nd$  and the following Spin Hamiltonian:

$$H = S \cdot A \cdot I + g \cdot \mu_B \cdot B \cdot S \tag{1}$$

where  $A$  – tensor of HFS and  $g$  –  $g$ -tensor,  $B$  – magnetic field,  $\mu_B$  – Bohr magneton. As seen from Fig. 2 the experimental resonance fields fit well to the calculated curves. Obtained here  $g$  values ( $g_1 = \{4.05; 2.128; 0.819\}$ ;  $g_2 = \{4.203; 1.838; 0.719\}$ ) are close to the values from [3].

This work was supported by the Russian Science Foundation (grant no. 16-12-00041).

1. Thiel C.W., Sun Y., Macfarlane R.M., Böttger T., Cone R.L.: J. Phys. B: At. Mol. Opt. Phys. **45**, 124013 (2013)
2. Zhou W., Yang J., Wang J., Li Y., Kuang X., Tang J., Liang H.: Optics express **20**, A510 (2012)
3. Wolfowicz G., Maier-Flaig H., Marino R., Ferrier A., Vezin H., Morton J.J.L., Goldner P.: Phys. Rev. Lett. **114** (1-5), 170503 (2015)

## Dipolar Relaxation of Multiple Quantum Coherences of One-Dimensional Systems in Multiple Quantum NMR

G. A. Bochkin, E. B. Fel'dman, and S. G. Vasil'ev

Theoretical Department, Institute of Problems of Chemical Physics of Russian Academy of Sciences, Chernogolovka 142432, Russian Federation, efeldman@icp.ac.ru

Multiple quantum (MQ) NMR [1] is an important method for the investigations of problems of quantum information processing such as transmission of quantum information and decoherence processes. MQ NMR not only creates multi-qubit coherent states but also allows the investigation of their relaxation under the action of the correlated spin reservoir [2].

MQ NMR dynamics of one-dimensional systems can be investigated analytically [3] on the preparation period of the MQ NMR experiment [1]. Relaxation of the MQ NMR coherences can be studied on the evolution period of the MQ NMR experiment. This period begins immediately after the preparation period and the density matrix at the end of the preparation period can be used as the initial state for the relaxation process. We suggested [4] to study relaxation which is caused by the ZZ-part of the dipole-dipole interactions (ZZ-model).

It is shown that the MQ NMR coherence of the zeroth order is not subject to relaxation in the ZZ-model. Experimental data obtained on quasi-one-dimensional chain of  $^{19}\text{F}$  nuclei in calcium fluorapatite  $\text{Ca}_5(\text{PO}_4)_3\text{F}$  demonstrate that MQ NMR coherence of the zeroth order decays due to the flip-flop part of the DDI. Relaxation ends with the stationary non-zero intensity of that MQ coherence. The analytical expression for the stationary intensity was obtained. It is in a good agreement with the experimental data.

The dipolar relaxation of the MQ NMR coherences of the plus/minus second orders was also investigated. The obtained results are in a close agreement with the experimental data.

The work is supported by the Russian Foundation for Basic Research (Grants no. 16-03-00056 and no. 16-33-00867) and the Program of the Presidium of RAS 1.26 Electron Spin Resonance, Spin-Dependent Electron Effects and Spin Technologies (grant no. 0089-2015-0191).

1. Baum J., Munowitz M., Garroway A.N., Pines A.: *J. Chem. Phys.* **83**, 2015 (1985)
2. Kaur G., Ajoy A., Cappellaro P.: *New J. Phys.* **15**, 093035 (2013)
3. Doronin S.I., Maksimov I.I., Fel'dman E.B.: *J. Exp. Theor. Phys.* **91**, 597 (2000)
4. Bochkin G.A., Fel'dman E.B., Vasil'ev S.G.: *Zeitschrift fur Phys. Chemie* **230** (2016)

## Microwave Pulses Storage by Using Spin-Frequency Comb Protocol Combined with Gradient Pulses of Magnetic Field

**K. I. Gerasimov<sup>1,2</sup>, S. A. Moiseev<sup>1,2</sup>, V. I. Morozov<sup>3</sup>, and R. B. Zaripov<sup>1,2</sup>**

<sup>1</sup> Zavoiisky Physical-Technical Institute, Russian Academy of Sciences, Kazan 420029, Russian Federation, kigerasimov@mail.ru

<sup>2</sup> Kazan Quantum Center, Kazan National Research Technical University, Kazan 420111, Russian Federation

<sup>3</sup> A. E. Arbuзов Institute of Organic and Physical Chemistry, Kazan 420088, Russian Federation

Last decade demonstrates an increasing interest to quantum information science. Herein, elaboration of quantum memory (QM) devices plays a crucial role in developing of universal quantum processing and long-distance communication [1, 2]. There are a number of main requirements to the QM devices, such as high efficiency, fidelity and capacity, long time of storage and presence of on-demand functions in information retrieval. Various materials are investigated for quantum storage and many QM protocols are examined for practical usefulness in QM. One of the perspective QM scheme is an atomic-frequency comb (AFC) protocol [3] and its broadband counterpart [4] which are promising of multi-mode quantum storage. In this protocol, a record storage of more than 1000 light pulses has been already demonstrated [5]. Cavity enhanced AFC protocol has a rather high efficiency [6]. Recently cavity assisted AFC protocol on natural electron-nuclei spin transitions has been demonstrated in microwave region [7]. We used spin ensemble of stable TCNE radical revealing nine almost equidistant hyperfine lines in ESR spectrum so we called the studied quantum memory scheme by spin-frequency comb (SFC) protocol.

The well-known disadvantage of AFC/SFC protocols is a fixed time delay of the retrieved signal pulses which is determined by a spectral distance of the periodic frequency lines. In this work, we modify SFC protocol by combining its implementation with control gradient pulses of quasi-stationary magnetic field providing noise-free controlling the excited spin coherence and on demand the signal pulse retrieval, correspondingly. Here we also show that using gradient pulses of magnetic field technique could provide essential increasing the quantum memory capacity. Experimental results demonstrate new useful properties for the coherent control of electron-nuclear spin ensemble that could be implemented for broadband microwave or optical-microwave quantum memory protocols.

We are grateful to the RFBR grant no. 15-42-02462 for financial support.

1. Tittel W., Afzelius M., Chaneliere T., Cone R., Kroll S., Moiseev S., Sellars M.: *Laser & Photonics Reviews* **4**, 244–263 (2010)
2. Heshami K., England D.G., Humphreys P.C., Bustard P.J., Acosta V.M., Nunn J., Sussman B.J.: *Journal of Modern Optics* **63**, 2005–2028 (2016)
3. de Riedmatten H., Afzelius M., Staudt M.U., Simon C., Gisin N.: *Nature* **456**, 773–777 (2008)
4. Moiseev S.A., Le Gouët J.-L.: *J. Physics B: Atom, Mol. & Opt. Phys.* **45**, 124003–7 (2012)
5. Bonarota M., Le Gouët J.L., Chanelière T.: *New Journal of Physics* **13**, 0130131–13 (2011)
6. Sabooni M., Li Q., Kroll S., Rippe L.: *Phys. Rev. Lett.* **110**, 1336041–5 (2013)
7. Gerasimov K.I., Moiseev S.A., Morozov V.I., Zaripov R.B.: *Phys. Rev. A* **90**, 0423061–6 (2014)



---

## SECTION 6

# ELECTRON SPIN BASED METHODS FOR ELECTRONIC AND SPATIAL STRUCTURE DETERMINATION IN PHYSICS, CHEMISTRY AND BIOLOGY

## Spin Interactions and Structure in the Condensed Phase

**M. K. Bowman**

Department of Chemistry, The University of Alabama, Tuscaloosa, Alabama 35487, USA,  
mkbowman@ua.edu

The interaction of an unpaired electron spin with the spins of nuclei or other electrons has many consequences in the spectroscopy, spin dynamics, reactivity and chemistry of that unpaired electron. Strong interactions are readily seen in the simple CW-EPR spectrum as resolved hyperfine or zero-field splittings. Weak splittings are often unresolved and a number of techniques are used to selectively reveal small splittings, such as, ENDOR, PELDOR, ESEEM and HYSCORE. It is possible to describe each of them as a double resonance method.

Spin interactions also affect transition moments and selection rules, allowing measurement of “forbidden” transitions by EPR, ELDOR and ENDOR and nutational frequencies by pulsed experiments. “Forbidden” transitions provide an independent measurement of hyperfine or zero-field splittings and, in addition, allow spectra to be dispersed in a second dimension to improve resolution of overlapping transitions, Fig. 1. Nutational spectra can be very helpful in assigning transitions and determining the total spin  $S$ .

Interactions between electron spins are responsible for cross-relaxation, spin and spectral diffusion, spin-lattice and spin-spin relaxation that play a major role in spin dynamics and phenomena such as dynamic nuclear polarization. The interactions between electron spins play an important role in controlling the total spin multiplicity  $S$ . This affects electron transfer rates, chemical reactions, and allows optical, electrical and chemical detection of EPR. The spin selection rules in chemical reactions also enable control of chemical reactions by resonant microwaves.

The spin interactions are very sensitive to the arrangement and geometry of the spins, making them very useful for determining structure and driving the development of magnetic resonance methods to measure spin interactions.

The financial support of the National Science Foundation (grant no. 1416238) is gratefully acknowledged.

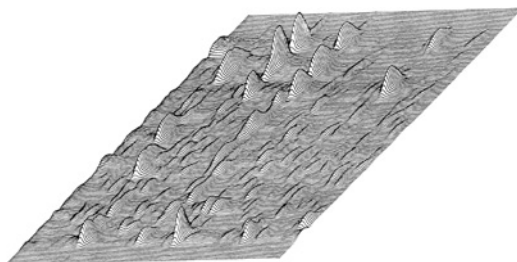


**Fig. 1.** 2D EPR/ESEEM spectrum of Aluminum in a quartz crystal.

## EPR Studies of Doped TiO<sub>2</sub> Photocatalysts: Structures, Properties and Dynamics of Paramagnetic Centers in the Lattice and on the Surface

**A. I. Kokorin<sup>1</sup> and A. I. Kulak<sup>2</sup>**

<sup>1</sup> N. Semenov Institute of Chemical Physics RAS, Moscow 119991, Russian Federation, alex-kokorin@yandex.ru

<sup>2</sup> Institute of General and Inorganic Chemistry NANB, Minsk 220072, Belarus, kulak@igic.bas-net.by

In this report we will present our experimental results on structural peculiarities of TiO<sub>2</sub> of various types doped in the lattice or surface-modified with vanadium ions at different content.

Hamiltonian parameters were calculated as described in [1, 2]. Two types of structural dynamics of V<sup>4+</sup> centers on the surface of nanostructured TiO<sub>2</sub> were observed and analyzed: transitions between aggregated and isolated V<sup>4+</sup> centers (Fig. 1) and among three different V<sup>4+</sup> isolated complexes forming on the surface of nanoparticles (Fig. 2) as a function of the vanadium concentration, TiO<sub>2</sub> composition and time of incubation in the suspension. All changes will be discussed quantitatively in the report.

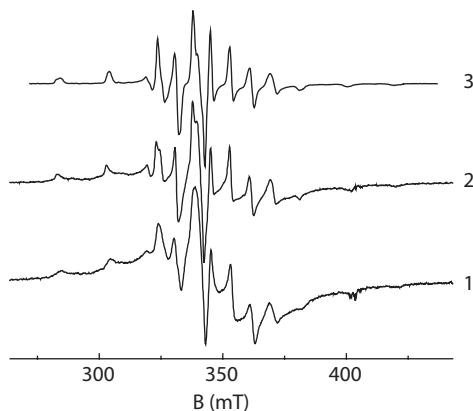


**Fig. 1.** EPR spectra of the P-25 particles after: 1 – 10 min, 2 – 6 days, 3 – 75 days of incubation in 0.15 cm<sup>3</sup> of 0.65 M ascorbic acid in H<sub>2</sub>O-C<sub>2</sub>H<sub>5</sub>OH = 3:2 solution. [V<sup>4+</sup>] = 1.8 · 10<sup>20</sup> cm<sup>-3</sup>; T = 77 K.

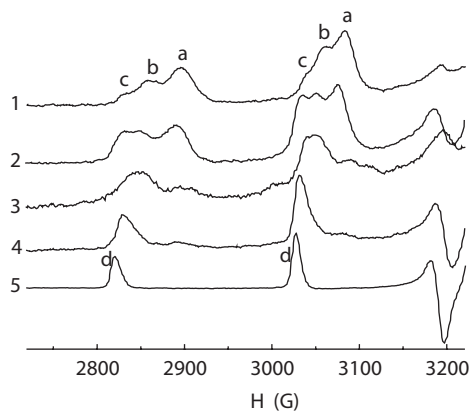


**Fig. 2.** Low-field lines of the EPR spectra of Hombicat UV100 (1, 2) and Degussa P-25 (3, 4) particles after: 1 – 10 min, 3 – 25 h, 2, 4 – 15 days incubation in 0.15 cm<sup>3</sup> of 0.75 M ascorbic acid.  $[V^{4+}]_0 = 4 \cdot 10^{19}$  (1, 2) or  $2 \cdot 10^{19}$  (3, 4) spin/g. 5 – 0.01 M  $VO^{2+}$  ions in  $H_2O-C_2H_5OH = 3:2$ .

This work is partially supported by the RFBR project no. 16-53-00136-Bel\_a.

1. Kokorin A.I., Arakelian V.M., Arutyunian V.M.: Russ. Chem. Bull., Int. Ed. **52**, no. 1, 93 (2003)
2. Kokorin A.I., Kulak A.I. In: Proc. of V Int. Conf. "Atmosphere, Ionosphere, Safety", Kaliningrad, pp. 257–263 (2016)

## EPR Spectroscopy for Studying the Structure and Dynamics of Supercritical Fluids

**E. Golubeva**<sup>1,2</sup>

<sup>1</sup> Chemistry Department, Lomonosov Moscow State University, Moscow 119991, Russian Federation, legol@mail.ru

<sup>2</sup> The Institute of Chemistry and Biology, Immanuel Kant Baltic Federal University, Kaliningrad 236041, Russian Federation

In this lecture the short review on application of EPR spectroscopy to study the local structure and dynamic of supercritical fluids (SCF) will be discussed. The fundamental and applied research in the field of SCF is intensively developed in the world from the end of the last century. The unique properties of SCF (tunable density, high solubility of many substances, low viscosity, negligible surface tension, etc.) allow realizing of variety of new effective technological processes based on applying of SCF solvents. The conversion from traditional solvents to SCF (e.g., supercritical carbon dioxide) also enables obtaining materials with unique properties which can not be synthesized in traditional ways. Most of the technologies based on SCF employment completely satisfy all principles of “green” chemistry and industry.

Experiments have shown solute-solvent interactions in supercritical fluids to be higher than those in homogeneous liquids, causing effective local densities of solvent around solutes to be several times higher than bulk density, demonstrating effect of “clustering”. UV, fluorescence spectroscopy, photoionization techniques, and, in less degree, electron paramagnetic resonance have been used to study these effects. Some examples of encouraging possibilities of spin probe method for detecting the clustering in SCF and studying the features of Heisenberg spin exchange will be discussed in the lecture [1, 2].

No less interesting is to study the interactions in ternary systems: SCF-spin probe-polymer or porous matrix. The interest to these systems is explained by high importance of development of progressive technologies for obtaining new functional materials impregnated by metal clusters, pharmaceutically active substances (FAS), etc. In spite of the obvious advantages of using spin probe method to investigate mechanistic aspects of molecules or clusters penetration into polymers in situ, to study the dynamics of paramagnetic molecules inside the polymer or porous structures and the features of their release into the environment due to dissolution, swelling or degradation of the matrix, this approach was used only in a very few publications [3]. The first results and perspectives of using spin probe method for study the controlled release of FAS and controlled degradation of matrixes for tissue engineering in silica, in vitro and in vivo will be outlined [4].

The research was supported by RFBR (grant no. 16-03-00333).

1. Shaulov A.Yu.: JETP **63**, 157 (1972)
2. Carlier C., Randolph T.W.: AIChE **39**, 876 (1993)
3. Harbron E.J. *et al.*: Journal of Polymer Science, Part B: Polymer Physics **43**, 2097 (2005)
4. Golubeva E.N. *et al.*: Russian Journal of Physical Chemistry B **10**, (2016)

## The Development of Nitroxide Spin Probe Technique for Determination of Molecular Orientation Distribution Function

**A. Kh. Vorobiev<sup>1</sup> and N. A. Chumakova<sup>2</sup>**

<sup>1</sup> Department of Chemistry, M. V. Lomonosov Moscow State University, Moscow 119992, Russian Federation, a.kh.vorobiev@gmail.com

<sup>2</sup> Department of Chemistry, M. V. Lomonosov Moscow State University, Moscow 119992, Russian Federation, harmonic2011@yandex.ru

The partial molecular orientation alignment is an important feature of the materials such as liquid crystals, biological tissues, stretched polymers, artificial membranes, etc. The recording and simulation of EPR spectra of nitroxide probes is one of the most informative methods of investigation of molecular orientation order. The widespread method of simulation of EPR spectra and description of molecular orientation is based on the stochastic Liouville equation for probe molecule in the mean-field potential [1]. The alternative method is the model-free EPR spectra simulation based on expansion of orientation distribution function in a series of order parameters. In the presented work, these two descriptions of orientation distribution are compared using the experimental data for different nitroxides in nematic and smectic liquid crystalline materials.

The determination of orientation distribution was performed in presented work by the following:

- determination of magnetic parameters using the ESR spectra of disordered samples;
- recording of the detailed angular dependencies of ESR spectrum for oriented ordered sample (up to 20 spectra with different orientation of the sample relative too magnetic field);
- joint numerical simulation of these spectra using least square fitting for determination of varied parameters.

The results for the samples with negligible molecular rotations are presented. The symmetry limitations are discussed. The order parameters up to the tenth rank were determined. The evolution of orientation distribution function in course of light-induced reorientation was quantitatively characterized. The direct description of the orientation distribution function by series of order parameters is concluded to be preferable in the case of rigid limit EPR spectra. The limitation of this approach is the small resolution of the rigid limit spectra and applicability of the approach to polymeric and glassy materials only.

The ESR spectra of oriented liquid crystals should be simulated taking into account the molecular rotational mobility. The mixed model jointly comprising the mean field potential and expansion of orientation distribution function in a series of order parameters was developed for simulations of EPR spectra in liquid crystalline media. The stochastic Liouville equation in the potential was solved for description of the molecular rotation mobility. The rotation diffu-

sion and quasy-librations were used for description of molecular rotations. The distribution of the local potential was described by series of order parameters.

Results of spectra simulations for series of nitroxides in nematic and smectic liquid crystals are presented. The order parameters up to 18-th rank were determined. The orientation ditribution functions obtained are presented. The biaxiality of the nitroxide probe and macroscopic biaxiality of the samples are analyzed and characterized. The peculiarities of rotation moves for nitroxides with different structure in the different media are demonstrated.

This work was supported by the Russian Foundation for Basic Research, Grant no. 14-03-00323.

1. Budil D.E., Lee S., Saxena S., Freed J.H.: *J. Magn. Reson. Ser. A* **120**, 155 (1996)

## Determining the Structure and Magnetic Properties of Ytterbium Impurity Centers in Synthetic Forsterite by X-band EPR Spectroscopy

**V. Tarasov<sup>1</sup>, A. Sukhanov<sup>1</sup>, and E. Zharikov<sup>2,3</sup>**

<sup>1</sup> Zavoisky Physical-Technical Institute, Russian Academy of Sciences, Kazan 420029, Russian Federation, tarasov@kfti.knc.ru

<sup>2</sup> Prokhorov General Physics Institute of the Russian Academy of Sciences, Moscow 119991, Russian Federation, evzh@mail.ru

<sup>3</sup> Mendeleev University of Chemical Technology of Russia, Moscow 125047, Russian Federation, evzh@mail.ru

It is known that some trivalent impurity ions in synthetic forsterite have a tendency to the formation of dimer associates consisting of two closely situated impurity ions with a magnesium vacancy between them. The concertation of these associates is much higher than that to be expected for the statistical distribution of the impurity trivalent ions in the forsterite host. This effect of the dimer self-organization of trivalent ions in forsterite was observed for the Cr<sup>3+</sup> [1], Ho<sup>3+</sup> [2] and Tb<sup>3+</sup> [3] ions Here we present the results of the application of X-band electron paramagnetic resonance (EPR) to studying structure of paramagnetic centers formed by the Yb<sup>3+</sup> ions in forsterite.

The measurements were performed at helium temperatures by the ELEXSYS E580 EPR spectrometer. It is found that ytterbium ions substitute Mg<sup>2+</sup> ions in the M2 positions of the forsterite crystal lattice as single ions and in the M1 positions as the dimer associates consist-ing of two ions in the M1 position the associate of dimeric ions of ytterbium, consisting of two ions in the M1 position, located approximately at 0.6 nm along the crystal *c*-axis.

This work was supported in part by RFBR and the Government of the Republic of Tatarstan according to the research project no. 15-42-02324.

1. Shakurov G.S., Tarasov V.F.: Appl. Magn. Reson. **21**, 597 (2001)
2. Konovalov A.A., Lis D.A., Malkin B.Z. *et al.*: Appl. Magn. Reson. **28**, 267(2005)
3. Konovalov A.A., Lis D.A., Subbotin K.A. *et al.*: Appl. Magn. Reson. **45**, 193 (2014)



## Spins of Current Carriers as a Probe of Physical and Chemical Transformations in Conductors

A. M. Ziatdinov

Institute of Chemistry, Far-Eastern Branch of the Russian Academy of Sciences,  
Vladivostok 690022, Russian Federation, ziatdinov@ich.dvo.ru

The conduction ESR (CESR) technique is one of the most powerful methods for studying the physical and chemical transformations in conductors because the shape and intensity of resonance signal vary significantly at these events. In this presentation the CESR capabilities as the instrument for study of physical and chemical transformations in graphite and graphite intercalation compounds (GICs) are considered. The following problems are discussed in detail.

Conduction electron spins as a probe of magnetic properties of chemical reaction front in graphite and its compounds.

The measurements of CESR signal intensity as a method of studying the variations of chemical potential at physical and chemical transformations in graphite and its compounds.

The CESR signal linewidth temperature dependence peculiarities as a source of unique information about the current carrier spin relaxation channels appearing at the physical and chemical transformations in intercalate subsystem.

The determination of layer and interlayer conductivities in graphite and GICs from CESR signal data.

The estimation for density of states of current carriers at the Fermi level for nanosized graphite particles (nanographites) and their compounds using the CESR and static magnetic susceptibility data.

The application of CESR method for study of structural incommensurate states of conductors. Temperature evolution of structural incommensurate states of matter in the soliton regime of lattice displacement modulation. The relationship between the phase and amplitude of incommensurate modulation.

The methods for increasing the capabilities of CESR-spectroscopy by a choice of experimental configuration and sample sizes.

All considered problems are illustrated by the original results of our investigations.

---

---

## SECTION 7

# LOW-DIMENSIONAL SYSTEMS AND NANO-SYSTEMS

## Level-Anticrossing Spectroscopy of Excited States in Semiconductors and Semiconductor Nanostructures

**N. G. Romanov, A. N. Anisimov, V. A. Soltamov, and P. G. Baranov**

Ioffe Institute, St. Petersburg 194021, Russian Federation, nikolai.romanov@gmail.com

The results of application of level anticrossing (LAC) spectroscopy for investigations of two classes of nanostructures, i.e GaAs/AlGaAs quantum wells and superlattices grown by molecular beam epitaxy and silicon carbide crystals of different polytypes, which can be considered as natural superlattices, are reported. LAC spectroscopy was shown to be very suitable for obtaining important information on shortly lived excited states and for a local diagnostics of nanostructures including single defect spectroscopy.

LAC detected via photoluminescence in GaAs/AlGaAs quantum wells and superlattices made it possible measuring the electron and hole  $g$ -factors and the exchange splitting parameters for shortly lived ( $\tau_R \leq 1$  ns) heavy-hole excitons in the systems with type-I band alignment, to follow variation of these parameters type-I to at type-II transition and to reveal the hidden anisotropy of the exciton localization.

A family of vacancy-related ( $V_{Si}$ ) color centers with  $S = 3/2$  in hexagonal (4H, 6H) and rhombic (15R) polytypes of CMOS-compatible silicon carbide (SiC) was shown to be promising for chip-scale quantum technologies based on ensembles as well as on single centers. Similar to the spin  $S = 1$  nitrogen-vacancy (NV) defect in diamond,  $V_{Si}$  centers in SiC possess selectively addressable spin states through optically detected magnetic resonance. Optically detected LAC has been demonstrated for a family of  $S = 3/2$  centers in the ground and excited ( $\tau_R$  of the order of ns) states. It was concluded that sharp and strong variations of the IR photoluminescence intensity at LAC can be used for an all-optical sensing of the magnetic field and temperature. A giant thermal shift was found for the excited-state zero-field splitting of the silicon vacancy centers in 4H-SiC. In contrast, the zero-field splitting in the ground state of these centers does not reveal detectable temperature shift. Using these properties, an integrated magnetic field and temperature sensor can be implemented on the same center.

This work was supported by the Russian Science Foundation under Agreement no. 14-12-00859.

## Magnetic Investigation of One-Dimensional Organic Conductors, (TMTTF)<sub>2</sub>X

M. Asada<sup>1</sup> and T. Nakamura<sup>1,2</sup>

<sup>1</sup> Institute for Molecular Science, Okazaki 444-8585, Japan

<sup>2</sup> The Graduate University for Advanced Studies, Okazaki 444-8585, Japan,  
t-nk@ims.ac.jp

One-dimensional conductors based on (TMTCF)<sub>2</sub>X (C = S, Se) are some of the most extensively studied materials among organic conductors. They possess various ground states including the spin-singlet (SS), commensurate antiferromagnetic state (C-AF), incommensurate spin density wave (IC-SDW) and superconductivity (SC), with applied pressures or counter anions, X [1]. Moreover, findings of charge-ordering (CO) and related phenomena in (TMTTF)<sub>2</sub>X have attracted significant recent attention [2].

(TMTTF)<sub>2</sub>Br undergoes antiferromagnetic transition at 16 K ( $T_N$ ). But it is located on the proximity between C-AF and IC-SDW phase in the generalized phase diagram. Previously, we examined the magnetic structure of the antiferromagnetic state of (TMTTF)<sub>2</sub>Br by <sup>1</sup>H-NMR spectroscopy at 4.2 K [3]. We clarified that the wave-number of the antiferromagnetic state is commensurate  $Q = (1/2, 1/4, 0)$  with amplitude  $0.14\mu_B/\text{molecule}$  at 4.2 K. The commensurate antiferromagnetic state of (TMTTF)<sub>2</sub>Br was also confirmed by <sup>13</sup>C-NMR measurements [4]. Recently Kawamoto and coworker found anomalous <sup>13</sup>C-NMR spectra change in (TMTTF)<sub>2</sub>Br below 4.2 K [5]. This observation suggests possible successive phase transition around 4.2 K.

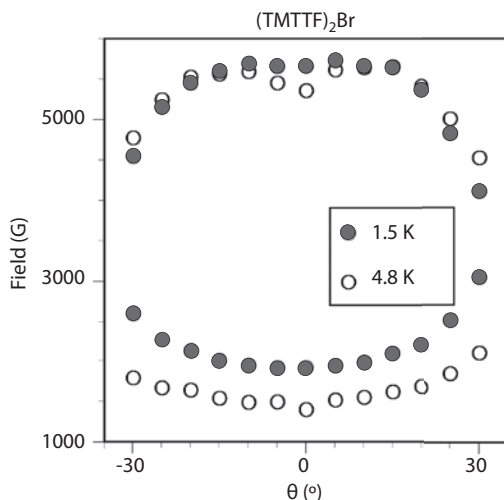


**Fig. 1.** Angular dependence of the antiferromagnetic resonance in (TMTTF)<sub>2</sub>Br (easy-intermediate plane: X-band).

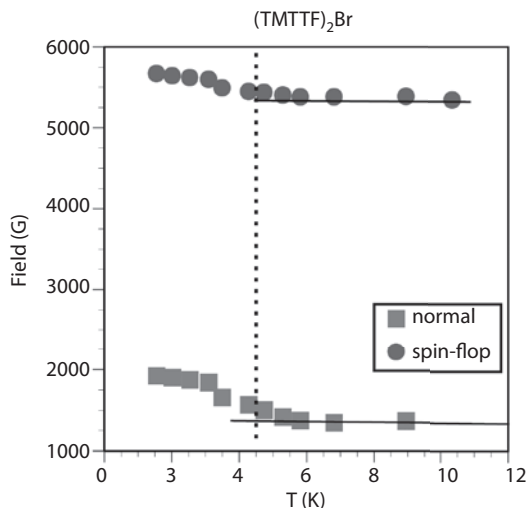


Fig. 2. Temperature dependence of AFMR modes (normal and spin-flop).

Hence we also investigated antiferromagnetic resonance (AFMR) of a single crystal of  $(\text{TMTTF})_2\text{Br}$ . The X-band ESR experiments were carried out using Bruker EleXsys 500 with Oxford Cryostat E910. The temperature range was between 1.5 K and 10 K.

Figure 1 shows the angular dependence of AFMR modes (normal mode and spin-flop mode) at 4.8 K and 1.5 K. The AFMR modes seem to enhance at 1.5 K, indicating development of the magnetic moment of the AF sub-lattices even at low-temperatures ( $T \ll T_N/2$ ). Temperature dependence of the two antiferromagnetic resonance (AFMR) modes also shows anomalous increase below 5 K. According to the detailed analysis of the AFMR experiment results, the shift of the AFMR field suggests change of the magnetization of the AF sub-lattice (namely, the amplitude of the AF) [6]. We also carried out  $^2\text{H}$ -NMR measurements for deuterated  $(\text{d}_{12}\text{-TMTTF})_2\text{Br}$  to investigate charge distribution by the quadrupole splitting at low temperatures. Possible sub-phases in the antiferromagnetic state are discussed.

The work was supported by a Grant-in-Aid for Scientific Research B (no. 20340095) from the Ministry of Education, Culture, Sports, Science and Technology, Japan.

1. (a) Ishiguro T., Yamaji K., Saito G.: *Organic Superconductors* (Springer-Verlag, Berlin/Heidelberg, 1998) 2nd ed. and references therein; (b) Jérôme D.: *Science* **252**, 1509 (1991)
2. (a) Chow D.S., Zamborszky F., Alavi B., Tantillo D.J., Baur A., Merlic C.A., Brown S.E.: *Phys. Rev. Lett.* **85**, 1698 (2000); (b) Monceau P., Nad F.Ya., Brazovskii S.: *Phys. Rev. Lett.* **86**, 4080 (2001)
3. Nakamura T., Nobutoki T., Kobayashi Y., Takahashi T., Saito G.: *Synth. Met.* **70**, 1293 (1995)
4. (a) Barthel E., Quirion G., Wzietek P., Jérôme D., Christensen J.B., Jørgensen M., Bechgaard K.: *Europhys. Lett.* **21**, 87 (1993); (b) Hirose S., Liu Y., Kawamoto A.: *Phys. Rev B* **88**, 125121 (2013)
5. T. Ihachi *et al.*, JPS Spring meeting 2015, 21aAs-2.
6. Ohta H., Yamauchi N., Nanba T., Motokawa M., Kawamata S., Okuda K.: *J. Phys. Soc. Jpn.* **62**, 785 (1993)

## ESR Reveals Doping-Induced Change of Spin Structure in a “Triangular” Antiferromagnet

**A. I. Smirnov<sup>1</sup>, T. A. Soldatov<sup>1</sup>, T. Kida<sup>2</sup>, A. Takata<sup>2</sup>, M. Hagiwara<sup>2</sup>,  
O. Petrenko<sup>3</sup>, and M. Zhitomirsky<sup>4</sup>**

<sup>1</sup> P. L. Kapitza Institute RAS, Moscow 119334, Russian Federation, smirnov@kapitza.ras.ru

<sup>2</sup> AHMF Center, Osaka University, Osaka 560-0043, Japan

<sup>3</sup> Warwick University, CV4-7AL Coventry, UK

<sup>4</sup> CEA-INAC, Grenoble 38054, France

The ground state of the two-dimensional Heisenberg antiferromagnet on a triangular lattice (AFMTL) is strongly degenerated in a molecular field approximation. The selection of the real ground state is performed by the so-called order-by-disorder mechanism, implying thermal and quantum fluctuations, lifting a degeneracy, see, e.g. [1]. Even a weak random potential of impurities was shown to prevent these fluctuations and, thus, may be a reason of a cardinal change of the spin structure of AFMTL [2]. We have checked these theoretical principles in experiments with  $S = 5/2$  AFMTL  $\text{RbFe}(\text{MoO}_4)_2$  [3], doped with up to 15% K (this means substitution of Rb per K). The susceptibility shows a reduced Néel temperature, but the Néel transition is almost as sharp as in a pure compound. The  $1/3$ -magnetization plateau, being an evidence of a phase, stabilized by fluctuations, was completely suppressed by doping in correspondence with [2]. The results of the present multifrequency ESR study in a range 25–150 GHz reveal a strong change of the antiferromagnetic resonance spectrum – the descending branch observed in pure samples, disappears completely in doped samples, indicating a change of the ground state. The theoretical analysis of the spectra of the proposed spin configurations is in a correspondence with “Y-type” structure (one sublattice opposite field, two sublattices tilted) for the pure compound, while for the doped samples the spectrum indicates the “anti-Y” structure (one sublattice along field and two-tilted). These facts directly demonstrate, that preventing spin fluctuations by a weak random potential really results in a drastic change of the spin structure.

1. Chubukov A.V., Golosov D.I.: *Journal of Physics: Condensed Matter* **3**, 69 (1991)
2. Maryasin V.S., Zhitomirsky M.E.: *Phys. Rev. Lett.* **111**, 247201 (2013)
3. Svistov L.E. *et al.*: *Phys. Rev. B* **67**, 094434 (2003)

## Unusual Magnetic Excitations in a Weakly Ordered Spin-1/2 Chain Antiferromagnet $\text{Sr}_2\text{CuO}_3$ : Possible Evidence for the Goldstone-Higgs Interaction

S. S. Sosin<sup>1</sup>, E. G. Sergeicheva<sup>1</sup>, and I. A. Zaliznyak<sup>2</sup>

<sup>1</sup> P. Kapitza Institute for Physical Problems, Moscow 119334, Russian Federation, sosin@kapitza.ras.ru

<sup>2</sup> Brookhaven National Laboratory, Upton, New York 11973, USA

We report on an electron spin resonance (ESR) study of a nearly one-dimensional (1D) antiferromagnet  $\text{Sr}_2\text{CuO}_3$ , known as one of the best realizations of a spin-1/2 chain system (with the ratio of an inter- to intra-chain exchange interaction  $J'/J \leq 5 \cdot 10^{-4}$ ,  $J \approx 2800$  K). It undergoes a phase transition into an antiferromagnetic state only below  $T_N = 5.5$  K, with an extremely small value of the magnetic order parameter  $\langle \mu \rangle = 0.06\mu_B$  [1]. Consequently,  $\text{Sr}_2\text{CuO}_3$  presents an ideal model material for exploring effects of an extremely weak symmetry breaking in a system of coupled quantum-critical spin-1/2 chains.

The ESR spectra were measured using a set of transmission type spectrometers covering frequency range 25–140 GHz at fields up to 12 T in a temperature range 0.5–50 K. At  $T > T_N$  in the disordered Luttinger-spin-liquid phase the system reveals an ideal Heisenberg-chain behavior with only very small, field-independent linewidth  $\sim 1/T$ . In the ordered state below  $T_N$  for all directions of the applied magnetic field we identify antiferromagnetic resonance (AFMR) modes with two gaps  $\Delta_1 = 23.0$  GHz and  $\Delta_2 = 13.3$  GHz rendered by a small anisotropy to the two Goldstone magnons. This type of spectrum is well described by the pseudo-Goldstone magnons in the model of a collinear biaxial antiferromagnet. Additionally, we observe a dominant resonant response with peculiar properties, which is not anticipated by the conventional theory of the Goldstone spin waves [2]. The nature of the spin system in  $\text{Sr}_2\text{CuO}_3$  allows one to suggest that this new mode is due to a coupling of one of the Goldstone magnon branches with the amplitude fluctuations of the order parameter (“Higgs” mode), which provides a plausible mechanism by which it can acquire a field-dependent “mass”. At the origin of such coupling could be the spin anisotropy, which favors different amplitude of the ordered moment depending on its alignment with respect to the easy/medium/hard axis.

1. Kojima K.M. *et al.*: Phys. Rev. Lett. **78**, 1787 (1997)

2. Sergeicheva E.G. *et al.*: arXiv:1603.05869 (2016)



## Ferromagnetic Resonance of Localized Nonuniform States in Magnetic Nanostructures

R. V. Gorev<sup>1</sup>, M. V. Sapozhnikov<sup>1</sup>, E. V. Skorohodov<sup>1</sup>,  
and V. L. Mironov<sup>1,2</sup>

<sup>1</sup> Institute for Physics of Microstructures RAS, Nizhny Novgorod, 603950, Russian Federation

<sup>2</sup> Lobachevsky State University of Nizhny Novgorod, Nizhny Novgorod 603950, Russian Federation  
mironov@ipmras.ru

We report the micromagnetic modeling of ferromagnetic resonance (FMR) for localized non-uniform states in different thin film ferromagnetic nanostructures. The FMR frequency spectra and spatial distributions of the oscillation amplitude are calculated by numerical solution of Landau-Lifshitz equation using the standard Object Oriented MicroMagnetic Framework (OOMMF) code [1]. As an example here we present the results for localized FMR modes associated with domain wall in permalloy nanowire and for skyrmion state in thin film multi-layer structure Co/Pt spatially modified by ion beam.

The spectrum of the magnetization oscillations in the nanowire with transverse domain wall is shown in Fig. 1a. The intense peaks 1 and 2 correspond to the oscillations localized in the domain wall area. Appropriate distributions of the FMR amplitude are shown in Fig. 1c, d.

Another perspective objects are skyrmions states in CoPt multilayer films with perpendicular anisotropy, locally irradiated with He focused ion beam [2], that the irradiation leads to local decrease of the anisotropy. Fig. 2 shows the

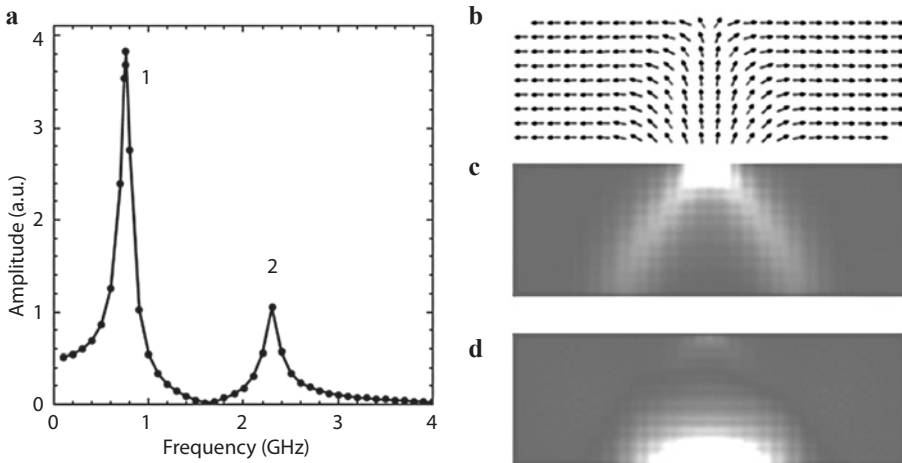


**Fig. 1.** a The spectrum of magnetization oscillations in the nanowire with transverse domain wall; b the magnetization distribution in the domain wall; c and d the FMR amplitude distributions associated with the peak 1 and 2 respectively.

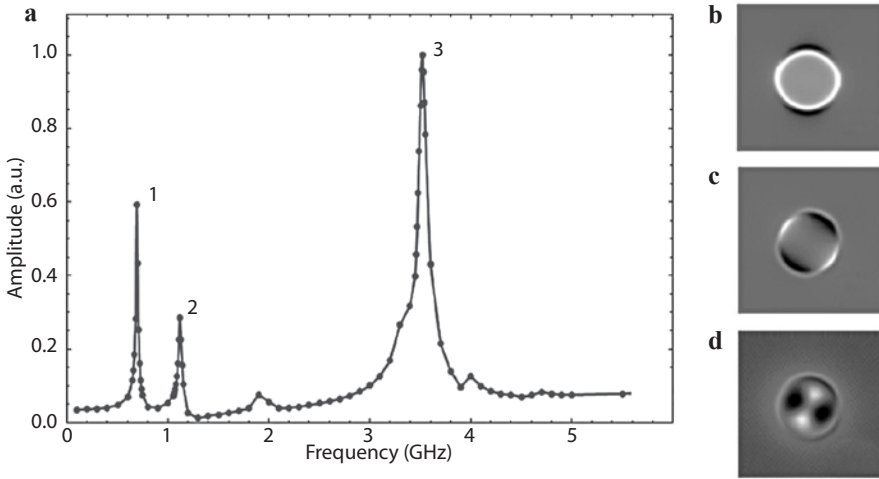


**Fig. 2.** **a** The spectrum of the magnetization oscillations for the skyrmion states in the CoPt with circular areas of modified anisotropy; **b**, **c** and **d** are distribution of the FMR amplitude associated with the peak 1, 2 and 3 respectively.

spectrum of the magnetization oscillations in such structure. The peaks 1 and 2 are associated with the localized oscillations within the irradiated areas (the diameter is 100 nm) (see Fig. 2b, c). The peak 3 is connected with the resonance of the film as a whole (see Fig. 2d).

Evidently the controlled rearrangement of nonhomogeneous states in ferromagnetic nanostructures can be exploited to create tunable magnetic components of the microwave electronics.

The financial support of the Russian Science Foundation (Grant no. 16-12-10254) is gratefully acknowledged.

1. Donahue M.J., Porter D.G.: "OOMMF User's Guide", Interagency Report NISTIR 6376, NIST, Gaithersburg, <http://math.nist.gov/oommf>
2. Sapozhnikov M.V., Vdovichev S.N., Ermolaeva O.L., Gusev N.S., Fraerman A.A., Gusev S.A., Petrov Yu.V.: *Appl. Phys. Lett.* **109**, 042406 (2016)

## Ferromagnetic Resonance in Exchange-Related Ferromagnet-Paramagnet Multilayer Structures

A. A. Fraerman<sup>1</sup>, E. V. Skorohodov<sup>1</sup>, S. N. Vdovichev<sup>1</sup>,  
R. V. Gorev<sup>1</sup>, and E. S. Demidov<sup>2</sup>

<sup>1</sup> Institute for Physics of Microstructures, Nizhny Novgorod 603950, Russian Federation,  
evgeny@ipmras.ru

<sup>2</sup> Nizhny Novgorod State University, Nizhny Novgorod 603950, Russian Federation

Multilayer metallic magnetic structures attract great interest in recent years. One of the most important characteristics of such systems is the interlayer exchange interaction between magnetic layers. This interaction determines properties of devices which can be made on the basis of multilayer magnetic structures (magnetic sensors, memory elements and etc.). For many applications it is important that the value of the interaction between the layers was not fixed and had the opportunity to control. Therefore, of particular interest is to study of the interlayer interaction in F/f/F systems, where F is a “strong” ferromagnet with a Curie temperature significantly higher than room temperature ( $T_F > 500$  K), f is a weak ferromagnet, for which the Curie temperature  $T_f < T_F$  and close to the room temperature  $T$ . The interest for such structures due to possibility of uses one as “magnetic” refrigerators. The principle of work such magnetic refrigerators is based on the magnetocaloric effect [1, 2].

We investigated a series of F/f/F multilayer structures  $\text{Ni}_{80}\text{Fe}_{20}/\text{Ni}_{65}\text{Cu}_{35}/\text{Co}_{60}\text{Fe}_{40}$  with thicknesses of  $\text{Ni}_{65}\text{Cu}_{35}$  layer in the range of 6–22 nm by method of ferromagnetic resonance in the temperature range 77–300 K. It was found that interaction between the  $\text{Ni}_{80}\text{Fe}_{20}$  films and  $\text{Co}_{60}\text{Fe}_{40}$  is ferromagnetic nature for thicknesses of  $\text{Ni}_{65}\text{Cu}_{35}$  less than 15 nm; for the thickness of 20 nm interaction change the sign depending on the temperature and can be ferromagnetic or antiferromagnetic type. It was used the phenomenological theory of phase transitions Landau for an accurate description of the experimental results. It was identified collinear and noncollinear magnetic state for different temperatures which depend on the external magnetic field and thickness of layer  $\text{Ni}_{65}\text{Cu}_{35}$ . The financial support of the Foundation for Basic is gratefully acknowledged.

1. Pecharsky V.K., Gschneidner K.A.: Phys. Rev. Lett. **78**, 4494 (1997)
2. Fraerman A.A., Shereshevskii I.A.: JETP Lett. **101**, 618 (2015)

## ESR Study of Electron States in Ge/Si Heterostructures with Nanodisc Shaped Quantum Dots

**A. F. Zinovieva<sup>1</sup>, V. A. Zinovyev<sup>1</sup>, A. V. Nenashev<sup>1,2</sup>,  
L. V. Kulik<sup>2,3</sup>, and A. V. Dvurechenskii<sup>1,2</sup>**

<sup>1</sup> Rzhanov Institute of Semiconductor Physics SB RAS, Novosibirsk 630090, Russian Federation, aigul@isp.nsc.ru

<sup>2</sup> Novosibirsk State University, Novosibirsk 630090, Russian Federation

<sup>3</sup> Institute of Chemical Kinetics and Combustion, Novosibirsk 630090, Russian Federation

Quantum dot (QD) semiconductor systems are excellent candidates for realization of quantum computation and spintronics devices. Recent theoretical work [1] proposed the approach for implementation of quantum logic operations without gate-addressing to individual qubit in two-qubit system. Ge/Si QD system allowing localization of two electrons with different  $g$ -factors nearby the same

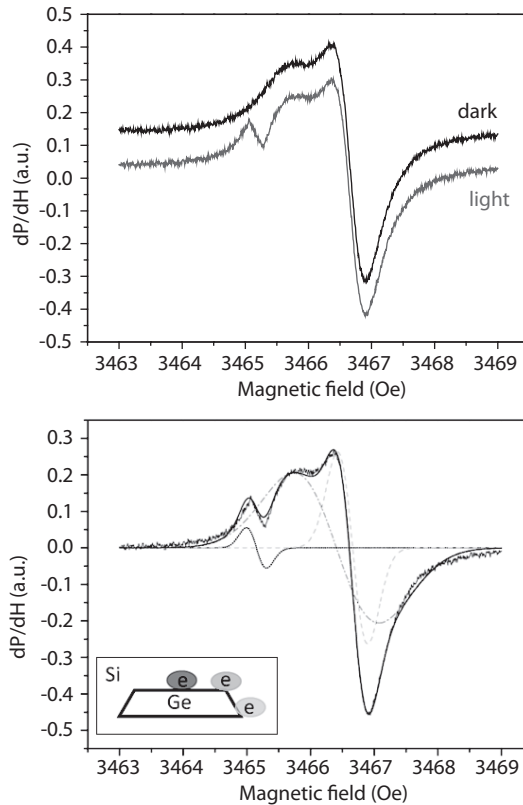


**Fig. 1.** ESR spectra obtained on the sample with nanodiscs under illumination (lower spectrum) and in the dark (upper spectrum).

QD [2] can be considered as the appropriate system for the realization of this idea. These electrons can serve as a pair of qubits and difference of  $g$ -factors should provide the selective access to each qubit. The present work demonstrates the simultaneous localization of three electrons with different  $g$ -factors on the same QD by use of electron spin resonance (ESR) method. It was revealed that the shape and size of QDs are crucial for realization of this type localization. The nanodisc shaped QD allows to localize three electrons in opposite to the case of lens shaped or pyramidal QD that can localize only two electrons with different  $g$ -factors [2]. Structures under study contain three layers of nanodisc shaped GeSi QDs with height  $h \approx 10$  nm and base size  $l \approx 200$  nm, grown by molecular-beam epitaxy. Each layer of nanodiscs is grown by deposition of 7.5 monolayers of Ge at 700 °C. The ESR study was performed with X-band ( $\nu \sim 9$  GHz) ESR spectrometer at 4.5 K. A simultaneous localization of three electrons with different  $g$ -factors was obtained under illumination of the samples. Analysis of angular dependencies of ESR spectra allows us to perform the assignment of the signals. All signals have the different orientation dependence of  $g$ -factors. This difference originates from different spatial electron localization corresponding to different  $\Delta$ -valleys in Si. Two ESR signals observed in the dark, as well as under illumination, are related to electrons localized due to strain at the top edges and base edges of nanodiscs, while the third ESR signal observed only under illumination is isotropic and related to electrons localized in the Si layer above the central parts of the nanodiscs due to Coulomb interaction with photo-holes. The comparison with ESR results obtained on the structures with the lens shaped QDs was performed. In the case of lens shaped quantum dots only two ESR signals corresponding to electrons localized at the QD top and base edges of QDs were observed.

The authors are grateful to V. A. Armbrister for the growth of quantum dot structures. This work was funded by State assignment no. 0306-2015-0025.

1. Nenashev A.V., Zinovieva A.F., Dvurechenskii A.V., Gornov A.Yu., Zarodnyuk T.S.: *Journal of Applied Physics* **117**, 113905 (2015)
2. Zinovieva A., Stepina N., Dvurechenskii A., Kulik L., Mussler G., Moers J., Grützmaier D.: *Solid State Phenomena* **233-234**, 415 (2015)

## Spin-1/2 Chain Magnet $\text{BaAg}_2\text{Cu}[\text{VO}_4]_2$ Studied by Magnetic Resonance Technique

**E. Vavilova<sup>1</sup>, Y. Krupskaya<sup>2</sup>, M. Schäpers<sup>2</sup>, A. U. B. Wolter<sup>2</sup>,  
H.-J. Grafe<sup>2</sup>, A. Möller<sup>3</sup>, B. Büchner<sup>2</sup>, and V. Kataev<sup>1,2</sup>**

<sup>1</sup> Zavoisky Physical-Technical Institute, Russian Academy of Sciences, Kazan 420029,  
Russian Federation, jenia.vavilova@gmail.com

<sup>2</sup> Leibniz-Institute for Solid State and Materials Research IFW Dresden, Dresden, Germany

<sup>3</sup> Institute of Inorganic Chemistry and Analytical Chemistry, Johannes Gutenberg University Mainz,  
Mainz 55128, Germany

Here we report the study of  $\text{BaAg}_2\text{Cu}[\text{VO}_4]_2$  compound that contains Cu(II)  $S = 1/2$  ions on a distorted two-dimensional triangular lattice interconnected via  $[\text{VO}_4]$  by High-Field/Frequency Electron Spin Resonance (HF-ESR) and Nuclear Magnetic Resonance (NMR) spectroscopies. DFT band structure calculations, quantum Monte-Carlo simulations, and high-field magnetization measurements show that the magnetism of this compound is determined by a superposition of ferromagnetic (FM) and antiferromagnetic (AFM) uniform spin-1/2 chains with nearest neighbour exchange couplings of  $J_{\text{FM}} = -19$  K and  $J_{\text{AFM}} = 9.5$  K [1]. The analysis of the low-temperature HF-ESR spectra shows that its peculiar structure is due to the development of the anisotropic internal fields corresponding to FM and AFM correlations in the respective Cu spin chains. The  $^{51}\text{V}$  NMR spectra clearly show the signals from  $^{51}\text{V}$  nuclei in the two types of chains. The analysis of the temperature evolution of the HF-ESR and NMR spectra confirms a theoretical predictions of the superposition of FM and AFM Cu(II) spin-1/2 chains in the studied material.

This work was supported by the DFG through Grants no. KA1694/8-1; WO 1532/3-2, and no. SU 229/10-2, and partially supported by the Russian Foundation for Basic Research through project RFBR 14-02-01194.

1. Tsirlin *et al.*: PRB **85**, 014401 (2012)

## Application of Ferromagnetic Resonance for Investigation of Magnetic Properties of Strained Permalloy Microparticles

D. A. Biziyayev<sup>1</sup>, A. A. Bukharaev<sup>1,2</sup>, Yu. E. Kandrashkin<sup>1</sup>,  
T. F. Khanipov<sup>1</sup>, L. V. Mingalieva<sup>1</sup>, and N. I. Nurgazizov<sup>1,2</sup>

<sup>1</sup> Zavoisky Physical-Technical Institute, Russian Academy of Sciences, Kazan 420029,  
Russian Federation, niazn@mail.ru

<sup>2</sup> Kazan Federal University, Kazan 420008, Russian Federation

It is well known that a mechanical tension in magnetic particles changes of its magnetic properties (magnetic anisotropy, coercitivity, direction of the magnetization axes, and other). Possibility of its using for creation of more energy-efficient logical elements of micro- and a nano-electronics caused formation of new direction named “straintronic” [1].

In this work was investigated of magnetic properties of the ordered array of permalloy (75%Ni, 25%Fe) microparticles with sizes of  $25 \times 25 \times 0.2$  mkm<sup>3</sup>. A glass substrate was elastic bended during process of the particles formation. Unbending of the substrate after the end of the process was created the compression of particles in one direction.

A saturation magnetization ( $M_s$ ) and a magnetic anisotropy field ( $H_k$ ) of the sample was calculated from the angular dependence of a ferromagnetic resonance (FMR). Calculation was based on the solution of the Landau-Lifshitz-Gilbert equation for thin film [2]. It was founded a mechanical strain of the Py particles (relative change of the lateral sizes about 0.2%) was resulted increasing of the  $H_k$  from 0.45 mT to 1.06 mT. Uniformity of particles (both by the sizes and by the intensity of compression) is important for correct interpretation of FMR spectrums. It was checked by a magnetic force microscopy (MFM), because MFM allows to investigate physical properties of one particle. The identical MFM images of the particles located in different areas allowed to verify of the sample uniformity. Moreover computer simulations of the MFM images of Py particles were carried out with using the  $M_s$  and  $H_k$  values obtained by FMR. The accuracy of the FMR data was additional confirmed by a good agreement of the model and of the experimental MFM images.

This study was partly supported by the Presidium of the RAS.

1. Roy K.: Appl. Phys. Lett. **103**, 173110 (2013)
2. Belyaev B.A., Izotov A.V.: Physics of the Solid State **49**, 1731 (2007)

---



---

## SECTION 8

# OTHER APPLICATIONS OF MAGNETIC RESONANCE

## Nanoscale Magnetic Resonance Microscopy

**A. Volodin**

Laboratorium voor Vaste-Stoffysica en Magnetisme, KU Leuven, Leuven 3001, Belgium,  
alexander.volodin@fys.kuleuven.be

Magnetic Resonance Microscopy (MRM) – one of the most rapidly developing and promising directions of scanning probe microscopy, which is based on the magnetic resonance (MR) phenomenon. Whereas the use of typical magnetic resonance analytical tools is limited to objects of millimeter size, the MRM advances them to a nanoscale. Traditional induction-detection methods cannot be used in MRM at sub-micrometer lengthscales. At present the best alternative approaches are mechanical and optical MR detections which are based on the use of micromechanical resonators and on the luminescence of nitrogen-vacancy (NV) centers in diamond correspondingly. The decisive role of a unique ultra-high sensitive equipment has led to the achievement of remarkable success in the development of MRM, bringing it close to the detection of a single-proton spin. We will discuss some “unconventional” MRM applications, that can be implemented without the need for a unique instrumentation and exotic environment for MR monitoring.

Ultrasensitive attonewton force level mechanical sensors, ultra-high vacuum and low temperature conditions are no longer necessary in the case of ferromagnetic resonance (FMR) based MRM. Due to thousand-fold increase in MR signal standard industrial force microscopy cantilevers can be used in MRM as mechanical FMR sensors even under ambient conditions. Piezoresistive mechanical detector for FMR (Fig. 1) proposed in [1] has been successfully applied to study the modification of the FMR spectra of structured Co/CoO films [2] induced by a spatially modulated exchange bias. The micromagnetic probe tip localizes the FMR collective mode beneath the probe and provides true imaging capabilities.

Optical detection of photons emitted from NV centers for detecting MR is typically performed using sophisticated equipment with single-photon sensitivity. An alternative non-optical technique consisting in the direct photoelectric readout of the electron-spin resonance of NV centers which was recently pre-

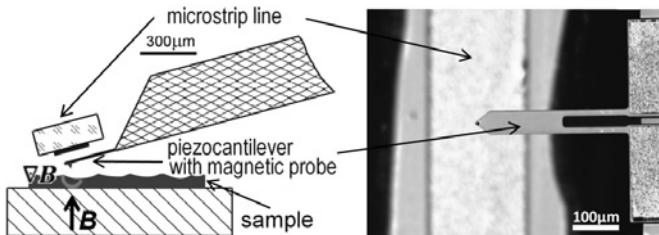


**Fig. 1.** Piezoresistive mechanical detector of FMR.

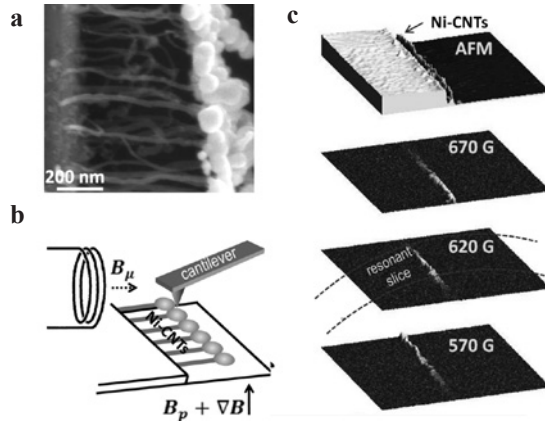


**Fig. 2.** Selective actuation of the nanotube array (a) by means of FMR induced in the array under combined action of magnetic and rf fields (b). AFM (top) and oscillation images (c) showing displacement of the actuated region by the applied magnetic field.

sented in [3] could potentially greatly simplify MRM instrumentation based on the NV-centers.

Another non-traditional MRM application is related to observation of mechanical oscillations in nanostructured sample excited by MR. We introduced the use of FMR to actuate mechanical resonances in as grown arrays of carbon nanotubes loaded with Ni particles (Ni-CNTs) (Fig. 2a) [4]. The vibrations of the Ni-CNTs are actuated by relying on the driving force that appears due to the FMR excited in the Ni particles. The Ni-CNT oscillations are detected mechanically by a standard atomic force microscopy (AFM) cantilever (Fig. 2b). The acquired oscillation images of the Ni-CNT uniform array (Fig. 2c) reveal clear maxima in the spatial distribution of the oscillation amplitudes. We attribute these maxima to the “sensitive slices”, i.e. the spatial regions of the Ni-CNT array where the FMR condition is met. Similar to MR imaging the sensitive slice is determined by the magnetic field gradient and moves along the Ni-CNT array as the applied magnetic field is ramped. This remote actuation can be effectively implemented also for arrays of other magnetic nanomechanical resonators.

The MRM as fully three-dimensional nanoscale-resolution scanned probe technique is improving rapidly and its successful applications confirm this and indicate its promising potential.

1. Volodin A. *et al.*: Rev. Sci. Instrum. **76**, 063705 (2005)
2. Volodin A. *et al.*: Appl. Phys. Lett. **85**, 5935 (2004)
3. Bourgeois E. *et al.*: Nature Comm. **6**, 8577 (2015)
4. Volodin A. *et al.*: ACS Nano **7**, 5777 (2013)

## Recent Developments in Microwave & Magnetic Resonance Detection of Explosive/Illicit Materials

**B. Z. Rameev<sup>1,2</sup>, B. Çolak<sup>3</sup>, İ. S. Ünver<sup>1</sup>, and G. V. Mozzhukhin<sup>1</sup>**

<sup>1</sup> Gebze Technical University, Gebze/Kocaeli 41400, Turkey, rameev@gtu.edu.tr

<sup>2</sup> Zavoisky Physical-Technical Institute, Russian Academy of Sciences, Kazan 420029,  
Russian Federation

<sup>3</sup> Karabük University, Karabük 78050, Turkey

The detection of explosives and illicit substances is a very important problem nowadays. In the aviation and public security, there is a problem of non-invasive detection of the explosives in the baggage, suits, cars, and others. Especially, improvised explosive devices (IEDs) made of homemade explosive materials has become an issue of growing importance. It has been shown that both time-domain NMR and MW dielectric spectroscopy are potentially very effective techniques to detect content of concealed liquids [1–3]. The later technique could be applied in combination with time-domain NMR to obtain better discrimination between benign and threat liquids especially for the case of very large group of liquids (i.e. in the situation that usually met in air-check points). In this work, recent developments in the field of magnetic resonance and microwave detection of liquid substances are reviewed.

The work was supported by NATO Science for Peace and Security Programme, NATO SPS project no. 985005 (G5005) and East Marmara Development Agency (MARKA), project no. TR42/16/ÜRETİM/0013.

1. Rameev B.Z., Mozzhukhin G.V., Aktaş B.: *Appl. Magn. Reson.* **43**, no. 4, pp. 463–467 (2012)
2. Apih T., Rameev B., Mozzhukhin G., Barras J., eds.: *Explosives Detection using Magnetic and Nuclear Resonance Techniques*, NATO Science for Peace and Security Series B: Physics and Biophysics, Dordrecht, The Netherlands: Springer, 2014.
3. Divin Y., Lyatti M., Poppe U., Urban K.: *Physics Procedia* **36**, 29–34 (2012)

## Advantages of SLASH (Slow Low Angle SHot) Sequence in Low-Field MRI of Hyperpolarised Gases

**K. Safullin<sup>1,2</sup>, P.-J. Nacher<sup>2</sup>, and C. Talbot<sup>2</sup>**

<sup>1</sup> Kazan Federal University, Kazan 420008, Russian Federation, kajum@inbox.ru

<sup>2</sup> Laboratoire Kastler Brossel, ENS, UPMC, CNRS, Coll. Fr., Paris 75005, France, nacher@lkb.ens.fr

Lung MRI using polarised  $^3\text{He}$  (or  $^{129}\text{Xe}$ ) gas provides a detailed information about condition of lung airways, ventilation properties, function and microstructure [1, 2]. MRI of hyperpolarised gases is usually performed with fast data acquisition but high spatial resolution lead to rapid signal attenuation induced by gas diffusion.

We introduce a  $k$ -space sampling scheme suitable for Slow Low Angle SHot (SLASH) acquisition and report on its advantages over traditional fast acquisition strategies (FLASH). The proposed  $k$ -space sampling strategy consists of a series of anisotropic partial acquisitions with a reduced resolution in the read direction [3]. It allows to significantly reduce diffusion-induced signal attenuation but still provides a high isotropic resolution and/or an increased signal-to-noise ratio (SNR). Slow acquisition requires long  $T_2$  values in lungs which occurs at low magnetic fields.

The experimental demonstration of SLASH imaging advantages is performed on sets of phantom cells filled with hyperpolarised  $^3\text{He}$ - $\text{N}_2$  gas mixtures using a low-field MRI setup [4] at 2.7 mT.  $^3\text{He}$  was polarised by metastability exchange optical pumping technique up to 40–50%. Obtained SLASH images of gas cells have higher spatial resolution and SNR than FLASH images. Our results show that SLASH imaging also allows to measure apparent diffusion coefficients for an extended range of times.

This work was supported in part by a EU Marie Curie Research and training network (PHeLINet) and by the FPGG (Pierre-Gilles de Gennes) foundation.

1. Möller A., Harald E. *et al.*: *Magnet. Reson. Med.* **47**(6), 1029 (2002)
2. van Beek, Edwin J.R. *et al.*: *J. Magn. Reson. Im.* **20**(4), 540 (2004)
3. Safullin K., Nacher P.-J., Talbot C.: *J. Magn. Reson.* **227**, 72 (2013)
4. Nacher P.-J., Pellisier M., Tastevin G.: *Proc. Intl. Soc. Mag. Reson. Med.* **15**, 3290 (2007)

## Double NMR-NQR for Studies of N-14 Nuclei

**G. V. Mozzhukhin<sup>1</sup>, D. A. Shulgin<sup>1</sup>, I. G. Mershev<sup>2</sup>, and B. Z. Rameev<sup>1,3</sup>**

<sup>1</sup> Gebze Technical University, Gebze/Kocaeli 41400, Turkey, mgeorge@gtu.edu.tr

<sup>2</sup> Immanuel Kant Baltic Federal University, Kaliningrad 236014, Russian Federation

<sup>3</sup> Zavoisky Physical-Technical Institute, Russian Academy of Sciences, Kazan 420029, Russian Federation, Russian Federation

Nuclear Quadrupole resonance (NQR) of nitrogen nuclei  $^{14}\text{N}$  in solids is an important tool for studies of molecular crystals. However, the NQR spectra of N nuclei are in low frequency range (100 kHz–6 MHz). Besides, the nitrogen ratio in the case of large organic molecules are usually small in comparison with hydrogen atoms. Thus, the signal-to-noise ratio (SNR) of NQR signals is rather small. On the other hand, it is possible to improve the SNR of  $^{14}\text{N}$  using double resonance approaches. In an organic material, the  $^1\text{H}$  nuclear magnetic resonance (NMR) may be used for detection of weak signal of the quadrupole  $^{14}\text{N}$  nuclei neighboring to the resonating protons. The following double resonance approaches are commonly applied: i) detection of a change in NMR signal intensity after so-called level-crossing procedure in the double NQR-NMR system; ii)  $^{14}\text{N}$  NQR enhanced by Zeeman pre-polarization or by  $^1\text{H}$ – $^{14}\text{N}$  level crossing after a preparatory static (not necessary homogeneous) magnetic field; iii) triple resonance method or quadrupole-quadrupole enhanced NQR; iiiii) an approach based on cross-relaxation enhancement by application of a low magnetic field [1, 2].

In this work, we report the results of studies based on the level-crossing approach. This method is based on the spin polarization transfer between the proton and nitrogen subsystems during adiabatic demagnetization of the sample. The procedure consists of the following steps: 1) The sample is polarized at high fields (in our case, it is 0.575 T that corresponds to the proton resonance frequency of about 24.48 MHz). 2) The sample is transferred from a high-field region in the NMR probe to a zero field in NQR probe. 3) the  $^{14}\text{N}$  quadrupole system is saturated by RF irradiation. 4) the saturated sample is moved back to the high field region for the proton NMR detection. During this transfer, the proton NMR energy levels and nitrogen NQR levels “crosses” (i.e. the difference between the  $^1\text{H}$  and  $^{14}\text{N}$  levels became equal to each other for a short time) that results in an attenuation of the proton NMR signal.

Our experimental system includes a two-channel Apollo Tecmag NMR/NQR console, NMR probe for 24.5 MHz, homemade NQR probe for 200 kHz–6 MHz, homemade electronic unit to control a pneumatic transfer between the NMR & NQR probes, inductively switched pneumatic valves, an air pump with pressure tank, a PTFE pneumatic transfer and plastic feeding lines. The distance between NMR and NQR probes is near 50 cm. The cycle time is near 40 ms. The urea  $\text{CO}(\text{NH}_2)_2$  and carbamazepine  $\text{C}_{15}\text{H}_{12}\text{N}_2\text{O}$  samples have been studied using the

double resonance setup. Possible applications of the developed double-resonance spectrometer for various NQR experiments are also discussed.

The work was supported by NATO Science for Peace and Security Programme, NATO SPS project no. 985005 (G5005) and Research Fund of Gebze Technical University, grant no. BAP 2015-A-19). D. Shulgin acknowledges the support of TÜBİTAK under 2216-Research Fellowship Programme for International Researchers.

1. Blinc R., Apih T., Seliger J.: *Appl. Magn. Reson.* **25**, 523–534 (2004)
2. Mozzhukhin G.V., Rameev B.Z., Kupriyanova G.S., Aktaş B. in: *Magnetic Resonance Detection of Explosives and Illicit Materials* (T. Apih, B. Rameev, G. Mozzhukhin, J. Barras, eds.), NATO Science for Peace and Security Series B: Physics and Biophysics, Springer, 2014, pp. 45–59.

## EPR Study of Special Cases of the Jahn-Teller Effect Realized in the Fluorite Type Crystals with d-Ion Dopants

V. A. Ulanov<sup>1,2</sup>

<sup>1</sup> Kazan State Power Engineering University, Kazan 420066, Russian Federation, ulvlad@inbox.ru

<sup>2</sup> Zavoisky Physical-Technical Institute, Russian Academy of Sciences, Kazan 420029, Russian Federation

Most of the impurity d-ions forming paramagnetic complexes in the fluorite type crystals have the doubly or triply degenerated ground orbital states and, consequently, are the objects displaying the Jahn-Teller effect. In the fluorites the impurity d-ions form the paramagnetic  $[\text{MeF}_8]^{k-}(\text{O}_h)$  clusters. Among them the clusters with triply degenerated ground orbital states display peculiar features arising mainly from two facts: 1) the number of nuclei in such cluster is 9; 2) the ground orbital states of the cluster are mixed by spin-orbit interaction. As consequences, the schemes of multimode vibronic interactions are possible in the  $[\text{MeF}_8]^{k-}(\text{O}_h)$  clusters with triply degenerated ground orbital states, and tunneling motion of these clusters between their adiabatic wells can be realized both with and without spin flips. It was found by EPR that the complexes with degenerated ground orbital states have the multiwell ground potential sheets. At low temperatures the magnetic properties of the complexes can be described by static spin Hamiltonian, but some peculiarities are observed in their EPR spectra at special orientations ( $B_0 \parallel \langle 001 \rangle$ ,  $B_0 \parallel \langle 110 \rangle$  and  $B_0 \parallel \langle 111 \rangle$ ). These peculiarities arise due to the reorientations of the complex with and without spin flip realizing as tunneling and overbarrier motion of the complexes between potential wells. At high temperatures the reorientations via excited vibronic states become very intensive.

Some special cases of the Jahn-Teller effect were revealed by EPR in the fluorite type crystals activated by d-ions: 1) the Jahn-Teller effect on the ground triply degenerated state accompanied with a pseudo-Jahn-Teller effect resulting in a very huge shift of the impurity d-ion into off-center position of a tetragonal type ( $\text{Cr}^{2+}$  in  $\text{BaF}_2$ ,  $\text{Cu}^{2+}$  in  $\text{SrF}_2$  and  $\text{BaF}_2$ ); 2) the Jahn-Teller effect on the doubly degenerated ground orbital states realized in the  $[\text{MeF}_8]^{k-}(\text{O}_h)$  impurity clusters associated with interstitial fluorine ions ( $\text{Cr}^{3+}$  and  $\text{Ti}^{3+}$  in  $\text{SrF}_2$ ); 3) pseudo-Jahn-Teller effect on the ground singlet orbital states of a  $[\text{MeF}_8]^{k-}(\text{O}_h, {}^{2S+1}\text{F})$  clusters stimulating the association of the cluster with an interstitial fluorine ion ( $[\text{CoF}_8]^{6-}$  impurity clusters associated with  $\text{F}_{\text{int}}^-$ ).

The Jahn-Teller effect producing a displacement of a paramagnetic ion from the geometric centre of the coordination polyhedron towards an off-centre position can be realized in the cases when the ion is far lighter than the ligand atoms and metal-ligand coordination bondings are weaker than ligand-lattice bondings. In such cases there must be realized an effective vibronic mixing of the excited electronic states to the high-symmetry ground state by low-symmetry nuclear motions. Our EPR data for  $\text{Cu}^{2+}$  in  $\text{SrF}_2$  and  $\text{BaF}_2$  indicate that a position of the



impurity copper is strongly non-central; it is shifted along the  $C_{4v}$  symmetry axis from the centre of its coordinational polyhedron by a distance of about 0.1 nm. This fact points at the Jahn-Teller effect of the  $(T_{2g} + A_{2u}) \otimes (a_{1g} + e_g + t_{1u})$  type producing six equivalent wells on the surface of the lowest adiabatic potential sheet. At temperatures below 30 K the  $[\text{CuF}_8]^{6-}(\text{O}_h)$  complex is mainly localized within one of the six adiabatic wells on the ground vibronic level; such localization corresponds to a  $[\text{CuF}_4\text{F}_4]^{6-}(\text{C}_{4v})$  complex. There is some possibility for the complex to cross a potential barrier and come into an adjacent well by tunneling and overbarrier jumps. Due to such molecular motion, the electron spin-lattice relaxation rate  $1/T_1$  grows rapidly on heating and its temperature dependence can be described by an Orbach-type process with excitations to two excited vibronic states of energy, 83 and 174  $\text{cm}^{-1}$ .

For the  $\text{Cr}^{3+}$  and  $\text{Ti}^{3+}$  impurity complexes formed in  $\text{SrF}_2$ , the Jahn-Teller effect is realized on a doubly degenerated ground orbital state which arises accidentally due to interaction of an impurity ion with interstitial fluorine ion locating in a tetragonal position. Negative charge of the latest compensates the excess positive charge of the impurity ion. In these cases  $E \otimes (b_1 + b_2)$  vibronic interaction scheme becomes very effective [2]. As result, each  $[\text{CrF}_4\text{F}_4\text{F}_{\text{int}}]^{6-}(\text{C}_{4v})$  complex acquires the four-well ground adiabatic potential sheet and each  $[\text{TiF}_4\text{F}_4\text{F}_{\text{int}}]^{6-}(\text{C}_{4v})$  complex the two-well ground potential sheet. There were observed the temperature dependences in the EPR spectra of the complexes which were attributed to the tunneling and overbarrier motions of the complexes under investigation.

EPR study of the  $\text{BaF}_2:\text{Co}$  crystals revealed two types of the paramagnetic complexes. First were the  $[\text{CoF}_8]^{6-}(\text{O}_h, {}^4\text{F})$  complexes being in the  ${}^4\text{A}_2$  ground orbital singlet states with effective spins  $S = 1/2$  and the second were the associates of the  $[\text{CoF}_8]^{6-}(\text{O}_h, {}^4\text{F})$  complexes with interstitial fluorine ions (the tetragonal  $[\text{CoF}_4\text{F}_4\text{F}_{\text{int}}]^{6-}(\text{C}_{4v})$  complexes). Relative concentration of the tetragonal complexes was rather high, and this fact pointed at a dipole instability of the  $[\text{CoF}_8]^{6-}(\text{O}_h, {}^4\text{F})$  complexes leading to energetically profitable process resulting in the formation of the  $[\text{CoF}_4\text{F}_4\text{F}_{\text{int}}]^{6-}(\text{C}_{4v})$  associates.

## Proton NMR Dipolar-Correlation Effect as a Method for Investigating Segmental Diffusion in Polymer Melts

**A. Lozovoi<sup>1,2</sup>, C. Mattea<sup>1</sup>, N. Fatkullin<sup>2</sup>, and S. Stapf<sup>1</sup>**

<sup>1</sup> Department of Technical Physics II, Technische Universität Ilmenau, 98684, Germany, Artur.Lozovoi@tu-ilmenau.de

<sup>2</sup> Kazan Federal University, Kazan 420008, Russian Federation, nfatkull@gmail.com

During many decades in the investigations of polymer melts it was postulated that the main contribution to the relaxation effects is a result of the intramolecular magnetic dipole-dipole interactions between protons belonging to the same polymer segment. In [1–3] it was theoretically argued and experimentally shown, that this assumption is incorrect, at least for the proton spin-lattice relaxation in polymer melts. Moreover, the separation of inter- and intramolecular contributions to the spin-lattice relaxation rate, and the observation of their respective frequency dispersion, allows one to extract the time-dependence of the relative mean-squared displacements of polymer segments of different polymer chains and also to discriminate between different models of polymer dynamics. In this research the same approach is used to probe the spin-spin relaxation.

A novel method for the investigation of segment displacements in high molecular weight polymer melts is presented. Based on the Dipolar-Correlation Effect (DCE) of the proton Hahn Echo (HE), the DCE build-up function of the HE signal at time moments  $t$  and  $t/2$  is introduced  $I^{DC}$ . The initial rise of this function at times  $t < T_2^{\text{eff}}$ , where  $T_2^{\text{eff}}$  is the effective spin-spin nuclear magnetic relaxation time, contains additive contributions from both inter- and intramolecular magnetic dipole-dipole interactions. In this scenario the intermolecular term of this function depends on the relative mean squared displacements of polymer segments from different macromolecules. This provides experimental access to polymer segment displacements in high molecular weight polymer melts at the millisecond range. This time scale is hardly accessible by other experimental techniques. The expression, which describes the connection between  $I^{DC;\text{inter}}$  and  $\langle \tilde{r}^2(t) \rangle$ , is as follows:

$$\langle \tilde{r}^2(t) \rangle = \left( \frac{9\pi}{5} f(\alpha) \sqrt{\frac{2}{3\pi}} \gamma^4 \hbar^2 n_s \frac{t^2}{\ln\left(\frac{1}{1 - I^{DC;\text{inter}}(t)}\right)} \right)^{\frac{2}{3}}. \quad (1)$$

The feasibility of the method is illustrated by experimental investigations of protonated and deuterated polybutadiene melts (PB) with molecular mass 196000 at temperatures of 308 K and 338 K [4]. The experiments are carried out on the Bruker Minispec mq 40 in Technical University of Ilmenau (Germany). The time dependence of MSD is presented on Fig. 1 with the use of time-temperature superposition. The observed exponent of the dependence  $\alpha = 0.32 \pm 0.03$  is close

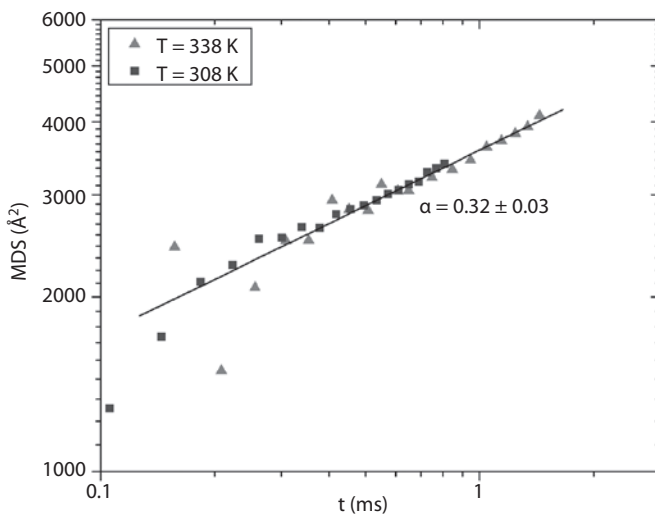


**Fig. 1.** The time dependence of the mean-squared displacements for polybutadiene of  $M = 196000$  at  $T = 308$  K (■) and  $T = 338$  K (▲). Time-temperature superposition is used.

to the tube-reptation model predictions. The intermolecular proton magnetic dipole-dipole contribution to the total proton HE NMR signals is found out to be larger than 50% and increasing with time, which contradicts the corresponding predictions of the tube-reptation model.

1. Kimmich R., Fatkullin N., Seitter R.-O., Gille K.: *J. Chem. Phys.* **108**, 2173 (1998)
2. Kehr M., Fatkullin N., Kimmich R.: *J. Chem. Phys.* **126**, 1 (2007)
3. Kehr M., Fatkullin N., Kimmich R.: *J. Chem. Phys.* **127**, 1 (2007)
4. Lozovoi A., Mattea C., Herrmann A., Roessler E.A., Stapf S., Fatkullin N.: *J. Chem. Phys.* **144**, 241101 (2016)

## Electron Transfer Pathways in Molecular Triads Centered by Aluminum Porphyrin

**Yu. E. Kandrashkin<sup>1</sup>, P. K. Poddutoori<sup>2</sup>, and A. van der Est<sup>2</sup>**

<sup>1</sup> Zavoiisky Physical-Technical Institute, Russian Academy of Sciences, Kazan 420029, Russian Federation, spinalgebra@gmail.com

<sup>2</sup> Department of Chemistry, Brock University, St. Catharines, L2S 3A1 Canada

Several types of the molecular complexes centered by aluminum(III) porphyrin (AlPor) have been assembled recently. They demonstrate a wide range of the photoexcited phenomena including intramolecular energy transfer and multi-step charge transfer. Here, we report on transient EPR (TREPR) studies of the charge-separated states of such triads with two different types of acceptors, free-base porphyrin (H2Por) and anthraquinone (AQ). The acceptors are covalently bound to the Al(III) metal via a linker and the donor tetrathiafulvalene (TTF) is attached by coordinating an appended pyridine to Al(III) on the opposite face of the porphyrin [1, 2]. The length of the bridge between AlPor and TTF has been varied by the incorporating varying numbers of phenyl groups.

Photoexcitation of the triad TTF-AlPor-H2Por in the liquid crystal 5CB leads to formation of the radical pair  $\text{TTF}^+\text{H2Por}^-$  at room temperature [1]. The analysis of the TREPR spectra shows that the main contribution to the signal comes from the singlet-born pairs. However some contribution from the triplet-born pairs is required to explain the time dependence of the spectra. The triplet contribution can be rationalized as resulting from partial formation of the charge-transfer states from the excited triplet state of H2Por.

In the triads with AQ as the acceptor, the TREPR signal of the radical pair  $\text{TTF}^+\text{AQ}^-$  has been observed in the glass phase (225 K) and at just above the glass transition (250 K) of the solvent *o*-dichlorobenzene [2]. The spectra at 225 K are well described by assuming a rigid environment and that the radical pair is formed by singlet electron transfer and has weak exchange coupling. Just above the glass transition (250 K) the spectrum changes dramatically and contributions from molecules in both the rigid and isotropic limits are observed. In the isotropic limit, the dipolar coupling term is averaged to zero and the *g*-anisotropy is also averaged resulting in a polarization pattern that is dominated by the exchange coupling. The analysis of the data indicates that the exchange coupling is negative. The time dependence of the spectra suggests that some triplet electron transfer also occurs and that spin selective recombination from the radical pair states with singlet character takes place.

The work was partially supported by RFBR, research project 16-03-00586 A.

1. Kandrashkin Yu.E., Poddutoori P.K., van der Est A.: Appl. Magn. Reson. **47**, 511 (2016)
2. Poddutoori P.K., Kandrashkin Yu.E., van der Est A.: ZPC, DOI 10.1515/zpch-2016-0826 (2016)

## Beating of Light During Photon Echo. Observation and Application

V. N. Lisin<sup>1</sup>, A. M. Shegeda<sup>1</sup>, and V. V. Samartsev<sup>1,2</sup>

<sup>1</sup> Zavoiisky Physical-Technical Institute, Russian Academy of Sciences, Kazan 420029,  
Russian Federation, valerylisin@gmail.com

<sup>2</sup> Kazan Federal University, Kazan 420008, Russian Federation

The term “echo” refers to coherent radiation from a medium in the form of a short pulse, caused by restoration of phase of separate radiators after the change of sign of their relative frequency. The frequency of the coherent radiation splits if a pulsed perturbation shifts the transition frequency of radiators for the different amount during echo-pulse. It is known that when two coherent waves of nearly same frequencies interfere, we get beats. The inverse period of the beats is equal to the frequency difference (splitting). The frequency splitting should be large enough to beat period was shorter than the duration of the echo-response and hence the beats of a waveform of an echo pulse can be observed.

In this way we measured Zeeman splitting of optical line  ${}^4I_{15/2} \rightarrow {}^4F_{9/2}$  of the impurity ion  $\text{Er}^{3+}$  in two crystal matrices  $\text{LuLiF}_4$  and  $\text{YLiF}_4$  [1] and the pseudo-Stark splitting of R1-line of  $\text{Cr}^{3+}$  ion in ruby [2].

It was shown that the pseudo-Stark splitting  $Z_E = 2\partial\nu/\partial E \cdot \langle E \rangle$  and Zeeman splitting  $Z_H = 2\partial\nu/\partial H \cdot \langle H \rangle$  are determined by the average values of the electric field  $\langle E \rangle$  and magnetic field  $\langle H \rangle$  of pulses over the optically excited volume.

It was also shown that inverse modulation period  $1/T$  of the echo waveform (see Fig. 1) is equal Zeeman splitting ( $1/T = Z_H$ ) or pseudo-Stark splitting ( $1/T = Z_E$ ):

$$1/T = Z_H = 2\partial\nu/\partial H \cdot \langle H \rangle, \quad 1/T = Z_E = 2\partial\nu/\partial E \cdot \langle E \rangle. \quad (1)$$

In the case of electric pulses (EP), see Fig. 1a, it was determined the value of the parameter  $2\partial\nu/\partial E = 0.214 \text{ MHzV}^{-1}\text{cm}$ . It is in good agreement with the results ( $0.228 \text{ MHzV}^{-1}\text{cm}$ ) [M. Cohen and N. Bloembergen (1964)]. The value of  $\langle E \rangle$  was calculated.

In the case of magnetic pulses (MP), see Fig. 1b, which field is directed along the C-axis of symmetry of the crystal matrix, it was considered that parameter  $2\partial\nu/\partial H \sim (g_e \pm g_g)$  is proportional to the difference (sum)  $g$ -factors of the excited  ${}^4F_{9/2}(g_e)$  and the ground  ${}^4I_{15/2}(g_g)$  states for  $\pi$ - ( $\sigma$ ) polarizations of the light pulses. It helped to find not only the difference or the sum of the  $g$ -factors of the ground and excited optical states, but the values themselves.

The  $g_e$  and  $g_g$  values to  $\text{YLiF}_4:\text{Er}^{3+}$  and  $g_g$  to  $\text{LuLiF}_4:\text{Er}^{3+}$  coincide with the known values. The value of the  $g$ -factor  $g_e$  to the excited state  ${}^4F_{9/2}$  in  $\text{LuLiF}_4:\text{Er}^{3+}$  was measured for the first time:  $g_e = 9.6$ .

In our study we measured the pseudo-Stark and Zeeman splitting of optical lines and determined electric parameter  $\partial\nu/\partial E$  and magnetic parameters  $g_e$  and  $g_g$  of echo active ions. The values of the electric and magnetic fields were

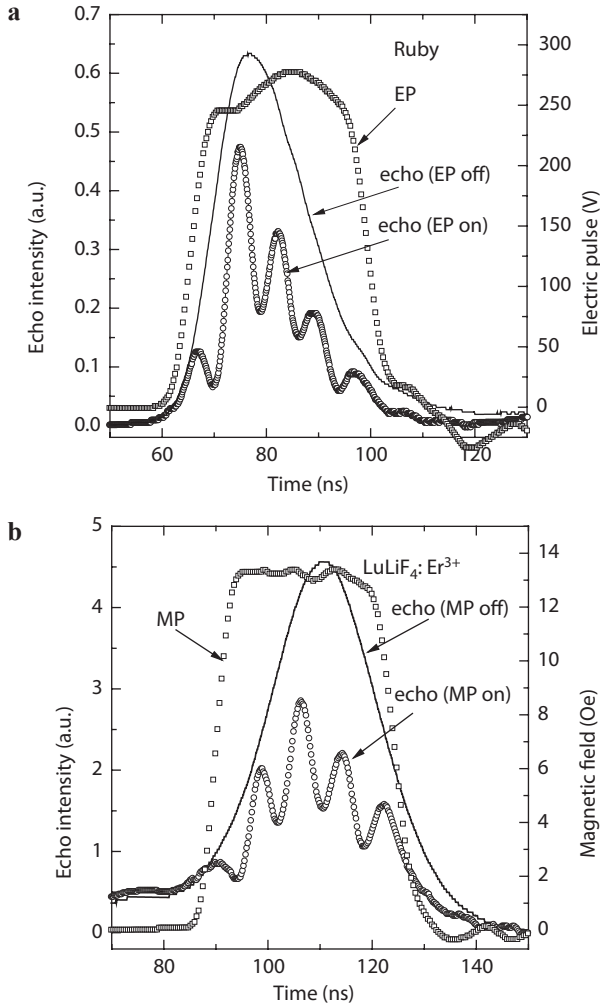


**Fig. 1.** Beating of light during photon echo under action: **a** electric, **b** magnetic pulse in a ruby (thickness is 4.5 mm) and LuLiF<sub>4</sub>:Er<sup>3+</sup> accordingly.

considered known (they were calculated). If parameter values are known, it is possible to determine the amplitude of the electric or magnetic pulses, using the relation (1). For example, if the electric or magnetic field created by the pulse changes the dipole-dipole interaction of the ion with the environment. This fact can be used to determine the distance to the centers of the environment by measuring the modulation period of the echo waveform.

The financial support of the Foundation for Basic Research (grant no. 14-02-00041a) and RAS program “Fundamental optical spectroscopy and its applications” is gratefully acknowledged.

1. Lisin V.N., Shegeda A.M., Samartsev V.V.: Laser Phys. Lett. **12**, 025701 (2015)
2. Lisin V.N., Shegeda A.M., Samartsev V.V.: Laser Phys. Lett. **13**, 075202 (2016)

## Conversions and Transformations: Deformation-Induced Chemical Bonding in Pharmaceutics

**D. S. Rybin<sup>1</sup>, G. N. Konygin<sup>1</sup>, V. E. Porsev<sup>1</sup>, D. R. Sharafutdinova<sup>2</sup>,  
G. G. Gumarov<sup>3</sup>, V. Yu. Petukhov<sup>3</sup>, I. P. Arsenyeva<sup>4</sup>, and V. V. Boldyrev<sup>5</sup>**

<sup>1</sup> Physical-Technical Institute UrB RAS, Izhevsk 426001, Russian Federation, dsrybin@ftiudm.ru

<sup>2</sup> A. E. Arbuzov Institute of Organic and Physical Chemistry KazSC RAS, Kazan 420088,  
Russian Federation, drsh@iopc.knc.ru

<sup>3</sup> Zavoisky Physical-Technical Institute, Russian Academy of Sciences, Kazan 420029,  
Russian Federation, gumarov@kfti.knc.ru

<sup>4</sup> Moscow State Open University, Moscow 107996, Russian Federation, arsenyeva\_i@mail.ru

<sup>5</sup> Institute of Solid State Chemistry and Mechanochemistry SB RAS, Novosibirsk 630128,  
Russian Federation, boldyrev@solid.nsc.ru

Studying the physical mechanisms of deformation induced transformations in molecular crystals and developing the methods of solid state mechanochemical synthesis resulted in the appearance of a new prospective trend in pharmaceutics. Without changing the chemical composition, one can transform a molecular crystal into a new state with unique physical-chemical properties, increasing the biochemical activity of the substance significantly. Thus, there appears a principal possibility of not only producing highly effective pharmaceutical products but also minimizing the cost and terms of their development.

The physical mechanisms of the deformation-induced structural transformations in molecular crystals, including morphological changes, amorphization and molecular polymorphous conversions in nano-dispersed bioinorganic compounds are discussed in this work. Integrated study using direct structural and structure-sensitive spectroscopic methods allowed obtaining the data on polymorphous transformations, taking place during mechanical activation in calcium gluconate monohydrate (CG).

One of the possible reasons for lattice polymorphous transformations and amorphization, observed in the course of mechanical activation of low-symmetry molecular crystals, might be the spatial molecular isomerization and complexation. It was revealed the formation of two-dimensional structures in the process of mechanical activation of bioinorganic compounds.

The reported study was partially supported by RFBR, research project no. 16-03-01131-a.

---



---

## SECTION 9

PERSPECTIVES OF MAGNETIC RESONANCE  
IN SCIENCE AND SPIN-TECHNOLOGY.  
THEORY OF MAGNETIC RESONANCE

## Advanced Pulse EPR Studies of the Water Oxidation Cycle in Photosynthesis

**W. Lubitz**

Max Planck Institute for Chemical Energy Conversion, Mülheim/Ruhr 45470, Germany,  
wolfgang.lubitz@cec.mpg.de

Advanced pulse EPR and related double resonance techniques are versatile tools for studying (bio)catalytic systems containing transition metals as active sites [1]. In the past such investigations have been impeded by fast magnetic relaxation and sensitivity problems of the methods used. Recently, these limitations have been overcome by performing the experiments at higher microwave frequencies (95 GHz, W-band) and by the development of ELDOR-detected NMR (EDNMR) [2], a double resonance method with intrinsic high sensitivity and large bandwidth compared to the traditionally employed ENDOR technique.

In this contribution the catalytic water oxidation reaction in photosystem II (PSII) of oxygenic photosynthesis is presented as an example. In this large protein complex water oxidation takes place at an oxygen-bridged tetranuclear manganese calcium cluster ( $\text{Mn}_4\text{O}_x\text{Ca}$ ) located in the D1 protein subunit of PSII [3]. The cofactor's reaction cycle is comprised of 5 distinct redox intermediates  $S_n$ , where the subscript indicates the number of stored oxidizing equivalents in the manganese cluster ( $n = 0-4$ ) required to split two water molecules and

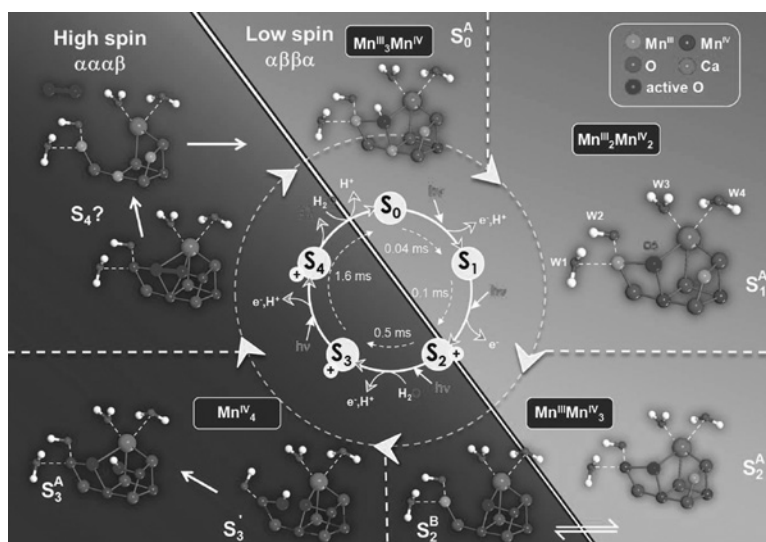


**Fig. 1.** Water oxidation cycle in PSII of oxygenic photosynthesis, showing the structures of the reaction intermediates, the oxidation states of the Mn ions and the 2 water molecules entering the cycle leading to  $\text{O}_2$  release in the S3-S4-S0 transition [7].

release one O<sub>2</sub>. A redox-active tyrosine residue couples the fast photoinduced single-electron charge separation to the slow catalytic four-electron water oxidation process. The S-states are trapped by laser flash/freeze techniques and their electronic structure is studied by advanced EPR techniques (ENDOR, ESEEM/HYSCORE, EDNMR). These data are corroborated by DFT calculations. The results give information on the spin and oxidation states of the manganese ions and the spin coupling in the cluster, the function of the Ca<sup>2+</sup>, the effect of the amino acid surrounding, and the binding, location and reaction dynamics of the 2 substrate water molecules, the O-O bond formation and the release of molecular oxygen [4, 5]. A robust model for the water oxidation mechanism is derived, in which the spin states are playing an important role [6, 7]. A scheme with the structure of the S-state intermediates is shown in Fig. 1. The information gained from PSII can be used for the design of bioinspired catalysts for water oxidation, which will also be discussed.

1. Cox N., Nalepa A., Pandelia M.E., Lubitz W., Savitsky A.: *Methods in Enzymology*, vol. 563, pp. 211–249. Oxford: Elsevier 2015.
2. Cox N., Lubitz W., Savitsky A.: *Mol. Phys.* **111**, 2788–2808 (2013)
3. Umena Y., Kawakami K., Shen J.-R., Kamiya N.: *Nature* **473**, 55–60 (2011); Suga M. *et al.*: *Nature* **517**, 99–103 (2015)
4. Cox N., Pantazis D.A., Neese F., Lubitz W.: *Acc. Chem. Res.* **46**, 1588–1596 (2013)
5. Cox N., Retegan M., Neese F., Pantazis D.A., Boussac A., Lubitz W.: *Science* **345**, 804–808 (2014)
6. Krewald V., Retegan M., Cox N., Messinger J., Lubitz W., DeBeer S., Neese F., Pantazis D.A.: *Chem. Sci.* **6**, 1676–1695 (2015)
7. Krewald, V., Retegan, M., Neese F., Lubitz W., Pantazis D., Cox N.: *Inorg. Chem.* **55**, 488–501 (2016)

## Perspectives of Hyperpolarization and its Role in Structural Biology

**R. Kaptein**

Bijvoet Centre, Utrecht University,  
Utrecht 3584 CH, The Netherlands, r.kaptein@uu.nl

After many years of lingering existence, the field of hyperpolarization has seen a renaissance during the last 10 to 15 years. In this lecture I will give an overview of the developments in this field, in particular on DNP, CIDNP and related radical-pair phenomena, and parahydrogen based polarization such as PHIP and SABRE. After a short historic introduction the present status and some future perspectives will be discussed with special focus on their role in structural biology.

Renewed interest in DNP stems from two major developments. First, the fact that high-field gyrotrons became available provided a large boost to solid state NMR studies of large proteins [1]. Secondly, in “Dissolution DNP” polarization is generated at low field (1–2 °K) and after rapid thawing transferred to the spectrometer field [2]. This allows applications in solution NMR and MRI. Applications of Photo-CIDNP range from solid state studies of large biological complexes [3] to detailed mechanisms of photoreactions in solution [4]. Among the many manifestations of the radical-pair mechanism an interesting one is that in bird navigation [5] as this may be one of the rare examples of quantum effects in biology. Finally, parahydrogen based polarization as observed in PHIP and SABRE experiments can be extremely large. It can be used in material science [6] and (potentially) in MRI [7]. A description of SABRE in terms of level anti-crossings (LACs) provides a qualitative understanding of the effect [1].

1. Griffin and coworkers: *Accounts Chem. Res.* **46**, 1933 (2013)
2. Ardenkjaer-Larsen and coworkers: *PNAS* **100**, 10158 (2003)
3. Jeschke, Matysik, Ivanov *et al.*: *J. Chem. Phys.* **144**, 144202 (2016)
4. Morozova, Kaptein, Yurkovskaya: *J. Phys. Chem. B* **116**, 12221 (2012)
5. Hore, Mouritsen *et al.*: *PNAS* **113**, 4634 (2016)
6. Koptug, Kaptein *et al.*: *ChemCatChem* **4**, 2031 (2012)
7. Duckett and coworkers: *Prog. NMR Spectr.* **67**, 1–48 (2012)
8. Ivanov, Kaptein *et al.*: *Prog. NMR Spectr.* **81**, 1–36 (2014)

---

## **Gd(III) Based Markers for Pulsed Dipolar Spectroscopy: Features, Theory, Instrumentation and Optimization of Measurements**

**A. Raitsimring**

Department of Chemistry and Biochemistry, University of Arizona, Tucson, Arizona 85721-0041,  
USA, arnold@u.arizona.edu

This presentation addresses various aspects of the recently introduced Gd(III)-based tags for measuring distance, distance variation and distance distribution between attachment sites in biological objects by pulsed dipolar spectroscopy (PDS). The advantages, such as the ability to perform measurements at cryogenic temperatures and high repetition rates simultaneously, the use of very short flipping and observation pulses without mutual interference, the lack of orientational selectivity, as well as the shortcomings, such as the limited mw operational frequency range, intrinsically small amplitude of oscillation related to dipolar interactions and the need for specialized equipment to realize the potential of these tags and avoid distortions in PDS time domain patterns are discussed. The particulars of Gd(III) tags phase relaxation are considered in order to reach optimal pulse settings. Finally, *pro et contra* of traditional nitroxide labels vs Gd(III) tags are deliberated as well as feasible options to further increase sensitivity and range of distance when the latter are used.

This work was supported by two consecutive BSF (Bi-National Science Foundation, USA-Israel) four-year grants (2002175;2006179) to A. R. and D. Goldfarb; PNNL (EMSL) User Support Award, ID: 44607; and National Science Foundation awards (DBI-0139459, DBI-9604939 and BIR-9224431). D-band experiments were performed at Argonne National Laboratory under the supervision and direct participation of Dr. O. Poluektov, and were supported by the U.S. Department of Energy, Office of Basic Energy Sciences, Division of Chemical Sciences, Geosciences, and Biosciences, under Contract W-31-109-Eng-38.

## Can Spin Chemistry Explain all Effects of Electromagnetic Fields on Living Organisms?

**G. I. Likhtenshtein**

Department of Chemistry, Ben-Gurion University, Beer-Sheva, Israel, gertz@bgu.ac.il;  
Institute of Problems of Chemical Physics, Russian Academy of Science, Chernogolovka,  
Moscow Region, Russian Federation

During the last six decades, the escalated use of various wireless communication devices, which emit non-ionizing radiofrequency radiation (RFR) of audio and TV broadcasting and high frequency electromagnetic fields (MV) of wireless communication technology, have raised concerns among the general public regarding the potential adverse effects on human health. In spite of large body of investigation of the effects of *in vitro* and *in vivo* exposures of animals and humans or their cells to RF and MV fields, data reported in scientific publications are contradictory. This minireview is an attempt of critical analysis of these data from point of basic conceptions of spin chemistry, that is, radical pair mechanism (RPM) and resonance nature of electromagnetic radiation absorption in low and mediate permanent magnetic field (PMF). Potential affection of very strong PMF on anisotropic diamagnetic system, say, biological lipid membranes and fluidity biological liquids can be also taken in consideration. According to theory, in low magnetic field of earth resonance non-heat low intensity of the RF can be observed and be biologically effective in area of about 1 MHz, which related to hyper fine electron-spin nuclear-spin interactions. Molecular compass models of magnetoreception of birds and some other living organisms as result of RF adsorption in the earth magnetic field is excellent demonstration of advantages of modern spin chemistry. As far as concern the MV radiation, such effects can be expected in mediate and strong PMF in radical processes such as oxidation of lipid, proteins, DNA and other molecules, and corresponding steps in active centers of metalloenzymes. Similar fields are widely used in magnetic tomography and magnetic bracelets. Various non resonance effects of permanent and electromagnetic fields of different strength and frequency, including geomagnetic phenomena, on physiological, biochemical and biophysical properties of living organism and its components were reported. The Lorentz magnetic forces of RF and MW fields are very weak and also can not provide a magneto-reception mechanism. Therefore all findings which don't fit to "a Procrustean bed" of the spin chemistry can be considered as annoying artefacts or intriguing challenging problems for future.

## **EPR Spectroscopy of Pulse Double Electron-Electron Resonance (PELDOR). Some Results and Prospects**

**Yu. D. Tsvetkov**

V. V. Voevodsky Institute of chemical kinetics and combustion SB RAS, Novosibirsk-630090,  
Russian Federation

The report will discuss the main features of PELDOR spectroscopy to studies of the dipolar spin-spin interactions-determining the distances and distribution functions at the distances for pairs of spins, determine the number of spins in the group, studying the characteristics of the spatial organization of the spin system (fractal effects, geometry radical pairs). Examples will be given of the study of radical and spin-labeled systems using PELDOR and identifies opportunities for future applications of PELDOR.

## Revealing Structures of Immobilized Catalysts by Solid State NMR

**G. Buntkowsky**

Institute of Physical Chemistry, Technical University Darmstadt, Darmstadt, Germany D-64287,  
gerd.buntkowsky@chemie.tu-darmstadt.de

Despite the tremendous importance of heterogeneous catalysis for large-scale industrial chemistry, there is still a huge gap in detailed knowledge of the processes and reaction intermediates on the surfaces of the catalysts. The combination of conventional and Dynamic Nuclear Polarization (DNP) enhanced solid-state NMR spectroscopy, X-ray diffraction, electron microscopy, chemical modelling and quantum chemical calculations has evolved into one of the most powerful characterization tools to fill this gap and study solid catalysts and chemical processes on their surface. These techniques give an unprecedented view in the chemistry of immobilized homogeneous transition metal catalysts, supported e.g. on silica or crystalline nanocellulose (CNC) or polymer based core shell structures as carriers or reactants and reaction intermediates on transition metal nanoparticles (MNPs). The contribution presents recent examples from our group about solid-state NMR spectroscopic characterizations of mono- or binuclear Rhodium, Ruthenium and Iridium catalysts. The focus is set to the immobilization of Wilkinson's type catalyst and dirhodium-acetate dimer (Rh<sub>2</sub>ac<sub>4</sub>). These are linked covalently to high-surface silica or crystalline nanocellulose support materials, employing amine, phosphine, pyridyl or carboxyl functions on the surface of the support materials. Combinations of <sup>13</sup>C, <sup>15</sup>N, <sup>29</sup>Si and <sup>31</sup>P CP MAS, J-resolved, <sup>31</sup>P MAS and HETCOR solid-state NMR techniques are employed to monitor the preparation of the catalyst. Moreover, by DNP enhanced solid-state NMR it is feasible to detect different carboxyl and amine binding sites in natural abundance at a fast time scale. The interpretation of the experimental chemical shift values for different binding sites is corroborated by quantum chemical calculations on dirhodium model complexes.



# Supramolecular Organization: What Can We Learn from Magnetic Resonance

**H. W. Spiess**

Max-Planck-Institute for Polymer Research, Mainz D-55021, Germany,  
spiess@mpip-mainz.mpg.de

Supramolecular functional nanostructures are in the focus of current soft matter science. They occur in advanced synthetic as well as in biological systems through self-assembly of carefully chosen building blocks. Secondary interactions such as hydrogen bonding, aromatic pi-interactions, electrostatic forces, and chirality are of central importance. Here, NMR spectroscopy provides unique and highly selective information on structure and dynamics of such systems, e.g., on hydrogen bond networks, stacking, and cooperative molecular motions of the building blocks in pi-conjugated polymers, supramolecular assemblies based on disc-like entities, and metal organic frameworks. Moreover, EPR spectroscopy provides unique information about thermoresponsive polymers and partially disordered proteins.

For full structural and dynamic elucidation, the spectroscopic data have to be combined with other techniques, in particular X-ray scattering, microscopy, dielectric spectroscopy and last, but not least, quantum chemical calculations. Recent examples of such multi-technique approaches will be presented and the findings will be related to the function of such materials, such as conductivity.

1. Hansen M.R., Graf R., Spiess H.W.: *Acc. Chem. Res.* **46**, 1996–2007 (2013)
2. Graf R., Hansen M.R., Hinderberger D., Muennemann K., Spiess H.W.: *Phys. Chem. Chem. Phys.* **16**, 9700–9712 (2014)
3. Hansen M.R., Graf R., Spiess H.W.: *Chem. Rev.* **116**, 1272–1308 (2016)

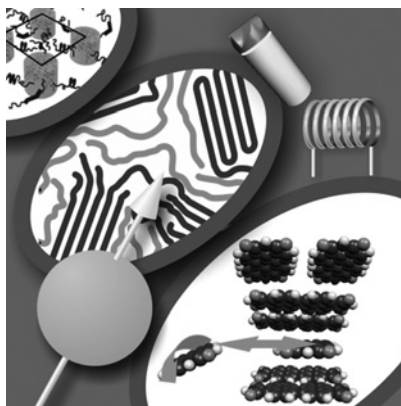


**Fig. 1.** Magnetic resonance techniques for elucidating structure and dynamics of supramolecular systems.

## Unexpected Changes in EPR Spectra of Liquid Solutions of Nitroxide Biradicals

**A. I. Kokorin**

N. Semenov Institute of Chemical Physics RAS, Moscow 119991, Russian Federation,  
alex-kokorin@yandex.ru

Less than in two years after synthesis of first stable nitroxide biradicals, several authors have independently created quantitative theory of fast intramolecular spin exchange [1–3], which was augmented for the case of slow electron spin exchange [4] and presented in details in [5]. The basic principle of these theories is the isotropy of such spin exchange, hence, the central symmetry of EPR spectra of biradicals in low-viscous solutions. In viscous solvents such as ionic liquids (ILs), till the last year, EPR spectra were also symmetric [6, 7].

Present paper presents our recent experimental results obtained for three biradicals:

B3 =  $R_5^{NO}-CH=N-N=CH-R_5^N$ , B4 =  $R_5^{NO}-CH=N-N=C(CH_3)-R_5^N$ , and C5 =  $R_5^N-C(CH_3)=N-N=C(CH_3)-R_5^N$  dissolved in ethanol and bmimBF<sub>4</sub> (Fig. 1).

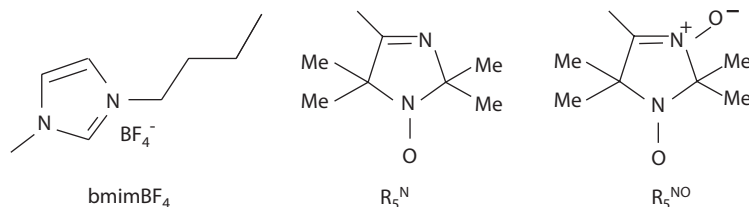


**Fig. 1.** Structures of imidazoline nitroxide rings  $-R_5^N$ ,  $-R_5^{NO}$ , and of bmimBF<sub>4</sub> ionic liquid.

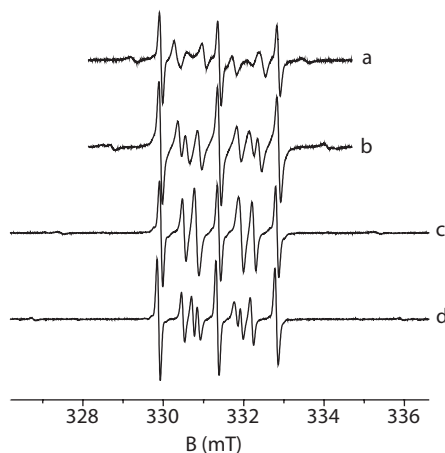


**Fig. 2.** EPR spectra of B3 (a, b) and B4 (c, d) in ethanol solutions at 310 (a), 350 (b, d) and 290 (c) K.

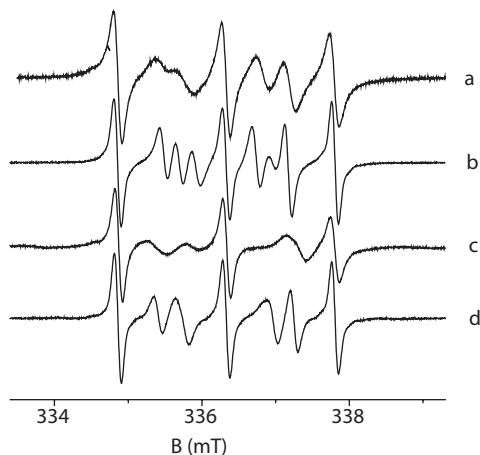


**Fig. 3.** EPR spectra of B4 (a, b) and B3 (c, d) in  $\text{bmimBF}_4$  solutions at 350 (a, c) and 390 (b, d) K.

EPR spectra were recorded on X-band Bruker EMX-8 spectrometer at various temperatures, and spin-Hamiltonian parameters were calculated as described in [5, 6].

In the paper, our recent results obtained for three nitroxide biradicals B3-C5 dissolved in ethanol and  $\text{bmimBF}_4$  are presented and discussed, EPR spectra of biradicals B3 and B4 with asymmetric structures in ethanol at all temperatures are “classical” with central symmetry (Fig. 2), though they become absolutely asymmetric in  $\text{bmimBF}_4$  solutions (Fig. 3). In the contrast, EPR spectra of symmetric biradical C5 in both solvents are asymmetric (Fig. 4, 5). For correct explanation of these results, we will need further co-operation with quantum chemists and other theoreticians.

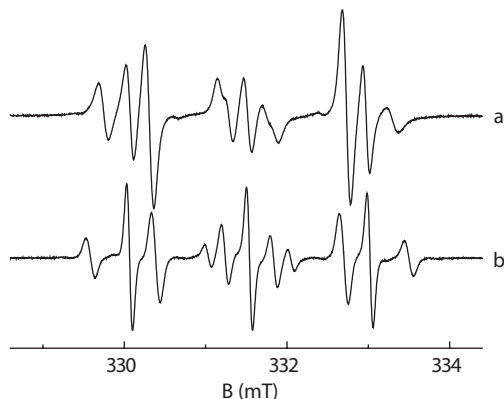


**Fig. 4.** EPR spectra of C5 in ethanol solution at 260 (a) and 355 (b) K.

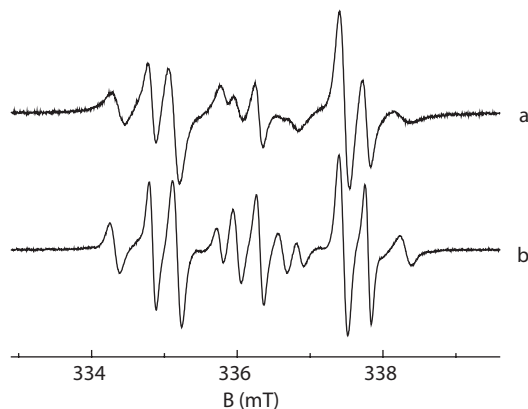


**Fig. 5.** EPR spectra of C5 in bmimBF<sub>4</sub> solutions at 350 (a) and 390 (b) K.

The author thanks Drs. B. Y. Mladenova-Kattnig, O. I. Gromov, Profs. G. Grampp and E. N. Golubeva, I. A. Grigor'ev for their valuable help at some steps of the work.

1. Luckhurst G.R.: *Molec. Phys.* **10**, 543 (1966)
2. Glarum S.H., Marshall J.H.: *J. Chem. Phys.* **47**, 1374 (1967)
3. Lemaire H.: *J. Chim. Phys.* **64**, 559 (1967)
4. Parmon V.N., Zhidomirov G.M.: *Mol. Phys.* **27**, 367 (1974)
5. Parmon V.N., Kokorin A.I., Zhidomirov G.M.: *Stable Biradicals*. Nauka, Moscow, 1980.
6. Kokorin A.I. in: *Ionic Liquids, Theory, Properties, New Applications*. InTech Publ., Rijeka, p. 183–200, 2011.
7. Kokorin A.I., Golubeva E.N. *et al.*: *Appl. Magn. Reson.* **44**, no. 9, p. 1041–1051 (2013)

---

## POSTERS

## NMR Investigation of Conformational Changes in Calcium Gluconate

**M. M. Akhmetov<sup>1</sup>, G. G. Gumarov<sup>1</sup>, V. Yu. Petukhov<sup>1</sup>, G. N. Konygin<sup>2</sup>,  
D. S. Rybin<sup>2</sup>, and A. B. Konov<sup>1</sup>**

<sup>1</sup> Zavoisky Physical-Technical Institute, Russian Academy of Sciences, Kazan 420029,  
Russian Federation, mansik86@mail.ru

<sup>2</sup> Physical-Technical Institute Ural Branch of RAS, Izhevsk, Russian Federation, dsrybin@mail.ru

Practically all biochemical processes are accompanied by conformational changes, i.e., the nature of the interaction and the structure of the resulting reaction products are determined by the spatial structure and the possibility of mutual adjustment (including conformation) of molecules involved. Gluconate is one of the most famous polyhydroxycarboxylates of high biological value that stipulates their widespread use in the pharmaceutical industry [1]. There are a number of NMR studies on the conformation of aldonic acids, especially in the aqueous gluconic acid solution [2]. However, to the best of our knowledge, no studies the conformational structure of calcium gluconate in the aqueous solution are available. This paper presents the results of studies of conformational changes of calcium gluconate in the aqueous solution as a function of the concentration.

NMR spectra were measured on an AVANCE 400 spectrometer (Bruker) in the magnetic field of 9.395 T. Resonance on <sup>1</sup>H nuclei for solutions of calcium gluconate was observed at the frequency of 400 MHz. The pulse sequence homonuclear correlation spectroscopy, <sup>1</sup>H-<sup>1</sup>H COSY, was used to establish links between the individual nuclei of the molecule.

The <sup>1</sup>H NMR spectra of calcium gluconate D<sub>2</sub>O solutions showed the shift of some lines, and the change of their shape as a function of the concentration. It is known that this indicates the presence of intermolecular hydrogen bonds [3]. The most noticeable shift is observed for lines H2 and H3 corresponding to protons next to the calcium atom in the calcium gluconate molecular structure.

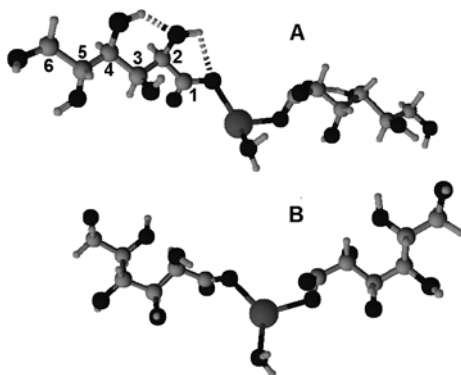


**Fig. 1.** Conformations in aqueous calcium gluconate solution: A-1-P, B-3G+.

The values of the spin-spin interaction constants (SSIC) obtained for calcium gluconate differ slightly from the corresponding values for the gluconic acid observed by Horton et. al. [4]. This suggests that conformations of molecules of gluconic acid and calcium gluconate in the aqueous solution are similar. The values of the coupling constants obtained for gluconic acid are interpreted within the dynamic equilibrium between two conformations: zigzag (planar) (1-P) and cyclic 3G<sup>+</sup>. The carbon skeleton in the zigzag conformation is coplanar, and is stabilized by well-defined intramolecular hydrogen bonds OH-4-O-2 (hydroxyl group at C2 and C4) and weaker bonds 2-O-OH-1. The cyclic 3G<sup>+</sup> form is formed from the planar one by the rotation along the C3-C4 residue of the carbon skeleton by 120° counterclockwise (Fig. 1). The conformational equilibrium is shifted strongly towards the zigzag shape.

The above model is consistent with our data on changes of torsion angles with the concentration. Obviously, if there is the intramolecular hydrogen bond 4-OH-O-2, the torsion angles of C2-C3 and C3-C4 are fixed. The appearance of additional intermolecular bonds with increasing concentration of the solution leads to the change of the remaining relatively free torsion angles along the bonds C4-C5 and C5-C6' as observed in the experiment.

The homonuclear 2D NMR spectrum of calcium gluconate shows intense cross-peaks from neighboring protons in the calcium gluconate molecule indicating that the molecule has primarily the zigzag configuration. The relatively low intensity of the H3-H4 cross-peak is probably due to the fact that the protons H3-H4 in the 1-P conformation are in the gauche position, and 3G<sup>+</sup> in the trans position. The same as in the case of gluconic acid, the equilibrium is strongly shifted towards the planar configuration. There is also a relatively weak cross peak H3-H6, which is not observed in the model 2D NMR spectrum. This cross-peak may indicate the presence of the cyclic conformation, particularly, the formation of the chelate complex due to the interaction of oxygen of the hydroxyl group at C6 with the calcium atom.

<sup>1</sup>H NMR studies of calcium gluconate samples made it possible to establish that intermolecular hydrogen bonds are formed with the increase in the concentration of the solution. The presence of two conformational structures for the calcium gluconate molecule in the aqueous solution 1-P and 3G<sup>+</sup>, with the predominance of the planar one was revealed.

1. Whitfield D.M., Stojkovsky S., Sarkar B.: *Coord. Chem. Rev.* **122**, 171–225 (1993)
2. Horton D., Walaszek Z., Ekiel I.: *Carbohydrate Research* **119**, 263–268 (1983)
3. March J.: *Organic Chemistry*, 381 c. Mir, 1987.
4. Horton D., Wander J.D.: *J. Org. Chem.* **39**, 13 (1974)

## Analysis of Manifestations of the Spin Coherence Transfer in EPR Spectra of Nitroxyl Radicals in Liquids

**M. M. Bakirov<sup>1</sup>, K. M. Salikhov<sup>1,2</sup>, and R. T. Galeev<sup>1</sup>**

<sup>1</sup>Zavoisky Physical-Technical Institute, Russian Academy of Sciences, Kazan 420029, Russian Federation, pinas1@yandex.ru

<sup>2</sup>Kazan Federal University, Kazan 420008, Russian Federation

The shape of the EPR spectra of the spin probes depends on the spin decoherence and spin coherence transfer between probes induced by the exchange and dipole-dipole interactions. The description of the EPR of nitroxide radicals often use simplified algorithms that do not take into account all the processes due to exchange and dipole-dipole interactions. In papers [1, 2] different algorithms of separating dipole-dipole and Heisenberg spin exchange interactions are proposed. In work [3] the theory was extended to include into consideration all magnetic nuclei of the spin probes. The exact theoretical expressions which describe the EPR spectrum of spin probes with exchange, dipole-dipole, and hyperfine interactions were derived [3]. For the chosen set of  $a_{\text{N}}$ ,  $\sigma$ ,  $1/T_2$ , constant of spin coherence transfer and constant of spin dephasing computer experiments with the model  $^{14}\text{N}$  nitroxide radical were performed. Analysis of these computer experiments were compared with input parameters. Results for some cases are shown in Fig. 1: input spin coherence transfer parameter  $K_{\text{sct}}C$  was set on x-axis and value of  $K_{\text{sct}}C$  that we got from EPR lineshape analysis is postpioned on

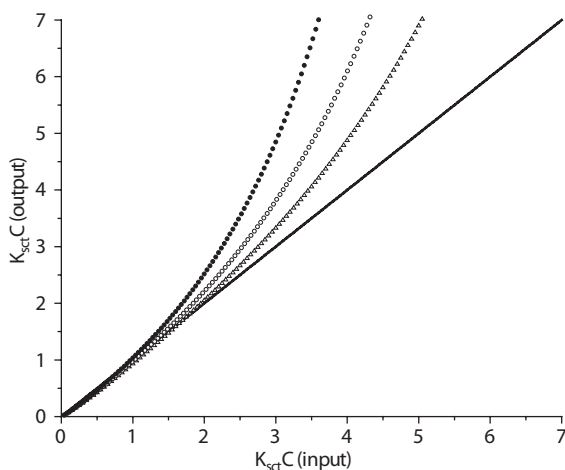


**Fig. 1.** Correlation between the input and output spin coherence transfer rate  $V = K_{\text{sct}}C$  used as the input of the computer simulation of the EPR spectrum and the value of the kinetic parameter  $K_{\text{sct}}C$  obtained by analyzing the dispersion contribution to the simulated EPR spectrum component. The bisector is shown as the solid line.



$y$ -axis. Parameters used in these simulations are:  $\Gamma_k = 0.2$  G,  $a_N = 16$  G,  $g = 2$ , number of protons = 12,  $a_p = 0.2$  G,  $K_{ex} = 0.05$  G L/mM,  $K_{dsct} = K_{dsd} = 0$  (open triangles);  $K_{ex} = 0.05$  G L/mM,  $K_{dsct} = 0.005$  G L/mM,  $K_{dsd} = 0.006$  G L/mM (open circles);  $K_{ex} = 0.05$  G L/mM,  $K_{dsct} = 0.01$  G L/mM,  $K_{dsd} = 0.012$  G L/mM (closed circles).

1. Salikhov K.M.: Appl. Magn. Reson. **38**, 237–256 (2010)
2. Peric M., Bales B., Peric M.: J. Phys. Chem. A **116**, 2855–2866 (2012)
3. Salikhov K.M., Bakirov M.M., Galeev R.T.: Appl. Magn. Reson. **47**, in press (2016)

## **First-Principles Solid-State Calculations and Pulsed EPR Measurements: a Study of Ionic Substitutions in Hydroxyapatite**

**T. Biktagirov<sup>1</sup>, M. Gafurov<sup>1</sup>, G. Mamin<sup>1</sup>, and S. Orlinskii<sup>1</sup>**

<sup>1</sup> Kazan Federal University, Kazan 420008, Russian Federation,  
tibbonktagirov@kpfu.ru

Density functional theory (DFT) calculations are widely used to characterize the electronic structure and magnetic resonance parameters of paramagnetic molecules. Here we address the versatility of plane-wave DFT for studying impurities in solids in combination with pulsed EPR techniques. We focus on hydroxyapatite  $\text{Ca}_{10}(\text{PO}_4)_6(\text{OH})_2$  (nano)crystals as a host lattice, since it is very tolerant to many ionic substitutions. We show that the calculation of magnetic resonance parameters in conjunction with EPR/ENDOR experiment can successfully complement first-principles thermodynamic analyses of the impurity localization. Next, we attempt to connect the results of electron spin-lattice relaxation measurements with the calculated phonon properties of the host crystal. Finally, we illustrate the capabilities of the combined experimental-computational approach for studying the interplay of oppositely charged substitution in the structure of hydroxyapatite nanopowders.

## Compare Acetonitrile and Solid-Phase Extractions for Sample Preparation of Plasma at Metabolom Study by NMR

**A. Bogaychuk<sup>1</sup>, M. Dambieva<sup>1</sup>, G. Kupriyanova<sup>1</sup>, and S. Babak<sup>1</sup>**

<sup>1</sup> Immanuel Kant Baltic Federal University, Kaliningrad 236041, Russian Federation, aleksandr.bogaychuk@gmail.com

In recent years actively developed metabolom research NMR methods for different pathologies [1]. Despite the seeming simplicity of sample preparation relative of other metabolom research methods, there are a number of conditions which are worth considering. For example, in the collection of blood samples is recommended to use heparin coated tubes in order to avoid signal overlap

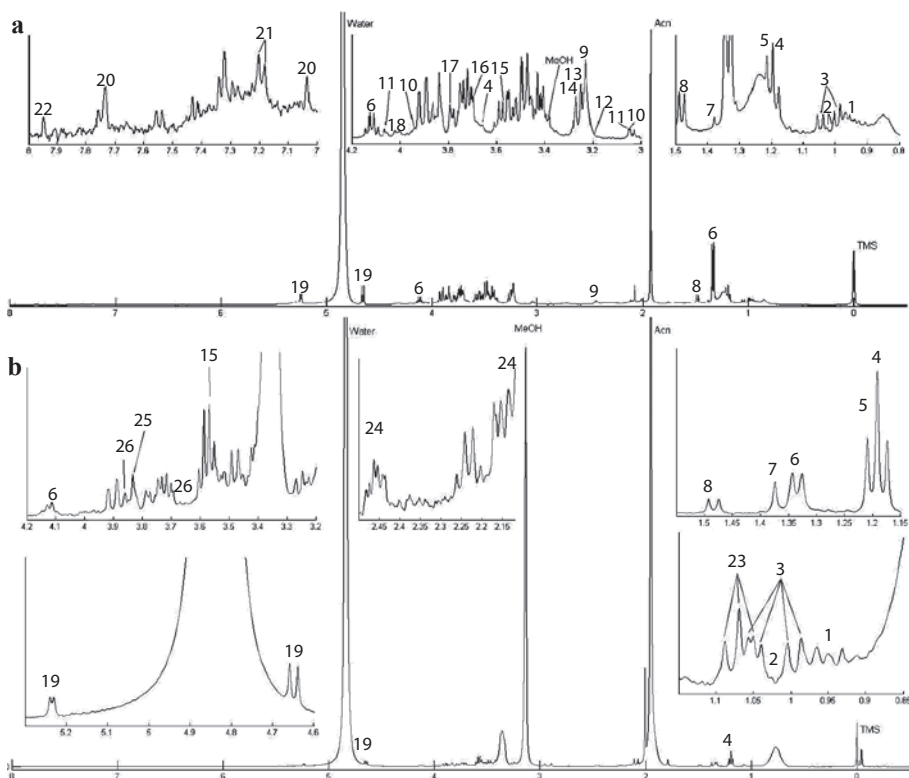


**Fig. 1.** <sup>1</sup>H spectra of plasma blood after acetonitrile (a) and solid-phase (b) extractions. In figure show signals from next metabolits: leucine (1), isoleucine (2), valine (3), ethanol (4), 3-hydroxybutyrate (5), lactate (6), 2-hydroxyisobutyrate (7), alanine (8), carnitine (9), creatine (10), creatinine (11), choline (12), betaine (13), trimethylamine N-oxide (14), glycine (15), ethylene glycol (16), guanidoacetate (17), fructose (18), glucose (19),  $\tau$ -methylhistidine (20), tyrosine (21), xanthine (22), propionate (23), glutamine (24), N-nitrosodimethylamine (25), glucitol (26).

[2]. Also it is necessary to pay attention to the terms and conditions of storage of samples [3].

If the collection and storage of samples for NMR studies are well understood and have precise instructions, the preparation of samples for the study of metabolites in the blood profile has very many variations, presented in comparative reviews [4]. Thus, the aim of our work was to compare the simplest and effective ways of sample preparation of plasma samples at metabolom research for informative NMR analysis.

The study was conducted on a healthy group aged 20 to 30 years. All patients had peripheral venous blood was taken in the morning before breakfast in a volume of 5 ml in a test tube with heparin. After that produce two different sample preparation: acetonitrile extraction, solid-phase extraction using SAKS or C8 column.

NMR spectra were recorded on a Varian 400 MHz spectrometer at 298 K.

Examples of the proton spectra are shown in Fig. 1.

Signals of 26 metabolites were identified. Estimate their concentration, measured the spin-lattice and spin-spin relaxation times.

1. Duarte I.F., Diaz S.O., Gil A.M.: *J. Pharmaceutical. Biomed.* **93**, 17 (2014)
2. Issaq H.J., Van Q.N., Waybright T.J., Muschik G.M., Veenstra T.D: *J. Sep. Sci.* **32**(13), 2183 (2009)
3. Pinto J., Rosario M., Domingues M., Galhano E., Pita C., Almeida M., Carreirade I.M., Gil A.M.: *Analyst.* **139**, 1168 (2014)
4. Sheedy J.R., Ebeling P.R., Gooley P.R., McConville M.J.: *Analytical Biochemistry* **398**, 263 (2010)

## Orientation Order and Rotation Mobility of Nitroxide Biradicals Determined by Quantitative Simulation of EPR Spectra

A. V. Bogdanov and A. Kh. Vorobiev

Chemistry Department, Lomonosov Moscow State University, Moscow 119991, Russian Federation

In the investigations of molecular dynamics and structure of liquids, glasses, polymers, colloids, and liquid crystals, the use of the spin probe technique is widely applied. It is generally agreed that for reliable interpretation of electron paramagnetic resonance (EPR) spectra in order to obtain information about rotation mobility and orientation order, the quantitative simulation of experimental spectra with the use of least-squares optimization should be performed. Among numerous spin probes used, biradical molecules show particular promise. Due to the large anisotropic electron-electron dipolar interaction, these probes are expected to have profound sensitivity towards orientation order and rotation movements of molecules in the investigated media. However, the problem of quantitative simulation of EPR spectra of biradicals in the slow-motional regime and in the ordered samples has not been solved until now.

In the present work the numerical simulation of EPR spectra of nitroxide biradical both in isotropic and aligned media was performed. The models suitable for description of the spectra of the probes, both in the rigid limit and in presence of rotation motions, were developed and successfully applied to model

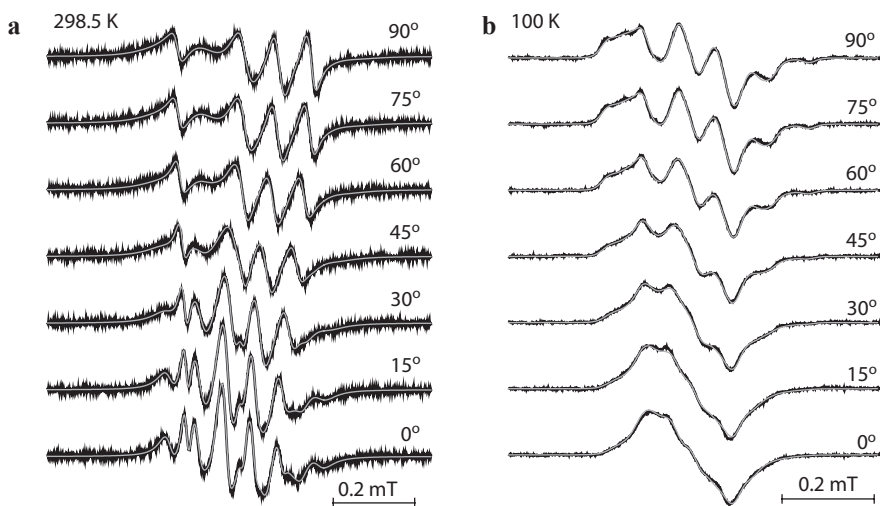


**Fig. 1.** Angular dependency of EPR spectra of the studied biradical in the smectic liquid crystal n-octylcyanobiphenyl at 298.5 K (a) and 100 K (b); experimental spectra (black lines) and results of numerical simulations (grey lines) are shown.

systems. The examples of spectra simulation are illustrated in Fig. 1 for the slow-motional regime (Fig. 1a) and in the rigid limit (Fig. 1b).

The simulation of EPR spectra allows obtaining the following information about molecular structure and dynamics: the values of orientation order parameters, the type of rotation mobility and its quantitative characteristics, the sign and value of the spin exchange constant of the biradical. Model systems used in this work include solutions of nitroxide biradical in a viscous solvent (squalane) in the range of temperatures 100–370 K and in the aligned liquid crystal *n*-octylcyanobiphenyl (8CB, 100–298.5 K). Unexpectedly, it was found that in 8CB the main orientation axis of biradical molecule is perpendicular to the longest molecular axis.

The authors acknowledge the financial support from RFBR (grant no. 16-33-60139 mol-dk and no. 14-03-00323a).

## Chemical Exchange in Water

**P. Dvořák and J. Lang**

Department of Low Temperature Physics, Faculty of Mathematics and Physics, Charles University,  
Prague 180 00, Czech Republic, [dvorak.p@gmail.com](mailto:dvorak.p@gmail.com), [Jan.Lang@mff.cuni.cz](mailto:Jan.Lang@mff.cuni.cz)

Several samples of  $\text{H}_2\text{O}/\text{D}_2\text{O}$  mixtures were prepared from water purified by a double distillation under the boiling point in a quartz apparatus. The chemical exchange on the millisecond time scale at various temperatures was studied by the measurements of the dependence of the spin-spin relaxation rate on the echo-time in the CPMG pulse sequence. The physical interpretation of the observed exchange process is discussed also in context of the original paper of Meiboom.

This work was supported by the Charles University through grant GA UK no. 112715.

1. Meiboom S.: J. Chem. Phys. **34**, 375 (1961)

## ESR Study of Mn-Heterovalent Ludwigite $\text{Mn}_{3-x}\text{Cu}_x\text{BO}_5$

R. M. Eremina<sup>1,2</sup>, I. V. Yatsyk<sup>1,2</sup>, E. M. Moshkina<sup>3</sup>, M. V. Rautskii<sup>3</sup>,  
L. N. Bezmaternykh<sup>3</sup>, H.-A. Krug von Nidda<sup>4</sup>, and A. Liodl<sup>4</sup>

<sup>1</sup>Zavoisky Physical-Technical Institute, Russian Academy of Sciences, Kazan 420029,  
Russian Federation

<sup>2</sup>Kazan Federal University, Kazan 420008, Russian Federation

<sup>3</sup>L. V. Kirensky Institute of Physics, Krasnoyarsk 660036, Russian Federation  
rmv@iph.krasn.ru

<sup>4</sup>Institut für Physik, University Augsburg, Augsburg 86135, Germany

$\text{Cu}_{1.8}\text{Mn}_{1.2}\text{BO}_5$  and  $\text{Cu}_{2.5}\text{Mn}_{0.5}\text{BO}_5$  single crystals were synthesized by the flux method. The grown single crystals have the form of orthogonal prisms with a length of 10 mm and a transverse size of about 2 mm. The sample belongs to

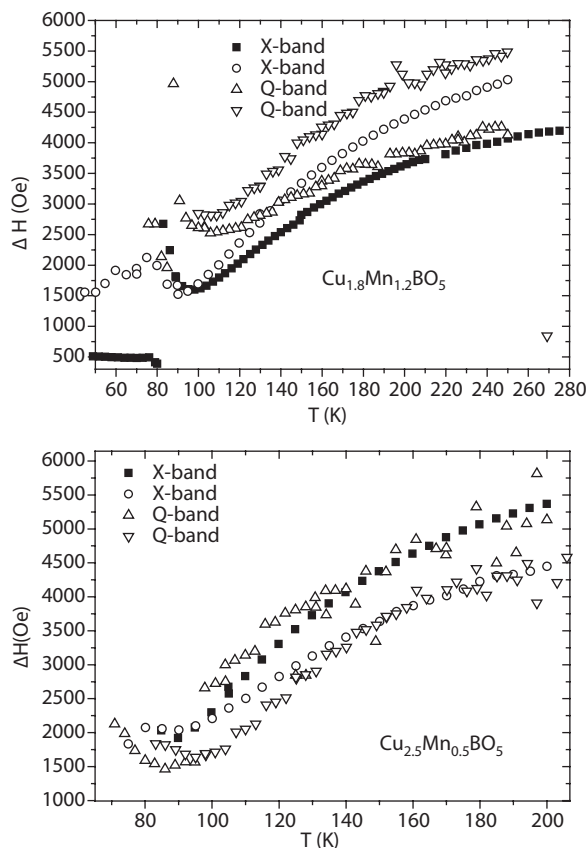


**Fig. 1.** Temperature dependence of ESR linewidth in X- and Q-band in two directions of magnetic fields for  $x = 1.8$  and  $x = 2.5$ .



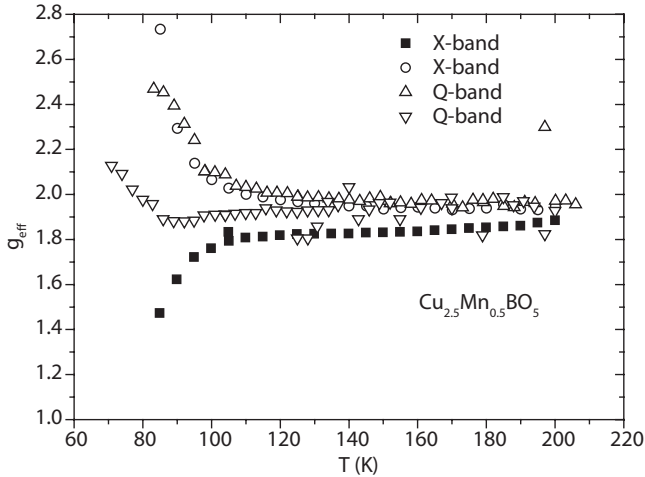


**Fig. 2.** Temperature dependence of effective  $g$ -factor in X- and Q-band in two directions of magnetic fields for  $x = 1.8$  and  $x = 2.5$ .

the space group  $P2_{1/c}$ . In the 75 K region, a feature in the magnetic susceptibility behavior is observed in both ZFC and FC regimes, which can be related to different temperature dependence of magnetization of different sublattices Mn and Cu.

ESR measurements were carried out in the paramagnetic regime at the temperature above the phase transition temperature  $T \sim 90$  K at the 9.48 GHz (X-band) and 34 GHz (Q-band) and two different orientation. In this temperature range the ESR spectrum of  $\text{Cu}_{1.8}\text{Mn}_{1.2}\text{BO}_5$  and  $\text{Cu}_{2.5}\text{Mn}_{0.5}\text{BO}_5$  consists of one broad exchange-narrowed resonance line. Near the phase transition the ESR linewidth exhibits its minimum value of about 1500 Oe in X-band and 2500 Oe in Q-band for  $\text{Cu}_{1.8}\text{Mn}_{1.2}\text{BO}_5$  and about 2000 Oe in X-band and 1500 Oe in Q-band for  $\text{Cu}_{2.5}\text{Mn}_{0.5}\text{BO}_5$  (Fig. 1).

In addition, for  $x = 1.8$  the linewidth shows a pronounced anisotropy which depended from frequency band and temperature, while for  $x = 2.5$  anisotropy of linewidth almost independent on frequency band and temperature.

A strong dependence of the effective  $g$ -factors on the orientation at a temperature below the phase transition was observed for both samples (Fig. 2). From the ESR measurements at the 9.48 GHz (X-band) and 34 GHz (Q-band) can be assumed that the anisotropy caused by complex magnetic structure of crystals and is suppressed by the external magnetic field.

This work was supported by the RFBR no. 16-32-50083.

## Electron Paramagnetic Resonance of $Ce^{3+}$ Ion in $Rb_2NaYF_6$ Single Crystal: Experiment and Theoretical Calculations of the Optical Spectra

M. L. Falin<sup>1</sup>, V. A. Latypov<sup>1</sup>, A. M. Leushin<sup>2</sup>, and S. L. Korableva<sup>2</sup>

<sup>1</sup>Zavoisky Physical-Technical Institute, Russian Academy of Sciences, Kazan 420029, Russian Federation, falin@kfti.knc.ru

<sup>2</sup>Kazan Federal University, Kazan 420008, Russian Federation

A family of crystals with the structure of cryolite-elpasolite  $A_3BCX_6$  ( $A^+$ ,  $B^+$ ,  $C^{3+}$  are mono- and trivalent metal cations, X is the halogen anion:  $F^-$ ,  $Cl^-$ ,  $Br^-$ ) is one of attractive types of crystals. Such compounds doped with rare-earth elements are promising materials for the practical usage in scintillators for X-rays, broadband tunable lasers etc. It is known that such crystals at room temperature have the cubic elpasolite structure with the space group  $O_h^5$ . It was established experimentally that many of them, e.g.,  $Cs_2NaYF_6$ ,  $Cs_2NaScF_6$  etc. keep this structure to low temperatures. It was assumed in many works that the symmetry of the  $Rb_2NaYF_6$  crystal also remains cubic in a wide temperature interval (4.2–300 K). However our study of paramagnetic defects in  $Rb_2NaYF_6$  using electron paramagnetic resonance (EPR) and optical spectroscopy showed that a phase transition (PT) takes place in this crystal at the temperature of 150 K [1, 2]. It was found that cubic ( $T_c$ ) paramagnetic centers of  $Yb^{3+}$  ions transform into centers of tetragonal symmetry ( $T_{tet}$ ). Simultaneously and independent of us the authors [3] studied the undoped  $Rb_2NaYF_6$  crystal by Raman spectroscopy and hydrostatic pressure, and established that the PT from the cubic into the disordered phase accompanied by the recovery of the soft mode occurs at  $T = 154$  K.

This report is concerned with investigation of the impurity paramagnetic centers formed by  $Ce^{3+}$  ions in the  $Rb_2NaYF_6$  single crystal. The presence of only one type of centers with tetragonal symmetry at low temperatures indicates that the  $Rb_2NaYF_6$  crystal has tetragonal symmetry. The obtained results confirm the fact established earlier that the studied crystal transfers from the cubic into the tetragonal phase with the temperature decrease.

Single crystals  $Rb_2NaYF_6$  doped with  $Ce^{3+}$  ions were grown by the Bridgman method. Experimental studies of EPR spectra were performed on a modified ERS-231 spectrometer (Germany) in the X-band. A CRYO202ESR helium flow thermostat (Russia) was used during EPR measurements at temperatures of 4.2–80 K.

The parameters of the corresponding spin Hamiltonians and the ground states were determined. Owing to the small temperature observation range, EPR of  $Ce^{3+}$  ions does not make it possible to study the impurity center in the cubic phase of the crystal at temperatures above the PT temperature. The further study of 4f energy levels of  $Ce^{3+}$  was performed on the basis of the theoretical interpretation of obtained and literature values of g-factors.

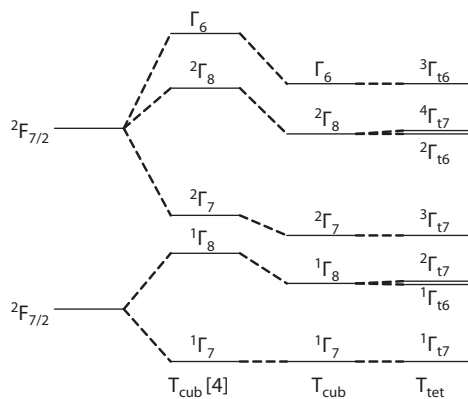


Fig. 1. Schematic energy-level diagram for six-coordinated  $\text{Ce}^{3+}$  in  $\text{Rb}_2\text{NaYF}_6$ .

A theoretical scheme of the energy levels of the  $T_{\text{tet}}$  of the  $\text{Ce}^{3+}$  ion was proposed, in which the calculated  $g$ -factors exactly correspond to the observed values (Fig. 1).

The crystal field (CF) parameters of the  $T_{\text{tet}}$  leading to this structure of the energy levels were established. The characteristic feature of the weak CF of tetragonal symmetry originating from the small rotations of octahedra  $\text{YF}_6$  (or substitutional  $\text{CeF}_6$ ) and  $\text{NaF}_6$  around the fourfold axis is that some cubic levels are almost not split. It is possible that this circumstance was the origin that the fact of the existence of low-symmetry phases of some elpasolites could not be established for a long time.

This study was supported by the grant of the Presidium of the Russian Academy of Sciences no. 32. A.M.L. was supported by the grant of the Kazan (Volga Region) Federal University (ND 02 VD 0211, theme no. 021110054 “Budget 14-54”).

1. Falin M.L., Gerasimov K.I., Latypov V.A., Leushin A.M., Khaidukov N.M.: Phys. Rev. B **87**, 115145 (2013)
2. Leushin A.M.: Phys. Sol. State **35**, 2558 (2013)
3. Krylov A.S., Vtyurin A.N., Oreshonkov A.S., Voronov V.N., Krylova S.N.: J. Raman Spectrosc. **44**, 763 (2013)
4. Aull B.F., Jøssens H.P.: Phys. Rev. B **34**, 6647 (1986)

## EPR and Optical Spectroscopy of $\text{Yb}^{3+}$ in Hexagonal Perovskite $\text{RbMgF}_3$ Single Crystal

M. L. Falin<sup>1</sup>, V. A. Latypov<sup>1</sup>, G. M. Safiullin<sup>1</sup>, A. M. Leushin<sup>2</sup>,  
and S. V. Petrov<sup>3</sup>

<sup>1</sup> Zavoiisky Physical-Technical Institute, Russian Academy of Sciences, Kazan 420029,  
Russian Federation, vlad@kfti.knc.ru

<sup>2</sup> Kazan Federal University, Kazan 420008, Russian Federation

<sup>3</sup> Kapitza Institute for Physical Problems of the RAS, Moscow 119334, Russian Federation

Fluoroperovskites  $\text{RbMgF}_3$  doped with transition metal ions attract attention due to their application in optically stimulated luminescence and usage as radiation detectors [1]. Only crystals activated with iron group ions were studied by electron paramagnetic resonance (EPR) and to the best of our knowledge, the studies of rare-earth ions in this crystal are absent.  $\text{RbMgF}_3$  has the hexagonal structure and the space group  $P63/mmc$  [2]. The crystal has two different crystallographic 6-fold  $\text{Mg}^{2+}$  positions. Analogously, there are two different crystallographic 12-fold  $\text{Rb}^+$  positions. This report is concerned with the investigation of the impurity paramagnetic centers formed by  $\text{Yb}^{3+}$  ions in the  $\text{RbMgF}_3$  single crystal.

The crystals were grown using the Bridgman method. Experimental studies of EPR spectra were performed on a modified ERS-231 spectrometer (Germany) in the X-band. A CRYO202ESR helium flow thermostat (Russia) was used during EPR measurements at temperatures of 4.2–80 K.

The parameters of the corresponding spin Hamiltonians, the ground states and their wave functions were determined. On the basis of the comparison of valence states and ion radii of  $\text{Rb}^+$ ,  $\text{Mg}^{2+}$  and  $\text{Yb}^{3+}$  [3] ions it is assumed that  $\text{Yb}^{3+}$  occupies one of  $\text{Mg}^{2+}$  states.

The Stark level energies of the  $\text{Yb}^{3+}$  multiplets were determined from absorption, luminescence and excitation luminescence spectra. These data and the  $g$ -factor of the ground state were used for the interpretation of the optical data within the crystal field theory.

This study was supported by the grant of the Presidium of the Russian Academy of Sciences no. 32. A.M.L. was supported by the grant of the Kazan (Volga Region) Federal University (ND 02 VD 0211, theme no. 021110054 “Budget 14-54”).

1. Dotzler C., Williams G.V.M., Rieser U., Robinson J.: Appl. Phys. **105**, 023107 (2009)
2. Dance J.M., Kerkouri N., Tressaud A.: Mat. Res. Bull. **14**, 869 (1979)
3. Shannon R.D.: Acta Crystallogr. A **32**, 751 (1976)

## **Spin Dynamics in the Vicinity of Levels Anticrossing**

**R. T. Galeev**

Zavoisky Physical-Technical Institute, Russian Academy of Sciences, Kazan 420029,  
Russian Federation, galeev@kfti.knc.ru

The response of model spin system on alternating magnetic field is considered. It is shown that rapid passage of the vicinity of levels anticrossing leads to non-linear response of spin system. Effect of levels anticrossing on the rate of magnetic relaxation and dynamic susceptibility is discussed. This research was supported in part by the program of presidium of RAS no. 1.26.

## Effect of Activation and Inhibition of $K_{ATP}^+$ -Channels on the NO Production in the Blood of Rats with Ischemic Stroke

S. A. Gavrilova<sup>1</sup>, O. G. Deryagin<sup>1</sup>, Kh. L. Gainutdinov<sup>2,3</sup>,  
V. V. Andrianov<sup>2,3</sup>, A. V. Golubeva<sup>1</sup>, G. G. Yafarova<sup>2,3</sup>, V. S. Iyudin<sup>2</sup>,  
A. V. Buravkov<sup>1</sup>, and V. B. Koshelev<sup>1</sup>

<sup>1</sup> Facility of Fundamental Medicine of Lomonosov Moscow State University, Moscow 119192, Russian Federation

<sup>2</sup> Zavoisky Physical-Technical Institute, Russian Academy of Sciences, Kazan 420029, Russian Federation

<sup>3</sup> Kazan Federal University, Kazan 420008, Russian Federation, kh\_gainutdinov@mail.ru

Nitric oxide (NO) and adenosine triphosphate-sensitive potassium ( $K_{ATP}^+$ ) channels play an important role in the mechanisms of ischemic damage of cells. NO hyperproduction in an ischemic stroke causes damage to the structural and regulatory components of the cells [1, 2], and NO binding to the mitochondrial transport chain enzymes inhibits cellular respiration [3]. Moderate activation of NO during the preconditioning may exert a neuroprotective effect, activating antioxidant enzymes, triggering anti-apoptotic mechanisms, and increasing the level of cerebral blood flow [1, 2]. The protective effect of the moderate NO production may also be mediated by activation of the  $K_{ATP}^+$ -channels [4]. The relationship between these elements in the system of the mechanisms of the neuroprotective effect of preconditioning has not been proved because of the absence of experimental approaches, distinct methods of NO detection and verification of the results obtained *in vivo*. The present study focuses on the relationship between the  $K_{ATP}^+$  channels and NO in cerebral ischemia.

The brain ischemic preconditioning (IP) was performed by alternately closing the right and left common carotid arteries (OSMA) for 5 minutes with 5 minutes reperfusion for 1 hour. Subsequently, the early (3 hours) and the delayed (24 hours) phases of the protective IP effect were studied. Measurement of NO content in brain tissue and venous blood were performed by the method of electron paramagnetic resonance (EPR). Quantitative EPR as the analytical method gives a large dynamic range with high sensitivity for measurements of different types of samples [5]. NO in our experiments was determined by the spin trapping, when the captured NO formed a stable radical  $(DETC)_2-Fe^{2+}-NO$ , which is detected by EPR spectroscopy [5]. The sample was weighted before the experiments. The sample mass was about 100 mg. Amplitude of EPR spectra was normalized on mass of sample. The details described by us previously [6].

The content of the complex  $(DETC)_2-Fe^{2+}-NO$  in the cortical brain structures in the control group of rats with OSMA was two times less than in the intact animals at all the time points. The average level of NO in the cerebral cortex of the intact animals made up 1.16 nm/g; after 5 hours of OSMA in the ischemia area was observed a minimum concentration of 0.3 nm/g, increasing as the distance from the damage area (of 0.48 nm/g) to 0.68 nm/g in the contralateral

hemisphere and 0.83 nm/g in the cerebellum. The average level of NO in 9, 24 and 72 h after OSMA was 0.62 nm/g and 0.65 nm/g and 0.75 nm/g respectively.

In the group of animals treated with a blocker of  $K_{ATP}^+$  channels glibenclamide, on the third day after the operation an increase of NO level by 65% was observed, compared with the control. Introduction of the activator of  $K_{ATP}^+$  channels, diazoxide a day before OSMA has led to a decrease of NO level at all time points on 25–41%. Thus, the relationship between  $K_{ATP}^+$  channels and NO in rats with ischemic preconditioning.

1. Jung K.H., Chu K., Ko S.Y. *et al.*: Stroke **37**, no. 11, 2744–2750 (2006)
2. Terpolilli N.A., Moskowitz M.A., Plesnila N.: J. Cereb. Blood Flow Metab. **32**, no. 7, 1332–1346 (2012)
3. Brown G.C., Cooper C.E.: FEBS Lett. **356**, no. 2-3, 295–298 (1994)
4. Sasaki N., Sato T., Ohler A. *et al.*: **101**, no. 4, 439–445 (2000)
5. Mikoyan V.D., Kubrina L.N., Serezhnikov V.A. *et al.*: Biochim. Biophys. Acta **1336**, no. 2, 225–234 (1997)
6. Gainutdinov Kh.L., Gavrilova S.A., Iyudin V.S. *et al.*: Appl. Magn. Reson. **40**, no. 3, 267–278 (2011)

## Magnetic Resonance Investigations of Core-Shell Composites Based on $\text{CaCu}_3\text{Ti}_4\text{O}_{12}$

**T. Gavrilova<sup>1,2</sup>, I. Yatsyk<sup>1,2</sup>, R. Eremina<sup>1,2</sup>, I. Gilmutdinov<sup>2</sup>,  
Y. Kabirov<sup>3</sup>, and J. Nikitina<sup>4</sup>**

<sup>1</sup> Zavoisky Physical-Technical Institute, Russian Academy of Sciences, Kazan 420029, Russian Federation, tatyana.gavrilova@gmail.com

<sup>2</sup> Kazan Federal University, Kazan 420008, Russian Federation, RERemina@yandex.ru

<sup>3</sup> Southern Federal University, Rostov-on-Don 344006, Russian Federation

<sup>4</sup> Institute of Solid State Chemistry RAS, Yekaterinburg 620990, Russian Federation

Composite materials attract much attention due to the manifestation of unexpected new physical properties in them. Studies of composite compounds with high values of magnetic susceptibility and dielectric permittivity are of

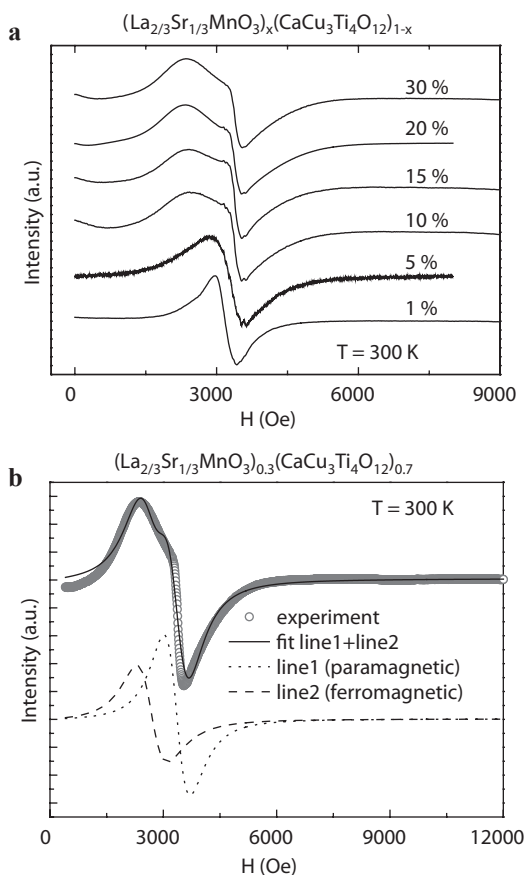


**Fig. 1.** **a** Concentration evolution of the ESR spectra of  $(\text{LSMO})_x(\text{CCTO})_{1-x}$  ( $x = 0.01, 0.05, 0.1, 0.15, 0.2, 0.3$ ); **b** decomposition of the ESR spectrum of  $(\text{LSMO})_x(\text{CCTO})_{1-x}$  ( $x = 0.3$ ) at room temperature in X-band.



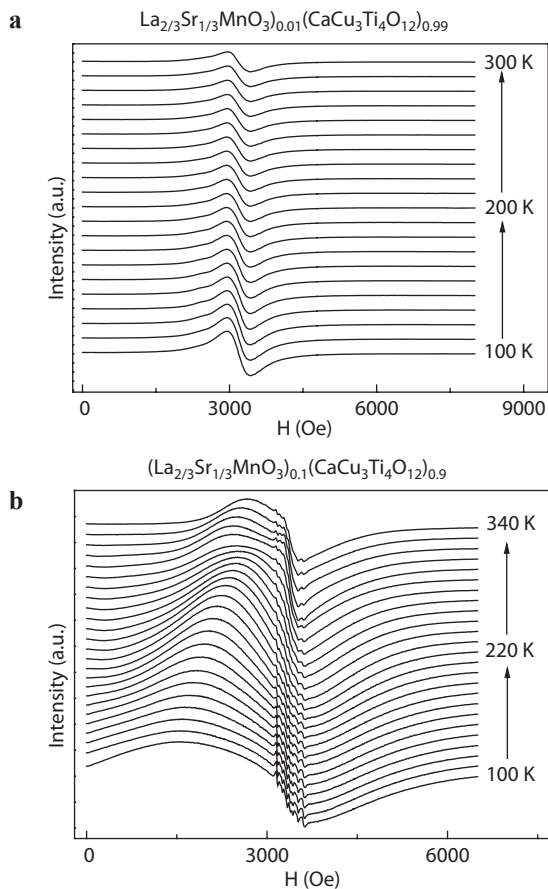


**Fig. 2.** Temperature evolution of the ESR spectra of  $(\text{LSMO})_x(\text{CCTO})_{1-x}$ : **a**  $x = 0.01$ ; **b**  $x = 0.1$  above  $T = 100$  K in X-band.

interest, which can be used in variety of applications. Here we investigate the materials which consist of two inorganic phases. One of the components of the composite material is  $\text{CaCu}_3\text{Ti}_4\text{O}_{12}$  (CCTO). The dielectric behavior of calcium copper titanate (CCTO) exhibits an extraordinary high dielectric constant and shows good thermal stability in a wide temperature range (100–600 K) [1]. As the second component of the composite material besides CCTO we chose the lanthanum-strontium manganite  $\text{La}_{2/3}\text{Sr}_{1/3}\text{MnO}_3$  (LSMO) to modulate the magnetic properties of the composite.

Magnetic resonance spectra of composites  $(\text{LSMO})_x(\text{CCTO})_{1-x}$  for  $x = 0.01, 0.05, 0.10, 0.15, 0.20, 0.30$  were measured on an ER 200 SRC (EMX/plus) spectrometer (Bruker) at the frequency of 9.4 GHz with a flow  $\text{N}_2$  Temperature Controller RS 232 cryostat (Bruker) in the temperature range from 100 to 300 K (Fig. 1, 2). It is clearly visible that the ESR spectrum of  $(\text{LSMO})_x(\text{CCTO})_{1-x}$  consists of two lines (except  $x = 0.01, 0.05$ ) (Fig. 1a): ferromagnetic line from

LSMO and paramagnetic line from CCTO. The decomposition of the ESR spectra of  $(\text{LSMO})_{0.3}(\text{CCTO})_{0.7}$  using two lines is presented in Fig. 2b at room temperature. The ESR spectrum of  $(\text{LSMO})_x(\text{CCTO})_{1-x}$  ( $x = 0.01, 0.05$ ) consist of one ESR line (Fig. 1a, 2a) with the linewidth larger than the value for pure CCTO. We believe that for  $(\text{LSMO})_x(\text{CCTO})_{1-x}$  ( $x = 0.01, 0.05$ ) ceramics there was formed the composite material when the ferromagnetic LSMO core “magnetize” the paramagnetic CCTO shell, how it was in the case  $(\text{SrFe}_{12}\text{O}_{19})_{0.05}(\text{CaCu}_3\text{Ti}_4\text{O}_{12})_{0.95}$  [3]. Based on our experimental results we suggeste that for concentration above  $x = 0.05$  (0.1, 0.15, 0.20, 0.30) ferromagnetic LSMO particles strong interact with each other.

The reported study was supported by RFBR, research project no. 16-32-00660.

1. Subramanian M.A., Li D., Duan N., Reisner B.A., Sleight A.W.: *J. Solid State Chem.* **151**, 323 (2000)
2. Koitzsch A., Blumberg G., Gozar A., Dennis B., Ramirez A.P., Trebst S., Wakimoto S.: *Phys. Rev. B* **65**, 052406 (2002)
3. Eremina R.M., Sharipov K.R., Yatsyk I.V., Lyadov N.M., Gilmudinov I.F., Kiiamov A.G., Kabirov Yu.V., Gavrilyachenko V.G., Chupakhina T.I.: *JETP* **123**, 127 (2016)

## Measurement of ESR Oscillating Magnetization Value in Strongly-Correlated Metals

**M. I. Gilmanov<sup>1,2</sup>, A. V. Semeno<sup>1</sup>, A. N. Samarin<sup>1,2</sup>, and S. V Demishev<sup>1,2,3</sup>**

<sup>1</sup> Prokhorov General Physics Institute of RAS, Moscow 119991, Russian Federation, gilmanov@lt.gpi.ru

<sup>2</sup> Moscow Institute of Physics and Technology, Dolgoprudny 141700, Moscow region, Russian Federation

<sup>3</sup> National Research University "Higher School of Economics", Moscow 101000, Russian Federation

The integral intensity of the resonance line is considered to be proportional to the static susceptibility of oscillating moments ( $\chi_0$ ) and requires significant additional efforts to be obtained in absolute values. Moreover, an oscillating magnetization  $M_0$  (the part of magnetization participating in magnetic resonance [1, 2]) is not always coincide with static magnetization  $M_{st}$  and this discrepancy could be a source of valuable information. Here we report a direct experimental method of measurement of the oscillating magnetization in metallic samples, which based on difference in resonant conditions for different mutual orientations of magnetic field and wave vector of high frequency radiation: Faraday's and Voigt's geometries. The position of the resonance in these two cases depends differently on the oscillating magnetization:  $\omega_0 = \gamma(H_1 + 4\pi M_0)$  and  $\omega_0^2 = \gamma^2 H_2(H_2 + 4\pi M_0)(1 + a^2)$  in Faraday and Voigt geometries respectively. Here  $\omega_0$  is frequency,  $H_1$ ,  $H_2$  – resonance fields,  $M_0$  – oscillating magnetization and  $a$  is a dissipation coefficient. This difference in resonance position for most of metallic systems is strong enough to precisely calculate the value of oscillating magnetization.

Presented technique was applied for two strongly-correlated metallic systems:  $\text{EuB}_6$  and  $\text{CeB}_6$ . Received values of oscillating magnetization was equal 920 Oe for  $\text{EuB}_6$  at  $T = 4.2$  K and 96 Oe for  $\text{CeB}_6$  at  $T = 1.8$  K which are in a good agreement with quantities obtained by other methods [1, 2].

This work was supported by Programs of RAS "Electron spin resonance, spin-dependent electronic effects and spin technologies", "Electron correlations in strongly interacting systems" and by RFBR grant no. 14-02-00800.

1. Semeno A.V. *et al.*: Phys. Rev. B **79**, 014423 (2009)

2. Demishev S.V. *et al.*: Phys. Rev. B **80**, 245106 (2009)

## EPR Investigation of the Radiation-Induced Transformation in Calcium Gluconate

**I. A. Goenko<sup>1</sup>, V. Yu. Petukhov<sup>1</sup>, I. V. Yatzyk<sup>1</sup>,  
G. N. Konygin<sup>2</sup>, D. S. Rybin<sup>2</sup>, I. N. Andreeva<sup>3</sup>,  
A. V. Anisimov<sup>3</sup>, and D. R. Sharafutdinova<sup>4</sup>**

<sup>1</sup> Zavoiisky Physical-Technical Institute, Russian Academy of Sciences, Kazan 420029, Russian Federation, ilya.goenko@mail.ru

<sup>2</sup> Physical-Technical Institute of the Ural Branch of the Russian Academy of Sciences, Izhevsk 426000, Russian Federation, konygin@fnms.udm.ru

<sup>3</sup> Kazan Institute of Biochemistry and Biophysics of the Kazan Scientific Center of the Russian Academy of Sciences, Kazan 420111, andreyeva@kibb.knc.ru

<sup>4</sup> A. E. Arbuzov Institute of Organic and Physical Chemistry of the Kazan Scientific Center of the Russian Academy of Sciences, Kazan 420088, drsh@iopc.ru

At present ionizing radiation is widely used in medical practice and particularly in the pharmaceutical industry for solving a series of problems, such as, e.g., radiation sterilization and modification of drugs.

Calcium gluconate (CG) is one of the commonly used pharmacological preparations for the therapy of diseases associated with hypocalcaemia. It is known that the mechanical activation of CG results in the increased bioavailability and efficacy of therapy [1]. At the same time, it was found that themechanochemical treatment of CG is accompanied by the appearance of the electron paramagnetic resonance (EPR) signal, which may indicate the formation of free radicals [2]. It is known that a similar effect is observed in the case of radiation exposure of the organic matter. Therefore, in this study we investigated changes in physical and chemical properties of CG after radiation exposure.

In the experiments, we used calcium gluconate monohydrate as a powder. A beam of electrons with the energy of 9 MeV, as well as a photon beam with the energy of 10 MeV produced on a linear accelerator were used as ionizing radiation. EPR spectra were measured on an EMX Plus spectrometer at the frequency of 9.3 GHz. Solid-state <sup>13</sup>C NMR spectra were measured on an AVANCE 400 spectrometer (Bruker) in the cross-polarization mode with the magic-angle rotation. Measurements of pH values were performed on a Radelkis OP-211/1pH-meter. The concentration of the measured CG solution for all samples was 10<sup>-2</sup> M. The electrospray ionization mass spectra (ESI-MS) were obtained on an AmazonX mass spectrometer (Bruker). Data were processed using the DataAnalysis 4.0 program (Bruker).

EPR spectroscopy revealed the formation of paramagnetic centers (free radicals) in CG after radiation exposure. The dependence of the intensity and shape of the EPR signal on the type of ionizing radiation was established. The dependence of the signal intensity of the structure of the initial sample was determined as well. The intensity of the EPR signal of the irradiated mechanically activated samples is much higher than that of conventional CG.

An important point in the modification process of drugs is the lack of the formation of new reactive elements. The mass spectroscopy study of irradiated samples revealed no formation of any new products.

No changes in the structure of CG before and after irradiation were observed by the solid-state  $^{13}\text{C}$  NMR experiments. The clarification of this issue requires additional experiments.

The correlation between the pH value of the calcium gluconate solutions and the EPR signal intensity was established. The most significant shift of the pH value was observed in the alkaline environment of the irradiated samples with a large number of paramagnetic centers.

Thus, the experimental data indicate the potential use of ionizing radiation for sterilization and radiation modification of CG. Presently, however, the nature of the new additional paramagnetic centers is not yet clear, but according to the Franck-Rabinovich concept in the radiolysis of organic compounds [3], the breakage of the C-H bonds and the removal of the hydrogen atom from lattice are the most probable origins.

1. Konygin G.N. *et al.*: Conference materials "Actual questions of pediatric surgery", vol. 56. ISMA, Izhevsk (2003)
2. Gumarov G.G. *et al.*: J. of Phys. Chem. **87**, 1578 (2013)
3. Blumenfeld L.A. *et al.*: EPR applications in chemistry (1962)

## Electron Spin Resonance on $\text{Eu}^{2+}$ Impurities in 3D Topological Semimetal

**Yu. V. Goryunov<sup>1</sup> and A. N. Nateprov<sup>2</sup>**

<sup>1</sup> Zavoiisky Physical-Technical Institute, Russian Academy of Sciences, Kazan 420029, Russian Federation, goryunov@kfti.knc.ru

<sup>2</sup> Institute of Applied Physics of the ASM, Kishenu 2028, Moldova

Three dimensional (3D) Dirac semimetal [1] is topological states of matter and can be represented as bulk analogue of graphene. Breaking symmetry in Dirac semimetal by means of magnetic field or magnetic impurities leads to unusual phenomena, for instance, negative magnetoresistance. Recently,  $\text{Cd}_3\text{As}_2$  was identified as a new topological semimetal (TS) hosting 3D Dirac fermions [2]. We studied the ESR in this TS doped by small impurity of Eu.

Measurements were performed at a frequency of 9.3 GHz for powder samples in the temperature range 8–370 K. At temperatures significantly above room the ESR spectrum consists of two almost symmetric resonant lines (see. Fig. 1a), the width and the position of which in the first approximation is a linear function of temperature (see Fig. 1b). The shift of the main line with a decrease in temperature occurs at a rate  $h_t = 1.43$  Oe/K. For low-field line  $h_t = 4.6$  Oe/K. Reducing of peak-to-peak linewidth ( $\Delta H_{pp}$ ) with increase in temperature occurs with rates, respectively, 0.75 Oe/K and 2.6 Oe/K. It should be emphasized that normally the temperature coefficient has opposite sign. At the 350 K,  $\Delta H_{pp} = 150$  and 190 Oe, intensity ratio is 4.4:1, respectively. The bases for attribution of the low-field line to not the ion europium  $\text{Eu}^{2+}$  is not available. X-ray studies have shown single-phase structure of samples.

It should be noted that the magnetic state of the  $\text{Eu}^{2+}$  ion is a pure spin state and almost is not affected by the orbital degrees of freedom and of the crystalline field influence. Therefore,  $g$ -factor for pure spin state of the europium ion is close to the  $g$ -factor of the free electron – 2.0. Ion  $\text{Eu}^{3+}$  has not a magnetic moment, and does not manifest itself in a magnetic resonance. Thus, significant deviations  $g$ -factor  $\text{Eu}^{2+}$  ion usually originate from mixed-valence state or a strong exchange interaction. The exchange interactions of localized spins in electronic systems with free charge carriers are reduced to two main types: a) direct exchange interaction with free carriers, which leads to a linear on temperature (Korringa) contribution in the linewidth of the ESR and to electronic Knight shift; b) indirect exchange interaction via the free charge carriers, so-called RKKY interaction [3] (incl. modified for valence band [4]) and the Dzyaloshinskii-Moriya interaction. All these models have been previously built on the basis of a quadratic dispersion law for charge carriers. In the case of Dirac topological semimetal, dispersion law for the free carrier is linear. Calculation of the RKKY interaction between the localized spins in the Dirac semimetal (i.e. for linear dispersion) was carried out in [5]. It showed that at a certain ratio of strength of the exchange interactions for internode and intranode

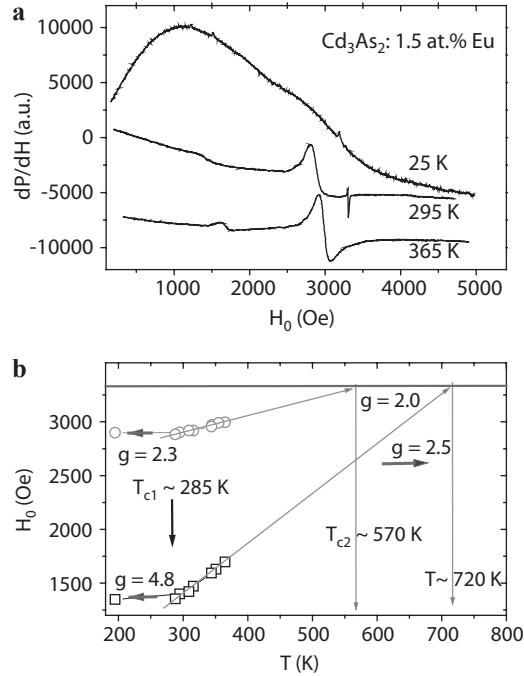


**Fig. 1.** **a** Types of ESR spectra  $\text{Eu}^{2+}$  ions in  $\text{Cd}_3\text{As}_2$ . At 25 K signal is the field derivative of the magnetoresistance. **b** The temperature dependences of the resonance fields.

processes, the nonoscillating (long-range) ferromagnetic component of RKKY interaction occurs. We believe that this explains the nature of the temperature dependence of the position and width of the observable  $\text{Eu}^{2+}$  resonance lines. However, given that in the semimetal, emergence of a free electron in the conduction band is accompanied by the emergence of a free hole in the valence band, in accordance with the ideas developed Kugel et al. [6], this should lead to microscale phase separation on ferromagnetic regions with different internal fields caused by the RKKY interaction, respectively, via the electrons or holes. In this case, in accordance with known mechanisms, sign magnetoresistance change is to occur. We observe it in sample doped by Eu. Thus, we first studied the magnetic resonance at localized magnetic moments in the topological semimetal and found an evidence of anomalously strong nonoscillating RKKY interaction between the magnetic impurities  $\text{Eu}^{2+}$ .

1. Young S.M., Zaheer S., Teo J.C.Y. *et al.*: Phys. Rev. Lett. **108**, 140405 (2012)
2. Borisenko S., Gibson Q., Evtushinsky D. *et al.*: Phys. Rev. Lett. **113**, 027603 (2014)
3. Ruderman M.A., Kittel C.: Phys. Rev. **96**, 99 (1954)
4. Bloembergen N., Rowland T.J.: Phys. Rev. **97**, 1679 (1955)
5. Hao-Ran Chang *et al.*: arXiv:1509.04741v1 [cond-mat.mes-hall] (2015)
6. Kugel K.I., Rakhmanov A.L., Sboychakov A.O.: Phys. Rev. Lett. **95**, 267210 (2005)

## Correlation of EPR and Biochemical Results of Iron Metabolism Study in Serum of Professional Athletes

**M. I. Ibragimova<sup>1</sup>, A. I. Chushnikov<sup>1</sup>, G. V. Cherepnev<sup>2</sup>,  
and V. Yu. Petukhov<sup>1</sup>**

<sup>1</sup> Zavoiysky Physical-Technical Institute, Russian Academy of Sciences, Kazan 420029, Russian Federation, [ibragimova@kfti.knc.ru](mailto:ibragimova@kfti.knc.ru)

<sup>2</sup> Health Service of Kazan Federal University, Kazan 420012, Russian Federation, [rkb2\\_rt@mail.ru](mailto:rkb2_rt@mail.ru)

It is well known that the iron plays an important physiological role in the life support and the violation of Fe metabolism, in particular, in sportsmen, may have a direct negative impact on the professional capabilities of the athlete. It is assumed that virtually all serum iron is associated with such proteins as transferrin ( $\text{Fe}^{3+}$ -Tf), although it can also join some other proteins and free amino acids. In clinical practice the biochemical determination of the serum iron concentration consists of measuring the optical density of the colored complexes formed under the release of  $\text{Fe}^{3+}$  from iron-binding serum proteins in an acidic medium with subsequent chemical reduction of  $\text{Fe}^{3+}$  up to  $\text{Fe}^{2+}$  and the reaction of the latter with chromogens. At the same time the method of EPR spectroscopy allows to estimate directly the quantity of paramagnetic  $\text{Fe}^{3+}$  ions in Tf. Therefore, the aim of this work was to study the correlation between the  $\text{Fe}^{3+}$  concentration in Tf determined from EPR spectra and that of serum iron measured by the absorption photometry using ferrozine as a chemical reagent.

EPR spectra were recorded on equal amounts of serum samples on a Varian E-12 spectrometer ( $\nu = 9.38$  GHz,  $T = 77$  K). For the quantitative estimation of

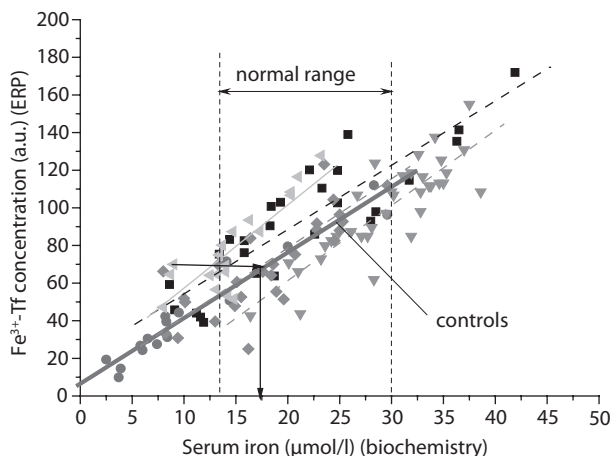


**Fig. 1.** Correlation between the  $\text{Fe}^{3+}$  concentration in Tf determined from EPR spectra and that of serum iron measured by biochemistry analysis for sportsmen and controls. As an example, the arrows indicate that the data of biochemical analysis can be underestimated by more than two times.



the results the reference spectrum of anthracite was also recorded. Serum iron was determined on a “Cobas integra 400 plus” analyzer. A group of professional sportsmen from four continental hockey League teams consisted of 115 persons. The randomly selected reference group of 16 controls included the volunteers (healthy individuals) and patients with different diagnoses (iron deficiency anemia, hypertension, ischemic heart disease and cirrhosis of the liver).

The results of the investigations are presented on Fig. 1. It can be seen from the figure that the data for controls obtained by both methods are well correlated (Pearson correlation coefficient  $r = 0.97$ ) and can be approximated by a straight line ( $y = 3.49x + 3.4$ ). These results indicate that all serum iron was bound to transferrin. At the same time for sportsmen the data of EPR spectroscopy in most cases were either overestimated or underestimated with respect to biochemical analysis data ( $r \cong 0.81$ ).

It should be noted that approximately for 75% of sportsmen such index as the total iron binding capacity of serum does not reach the lower limit of norm and this is indicative of the excessive iron accumulation in the body. Understating serum iron values in sportsmen as compared with EPR data may be due to the incomplete release of  $\text{Fe}^{3+}$  ions from Tf during the biochemical analysis. One would assume that the high saturation of Tf with  $\text{Fe}^{3+}$  ions can cause changes in the nearest environment of the paramagnetic ions, however, changes in the EPR line shape of  $\text{Fe}^{3+}$ -Tf was not revealed. The reason for the overstatement of serum iron values may be binding iron not only with Tf but with other proteins or free amino acids in the event of the excess iron accumulation in the body. However in any case these complexes are not paramagnetic (in EPR spectra new additional lines were not detected). Intense physical activities as well as the reception of biologically active preparations may be the cause of the iron metabolism disorder for professional sportsmen and as the result, the protocol measurements, which are used in the biochemical analysis of serum iron, lead to erroneous results.

Thus, the studies give reason to assume that EPR spectroscopy can be of practical application in sports medicine, as it will provide an opportunity to determine the mechanisms of disorders of the iron metabolism in cases of its excessive accumulation in the body, as well as to determine the correct choice of biologically active substances.

The work was supported by The Program of Fundamental Research of Pre-sidium RAS – 1.26II.

## Magnetic Susceptibility of an Antiferromagnetic System with Disorder: Griffiths Phase and Phases with an Intermediate Magnetic Order

**T. V. Ischenko<sup>1</sup>, A. N. Samarin<sup>1,2</sup>, and S. V. Demishev<sup>1,2,3</sup>**

<sup>1</sup> Prokhorov General Physics Institute of RAS, Moscow 119991, Russian Federation, t.ischenko@mail.ru

<sup>2</sup> Moscow Institute of Physics and Technology, Dolgoprudny 141700, Russian Federation

<sup>3</sup> National Research University Higher School of Economics, Moscow 101000, Russian Federation

In the present work, a generalization of the approach [1] for the description of the magnetic susceptibility in disordered antiferromagnets, in which the formation of long-range magnetic order is preceded by the appearance of the magnetic phase with an intermediate magnetic order, is considered. Following the suggested simple model, an analytical expression for the magnetic susceptibility  $\chi(T)$  valid for an arbitrary relationship between the temperature  $T$  and the characteristic value of the exchange integral  $J$  in disordered antiferromagnets is obtained. The model describes the transition to the antiferromagnetic phase with long-range magnetic order at low temperatures (including the case of the opening of a spin gap), the area of quantum critical Griffiths phase (phase with an intermediate magnetic order), where magnetic susceptibility is described by the power law  $\chi = 1/T^\zeta$  ( $\zeta < 1$ ), and high-temperature Curie-Weiss law with the paramagnetic temperature, depending on the characteristics of the Neel temperatures distribution function in spin clusters. The estimation of the characteristic size of the spin clusters forming Griffiths phase is considered. The application of the developed approach to the description of the electron spin resonance characteristics in experimental systems where the disorder driven quantum critical regime (germanium cuprate doped with magnetic impurities, VOx-nanomaterials, etc.) is observed.

This work was supported by programmes of Russian Academy of Sciences “Electron spin resonance, spin-dependent electronic effects and spin technologies” and “Electron correlations in strongly interacting systems”.

1. Demishev S.V.: *phys. status solidi (b)*, **247**, no. 3, 676 (2010)

## Determination of Magnetic Anisotropies Parameters and Miscut Angles for Epitaxial Thin Films Grown on Vicinal (111) Substrates Using Ferromagnetic Resonance

A. V. Izotov<sup>1,2</sup>, B. A. Belyaev<sup>1,2,3</sup>, and P. N. Solovev<sup>1,2</sup>

<sup>1</sup> Siberian Federal University, Krasnoyarsk 660041, Russian Federation

<sup>2</sup> Kirensky Institute of Physics, Krasnoyarsk 660041, Russian Federation

<sup>3</sup> Reshetnev Siberian State Aerospace University, Krasnoyarsk 660041, Russian Federation, [platon.solovev@gmail.com](mailto:platon.solovev@gmail.com)

The ferromagnetic resonance (FMR) is a powerful and convenient technique that allows for accurate measurements of magnetic anisotropy parameters for various thin-film ferromagnetic structures. This technique is of particular importance in the case of epitaxial films, where a complex combination of magnetocrystalline, uniaxial, and unidirectional anisotropies may exist [1]. Recently, thin epitaxial ferromagnetic films grown on vicinal single-crystal Si substrates have attracted particular interest because of the possibility to specifically modify magnetic properties of the films by controlling the atoms steps high and width on the substrate surface [2, 3]. In this work, we present our developed method for determining magnetic anisotropy parameters of thin epitaxial films grown on vicinal Si(111) substrates as well as substrates polar and azimuthal miscut angles.

The proposed method is based on the fitting of the experimentally measured ferromagnetic resonance field angular dependence of the investigated film by the theoretical curve. This theoretical curve is calculated using Smith and Suhl formula for the ferromagnetic resonance equation and magnetization equilibrium condition. In order to take into account polar ( $\delta$ ) and azimuthal miscut angles of the vicinal substrate in the model of a thin single-crystal ferromagnetic film, we introduce these angles into the expression for the magnetocrystalline magnetic anisotropy energy density [1]. We developed a numerical procedure that enabled us to extract the model parameters from the experimental in-plane angular dependence of the FMR field. To increase the accuracy of the method and to reduce the calculating time, we implemented the two following improvements: (i) a new approach for the solution of the system of nonlinear equations for equilibrium and resonance conditions; (ii) a new expression of the objective function for the fitting problem.

For testing of our proposed method, we studied epitaxial iron silicide thin films prepared by thermal deposition in ultrahigh vacuum on boron-doped atomically clean vicinal Si(111) substrates. Magnetic properties of the produced samples were investigated by the FMR scanning spectrometer [4] at the pump frequency  $f_0 = 3.329$  GHz. The obtained results demonstrate that the usage of the model of a film on a singular surface ( $\delta = 0^\circ$ ) leads to a significant deviation between experiment and theory for the studied here samples (Fig. 1). However, the use of our proposed film model on a vicinal surface ( $\delta \neq 0^\circ$ ) allowed us not only to determine precisely magnetic anisotropy parameters but also to retrieve the polar miscut angles that were in reasonably good agreement with the nominal values.

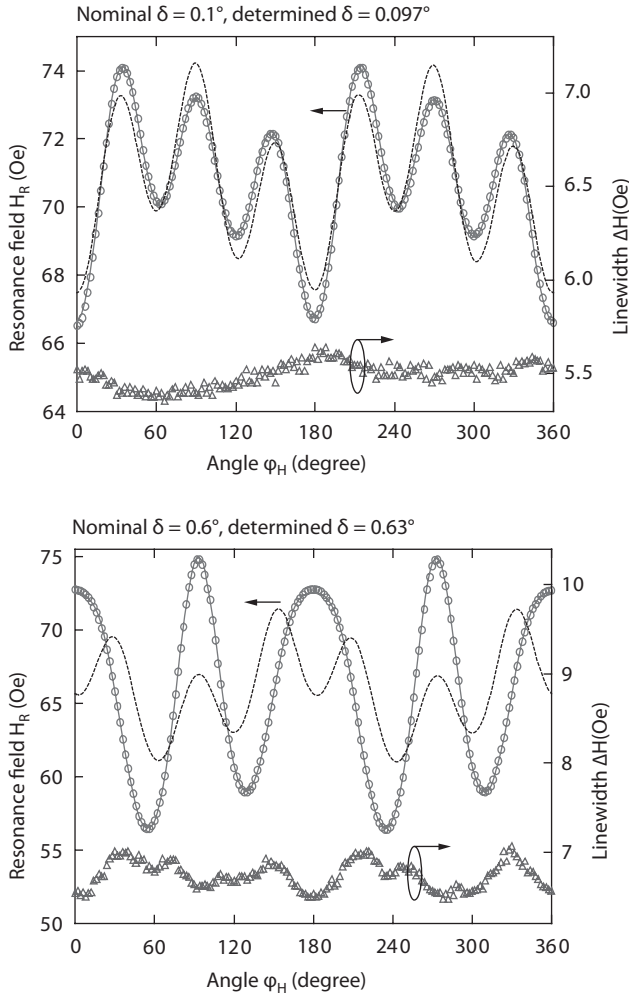


**Fig. 1.** Dependences of the resonance field  $H_R$  and FMR linewidth  $\Delta H$  on the sweeping magnetic field direction  $\varphi_H$ . Symbols correspond to the experimental measurements. Solid lines are the theoretical calculations for the model of a film on the vicinal surface with  $\delta \neq 0^\circ$ , while dashed lines show the theoretical results for the case of singular surface ( $\delta = 0^\circ$ ).

We note that the proposed method can be easily generalized to determine parameters of single-crystal films grown on substrates with an arbitrary cut.

This work was supported by the Ministry of Education and Science of the Russian Federation, task no. 3.528.2014K.

1. Belyaev B.A., Izotov A.V.: JETP Letters **103**, 41 (2016)
2. Ermakov K.S., Ivanov Yu.P., Chebotkevich L.A.: Phys. Solid State **52**, 2555 (2010)
3. Stupakiewicz A., Vedmedenko E.Y., Fleurence A., Maroutian T., Beauvillain P., Maziewski A., Wiesendanger R.: Phys. Rev. Lett. **103**, 137202 (2009)
4. Belyaev B.A., Izotov A.V., Leksikov A.A.: IEEE Sensors **5**, 260 (2005)

## Influence of the Outer-Sphere Anion on Electronic and Magnetic Properties of $[\text{Fe}(\text{3-CH}_3\text{O-Qsal})_2]\text{Y} \cdot n$ Solvent ( $n = 0, 1$ ) Complexes

**T. A. Ivanova<sup>1</sup>, I. V. Ovchinnikov<sup>1</sup>, O. A. Turanova<sup>1</sup>, L. V. Mingalieva<sup>1</sup>,  
I. F. Gilmutdinov<sup>2</sup>, and V. A. Shustov<sup>1</sup>**

<sup>1</sup> Zavoisky Physical-Technical Institute, Russian Academy of Sciences, Kazan 420029, Russian Federation, alex@kfti.knc.ru

<sup>2</sup> Kazan Federal University, Kazan 420008, Russian Federation

Based on Qsal-containing Fe(III) complexes, a number of compounds with interesting physical properties have been obtained. Thermo-induced spin transition, switching the spin state after light irradiation (LIESST effect), the coexistence of hysteretic behavior of the conductivity and spin-variable properties in the same temperature range were observed in these compounds. Synthesis and study of complexes of Fe(III) with substituted ligands X-Qsal open up new possibilities. According to previous works, solvation of the complexes, the type of outer-sphere anion Y and cooperative interactions between complexes are influenced on spin state of the  $[\text{Fe}(\text{X-Qsal})_2]\text{Y}$  complexes [1–3]. Magnetic properties of Fe(III) complexes with substituted X-Qsal ligands have been characterized by magnetic susceptibility measurements. Inter-molecular interactions, expected based on X-ray diffraction measurements, were not observed experimentally.

In this work, compounds of  $[\text{Fe}(\text{3-CH}_3\text{O-Qsal})_2]\text{Y}$  with Y = PF<sub>6</sub>, BF<sub>4</sub>, NCS, NO<sub>3</sub> и BPh<sub>4</sub> (samples **1**, **2**, **3**, **4**, **5** respectively) were synthesized by diffusion method for the first time and were characterized by methods ESR, magnetic susceptibility and X-ray diffraction measurements. Coexistence of spatially separated high-spin (solvated) and low-spin (non-solvated) fractions in these compounds has been observed. In low-spin complexes, the type of outer-sphere anion affects the crystal field symmetry (axial in samples **1–3** and rhombic in samples **4**, **5**) and magnitude of the lowest-orbital triplet splitting. In all samples the ground state is  $|d_{xy}\rangle$ . In low-spin fraction, low-temperature measurements ESR revealed the existence of dynamic antiferromagnetic correlations. In high-spin fraction, the shift of the resonance toward lower magnetic field values suggests presence of ferromagnetic inter-molecular interactions. Correlation of magnetic properties of investigated complexes with size, shape and chemical properties of outer-sphere anions is discussed.

The work was supported by the Grant of Presidium of RAS-1.26II.

1. Dias J.C., Vieira B., Santos I.C. *et al.*: *Inorg. Chim. Acta* **362**, 2076 (2009)
2. Sertphon D., Harding D.J., Hardinng P. *et al.*: *Eur. J. Inorg. Chem.* **5-6**, 788 (2013)
3. Sertphon D., Harding D.J., Hardinng P. *et al.*: *Eur. J. Inorg. Chem.* **3**, 432 (2016)

## Elucidating Mechanisms of Intramolecular Exchange Interaction in Substituted N,N'-Dioxy-2,6-Diazaadamantane Biradicals

O. N. Kadkin<sup>1</sup>, N. R. Khafizov<sup>2</sup>, T. I. Madzhidov<sup>2</sup>, and I. S. Antipin<sup>2</sup>

<sup>1</sup> Zavoisky Physical-Technical Institute, Russian Academy of Sciences, Kazan 420029, Russian Federation, oleg.kadkin@bk.ru

<sup>2</sup> Kazan Federal University, Kazan 420008, Russian Federation, nail-kh@yandex.ru

To elucidate exchange interactions mechanisms between the two nitroxyl radical groups, a series of N,N'-dioxy-2,6-diazaadamantanes with different substituents at the carbon atoms adjacent to the nitroxyl groups are studied using the quantum-chemical methods. Unrestricted DFT calculations at high levels of theory make it possible to determine theoretical values of the parameter,  $J$ , using breaking symmetry approach [1, 2]. The Mulliken spin population analysis shows that four different spin density transmission paths can be distinguished in the diazaadamantane cage, along which through-bond exchange interactions are achieved by spin-polarization mechanisms (see Fig. 1). Besides, owing to non-coplanarity of the nitroxyl groups, through-space overlap of their  $\pi$ -orbital systems in the center of molecule is possible that may contribute to a direct antiferromagnetic exchange interaction. Thus, the overall value of the  $J$  parameter can be considered as a result of four through-bond exchange interactions and one direct through-space interaction of antiferromagnetic nature.

The electron-withdrawing/electron-donating properties and steric effects of the substituents strongly affect the electron density distribution over the diazaadamantane cage. In some cases this leads to changing the sign of the  $J$  parameter due to the appearance of stronger antiferromagnetic components in some of the through-bond spin density transmission paths and a direct antiferromagnetic exchange interaction (see Table 1).

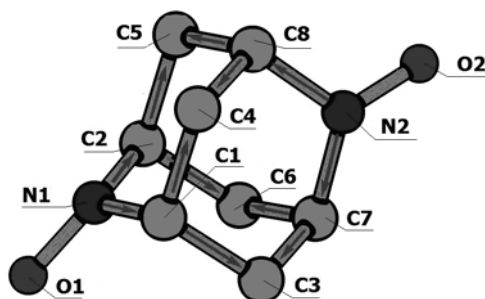


Fig. 1. Through-bond spin density transmission paths in the diazaadamantane cage.

**Table 1.** Values of the intramolecular exchange interaction parameter,  $J$  ( $\text{cm}^{-1}$ ), and Mulliken spin population for different substituents at atoms C1, C2, C7, and C8 (see Fig. 1).

| $R$   | $J$ ( $\text{cm}^{-1}$ ) | Mulliken spin population |        |        |        |        |        |        |
|---|--------------------------|--------------------------|--------|--------|--------|--------|--------|--------|
|   |                          | N1(N2)                   | O1(O2) | C1(C8) | C2(C7) | C3(C5) | C4     | C6     |
| CH <sub>2</sub> OH                            | 14.19                    | 0.45                     | 0.50   | 0.008  | -0.029 | 0.055  | 0.027  | 0.053  |
| H   | 11.87                    | 0.44                     | 0.53   | -0.028 | -0.025 | 0.045  | 0.012  | 0.075  |
| CBr <sub>3</sub>                              | 11.65                    | 0.40                     | 0.53   | 0.027  | -0.011 | 0.035  | 0.006  | 0.053  |
| CCl <sub>3</sub>                              | 9.26                     | 0.36                     | 0.56   | 0.045  | -0.004 | 0.031  | 0.031  | 0.032  |
| CF <sub>3</sub>                               | 7.33                     | 0.34                     | 0.58   | 0.061  | 0.010  | 0.022  | 0.032  | 0.021  |
| CH <sub>3</sub>                               | 6.56                     | 0.39                     | 0.54   | -0.032 | 0.028  | 0.047  | 0.045  | 0.053  |
| C <sub>3</sub> H <sub>7</sub>                 | 5.22                     | 0.40                     | 0.52   | 0.021  | 0.011  | 0.033  | 0.004  | 0.068  |
| C <sub>2</sub> H <sub>5</sub>                 | 4.43                     | 0.39                     | 0.53   | 0.037  | 0.032  | 0.026  | 0.006  | 0.053  |
| t-C <sub>4</sub> H <sub>9</sub>               | 4.39                     | 0.37                     | 0.52   | 0.059  | 0.016  | 0.030  | -0.023 | 0.083  |
| Br  | 1.45                     | 0.35                     | 0.57   | 0.008  | 0.006  | 0.025  | -0.012 | 0.066  |
| F   | 1.34                     | 0.34                     | 0.58   | 0.040  | 0.021  | 0.013  | -0.037 | 0.069  |
| Cl  | 0.33                     | 0.34                     | 0.58   | 0.039  | 0.036  | 0.013  | -0.045 | 0.075  |
| OCH <sub>3</sub>                              | 0.13                     | 0.38                     | 0.54   | 0.071  | 0.044  | 0.023  | -0.062 | 0.055  |
| CH <sub>2</sub> Cl                            | -1.93                    | 0.36                     | 0.55   | 0.060  | -0.014 | 0.056  | 0.048  | -0.009 |
| CH <sub>2</sub> C <sub>6</sub> H <sub>5</sub> | -2.46                    | 0.37                     | 0.52   | 0.038  | 0.017  | 0.037  | 0.050  | -0.034 |
| CH <sub>2</sub> F                             | -2.81                    | 0.36                     | 0.55   | 0.054  | -0.018 | 0.034  | 0.037  | -0.030 |
| CH <sub>2</sub> Br                            | -4.92                    | 0.34                     | 0.55   | 0.054  | -0.018 | 0.033  | 0.061  | -0.040 |

It is concluded that the intramolecular exchange interaction is mainly ferromagnetic in nature, but the  $J$  parameter gradually decreases, changing to the antiferromagnetic exchange interaction for the last four substituents, in the following sequence: CH<sub>2</sub>OH > H > CBr<sub>3</sub> > CCl<sub>3</sub> > CH<sub>3</sub> > C<sub>2</sub>H<sub>5</sub> > C<sub>3</sub>H<sub>7</sub> > *i*-C<sub>3</sub>H<sub>7</sub> > F > Br > OCH<sub>3</sub> > Cl > CH<sub>2</sub>Cl > CH<sub>2</sub>Br > CH<sub>2</sub>C<sub>5</sub>H<sub>6</sub> > CF<sub>3</sub>.

1. Noodleman L.: J. Chem. Phys.: **74**, 5737 (1981)
2. Noodleman L., Baerends E.J.: J. Am. Chem. Soc. **106**, 2316 (1984)

## Modeling of the Temperature Dependence of the EPR Spectra of Fullerene C60 Nitroxide Derivatives in Liquid

**I. T. Khairuzhdinov<sup>1</sup>, R. B. Zaripov<sup>1</sup>, K. M. Salikhov<sup>1</sup>,  
V. P. Gubskaya<sup>2</sup>, and I. A. Nuretdinov<sup>2</sup>**

<sup>1</sup> Zavoiisky Physical-Technical Institute, Russian Academy of Sciences, Kazan 420029, Russian Federation

<sup>2</sup> Arbuzov Institute of Organic and Physical Chemistry, Kazan, Russian Federation  
semak-olic@mail.ru

In this work were simulated EPR spectra of derivatives of fullerene C60 with two and four nitroxide radicals attached to fullerene sphere. It has been shown that nitroxide derivatives of fullerene undergo conformational changes in liquid solution. We performed a simulation of the temperature dependence of the EPR spectra in the 2-conformational model.

Let each conformation corresponds to a definite value of the exchange integral  $J_a$  and  $J_b$ ,  $J_{a,b} \ll kT$ , i.e. exchange interactions do not affect the dynamics of the conformational transitions. Then the dynamic equations for the joint (paired) spin density matrices  $\rho_a$  и  $\rho_b$ , described the conformation of a and b, can be written as follows:

$$\partial\rho_a/\partial t = (i/h)[\rho_a, H_a] - k_{ab}\rho_a + k_{ba}\rho_b = 0,$$

$$\partial\rho_b/\partial t = (i/h)[\rho_b, H_b] - k_{ba}\rho_b + k_{ab}\rho_a = 0,$$

where  $k_{ab} = \rho_{ab}/\tau_a$ ,  $k_{ba} = \rho_{ba}/\tau_b$ , here  $k_{ij}$  and  $\rho_{ij}$  are transition rate and transition probability from conformation  $i$  to conformation  $j$  respectively.

In the rotating frame Hamiltonian of each conformation is written as

$$H_j = (\omega_e^{(1)} - \omega)S_z^{(1)} + (\omega_e^{(2)} - \omega)S_z^{(2)} + a_j^{(1)}I_z^{(1)}S_z^{(1)} + a_j^{(2)}I_z^{(2)}S_z^{(2)} + J_j^{(1)}S^{(1)}S^{(2)} + \omega_S^{(1)}S_X^{(1)} + \omega_S^{(2)}S_X^{(2)},$$

where  $\omega_e^{(1)}$  is electron resonance frequency;  $a_j^{(k)}$  is HFI constant in conformation  $j$ ;  $\omega_S^{(k)}$  is Zeeman frequency in magnetic field ( $k = 1, 2; j = a, b$ ),  $J_j$  is exchange coupling in conformation  $j$ .

EPR signal in this situation determined by:

$$\text{EPR}_{\text{signal}} = \text{Sp}[(\rho_a + \rho_b)(S_Y^{(1)} + S_Y^{(2)})]$$

Whereas for tetradical derivatives of fullerene the situation more complicated. Also in this work we estimated values of energy activations  $E_a$  and transition rates  $k$  between two conformations. These values were estimated using Arrhenius equation

$$k = A\exp(-E_a/RT).$$



## Cloud Project for Storage and Processing of Medical Images Obtained by MRI of Zavoisky Kazan Physical Technical Institute

**R. Khabipov, I. Sitdikov, and Ya. Fattakhov**

Zavoisky Physical-Technical Institute, Russian Academy of Sciences, Kazan 420029,  
Russian Federation, [myster@mail.ru](mailto:myster@mail.ru)

Cloud computing is widely used in various areas of medicine including MRI [1–3]. The possibilities of using cloud technologies reduce costs of service and hardware resources, improve reliability, scalability and flexibility.

Therefore, the whole world admitted the need of transition to cloud computing in areas, that use large amounts of data for storage. The American Association of Health Insurance Portability and Accountability ACT (HIPAA) has ordered medical institutions to transfer data from local storage to cloud services. In medicine cloud computing it is expected the significant increasing. Many famous companies, who deal with medical have launched the service which based on cloud computing technologies [4–6]. The service operates with the DICOM standard and allows to store patient's medical data. It is flexible, safe and effective solution for medical institutions, which have to store large volumes of medical data.

But cloud-based solutions offered by manufactures of medical equipment are not universal. They are designed for a specific apparatus, and difficult to reconfigure. Public clouds can create potential problems of information leakage, because they don't have full control over the data. Also, according to Russian Federation rules, personal information must not kept in the territory of the other countries.

Currently, a cloud-based solution is being developed for MRI-scanners, which were created in the Kazan Physical Technical Institute. This will be a private cloud with access via web-browser. The project has versatility, i.e. project works not only with our MRI, but also with other medical equipment that supports DICOM 3.0 standard.

The main purpose of development is the ability to save and process medical images in the cloud. This will allow remote diagnosis, cooperative examination, the centralization of all data. It is possible for patients to access to their diagnoses. Diagnostic data, obtained by MRI, automatically will be sent to the cloud. A doctor will have real-time access, no matter where he is.

For data access it will be enough to have any device with a web-browser and access to the internet: a computer, a tablet, a smartphone. The cloud solution is planned to be universal with the ability of saving and processing any patient's diagnostic data.

The project consists of two main modules:

1. The server module is responsible for storage and processing of medical data and output of medical images on request from users.
2. Synchronization module is executed at the workstation, which is connected to the MRI scanner, and sends obtained medical images to the cloud server. The objective of the development of our project is to create a reliable, fast, easy to use system, that lets you view and process large amounts medical data. The project will extend and adapt to different hardware requirements and data formats. Access to data will be protected by separating users' rights.

Internet-resources:

1. <http://www.forbes.com/sites/centurylink/2013/05/02/why-healthcare-must-embrace-cloud-computing/>
2. <http://cyberleninka.ru/article/n/oblachnye-vychisleniya-v-meditisine>
3. <http://www.precisionit.com.au/solutions/medical-it-solutions/medical-cloud-computing>
4. <http://usa.healthcare.siemens.com/medical-imaging-it/multi-site-and-regional-solutions/image-sharing-archiving/features>
5. <http://www.itpro.co.uk/627952/what-is-cloud-computing>
6. [http://en.wikipedia.org/wiki/Cloud\\_computing](http://en.wikipedia.org/wiki/Cloud_computing)

## High Temperature Fast Field Cycling Study of Crude Oil

A. Lozovoi<sup>1</sup>, M. Hurlimann<sup>2</sup>, R. Kausik<sup>2</sup>, S. Stapf<sup>1</sup>, and C. Mattea<sup>1</sup>

<sup>1</sup> Department of Technical Physics II, Technical University of Ilmenau, Ilmenau 98684, Germany, Artur.Lozovoi@tu-ilmenau.de

<sup>2</sup> Schlumberger-Doll Research, Cambridge, Massachusetts 02139, United States

Nuclear magnetic resonance (NMR) has been widely used to study crude oil both in bulk and in reservoirs. Among other NMR methods, fast field cycling (FFC) relaxometry is of a particular interest for the laboratory research of oils, since it provides an opportunity to obtain information about the oil composition and molecular dynamics from a distribution of longitudinal relaxation times  $T_1$  as a function of Larmor frequency. Creating conditions similar to the oil wells, e.g. pressure, temperature, etc., allows one to predict the behaviour of the aforementioned oil characteristics in a borehole. This information helps to significantly improve the efficiency of oil extraction and transportation.

Conventional FFC probes do not provide an opportunity to perform measurements at the in-situ well temperature, which can exceed  $\sim 170$ – $175^\circ\text{C}$ . Therefore, the prediction of the features of the  $T_1$  distributions at that temperature has been made based solely on theoretical modeling and extrapolations from laboratory measurements. To enable direct experiments at these conditions, a high-temperature probe suitable for use in Stellar Spinmaster FFC2000 has been designed and constructed. This allows FFC experiments to be performed at temperatures up to  $200^\circ\text{C}$ .

Crude oil samples with known SARA (saturate, aromatic, resin, asphaltene) composition analysis were used for this high-temperature FFC study. As is well known, crude oils are a complex mixture of different molecules with a broad range of sizes, shapes and properties, resulting in complex molecular dynamics.

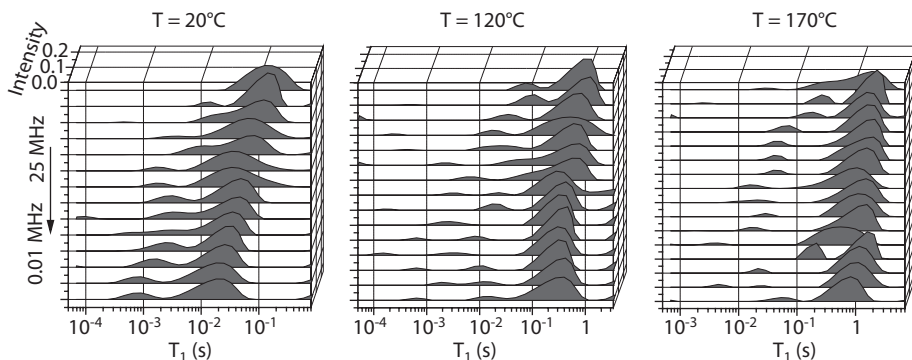


**Fig. 1.**  $T_1$  relaxation times distributions for crude oil with 12.9% asphaltene content for 3 temperatures obtained with the use of Inverse Laplace Transform.

Consequently, their NMR response cannot be described by a single relaxation time and one has to assume a broad distribution of  $T_1$ , generally obtained using an inverse Laplace transform (ILT) [1].

The focus of this research was on investigating the effect of asphaltene molecules in crude oils on the  $T_1$  relaxation time distribution at the high temperatures experienced downhole. This is of particular interest since the influence of even small amount of asphaltene on the rheological properties of oil is significant because of the tendency of these molecules to form porous aggregates. The mechanism of aggregation is not clearly understood and several models for this process can be found in the literature [2]. In this work, oils with different asphaltene content (12.9%, 6.6%, 0%) were studied. The measured longitudinal relaxation decays were recalculated into the distributions of  $T_1$  with the use of an ILT procedure. Resulting relaxation spectra for a range of frequencies from 0.01 MHz to 25 MHz at temperatures up to 170°C are shown in Fig. 1.

1. Freed D.E., Hurlimann M.D.: *Comptes Rendus Physique* **11**(2), 181–191 (2010)
2. Zielinski L., Saha I., Freed D.E., Hurlimann M.D., Liu Y.: *Langmuir* **26**(7), 5014–5021 (2010)

---

## **Manipulating Electron Spin Hyper-Polarization by Means of Adiabatic Switching of a Spin-Locking MW Field**

**N. N. Lukzen and K. L. Ivanov**

International Tomography Center SB RAS, Novosibirsk 630090, Russian Federation, luk@tomo.nsc.ru

A new method has been proposed allowing one to convert initial multiplet electron spin order into net electron polarization. It is based on hyper-polarizing a system of dipole-dipole coupled electron spins in the presence of a strong MW-field, which is subsequently slowly (adiabatically) reduced to zero. The technique can be useful for manipulating hyper-polarization, in particular, in cases where multiplet spin order gives the main contribution to electron hyper-polarization. The method allows one not only reversing the sign of the multiplet polarization but also converting it into net hyper-polarization without any loss of the spin order. Therefore net hyper-polarized signals can be used in ESR time-resolved spectroscopy to study, for instance, photoinduced charge separation in photo-voltaic cells. The difference of the form between thermal ESR spectrum of two dipole-dipole coupled electron spins (Pake doublet) and the spectrum resulting from adiabatic switching of the strong MW field will be analysed for the radical pair which appears in singlet state of two electron spins. The effect of setting the MW-field frequency will be investigated.

Financial support by the Russian Foundation for Basic Research (nos. 14-03-00380, 15-33-20716) is gratefully acknowledged.

## Hyperfine Structure of $\text{Er}^{3+}$ Ion in Bulk Copper

**S. Lvov** and **E. Kukovitsky**

Lab of Physics of Carbon Nanostructures and Composite Systems,  
Zavoisky Physical-Technical Institute, 420029, Russian Federation, sglvov@ya.ru

Hyperfine interaction (HFI) constant of  $\text{Er}^{3+}$  was determined by ESR method in copper-erbium dilute alloy. The constant was obtained by the comparison of experimental  $\text{Er}^{3+}$  spectrum recorded in X-band at 1.6 K and calculation of absorbed microwave power. Experimentally observed EPR spectrum in CuEr dilute alloy is superposition of spectra of even erbium isotopes with nuclear spin  $\mathbf{I} = 0$  and odd ones with  $\mathbf{I} = 7/2$ . Thus absorbed power is determined by solution of system of equations consisting of Maxwell equations and Bloch-Hasegawa equations for conduction-electrons magnetization, localized-moment magnetization with  $\mathbf{I} = 0$  and of separate equations for each  $m_I$  component of even isotope magnetization. We used system of equations supposed in [1] for our calculations. Least-squares method was applied to fit calculated spectrum to experimental one. HFI constant, localized-moment- and conduction-electron-spin-lattice relaxation rates and erbium concentration are the fitting parameters. Both experimental (red circles) and calculated (black solid line) spectra are shown on the Fig. 1 and demonstrate very good agreement.

Analysis showed that best fit of the spectra is achieved at  $A_{\text{hfs}} = 74.00 \pm 0.05$  G and the localized-moment spin-lattice relaxation time value  $2.6 \cdot 10^{-9}$  s with erbium concentration in very dilute limit. Spin dynamics of the Cu-Er system accounting these estimations are discussed.

1. Pifer J.H., Longo R.T.: Phys. Rev. B **4**, 3797 (1972)

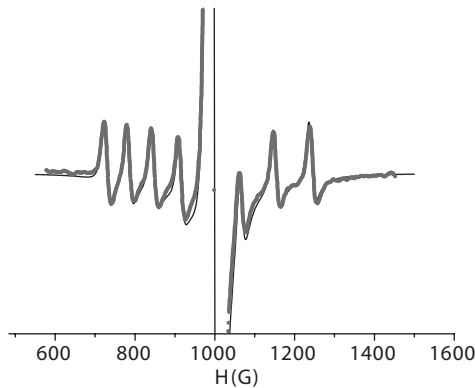


**Fig. 1.**

## NQR Relaxation Times Distribution of 5-Aminotetrazole Monohydrate

**S. Mamadazizov<sup>1</sup>** and **G. Kupriyanova<sup>1</sup>**

<sup>1</sup> Institute of physics and mathematics, Immanuel Kant Baltic Federal University, Kaliningrad 236016, Russian Federation, sultonazar.mamadazizov@mail.ru

Nuclear Quadrupole Resonance is efficient technique for solid samples investigation. NQR frequencies depend on Electric Field Gradient and nuclei's quadrupole moment. Modern multipulse sequences in NQR spectroscopy allow us to study the structure of molecular compounds, and the dynamic behavior of some nuclei.

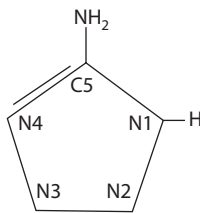


Fig. 1. 5-aminotetrazole monohydrate.

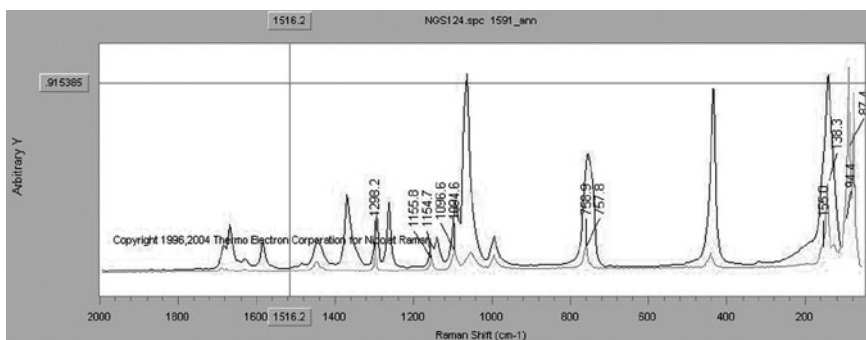


Fig. 2. Raman spectrum of 5-aminotetrazole monohydrate (95%).

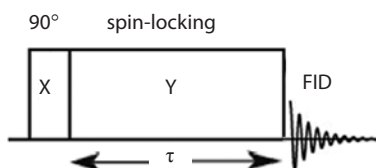
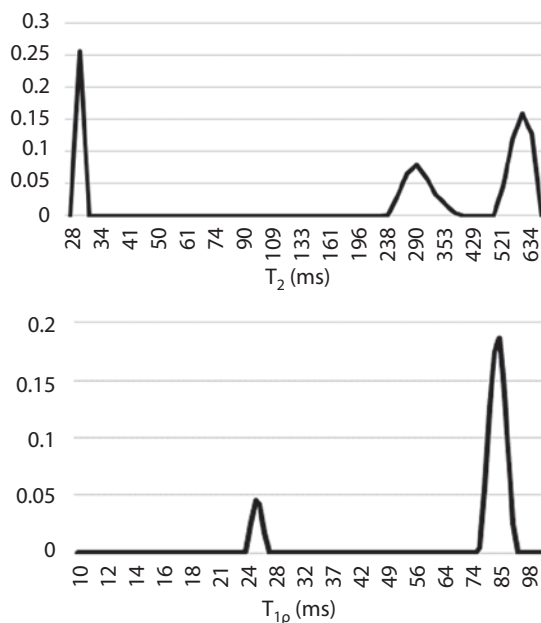


Fig. 3. Pulse sequence for spin-lattice relaxation time in the rotating frame  $T_{1\rho}$ .



**Fig. 4.** Relaxation times distribution.  $T_2$  is for N(3) and  $T_{1p}$  for N(4).

**Table 1.** NQR frequencies and relaxation times  $T_1$  and  $T_{1p}$  of ATZH.

| N(i) | $\nu_+$ (MHz) | $T_1$ (s) | $T_{1p}$ (s) |
|------|---------------|-----------|--------------|
| 1    | 2.74          | –         | –            |
| 2    | 3.615         | 1.6       | 0.4          |
| 3    | 3.7           | 1.8       | 0.6          |
| 4    | 3.33          | 1.1       | 0.08         |
| 5    | 3.144         | 1.5       | 1.1          |

Highly nitrogenous tetrazole (TZ) derivatives are quite interesting objects for NQR researches, because they find some practical implementations as components of pharmaceuticals, rocket propellants, explosives. In our work some results on  $^{14}\text{N}$  NQR relaxometry of 5-aminotetrazole monohydrate (ATZH) are presented. To identify our object with 98% accuracy Raman spectrum were obtained on LabRAM HR Ev spectrometer at Science Park of IKBFU. According to Raman spectrum, our object is indeed ATZH of technical purity 95% (Fig. 2)

The relaxation time of quadrupole nuclei depends on sample's degree of order. Thus, the crystal solids tend common to have longer relaxation times than amorphous. Some inverse-recovery and CPMG experiments were carried out to obtain the longitudinal  $T_1$  and transverse  $T_2$  relaxation times in ATZH[1]. Additionally spin-locking effect was studied to obtain the data on spin-lattice relaxation time in the rotating frame system  $T_{1p}$ . Pulse sequence for spin-locking effect is shown on Fig. 3. The pulse sequence for measurements of relaxation



time  $T_{1\rho}$  consists of  $90^\circ$  pulse and spin-locking pulse with variable duration. Second pulse keeps a magnetization vector in the rotating frame system.

Relaxation times data massive was processed by Regularized Inverse Laplace Transform. During proceeding, we used 50–200 approximation points. Number of iterations varied in the range from 100 to 200.  $T_2$  relaxation times distribution (see Fig. 4) consists of one peak at the range from 10ms to 40 ms and several peaks about hundreds ms. It is possible that short  $T_2$  refers to transverse relaxation time of surface nuclei, which are able to relax faster. Other peaks could belong to nonequivalent nuclei in the sample. Longitudinal relaxation times distribution are also multicomponent for all nuclei.  $T_1$  values could vary in the range of 1 s.

Another situation take places in case of  $T_{1\rho}$ . Only for N(4) (Fig. 4) distribution is multicomponent. For other nuclei short relaxation time peak (10–30 ms) is quite small in comparison with main peaks, which are about hundreds ms.

1. Mamadazizov S., Kupriyanova G.: Nuclear Quadrupole Resonance in 5-aminotetrazole monohydrate, "Magnetic Resonance: from fundamental research to practical application", p. 148–149. Book of abstracts, 2016.

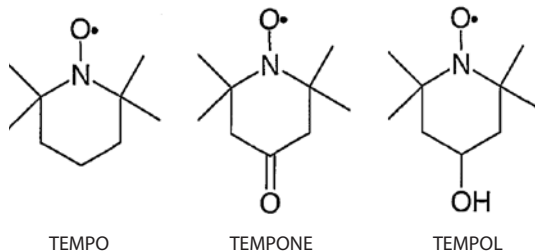
## Investigation of Influence Conformations of Nitroxyl Radicals on EPR Parameters by DFT Method

**A. Mamatova<sup>1</sup> and L. Savostina<sup>1,2</sup>**

<sup>1</sup> Kazan Federal University, Kazan 420008, Russian Federation, [mamatovaalinka@mail.ru](mailto:mamatovaalinka@mail.ru)

<sup>2</sup> Zavoisky Physical-Technical Institute, Russian Academy of Sciences, Kazan 420029, Russian Federation, [savostina.kfti@gmail.com](mailto:savostina.kfti@gmail.com)

Six-membered heterocyclic nitroxyl radicals have traditionally been used as spin labels in EPR experiments. It is widely known that the characteristic feature is the ability of these compounds is a cyclic molecule in different conformations: a bath, chair and twist. The aim of study was to investigate by DFT method impact on the parameters of the EPR spectra of the conformational structure nitroxyl radical (TEMPO, TEMPONE, TEMPOL)



Quantum chemical calculations of the structure and parameters of the EPR spectra of nitroxyl radicals by the ORCA software package using PB86 functional, B3LYP, BHandHLYP and basis sets SVP, TZVP, EPRII, EPRIII were carried out [1]. Calculations have shown that low-energy structure for all the compounds studied is the chair conformation.

The values of the parameters of EPR spectra (hyperfine interaction constant and  $g$ -factor) for the chair conformation are closest to the experimental data [2]. It was also shown that the most optimal combination of the functional / the basis for calculations of the structure of nitroxyl radicals is BP86/TZVP, and for calculations of the EPR spectra parameters – BHandHLYP/EPRII.

1. Neese F.: *Comp. Mol. Science* **2**, 73–78 (2012)
2. M. Kumara Dhas: *European J. of Biophysics* **2**, no. 1, 1–6 (2014)

## Development of Permanent Magnet System for Time-Domain NMR

**A. Maraşlı<sup>1</sup>, M. Maksutoğlu<sup>1</sup>, Y. Öztürk<sup>1</sup>, and B. Z. Rameev<sup>1,3</sup>**

<sup>1</sup> Gebze Technical University, Gebze/Kocaeli 41400, Turkey, amarasli@gtu.edu.tr

<sup>2</sup> TÜBİTAK, BİLGEM, Gebze/Kocaeli 41470, Turkey

<sup>3</sup> Zavoisky Physical-Technical Institute, Russian Academy of Sciences, Kazan 420029, Russian Federation

The most important and expensive part of the typical NMR system is a magnetic system. Superconducting cryocooled magnets, usually used to obtain high-field magnetic field, are very expensive and complex in construction. Taking into account that in many branches of NMR (including time-domain NMR or NMR relaxometry) obtaining of the magnetic field of moderate uniformity is enough, development of low-cost alternatives to the superconducting magnets is actual task.

In this work, a design of low-cost permanent magnet system for time-domain NMR measurements is presented. NdFeB permanent disc shaped magnets are fixed inside the cage made of soft iron. Pole caps made of low carbon iron are placed on each magnet to improve the magnetic field homogeneity. The magnetic flux density in air gap of constructed system has been measured and rather uniform magnetic field is observed in the magnet center. Test NMR measurements using the constructed magnetic system are also presented. Theoretical calculations of the designed magnet systems have been performed. For the fixed gap distance (50 mm without shims), we compared various experimental situations: 1) using only permanent magnet tablets inside the iron yoke (no shims), 2) with flat shims (of constant thickness), 3) with polynomial and spherically concaved shims. The best result has been obtained for the magnet with spherically concaved shim. We have also shown that the shim parameters are very sensitive to the pole gap distance.

The work was supported by NATO Science for Peace and Security Programme, NATO SPS project no. 985005 (G5005). A. Maraşlı (Ideamag LTD) and M. Maksutoğlu (Magde Cryo-Magnetic Systems LTD) also acknowledge the support of Ministry of Science, Industry and Technology under Teknogirişim Program.

## Molecular Mobility of n-Hexane in Silicalite-1 by 2D NMR Relaxo- and Diffusometry

**D. L. Melnikova<sup>1</sup>, T. V. Shipunov<sup>1</sup>, M. N. Makarov<sup>1</sup>,  
H. Zhou<sup>2</sup>, and B. I. Gizatullin<sup>1</sup>**

<sup>1</sup>Kazan Federal University, Kazan 420008, Russian Federation

<sup>2</sup>Chemical Technology, Lulea University of Technology, Lulea SE-91187, Sweden  
melndaria@gmail.com

Silicalite-1 is a nanoporous aluminosilicate with MFI (mordenite framework inverted) structure (diameter of channels is  $5.3 \times 5.6$  Å) prepared without aluminum [1]. Its unique properties allow using of this material in the chemical and petrochemical industries as catalyst, adsorbent and “molecular sieve”. Moreover, silicalites are model samples for investigation of fundamental physical processes of molecular diffusion, exchange etc [2, 3]. Main goals of this work were both investigation of molecular mobility of adsorbed n-hexane and study of structural features of silicalite-1. Samples of powder silicalite-1 were obtained from Lulea University of Technology, Sweden.

Pulsed NMR spectrometer Apollo (Tecmag) was used to study the 2D nuclear magnetic relaxation and self-diffusion in bulk and adsorbed n-hexane. Main characteristics of Apollo spectrometer are as follows: 300 MHz  $^1\text{H}$  resonance frequency, duration of  $\pi/2$  pulse  $7 \mu\text{s}$ , “dead time” of receiving tract  $\tau_d = 25 \mu\text{s}$ , inhomogeneity of the magnetic field – not more than 0.01 gauss/cm. Measurements of 1D and 2D correlation of relaxation times ( $T_1$ - $T_2$ ) and self-diffusion coefficients ( $T_1$ - $D$ ,  $T_2$ - $D$ ) were performed at 295 K by standard pulse sequences [4–6]. Estimation of exchange time between components with different  $T_2$  was carried out with the use of Goldman-Shen pulse sequence [7].

Three types of 2D correlation maps were presented on figure 1. Despite of the simple structure of silicalite-1 several components with different correlation parameters were observed on the set of  $T_1$ - $T_2$ - $D$  graphs. Based on literature data [3, 8–9], it can be assumed that components with different  $T_2$  relaxation times correspond to molecules of n-hexane in intra- and intercrystalline part of

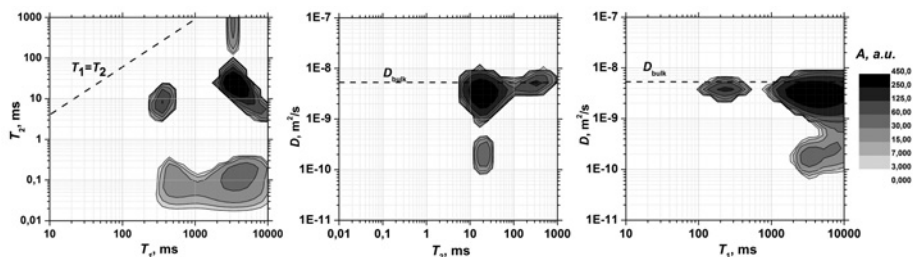


Fig. 1.  $T_1$ - $T_2$ ,  $T_2$ - $D$ ,  $T_1$ - $D$  correlation maps of n-hexane in silicalite-1.

silicalite-1. On the other hand, we attribute the presence of distribution of  $T_1$  relaxation times to exchange processes between different parts of silicalite-1. Moreover, the presence of the component with relaxation times  $T_1 = 350$  ms,  $T_2 = 10$  ms and self-diffusion coefficient close to the one of a bulk n-hexane  $D = 3.8 \cdot 10^{-9}$  m<sup>2</sup>/s implies that additional area or “defects” in the structure of silicalite-1 exists [9]. The component with  $D = 2 \cdot 10^{-10}$  m<sup>2</sup>/s cannot be associated with molecules of n-hexane in nanochannels because of its short  $T_2$  value. Goldman-Shen experiment was performed for a numerical estimation of self-diffusion coefficients of n-hexane molecules in nanochannels. The calculated self-diffusion coefficient of n-hexane molecules in silicalite-1 nanochannels was  $2.9 \cdot 10^{-11}$  m<sup>2</sup>/s.

Time dependence of self-diffusion coefficients of n-hexane in silicalite-1 was measured to correlate the obtained data with the structure of silicalite-1. Two self-diffusion coefficients, corresponding to restrictions with calculated size 4 and 34  $\mu\text{m}$ , were determined. These values correlate well with the sizes of silicalite-1 crystallites ( $30 \times 7 \times 7$   $\mu\text{m}$  [2]).

This work was supported by the Russian Foundation for Basic Research (Project no. 16-32-00169 mol\_a).

1. Tosheva L., Valtchev V.: Chem Materials **17**, 494 (2005)
2. Filippov A., Dvinskikh S.V., Khakimov A., Grahn M., Zhou H., Furo I., Antzutkin O.N., Hedlun J.: Magn. Res. Im. **30**, 1022 (2012)
3. Paciok E., Haber A., Maxime Van Landeghem, Blümich B.: Z. Phys. Chem. **226**, 1243 (2012)
4. Ernst R.R., Bodenhausen G., Wokaun A.: Principles of Nuclear Magnetic Resonance in One and Two Dimensions. Oxford: Oxford University Press 1987.
5. Monteilhet L., Korb J.-P., Mitchell J., McDonald P.J.: Phys. Rev. E. **74**, 061404 (2006)
6. Song Y.-Q., Venkataramanan L., Hurlimann M.D., Flaum M., Frulla P., Straley C.: J. Magn. Res. **154**, 261 (2002)
7. Valliulin R., Furo I.: J. Chem. Phys. **117**, 2307 (2002)
8. Uryadov A.V., Skirda V.D.: Magn. Res. Im. **19**, 429 (2001)
9. Takaba H., Yamamoto A., Hayamizu K., Oumi Y., Sano T., Akiba E., Nakao S.: Chem. Phys. Let. **393**, 87 (2004)

## Complex Downhole Apparatus for Magnetic Resonance Logging

**V. Murzakaev<sup>1</sup>, A. Bragin<sup>1</sup>, D. Kirgizov<sup>1</sup>, D. Nurgaliev<sup>2</sup>, A. Alexandrov<sup>2</sup>,  
A. Ivanov<sup>2</sup>, M. Doroginitckiy<sup>2</sup>, V. Skirda<sup>2</sup>, Ya. Fattakhov<sup>3</sup>, V. Shagalov<sup>3</sup>,  
A. Fakhрутдинov<sup>3</sup>, R. Khabipov<sup>3</sup>, and A. Anikin<sup>3</sup>**

<sup>1</sup> TNG Group Ltd, Bugul'ma, 423236, Russian Federation, vmurzakaev@rambler.ru

<sup>2</sup> Kazan Federal University, Kazan 420008, Russian Federation, kazanvs@mail.ru

<sup>3</sup> Zavoisky Physical-Technical Institute, Russian Academy of Sciences, Kazan 420029, Russian Federation, fattakhov@kfti.knc.ru

A complex device for downhole logging has been designed. The main purpose of the device is to obtain reservoir properties of a well by combining NMR data with simultaneous dielectric measurements. This combination must provide more reliable interpretation of data, especially in complicated collectors. The device consists of three blocks: electronic block, NMR probe and dielectric probe. Magnetic system for NMR is built of a set of SmCo permanent magnets. The main quality of this alloy is minimal temperature dependence of magnetization. Magnetic system generates three distant areas of magnetic field from where NMR signal is obtained: 1) 190 mm from device axis, saddle-point type, nearly homogeneous field; 2) 230 mm from device axis, saddle-point type, nearly homogeneous field; 3) 190 mm from device axis, gradient type magnetic field. The saddle-point areas have very high vertical resolution – about 3 cm, and allow to measure relaxation times, which are less disturbed by diffusion. The different depth of investigation allows to estimate drilling mud filtration of the rock. The gradient area at contrary allows to estimate the diffusion coefficient of fluid.

In order to achieve and grant high reliability of NMR data unique electronics has been designed: highly sensible receiver, noiseless power source, programmer built on FPGA and DSP chips, which could perform any kind of sequence, and the best methods of digital signal processing, RF power amplifier with active damping and self-protection circuits. To grant reliability of operation, all of electronics are operable from 0 to 150°C.

The software contains all tools for device management and tuning, and a set of logging sequences, which employ all common NMR logging methods: standard activation, activation of double TE and TW, 2D  $T_1$ - $T_2$  and  $T_2$ -D measurements.

The second part of apparatus is the device for scanning dielectric parameters of a rock is based on the method of a wave dielectric logging. The essence of the method is the measure of the characteristics of high frequency electromagnetic field excited by a device and propagated in the borehole and in surrounded stratum. The difference of phases and relation of the amplitudes between signals depends upon the electric capability of a surrounded stratum.

Having a measure of the difference of phases, one can determine the dielectric permeability of the surrounded stratum in which the electric field is propagated. It's known, that dielectric permeability of a water equals to 80 relative units, the dielectric permeability of the main minerals, which constitute a rock, equals to 4–6 relative units, and the dielectric permeability of petroleum – 2.5 relative

units. This way, having a measure the difference of phases, one can separate oil-saturated rocks from water saturated ones.

The exploitation of this device is intended at the extremely hard conditions: the pressure in a borehole cavity may amount to 800 atmosphere and the temperature at 130 °C. So all electronic devices are temperature-stabilized, enclosed in titan case and protected by radio transparent shell.

During successful testing of the device there were shown a possibility of the medium differentiation with different water and oil concentration.

## EPR Investigation of Some Complexes of Fe(III) with Pentadentate Ligand

I. Ovchinnikov, T. Ivanova, A. Suhanov, E. Frolova, O. Turanova,  
L. Mingalieva, and L. Gafiyatullin

Zavoisky Physical-Technical Institute, Russian Academy of Sciences, Kazan 420029,  
Russian Federation, fro-e@yandex.ru

The investigation of light-induced spin-state dynamics of Fe(III) spin crossover (SCO) materials recently was carried out by R. Bertoni and co-workers [1]. It was shown that the processes which started by femtosecond laser flash involves several steps in femtosecond, nanosecond and microsecond time scale. The last one is the time scale of our TR-EPR measurements. We apply the CW and TR-EPR spectroscopy to investigation of out-of-equilibrium dynamics of spin systems with thermally-induced SCO in solid state and in frozen solutions. An iron (III) complexes [FeSaltenX]BPh<sub>4</sub> (H<sub>2</sub>Salten = 4-azaheptamethylene-1,7-bis(salicylideneimine); X = Cl, BPh<sub>4</sub>, imidazole(Him), 4-methylpyridin (Pic)) has been synthesized, which spin crossover properties are quite sensitive to nature of X-ligand [2].

CW EPR study of powder samples shows that [FeSaltenPic]BPh<sub>4</sub> demonstrates thermally-induced SCO: LS ( $S = 1/2$ )  $\leftrightarrow$  HS ( $S = 5/2$ ), while the rest compounds remain in HS state at 5–300 K. Nevertheless, according to the EPR data, in frozen solutions all complexes manifested SCO properties, excepting [FeSaltenCl]BPh<sub>4</sub>, which demonstrate only coexistence of HS and LS centers at 5–180 K. TR-EPR experiments were performed at laser wavelength 532 nm and various power of a laser flash. The spectra of powder samples reveal the spin-polarization (SP) states for various Fe(III) centers in investigated compounds. Thus for [FeSaltenPic]BPh<sub>4</sub> was established the SP for  $S = 1/2$  only in a wide temperature interval (5–120 K). For [FeSaltenHim]BPh<sub>4</sub> we registered along with SP for  $S = 5/2$  the absorption line which corresponds to excite spin state. The nature of the last one is the object of further investigations.

The financial support of the Grant of Presidium of RAS-1.26II is gratefully acknowledged.

1. Bertoni R., Lorenc M. *et al.*: J. Mater. Chem. C. DOI: 10.1039/c5tc00854a (2015)
2. Ovchinnikov I., Ivanova T. *et al.*: Rus. Journ. Coord. Chem. **39**, 598 (2013)



## Development of New Approaches to NMR Data Processing in Time-Domain NMR

**O. V. Petrov and S. Stapf**

Institute of Physics, Ilmenau University of Technology, Ilmenau D-98684, Germany,  
oleg.petrov@tu-ilmenau.de

A many NMR techniques rely on measuring magnetization versus a variable parameter. Among them are  $T_1/T_2$  relaxometry, diffusometry, NOE and chemical exchange monitoring, as well as more specific stimulated-echo measurements of high-order correlation functions and multiple coherence buildups. The experiments often result in a signal of low signal-to-noise ratio, making an optimum data quantification a matter of great concern. Thereby, we present a simple, parameter-free method of measuring the total magnetization on arrays of NMR signals based on principle component analysis (PCA) [1, 2]. PCA has the advantage over measurements on individual signals of utilizing “the collective power of the data”. Conveniently, it is a black-box method in the sense that the user interaction is minimal and all parameters are estimated in one step.

Another problem which is often encountered in NMR relaxometry is how to treat non-exponential relaxation data. A common approach to such data analysis is resolve the relaxation function into a sum of exponentials by inverse Laplace transform (ILT) and deal with a quasi-continuous relaxation time distribution,  $g(\tau)$ . The key question is how to proceed with thus obtained  $g(\tau)$ , particularly whether any further quantification of  $g(\tau)$  as a function of experimental conditions is required. If the latter is the case, it is advisable to parameterize  $g(\tau)$  in terms of its moments which would characterize the centre of gravity, the span over the  $\tau$ -scale, and the symmetry of  $g(\tau)$ . Here we demonstrate how to calculate those moments on the logarithmic time scale, using a method originally introduced by Zorn for dielectric relaxation [3]. The method does not require calculation of  $g(\tau)$  through ILT and thus is free of ambiguities that may accompany such an inversion.

1. Stoyanova R., Kuesel A.C., Brown T.R.: J. Magn. Reson. A **115**, 265 (1995)
2. Stoyanova R., Brown T.R.: J. Magn. Reson. **154**, 163 (2002)
3. Zorn R.: J. Chem. Phys. **116**, 3204 (2002)

## Effects of Femtosecond Magneto-optics Based on Photon Echo and Practical Significance

I. Popov, N. Vashurin, and A. Bahodurov

Department of design and manufacture of radio equipment, Volga State University of Technology, Yoshkar-Ola 424000, Russian Federation, popov@volgatech.net

It demonstrates the ability to convert femtosecond time slots in the angle of rotation of the polarization of the stimulated photon echo (SFE) excited on the exciton states localized on the nanoscale crystal lattice defects textured thin semiconductor films. The angle of rotation of the polarization plane of the echo signal  $\varphi$  is determined by the type of product and the quantum transition amplitude of the magnetic field for the delay time between the exciting laser pulses. The value of this angle  $\varphi$  is greater than the value of the Faraday rotation by 3-4 orders of magnitude ( $10^3$ – $10^4$ ).

In this paper as the medium selected resonant excitonic states localized on the fibers of nanosize crystalline defects three layer thin ZnO/Si(P)/Si(B) (three layer for each 100 nm thick) prepared by magnetron sputtering. This film is made a prerequisite for the effect – different cleavage in the magnetic field of the upper and lower levels of the quantum transition [1]. Figure 1 shows the discovery nonFaraday SFE polarization plane rotation in a thin-layer film of ZnO/Si(P)/Si(B) at room temperature in a uniform longitudinal magnetic field.

From Fig. 1 it follows that registration by changing the angle  $\varphi$ , consisting of 7 or 8 degrees (depending on the plot function  $\varphi = f(\arctg \tau_{2/3})$ ) can determine the time interval  $\tau_{2/3}$ , was 180 degrees. Thus, the resolution of the recording time slot was no worse than  $180/7$  fs / degree. Using a precision polarization logger can increase the resolution of several orders of magnitude.

1. Alekseev A.I.: JETP Letters 9, no. 8, 472–475 (1969)

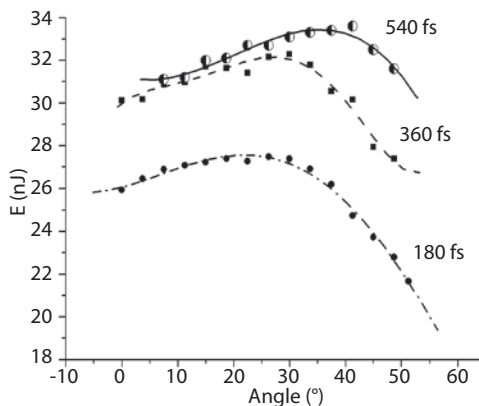


**Fig. 1.** The dependence of the rotation vector nonFaraday depending on the time interval between the second and third exciting pulses: 180 fs at  $\tau_{2/3}$  rotation angle was 25 degrees, with 360 fs – 32 degrees at 540 fs – 40 degrees.

## Consistent Paradigm of the Spectra Decomposition into Independent Resonance Lines

**K. M. Salikhov**

Zavoisky Physical-Technical Institute, Russian Academy of Sciences, Kazan 420029,  
Russian Federation

The shapes of the spin resonance spectra have been analyzed theoretically in the case, when the kinetic equation for the spin density matrix is linear. Examples of the random relaxation processes which lead to the linear kinetic equations for the spin coherences have been presented in short. A consistent approach has been described for the decomposition of the multicomponent spectra into individual resonance lines based on finding *independent collective modes* for the evolution of quantum coherences. For the model situations with two and three transitions between the energy levels the spectra are decomposed following this approach. The contributions of their collective evolution modes to the magnetic resonance spectra have been analyzed comprehensively. In the presence of the coherence transfer the shapes of resonance lines corresponding to these modes can be a mixture of *Lorentzian absorption and dispersion curves*. The results obtained make it possible to visualize in detail transformations of the spectra as a consequence of the coherence transfer caused by random relaxation processes. This consistent approach makes it possible to describe on a common platform the transformations of spectra at any coherence transfer rate: from the very slow coherence transfer rate which leads to line broadening, then to the rate which results in the coalescence of the spectral lines and further to the very fast rate which leads to exchange narrowed spectra. It is shown that in the limit of the fast coherence transfer corresponding to the exchange narrowing effect one collective mode gives the dominant contribution to the experimental spectrum, namely, in-phase evolution of all transition coherences. The shape of the resonance corresponding to this in-phase evolution is described by the narrowed *Lorentzian absorption curve*.

## Influence of Non-Stoichiometry on the Frustrated Honeycomb System $\text{Li}_3\text{Ni}_2\text{SbO}_6$

**T. Salikhov<sup>1</sup>, E. Klysheva<sup>1</sup>, M. Iakovleva<sup>1</sup>, E. Zvereva<sup>2</sup>,  
I. Shukaev<sup>3</sup>, V. Nalbandyan<sup>3</sup>, B. Medvedev<sup>3</sup>, and E. Vavilova<sup>1</sup>**

<sup>1</sup> Zavoisky Physical-Technical Institute, 420029, Russia

<sup>2</sup> Faculty of Physics, Moscow State University, Moscow 119991, Russian Federation

<sup>3</sup> Chemistry Faculty, Southern Federal University, 344090, Russian Federation

In the last years the layered oxides of alkali and transition metals are intensively investigated due to their potential applications as solid electrolytes and electrode materials in modern ionics. Recently, a new generation of layered complex metal oxides with honeycomb-based crystal structure where ordered mixed-layers of magnetic cations alternate with non-magnetic alkali metal layers has been a subject of intense research worldwide.

This work is devoted to the investigation of new quasi two-dimensional (2D) honeycomb-lattice compounds  $\text{Li}_3\text{Ni}_2\text{SbO}_6$  and  $\text{Li}_{0.8}\text{Ni}_{0.6}\text{Sb}_{0.4}\text{O}_2$ . Basic magnetic properties of  $\text{Li}_3\text{Ni}_2\text{SbO}_6$  have been reported recently [1, 2]. We are here to present the results of systematic study of their electronic and magnetic behavior.

The work was supported by Foundation for Basic Research (grant no. 14-02-01194 and no. 14-02-00245).

1. Zvereva E.A. *et al.*: Dalton Trans. **41**, 572 (2012)
2. Politaev V.V. *et al.*: J. Solid State Chem. **183**, 684 (2010)

## High-Frequency EPR Spectroscopy of YAG: Fe, Ce

**G. S. Shakurov<sup>1</sup>, G. R. Asatryan<sup>2</sup>, K. L. Hovhannesian<sup>3</sup>,  
and A. G. Petrosyan<sup>3</sup>**

<sup>1</sup> Zavoisky Physical-Technical Institute, Russian Academy of Sciences, Kazan 420029,  
Russian Federation, shakurov@kfti.knc.ru

<sup>2</sup> A. F. Ioffe Institute, St. Petersburg 19402, Russian Federation

<sup>3</sup> Institute for Physical Research, NAS RA, Ashtarak-2, 0203, Armenia

Yttrium aluminum garnet  $Y_3Al_5O_{12}$  (YAG) doped with transition and rare earth ions have many applications in the quantum electronics. The spectroscopic properties of these crystals are well researched. However, for some ions the EPR spectra have not been registered. In particular there are no EPR signals for  $Fe^{2+}$  ion in tetrahedral and  $Ce^{3+}$  in the octahedral environment. We undertook the study of YAG doped with Fe, Ce by high-frequency (65–850 GHz) tunable EPR spectroscopy method.

In the YAG:Fe<sup>2+</sup> crystal we registered EPR signal belonging to the Fe<sup>2+</sup> ion in the tetrahedral positions. Due to the low local symmetry ( $S_4$ ) the ground and the first excited electronic levels are singlets with a zero-field-splitting (ZFS) about 110 GHz. The angular dependence of the spectra indicates the existence of 6 magnetically nonequivalent positions occupied by the ion. Within the investigated frequency range the other excited levels were not detected, so the description is made on the basis of the effective spin Hamiltonian with  $S_{\text{eff}} = 1/2$ .

The second new spectrum we observed in this crystal was resonance transitions between two doublets with ZFS about 260 GHz. The same spectrum was found in the YAG:Ce<sup>3+</sup> crystal. The angular dependence of the spectra indicates the trigonal symmetry of the center. We supposed that this spectrum belong to the Ce<sup>3+</sup> ion in the octahedral position. Using the energy matrix of the fourth order were calculated angular dependences of EPR spectra and the obtained values of spectral parameters. Cerium ions could enter in the YAG:Fe crystal as an uncontrolled impurity, since this crystals was grown in the same growth system, which had previously been the growth of crystals with cerium. It is interesting to note that the intensity of EPR line of Ce<sup>3+</sup> in the YAG:Fe crystal was more than in the crystal YAG:Ce. Presumably the co doping of YAG:Fe crystal with Ce leads to the substitution of aluminum by cerium.

This work is supported by the RFBR grant no. 5-52-05040 Arm\_a and grant no. 15RF-003 of the State Committee of Science of Armenia.

## Synthesis and Characterization of $\text{Gd}_{1-x}\text{Sr}_x\text{MnO}_3$ ( $x = 0.5, 0.6, 0.7, 0.8$ )

**A. K. Shukla<sup>1</sup>, T. Maiti<sup>2</sup>, R. M. Eremina<sup>3,4</sup>,  
I. V. Yatsyk<sup>3,4</sup>, and H.-A. Krug von Nidda<sup>4</sup>**

<sup>1</sup> Physics Department, Ewing Christian College, Allahabad 211003, India, drkshukla@gmail.com

<sup>2</sup> Department of Materials Science and Engineering, Indian Institute of Technology, Kanpur, India, tmaiti@iitk.ac.in

<sup>3</sup> Zavoisky Physical-Technical Institute, Russian Academy of Sciences, Kazan 420029, Russian Federation, reremina@yandex.ru

<sup>4</sup> Kazan Federal University, Kazan 420008, Russian Federation

<sup>5</sup> Experimentalphysik V, Institute for Physics, Augsburg University, Augsburg D-86135 Germany

Recently perovskite type manganites  $\text{R}_{1-x}\text{A}_x\text{MnO}_3$  (where R is a trivalent rare-earth ion and A is divalent alkali earth ion) have attracted lot of attention from researchers because their properties are sensitive to external parameters like doping and temperature, hence offering opportunity to tailor spin-spin and spin-lattice interactions [1–3].

This talk reflects our effort to investigate the nature of interplay between spin & charge degrees of freedom and temperature evolution of magnetically ordered phases in  $\text{Gd}_{1-x}\text{Sr}_x\text{MnO}_3$ . High-density ceramics of  $\text{Gd}_{1-x}\text{Sr}_x\text{MnO}_3$  compositions were synthesized by conventional solid state route. All the starting powders were tested for loss on ignition (accounting for carbonates that evolve during firing) to reduce the driving force of secondary phase formation. Magnetic resonance spectra of ceramics  $\text{Gd}_{1-x}\text{Sr}_x\text{MnO}_3$  ( $x = 0.5, 0.6, 0.7, 0.8$ ) were measured on an ER 200 SRC (EMX/plus) spectrometer (Bruker) at the frequency of 9.4 GHz with a flow N<sub>2</sub> Temperature Controller RS 232 cryostat (Bruker) in the temperature range from 100 to 300 K (see Fig. 1 for  $x = 0.8$ ). Ceramic samples were placed in a glass tube with paraffin, were heated at 600 K in a magnetic field 10,000 Oe and then cooled to room temperature. We investigated the angular dependencies of magnetic resonance spectra at 150, 250 and 300 K for  $\text{Gd}_{0.2}\text{Sr}_{0.8}\text{MnO}_3$  oriented ceramic. It is clearly visible that the ESR spectrum of  $\text{Gd}_{0.2}\text{Sr}_{0.8}\text{MnO}_3$  consists of two lines (see Fig. 1). One line was observed near zero magnetic fields, second line with  $g \sim 2$  belongs to the exchange-narrowed resonance from manganese and gadolinium ions. Temperature dependence of magnetization along with that of ESR linewidth ( $\Delta H$ ), asymmetry parameter  $\alpha$  and  $g$ -factor were used to estimate the phase transition temperatures. Temperature dependencies of the magnetic resonance spectra for two direction of oriented ceramic were investigated, where maximum and minimum linewidth was observed. As can be seen from the Fig. 1b at temperatures from 200 to 300 K, there is a strong anisotropy of the linewidth for the two selected orientations. Phase transitions were observed at 200 and 300 K for  $\text{Gd}_{0.2}\text{Sr}_{0.8}\text{MnO}_3$ .

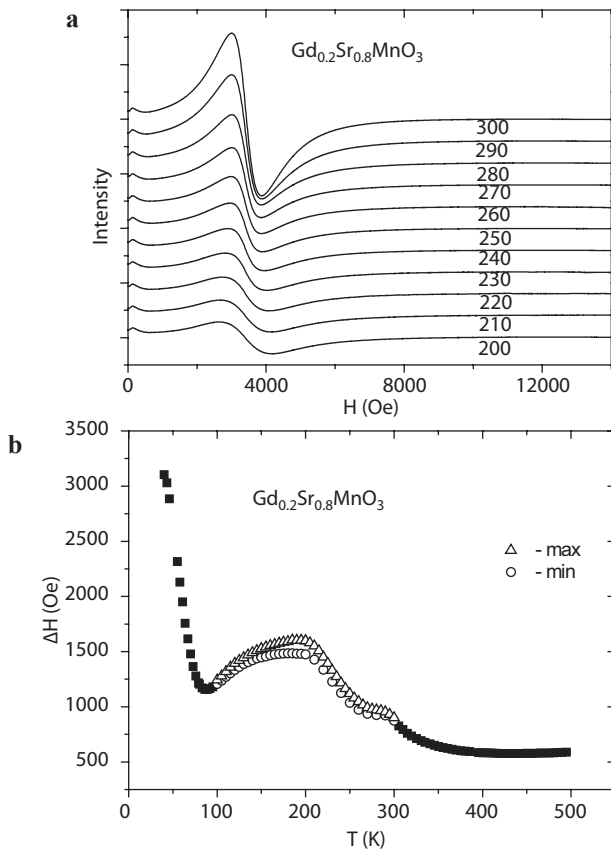


**Fig. 1.** **a** Temperature evolution of the ESR spectra of  $Gd_{0.2}Sr_{0.8}MnO_3$ , **b** temperature dependencies of ESR linewidth in X-band.

1. Fontcuberta J.: *Physique* **16**, 204 (2015)
2. Yingnam Z., Junjia L., Ziqing Z., Fuyang L., Xudong Z., Xiaoyang L., Wakimoto S.: *Chem. Res. Chi. Univ.* **31**, 699 (2015)
3. Joy L.K., Thomas S., Ananthraman M.R.: *J. Mag, Mag. Mat.* **398**, 174 (2016)

## Dysprosium Containing Clusters: Some Features of EPR of the Polycrystalline Samples

A. Sukhanov<sup>1</sup>, R. Galeev<sup>1</sup>, V. Voronkova<sup>1</sup>, A. Baniodeh<sup>2</sup>, and A. Powell<sup>2</sup>

<sup>1</sup> Zavoisky Physical-Technical Institute, Russian Academy of Sciences, Kazan 420029, Russian Federation, vio@kfti.knc.ru

<sup>2</sup> Karlsruhe Institute of Technology, University of Karlsruhe, Karlsruhe, Germany

The magnetic properties of molecular magnets based on rare-earth ions continue to attract much attention. This is particularly the case for coordination complexes containing lanthanide ions such as Dy<sup>III</sup>, for which a prolate ligand field with high axial symmetry will often result in an single-molecule magnet (SMM) behaviour.

The design of new SMMs on the basis of clusters with dysprosium ions requires the understanding of the correlation between the relaxation rate of the magnetization, anisotropy of the local magnetic properties of the Dy<sup>3+</sup> ion and spin-spin interactions in the cluster. The influence of the spin-spin interactions on SMMs properties of dysprosium containing clusters today is poorly studied. EPR is a useful method for studying the local magnetic properties of the paramagnetic ions and spin-spin interaction between ions in clusters. However, the EPR spectra of polycrystalline samples of such clusters can have some features due to the high anisotropy of the local magnetic properties of the Dy<sup>3+</sup> ions.

In this report we discuss these features by the example of EPR studies of compounds built up of tetranuclear Fe<sub>2</sub>Dy<sub>2</sub> and Al<sub>2</sub>Dy<sub>2</sub> clusters for which the anisotropy of the {g}-tensors of the Dy<sup>3+</sup> ions and the spin-spin interaction tensors {D} deviated strongly from uniaxiality as shown by EPR spectroscopy. The EPR study was carried out on polycrystalline samples at different temperatures down to 4 K and frequencies (X-, Q- and W-bands).

It was shown that only signals of clusters with g<sub>z</sub> oriented along external magnetic field are detected in these spectra, their intensity is small but the shape

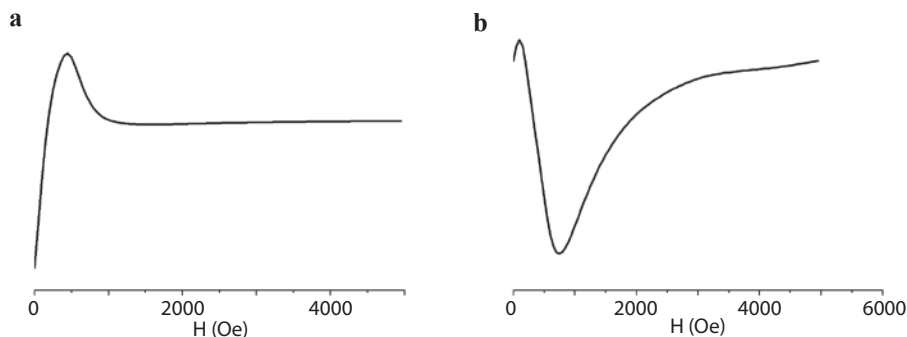


**Fig. 1.** Simulated polycrystalline spectra for the Dy-dimer in X-band,  $g_z = 19.2$ ,  $g_{xy} = 0.1$ ,  $D = 0.1 \text{ cm}^{-1}$ . **a** Orientations of {g}- and {D}-tensors coincide, **b** {g}-tensor is rotated by  $10^\circ$ .



---

of signals in the X-band depends strongly on the symmetry of the  $\{D\}$ -tensor (Fig. 1). In addition, the change of the EPR spectra are change due to the orientation of the crystallites by the external magnetic field. Especially clearly it is observed in Q-band (Fig. 1). The observed signal changes indicate that the number of clusters with  $g_z$  oriented along the external magnetic field increases under the effect of the external magnetic field.

This research is supported in part by the Program of the Presidium of the Russian Academy of Sciences no. 1.26.

## Investigation Magnetic Properties of the Mercury Chalcogenides

A. V. Shestakov<sup>1</sup>, I. I. Fazlizhanov<sup>1,2</sup>, I. V. Yatsyk<sup>1,2</sup>,  
M. I. Ibragimova<sup>2</sup>, V. A. Shustov<sup>2</sup>, and R. M. Eremina<sup>1,2</sup>

<sup>1</sup> Kazan Federal University, Kazan 420008, Russian Federation

<sup>2</sup> Zavoisky Physical-Technical Institute, Russian Academy of Sciences, Kazan 420029, Russian Federation, aleksey665@gmail.com

The mercury chalcogenides HgSe и HgTe in the zinc-blende (ZB) structure belong to a group of unique materials exhibiting the so-called inverted band structure [1] and it are semimagnetic semiconductors n-type ( $A^{II}B^{VI}$ ). Compound HgCdTe is the most widely used semiconductor with a variable band gap [2].

The samples were grown by continuous feeding of the melt. Grown crystal  $Hg_{0.76}Cd_{0.24}Te$  had n-type conductivity with concentration of  $10^{16}$ – $10^{17}$   $cm^{-3}$ , the sample was subjected to ion implantation by ions of  $Ag^+$  ion on ILU-3 accelerator. After implantation the sample was annealed in a sealed quartz tube in a saturated mercury atmosphere at a temperature of 300 °C for 20 days. Subsequent annealing of the crystal in the atmosphere of mercury ions the conductivity is inverted to p-type with carrier concentration of  $\sim 10^{14}$   $cm^{-3}$ . The experiments with different orientations of the sample relative direction field and with difference microwave power magnetic field were performed on a spectrometer Varian E12 at X-band frequency (9.36 GHz) at the temperature 4.2 K in three planes, perpendicular to the selected axis (0) in the plane of the axis (90), and at an angle

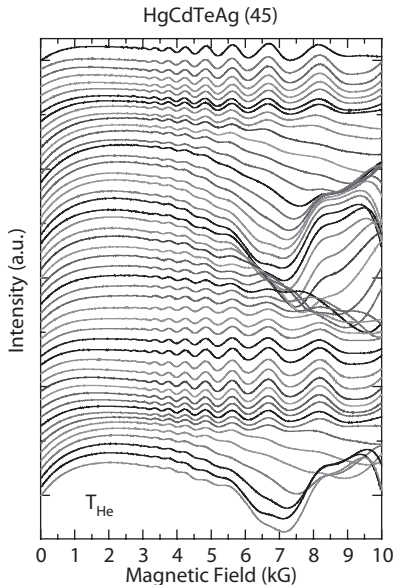


Fig. 1. Angular dependencies of microwave power derivative in HgCdSe:Ag<sup>+</sup>.

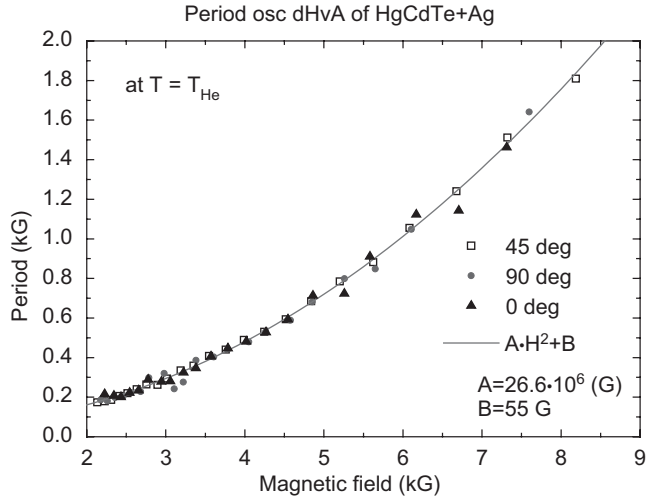


Fig. 2. The dependence of the period of quantum oscillations of the applied magnetic field in in HgCdSe:Ag<sup>+</sup>.

of 45 degrees to the selected direction. The angular dependencies of spectra of Hg<sub>0.76</sub>Cd<sub>0.24</sub>Te:Ag<sup>+</sup> single crystal are shown in Fig. 1.

Strong Shubnikov-de Haas (SdH) oscillations were observed in the derivative of microwave absorption ( $f = 9.4$  GHz) in the of Hg<sub>0.76</sub>Cd<sub>0.24</sub>Te:Ag<sup>+</sup> using electron-paramagnetic-resonance spectroscopy at low temperatures (4.2–20 K) and

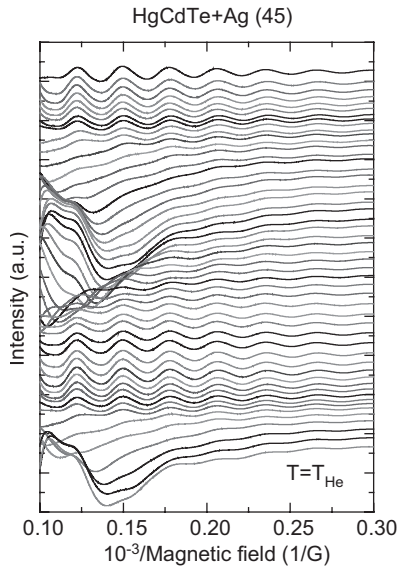


Fig. 3. Angular dependence of SdH oscillations of the microwave power derivative by various orientations of the sample in the reverse magnetic field.  $T = 4.2$  K.

in the magnetic field up to 10 kOe. The samples of  $2 \times 2 \times 2 \text{ mm}^3$  were placed in the cavity and the outside magnetic field was applied. The microwave absorption power derivative ( $dP/dH$ ) was registered in the experiments. Microwave current induces in the microwave field. Oscillations of the microwave power derivative correspond to the transverse magnetoresistance  $\Delta\rho/\rho$ . The fitting dependence of the period of high-frequency oscillations is described by formula  $\Delta H = A \cdot H^2 + C$ , where  $H$  – external magnetic field,  $A$ ,  $C$  – fitting parameters. Up to experimental error obtained parameters  $A$  and  $C$  are the same for all directions of the external magnetic field relative to the crystallographic axes of the crystal (see Fig. 2). Figure 3 shows the microwave absorption power derivative as a function of the inverse applied magnetic field. We estimate extreme cross sectional area according to the formula,  $\Delta H^{-1}(0) = 2.8 \cdot 10^{-5} \text{ Oe}^{-1}$ ;  $\Delta H^{-1}(45) = 3.0 \cdot 10^{-5} \text{ Oe}^{-1}$ ;  $\Delta H^{-1}(90) = 3.23 \cdot 10^{-5} \text{ Oe}^{-1}$ . From the oscillation period  $\Delta(H^{-1})$  of the SdH oscillations the carrier concentration has been determined according to  $n_s = e/(\pi\hbar\Delta(H^{-1}))$ . Concentration in the  $n_s \approx 1.5\text{--}1.7 \cdot 10^{21} \text{ cm}^{-2}$  was evaluated from oscillation period.

1. Veynger A., Zabrodskii A., Tisnek T., Biskupská G.: Phys. and Tech. Semiconductor (FTP) **32**, 557–563 (1998)
2. Winterfeld L., Agapito L.A., Li J., Kioussis N., Blaha P., Chen Y.P.: Phys. Rev. B **87**, 075A, 143 (2013)

## Photoinduced Spin States of Copper Porphyrin Dimers

**A. A. Sukhanov<sup>1</sup>, V. K. Voronkova<sup>1</sup>, and V. S. Tyurin<sup>2</sup>**

<sup>1</sup> Zavoisky Physical-Technical Institute, Russian Academy of Sciences, Kazan 420029,  
Russian Federation, ansukhanov@mail.ru

<sup>2</sup> A. N. Frumkin Institute of Physical chemistry and Electrochemistry RAS, Moscow 119071,  
Russian Federation

Aggregation of porphyrins have been investigated extensively using a range of different linkers to create new two- and three-dimensional supramolecular structures with varying optical and electronic properties [1–2]. Porphyrin aggregates play a special role in photosynthetic plants and organisms and self-assembled chromophore aggregates can be used as nonlinear optical materials. EPR and time-resolved (TR) EPR spectroscopy are a useful tool for studying the structure, the delocalization of unpaired electrons in these systems and photoinduced spin states. Understanding of the factors determining electron delocalization is of fundamental importance for the design and further development of supramolecular systems.

Earlier we studied the dimerization of aza-crown copper porphyrins in the presence of K(SCN) salt by EPR and TR EPR [3]. Porphyrins can be transferred from the diamagnetic singlet state to paramagnetic triplet state by optical excitation. Metalloporphyrins and their dimers can have different paramagnetic states under optical excitation. TR EPR allows direct detection of these states due to electron spin polarization.

In our previous work [3] we demonstrated the formation of the relatively long-lived excited four electron states after the laser irradiation. In this work, we study self-dimerization of copper complex of tetraethyl coproporphyrin (Fig. 1) by EPR and its photoinduced spin states by TR EPR (Fig. 2).

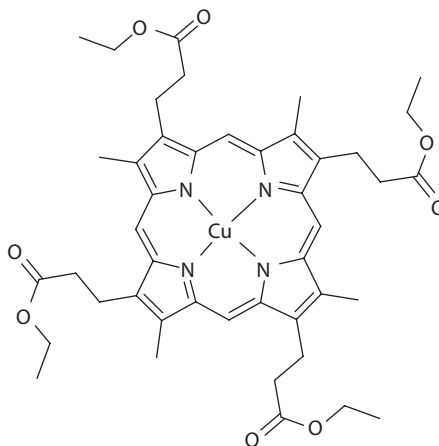


**Fig. 1.** Copper complex of tetraethyl copro-porphyrin (CuCPP-1).

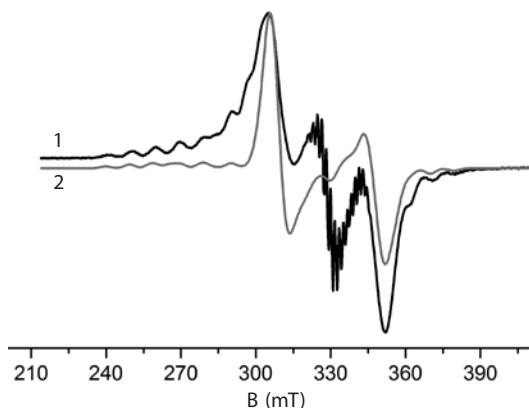


**Fig. 2.** Experimental CW EPR spectrum of CuCPP-1 at 100 K in chloroform/toluene (1) and simulated spectrum (2) describing the contribution of dimer fragments.

The dependence of the dimerization degree of on the type of solvent, possible structures of the system, the exchange interaction parameter between copper porphyrin fragments and the dynamics of the spin polarization of the photoinduced spin states of copper porphyrin dimer are discussed.

We are grateful to the Russian Foundation for Basic Research (project no. 16-03-00586-A) and Program of the Presidium of RAS no. 1.26 for partial financial support.

1. Sprafke J.K., Kondratuk D.V., Wykes M. *et al.*: *J. Am. Chem. Soc.* **133**, 17262(2011)
2. Kim D., Osuka A.: *J. Phys. Chem. A* **107**, 8791 (2003)
3. Kandrashkin Y.E., Iyudin V.S., Voronkova V.K. *et al.*: *Applied Magnetic Resonance* **44**, 967 (2013)

## High Frequency Zero Field EPR Spectroscopy of Thulium Impurity Centers in Synthetic Forsterite

**V. Tarasov<sup>1</sup>, N. Solovarov<sup>1</sup>, and E. Zharikov<sup>2,3</sup>**

<sup>1</sup> Zavoisky Physical-Technical Institute, Russian Academy of Sciences, Kazan 420029, Russian Federation, tarasov@kfti.knc.ru

<sup>2</sup> Prokhorov General Physics Institute of the Russian Academy of Sciences, Moscow 119991, Russian Federation, evzh@mail.ru

<sup>3</sup> Mendeleev University of Chemical Technology of Russia, Moscow 125047, Russian Federation, evzh@mail.ru

Recently much attention has been recently attracted by-rare earth ions in oxide crystals, which are regarded as materials for the practical implementation of quantum information devices. Here we report on the specific features of the EPR spectra of impurity thulium ions in synthetic forsterite discovered in low magnetic fields, when the Zeeman splitting between the hyperfine levels of thulium ions is much smaller than the inhomogeneous width of resonance transitions. The measurements were carried out on a broadband microwave EPR spectrometer [1] in the frequency range of 270–310 GHz.

Two narrow lines associated with the specificity of spin dynamics were observed in weak magnetic fields by a standard technique with the use of the modulation of the magnetic field. The increase in the resonance microwave absorption was observed in the zero magnetic field due to the Hanle effect known in optical spectroscopy. The lines corresponding to the decrease in the resonance absorption was detected in magnetic fields of  $\pm 11$  mT due to the strong saturation of the resonance transition owing to the drastic increase in the effective phase relaxation time in the magnetic field in which the linear Zeeman effect is absent. The observation of these lines enabled us to estimate the decoherence time of  $5 \cdot 10^{-8}$  s at the temperature of 4.2 K.

This work was supported in part by RFBR and the Government of the Republic of Tatarstan according to the research project no. 12-02-97018.

1. Tarasov V.F., Shakurov G.S.: Appl. Magn. Reson. 2, 571 (1991)

## Ethanol Clusters in Gasoline-Ethanol Blends

A. Turanov<sup>1,2</sup> and A. K. Khitrin<sup>2</sup>

<sup>1</sup> Zavoisky Physical-Technical Institute, Russian Academy of Sciences, Kazan 420029, Russian Federation, sasha\_turanov@rambler.ru

<sup>2</sup> Department of Chemistry, Kent State University, OH 44242, USA, akhitrin@kent.edu

Gasoline-ethanol blends are common motor fuels in several countries. The blend with 10% ethanol E10 is standard in the US. By using PFG 1H NMR we studied formation of ethanol clusters in the fuel blends. To study the effect of ethanol concentration on diffusion of ethanol molecules we used the “model” system, which was prepared by adding variable amounts of anhydrous ethanol to ethanol-free gasoline. The results are shown in Fig. 1. Figure 2 shows the temperature dependences of the diffusion coefficients of ethanol and benzene in the E10 blend.

$D_1 = 7.2 \cdot 10^{-5} \text{ cm}^2/\text{s}$  in Fig. 1 is the diffusion coefficient of isolated ethanol molecule. The diffusion coefficient of benzene  $D_b$  is shown for comparison. As one can see, a decrease in ethanol concentration causes dissociation of the clusters. As one can see in Fig. 2, clusters dissociation is also caused by increased temperature. Arrhenius dependences in Fig. 2 can be interpreted as following. For benzene, the molecule with fixed geometry, increased diffusion at elevated temperatures is a result of decreased viscosity of gasoline. For ethanol, in addition to the same effect of viscosity, there is an extra increase of diffusion due to dissociation of ethanol clusters. The activation energies in Fig. 2 are 39 kJ/mol and 60 kJ/mol for benzene and ethanol, respectively. There is a small amount of water in the E10 blend. Water molecules are attached to the ethanol clusters and have the same coefficient of diffusion.

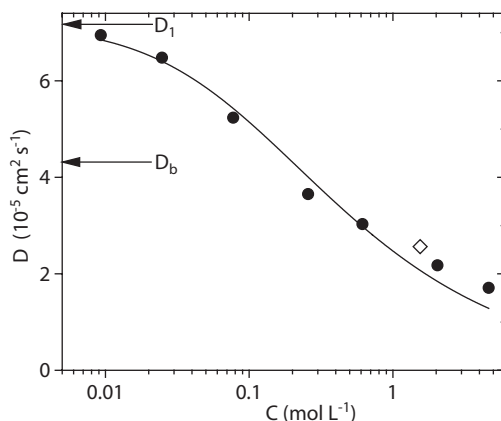


**Fig. 1.** Coefficient of diffusion of ethanol in prepared gasoline-ethanol blend as a function of ethanol concentration (●). The line is a theoretical fit by our model. (◊) is the value for E10 sample.



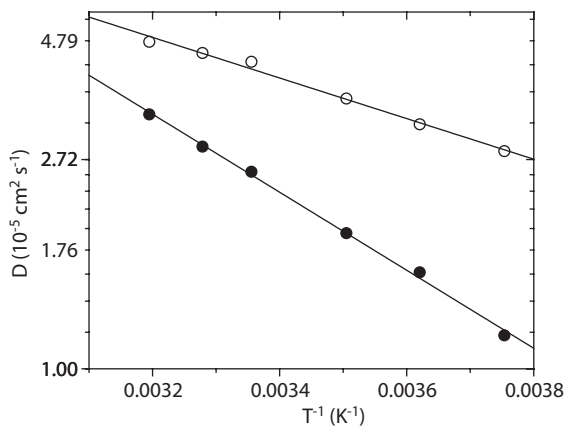


**Fig. 2.** Temperature dependence of the diffusion coefficients of ethanol ( $\bullet$ ) and benzene ( $\circ$ ) in the E10 gasoline blend.

Additional proof of the clusters formation has been obtained from chemical shifts measurements. It is well known that chemical shift of participating protons is greatly affected by the formation of hydrogen bonds. Significant increase of chemical shifts of ethanol OH group and water at increasing ethanol concentration or decreasing temperature is consistent with the formation of clusters, observed in the diffusion measurements.

## **New Protocol of Experiments for Determining the Rate of the Spin Coherence Transfer in a Course of the Spectral Diffusion when Spectra Have Resolved Multicomponent Structure**

**M. Yu. Volkov<sup>1</sup>, M. M. Bakirov<sup>1</sup>, R. T. Galeev<sup>1</sup>,  
A. A. Sukhanov<sup>1</sup>, and K. M. Salikhov<sup>1</sup>**

<sup>1</sup> Zavoisky Physical-Technical Institute, Russian Academy of Sciences, Kazan 420029,  
Russian Federation, mihael-volkov@yandex.ru

There are several relaxation processes which cause the spectral diffusion: the chemical exchange caused by the reversible chemical reactions, the spin exchange induced by the exchange interaction between paramagnetic species, etc. In a course of the spectral diffusion there occurs the spin coherence transfer between spins which belong to different sub-ensembles corresponding to different components of the NMR or EPR spectra. In the case of a relatively slow spectral diffusion the spin coherence transfer manifests itself remarkably. With increasing the rate of the spin coherence transfer, the shifting and the broadening of resonance lines occurs. In addition, the shape of these resonances become mixed, because they are sums of the absorption and of the dispersion terms [1, 2]. It was shown that the weight of the dispersion contribution opens a direct way for determining the rate of the spin coherence transfer [1–5]. In this report we suggest the way of experimental finding the weight of the dispersion contribution to the spectrum.

1. Salikhov K.M.: *Appl. Magn. Reson.* **38**, 237 (2010)
2. Salikhov K.M., Bakirov M.M., Galeev R.T.: *Appl. Magn. Reson.* (2016), DOI:10.1007/s00723-016-0818-0
3. Bales B.L.: *Inhomogeneously Broadened Spin-Label Spectra in: Biological Magnetic Resonance* (Berliner L.J., ed.) **8**, 77 (1989)
4. Bales B.L., Peric M.: *J. Phys. Chem. B* **101**, 8707 (1997)
5. Bales B.L., Peric M.: *J. Phys. Chem. A* **106**, 4846 (2002)

## Orientation-Dependent EMR Signals in Biological Tissues. Characteristics and Interpretation

**S. V. Yurtaeva<sup>1</sup>, V. N. Efimov<sup>2</sup>, V. V. Salnikov<sup>3</sup>, A. A. Rodionov<sup>4</sup>,  
and I. V. Yatsyk<sup>1</sup>**

<sup>1</sup> Zavoisky Physical-Technical Institute, Russian Academy of Sciences, Kazan 420029,  
Russian Federation, yurtaeva@mail.knc.ru

<sup>2</sup> IFMB, KFU, Kazan, 420008, Russian Federation, vefimov.51@mail.ru

<sup>3</sup> KIBB, RAS, Kazan, 420111, Russian Federation, salnikov\_russ@yahoo.com

<sup>4</sup> Kazan Federal University, Kazan 420008, Russian Federation, rodionovshurik@yandex.ru

The signals of electron magnetic resonance (EMR) in biological tissues depended on orientation are known since 60's. It is supposed that such signals are due to iron oxides crystalline particles emerging in biological tissues in the result of natural biomineralization possesses in living systems. The most widespread of them are ferrihydrite ( $5\text{Fe}_2\text{O}_3 \cdot 9\text{H}_2\text{O}$ ) in ferritin core and magnetite ( $\text{Fe}_3\text{O}_4$ ). These crystals play an important role in functioning of living systems as they provide the organism with the iron store and protect the cells from harmful radicals. And the growing of amount of them may be observed in different pathologies, for example, pathologies of brain, tumors and others.

The formation of such particles causes the appearance of magnetic properties in biological tissues which may be detected by the EPR technique. The signal is due to iron oxide nanoparticles. The nature of the signal, characteristics and their interpretation are still the subject of interest. The appearance of such signals in tissues is a manifestation of intensive biomineralization possesses. Up to date such EMR signals are rather widely investigated only in magnetotactic bacteria and in magnetoreception organs of insects. The present study is devoted

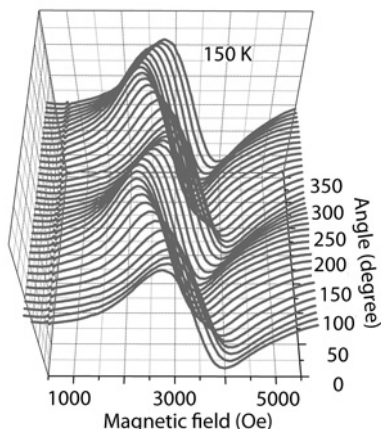


**Fig. 1.** EMR signal in rat lung.

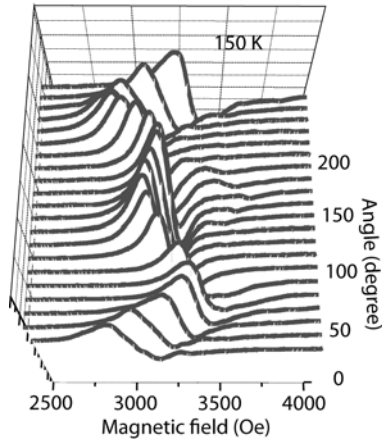


Fig. 2. EMR signal in snail heart.

to detailed investigation of such EMR signals in different pathologic tissues of mammals and snails.

It is known that such signals are not observed in tissues under physiological conditions (except for brain tissues [1] or sometimes liver and spleen). More often they are detected in pathological tissues. As the result of study of pathological tissues of human (cancer tumor) [2], and rats (microgravitation model [3], and spin cord injure model) and nerve tissue of snail the general characteristics of EMR signals were determined. The most important of them are: the dependence of resonance field ( $H_{res}$ ) on the orientation (Fig. 1–3) and characteristic non-monotonic temperature dependencies of  $H_{res}$ , linewidth ( $\Delta H$ ) and integral

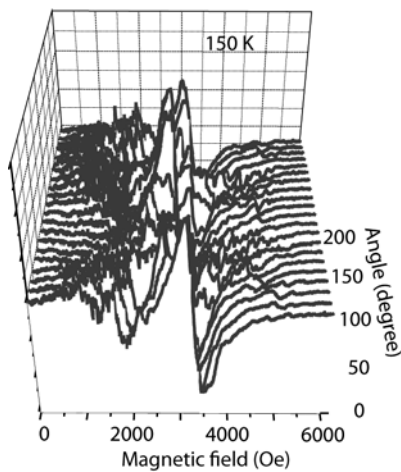


Fig. 3. EMR signal in rat muscle.

intensity ( $I$ ) within the temperatures 4–300 K. Within the temperatures 100–125 K there are anomalies in  $H_{\text{res}}$ ,  $\Delta H$  and  $I$ . It was found that all enumerated temperature features corresponded to magnetite characteristics and temperature anomalies within 100–125 K to Verwey phase transition in magnetite. Three types of anisotropic EMR signals characterised accordingly by axial anisotropy (Fig. 1), the sum of axial and cubic anisotropy (Fig. 2), and axial anisotropy with simultaneous registration of “noise-like” spectra (fine structure of EMR) (Fig. 3) were detected and investigated. Such different orientation behavior of the three types of signals reflects the variety of spatial forms of accumulation of biogenic magnetite in tissues.

There was also an attempt to visualize the distribution of these particles in tissues by transmission electron microscopy technique (TEM). For microscopic studies the samples with the most intensive EMR signals were chosen. The localization of crystalline nanoparticles was determined in the samples of tumor tissues and nerve ganglion of snail. The areas with large amount of crystalline particles were detected. TEM technique of double antibody immunogold labeling was used. Microscopic studies showed that crystalline particles may be arranged in chains or various ensembles.

The authors are thankful to Kh. L. Gainutdinov, L. N. Muranova, G. G. Yafarova and A. A. Ereemeev provided tissue samples for investigation.

The financial support of Scientific Program of Presidium of RAS 1.26 P during 2016 is gratefully acknowledged.

1. Brik A.B.: Ukr. J. Phys. Opt. **11**, Suppl. 1 S46–S61 (2010)
2. Yurtaeva S.V., Efimov V.N., Silkin N.I. *et al.*: Appl. Magn. Res. **42**, 299–311 (2012)
3. Yurtaeva S.V., Efimov V.N., Yafarova G.G., Ereemeev A.A., Iyudin V.S., Rodionov A.A., Gainutdinov Kh.L., Yatsyk I.V.: Appl. Magn. Res. (2016)

## EPR Study of the BaF<sub>2</sub> Crystals Activated by Nb<sup>4+</sup> Ions

E. R. Zhiteitsev<sup>1</sup>, R. B. Zaripov<sup>1</sup>, and V. A. Ulanov<sup>1,2</sup>

<sup>1</sup> Zavoisky Physical-Technical Institute, Russian Academy of Sciences, Kazan 420029, Russian Federation, ulvlad@inbox.ru

<sup>2</sup> Kazan State Power Engineering University, Kazan 420066, Russian Federation

The fluorite type crystals (CaF<sub>2</sub>, SrF<sub>2</sub>, and BaF<sub>2</sub>) are well known materials for various technical applications so far as they are transparent for optical waves in a very wide frequency region. Moreover, paramagnetic impurities of d-ions add them new properties with respect to radiofrequency radiation.

As these crystals have cubic structures in which each cation is located in the center of a coordination cube formed by eight fluorine anions, the impurity d-ions in the activated fluorites find itself in a cubic crystal field and can demonstrate the Jahn-Teller or pseudo-Jahn-Teller effects. When the impurity d-ion is not isovalent with respect to basic cation, a charge compensating defect can be formed in a vicinity of the impurity ion.

The goal of this EPR study was investigation of magnetic properties and molecular structure of paramagnetic centers formed by niobium impurities in the BaF<sub>2</sub>:Nb crystals. The niobium impurities were found in the Nb<sup>4+</sup> (4d<sup>1</sup>,  $S = 1/2$ ,  $I = 9/2$ ) states. The EPR spectra demonstrated a resolved hyperfine structures of 10 lines and some additional lines which were attributed to superhyperfine and quadrupole interactions. These spectra corresponded to tetragonal symmetry of magnetic properties of centers under study and were observed in the temperature region from 4.2 K to 300 K.

The parameters of these spectra at  $T = 300$  K are following:  $g_{\parallel} = 2.0018 \pm 0.0005$ ;  $g_{\perp} = 1.8584 \pm 0.0002$ ;  $a_{\parallel}^{\text{hfs}} = 172 \pm 8$  MHz;  $a_{\perp}^{\text{hfs}} = 605 \pm 3$  MHz. The observed superhyperfine structure pointed at the presence of two equivalent fluorine ligands located on the  $\langle 001 \rangle$  crystallographic directions. The values of the superhyperfine structure parameters for  $T = 300$  K were following:  $a_{\parallel}^{\text{hfs}} \approx 45$  MHz;  $a_{\perp}^{\text{hfs}} = 420 \pm 5$  MHz. The values of the EPR spectra parameters and EPR line widths changed with decreasing of the temperature.

The possible electronic and molecular structures of the centers under study and a role of the vibronic interactions on the magnetic properties of the centers are discussed.

## The Concentration Dependence of the Wings of a Dipolar-Broadened Line of Magnetic Resonance in a Magnetically Dilute Lattice of Spins

V. E. Zobov<sup>1</sup> and M. M. Kucherov<sup>2</sup>

<sup>1</sup> Kirensky Institute of Physics, Federal Research Center KSC SB RAS,  
Krasnoyarsk 660036, Russian Federation, rsa@iph.krasn.ru

<sup>2</sup> Institute of Space and Information Technology of Siberian Federal University,  
Krasnoyarsk 660074, Russian Federation

The line shape of correlation function can yield information about, e.g. the rate of equilibration in heterogeneous spin system that is relevant to the problems of ergodicity, thermalization, spin transport, and many-body localization [1, 2]. Its wings decrease exponentially with frequency when the spin autocorrelation function (ACF) has singular points on the imaginary time axis. The coordinates of the singular points that determine exponential decay were calculated for regular spin lattices [3].

In this paper we study the singularities of the ACF of magnetically dilute spin systems with the dipole-dipole interaction (DDI). Within the approximation of the self-consistent fluctuating local field theory, we derived the nonlinear equations for the ACF averaged over independent random arrangements of spins (magnetic atoms) in the diamagnetic lattice with various spin concentration. The equations take into account the specific character of the DDI. Firstly, due to the axial symmetry of secular part of the DDI in a strong constant magnetic field, the ACF longitudinal and transverse spin components are described by different equations. Secondly, the long-range nature of the DDI is accounted by division into deposits in local field from distant and near spins. Then we have written recurrence equations for the coefficients of the ACF series in the powers of time, and we found the numerical value of the coordinate of the nearest singular point on the imaginary time axis of the ACF which is equal to the convergence radius of series. It is shown that at strong magnetic dilution there is the logarithmic concentration dependence of the coordinate which in that case determined by clusters of close spins, proportion of which is small, but contribution to modulation frequency is large. As an example, crystals of silicon with a various concentrations of <sup>29</sup>Si [4] are considered for the magnetic field directions along the three crystallographic axes.

1. Dzheparov F.S.: J. Phys.: Conf. Ser. **324**, 012004 (2011)
2. Eisert J., Friesdorf M., Gogolin C.: Nature Physics **11**, 124 (2015)
3. Zobov V.E., Popov M.A.: JETP **97**, 78 (2003)
4. Hayashi H., Itoh K.M., Vlasenko L.S.: Phys. Rev. B **78**, 153201 (2008)

## EMR Searching of Quantum Behavior of Superparamagnetic $\gamma$ -Fe<sub>2</sub>O<sub>3</sub> Nanoparticles Fabricated in Dendrimeric Matrix

**N. E. Domracheva<sup>1</sup>, V. E. Vorobeva<sup>1</sup>, and M. S. Gruzdev<sup>2</sup>**

<sup>1</sup> Zavoisky Physical-Technical Institute, Russian Academy of Sciences, Kazan 420029, Russian Federation, ndomracheva@gmail.com

<sup>2</sup> G. A. Krestov Institute of Solution Chemistry, Ivanovo 153045, Russian Federation

In recent years, the study of magnetic nanoparticles (MNPs) has attracted considerable attention driven by both fundamental scientific interest and potential technological applications. Electron Magnetic Resonance (EMR) is one of the key tools for studying MNPs. We have investigated earlier [1] the EMR behavior of  $\gamma$ -Fe<sub>2</sub>O<sub>3</sub> nanoparticles fabricated in a second-generation poly(propylene imine) dendrimer using the classical theoretical approach [2] based on parameters derived from bulk materials. However, we observed a signal at half-field in the EMR spectra of our NPs (of approximately 2.5 nm). This feature is interpreted in the literature [3, 4] as an evidence of the discrete structure of the energy levels and, therefore, of the quantum nature of the system (where the whole energy spectrum of a NP considered as a giant exchange cluster).

In the present work we have tried to find new arguments in favor of the quantum nature of our  $\gamma$ -Fe<sub>2</sub>O<sub>3</sub>-MNPs. For this purpose the EMR spectra were recorded in both parallel and perpendicular configuration, i.e. with the  $H_1$  field of the microwave radiation parallel and perpendicular to the external  $H_0$  field. These alternative measurement configurations have different selection rules for

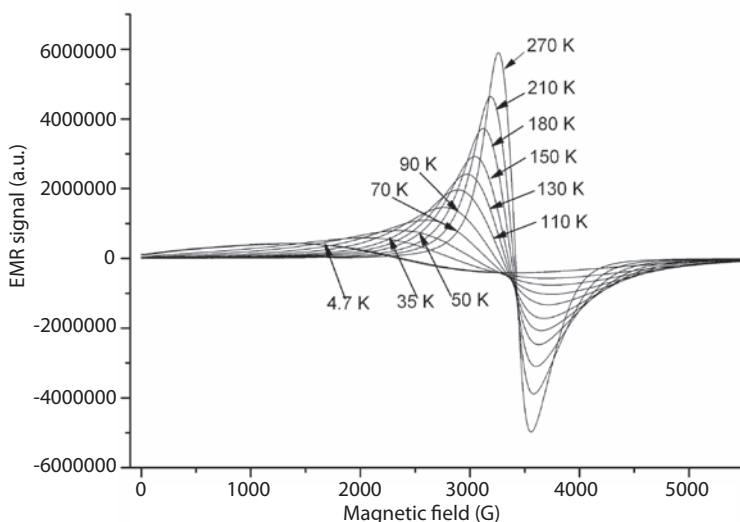


**Fig. 1.** EMR spectra of  $\gamma$ -Fe<sub>2</sub>O<sub>3</sub> NPs in dendrimer recorded at X-band in perpendicular configuration at various temperatures ( $\nu = 9.64$  GHz).



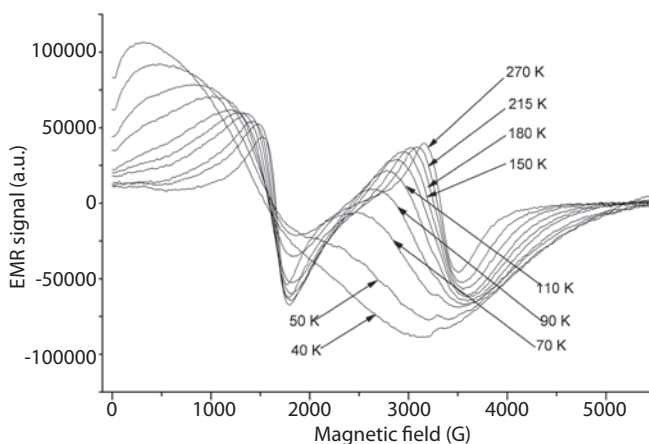


**Fig. 2.** EMR spectra of  $\gamma\text{-Fe}_2\text{O}_3$  NPs in dendrimer recorded at X-band in parallel configuration at various temperatures. The microwave frequency was  $\nu = 9.39$  GHz.

the allowed transitions between the total spin projections; therefore, this provides a means to perceive the quantum nature of the system.

EMR spectra of  $\gamma\text{-Fe}_2\text{O}_3$  NPs in dendrimer were measured at the X-band both in perpendicular and parallel configurations at various temperatures (Fig. 1 and 2). As seen, the behavior of the EMR spectra recorded in the perpendicular configuration with cooling of the sample is typical for superparamagnetic materials [1, 2, 4] and it was described in detail in our previous work [1]. A small signal at  $H_0/2$  (around 1500 G) is also observed, which is attributed to “forbidden” transitions between states with  $\Delta M = \pm 2$ , where  $M$  is the expectation value of  $\hat{S}_z$  and  $S$  the total spin of the MNP. If the model based on the giant spin is correct for the interpretation of the experimental results, then the intensity of the  $H_0/2$  signal must increase when the EMR spectra is recorded in the parallel configuration. As seen from Fig. 2, the EMR experiments performed in this configuration confirm this prediction. An increase in the intensity of the transitions at half field is clearly observed. Thus, this experiment opens the possibility to analyze the properties of MNPs by using a simple model based on the giant spin, in which the spin is associated with the whole MNP and, consequently, the system must be treated as a quantum object. In the near future, the simulation of the measured EMR spectra will be done, and the values of the total spin ( $S$ ) and zero-field splitting parameter ( $D$ ) for MNPs of the present studies will be obtained.

1. Domracheva N.E., Pyataev A.V., Manapov R.A., Gruzdev M.S.: *ChemPhysChem* **12**, 3009 (2011)
2. Raikher Yu.L., Stepanov V.I.: *JMMM* **316**, 417 (2007)
3. Fittipaldi M., Gatteschi D. et al.: *Phys. Rev. B* **83**, 104409 (2011)
4. Noginova N., Weaver T., Atsarkin V.A. et al.: *Phys. Rev. B* **77**, 014403 (2008)

## Counterion Effect on the Spin-Transition Properties of the Second Generation Iron(III) Dendrimeric Complexes

**N. E. Domracheva<sup>1</sup>, V. E. Vorobeva<sup>1</sup>, V. I. Ovcharenko<sup>2</sup>,  
A. S. Bogomyakov<sup>2</sup>, E. M. Zueva<sup>3</sup>, M. S. Gruzdev<sup>4</sup>,  
U. V. Chervonova<sup>4</sup>, and A. M. Kolker<sup>4</sup>**

<sup>1</sup> Zavoiisky Physical-Technical Institute, Russian Academy of Sciences, Kazan 420029, Russian Federation

<sup>2</sup> International Tomography Center, Novosibirsk 630090, Russian Federation

<sup>3</sup> Kazan State Technological Institute, Kazan 420015, Russian Federation

<sup>4</sup> G. A. Krestov Institute of Solution Chemistry, Ivanovo 153045, Russian Federation

The magnetic properties and the influence of counterions on the spin crossover properties of two novel Fe(III) dendrimeric complexes of the second generation, namely  $[\text{Fe}(\text{L})_2]^+\text{X}^-$ , where  $\text{L} = 3,5\text{-di}(3,4,5\text{-tris}(\text{tetradecyloxy})\text{benzoyloxy})\text{benzoyl-4-oxy-salicylidene-N}^7\text{-ethyl-N-ethylenediamine}$ ,  $\text{X} = \text{Cl}^-$  (**1**),  $\text{ClO}_4^-$  (**2**) have been studied for the first time by magnetic susceptibility and EPR in the wide (4.2–300 K) temperature range. EPR results showed that compound **1** contains about 94% of high-spin (HS,  $S = 5/2$ ) and ~6% of low-spin (LS,  $S = 1/2$ ) Fe(III) centers, and undergoes the antiferromagnetic ordering below 7 K, but the spin-crossover effect completely disappears in it. When the temperature is lowered from 300 to 30 K, the EPR integrated intensity of a broad line ( $g \approx 2$ ), which corresponds to the HS iron(III) centers, passes through a broad maximum at  $T_{\text{max}} \approx 100$  K, which indicates the formation of the short-range correlation effects. The anomalous broadening of this EPR line at low temperatures with the critical exponent  $\beta = 1.5$  upon approaching the long-range ordering transition from above indicates the quasi-two-dimensional antiferromagnetic nature of magnetism in complex **1**. The obtained results and DFT calculations allow us to conclude that  $\text{FeN}_4\text{O}_2$  octahedra in compound **1** are packed in the chains which form ionic bilayers. The compound **2** with  $\text{ClO}_4^-$  counterion demonstrates another magnetic behavior. EPR data show that compound **2** contains about 77% of LS and ~23% of HS Fe(III) centers. Complex **2** displays partial spin crossover ( $S = 5/2 \leftrightarrow 1/2$ ) of ~23% of the Fe(III) molecules above 150 K and undergoes the antiferromagnetic ordering below 10.2 K. HS and LS iron(III) centers are linked together and form a dimeric structure. Thus, the replacing of a counterion dramatically alters the magnetic structure of the compound. The large  $\text{ClO}_4^-$  anion leads to the formation of the dimer structure, while the small Cl anion promotes the formation of chain-like structures of Fe(III) centers in ionic bilayers.

---

## AUTHOR INDEX

|                     |           |
|---------------------|-----------|
| Akhmedzhanov, R. A. | 51, 53    |
| Akhmetov, M. M.     | 114       |
| Alexandrov, A.      | 162       |
| Ancelet, L. R.      | 34        |
| Andreeva, I. N.     | 136       |
| Andrianov, V. V.    | 130       |
| Anikin, A.          | 162       |
| Anisimov, A. V.     | 136       |
| Anisimov, A. N.     | 72        |
| Antipin, I. S.      | 146       |
| Arsentyeva, I. P.   | 99        |
| Asada, M.           | 73        |
| Asatryan, G. R.     | 169       |
| Atsarkin, V. A.     | 6         |
| Audran, G.          | 18        |
| <b>B</b> abak, S.   | 119       |
| Bagryanskaya, E.    | 16        |
| Bahodurov, A.       | 166       |
| Bakirov, M. M.      | 116, 182  |
| Baniodeh, A.        | 172       |
| Baranov, P. G.      | 72        |
| Belyaev, B. A.      | 143       |
| Bertet, P.          | 46        |
| Bezmaternykh, L. N. | 124       |
| Bienfait, A.        | 46        |
| Biktagirov, T.      | 118       |
| Biziyaev, D. A.     | 83        |
| Bochkin, G. A.      | 59        |
| Bogach, A. V.       | 25        |
| Bogaychuk, A.       | 119       |
| Bogdanov, A. V.     | 121       |
| Bogomyakov, A. S.   | 190       |
| Boldyrev, V. V.     | 99        |
| Bowman, M. K.       | 2, 31, 62 |
| Bragin, A.          | 162       |
| Brémond, P.         | 18        |
| Büchner, B.         | 27, 82    |
| Bukharaev, A. A.    | 83        |

|                      |                        |
|----------------------|------------------------|
| Buntkowsky, G.       | 108                    |
| Buravkov, A. V.      | 130                    |
| Bushev, P.           | 56                     |
| Carl, P.             | 43                     |
| Cherepnev, G. V.     | 140                    |
| Chervonova, U. V.    | 190                    |
| Chumakova, N. A.     | 38, 66                 |
| Chushnikov, A. I.    | 140                    |
| Çolak, B.            | 88                     |
| Dambieva, M.         | 119                    |
| Demidov, E. S.       | 79                     |
| Demishev, S. V.      | 25, 26, 135, 142       |
| Deryagin, O. G.      | 130                    |
| Dey, T.              | 27                     |
| Domracheva, N. E.    | 188, 190               |
| Doroginitcky, M.     | 162                    |
| Dvořák, P.           | 123                    |
| Dvurechenskii, A. V. | 80                     |
| Dzheparov, F. S.     | 30                     |
| Dzikovski, B.        | 8                      |
| Earle, K. A.         | 37                     |
| Efimov, V. N.        | 183                    |
| Eichhoff, U.         | 36                     |
| Eremina, R. M.       | 57, 124, 132, 170, 174 |
| Esteve, D.           | 46                     |
| Fakhrutdinov, A.     | 162                    |
| Falin, M. L.         | 126, 128               |
| Fatkullin, N.        | 94                     |
| Fattakhov, Ya.       | 149, 162               |
| Fazlizhanov, I. I.   | 57, 174                |
| Fel'dman, E. B.      | 59                     |
| Filipov, V. B.       | 25, 26                 |
| Fraerman, A. A.      | 79                     |
| Freed, J. H.         | 8                      |
| Frolova, E.          | 164                    |
| Gafiyatullin, L.     | 164                    |
| Gafurov, M.          | 118                    |
| Gainutdinov, Kh. L.  | 130                    |
| Galeev, R. T.        | 116, 129, 172, 182     |
| Galvosas, P.         | 34                     |
| Gavrilova, S. A.     | 130                    |
| Gavrilova, T.        | 57, 132                |
| Georgieva, E. R.     | 8                      |
| Gerasimov, K. I.     | 60                     |
| Gilmanov, M. I.      | 25, 26, 135            |
| Gilmutdinov, I. F.   | 132, 145               |

---

|                      |          |
|----------------------|----------|
| Gizatullin, B. I.    | 160      |
| Glushkov, V. V.      | 25       |
| Goenko, I. A.        | 136      |
| Golbeck, J.          | 42       |
| Golubeva, A. V.      | 130      |
| Golubeva, E.         | 65       |
| Gorev, R. V.         | 77, 79   |
| Gorka, M.            | 42       |
| Goryunov, Yu. V.     | 138      |
| Gostev, F.           | 42       |
| Grafe, H.-J.         | 27, 82   |
| Grampp, G.           | 14       |
| Gromov, I.           | 43       |
| Gruzdev, M. S.       | 188, 190 |
| Gubaidullin, F. F.   | 54       |
| Gubskaya, V. P.      | 148      |
| Gumarov, G. G.       | 99, 114  |
| Gushchin, L. A.      | 51, 53   |
| <b>Hagiwara, M.</b>  | 75       |
| Hara, S.             | 10       |
| Hermans, I. F.       | 34       |
| Hosseini, E.         | 7        |
| House, M.            | 50       |
| Hovhannesyan, K. L.  | 169      |
| Hurlimann, M.        | 151      |
| <b>Iakovleva, M.</b> | 27, 168  |
| Ibragimova, M. I.    | 140, 174 |
| Ischenko, T. V.      | 142      |
| Itkis, D.            | 41       |
| Ivanov, A.           | 162      |
| Ivanova, T. A.       | 145, 164 |
| Ivanov, K. L.        | 153      |
| Iyudin, V. S.        | 130      |
| Izotov, A. V.        | 143      |
| <b>Jhaveri, J.</b>   | 50       |
| <b>Kabirov, Y.</b>   | 132      |
| Kadkin, O. N.        | 146      |
| Kalachev, A.         | 53       |
| Kandrashkin, Yu. E.  | 83, 96   |
| Kaptein, R.          | 104      |
| Kataev, V.           | 27, 82   |
| Kattnig, D.          | 14       |
| Kausik, R.           | 151      |
| Kaustuv, M.          | 27       |
| Khabipov, R.         | 149, 162 |
| Khafizov, N. R.      | 146      |

|                       |              |
|-----------------------|--------------|
| Khairuzhdinov, I. T.  | 148          |
| Khanipov, T. F.       | 83           |
| Khitrin, A. K.        | 180          |
| Kida, T.              | 75           |
| Kirgizov, D.          | 162          |
| Kirillov, R. S.       | 54           |
| Klauss, H.-H.         | 24           |
| Klein, J. H.          | 39           |
| Klysheva, E.          | 168          |
| Kokorin, A. I.        | 63, 110      |
| Kolker, A. M.         | 190          |
| Konov, A. B.          | 114          |
| Konygin, G. N.        | 99, 114, 136 |
| Korableva, S. L.      | 53, 126      |
| Koroteev, V.          | 41           |
| Koshelev, V. B.       | 130          |
| Krasnorussky, V. N.   | 25, 26       |
| Krug von Nidda, H.-A. | 124, 170     |
| Krupskaya, Y.         | 82           |
| Kuchеров, M. M.       | 187          |
| Kukovitsky, E.        | 154          |
| Kulak, A. I.          | 63           |
| Kulik, L. V.          | 80           |
| Kupriyanova, G.       | 119, 155     |
| Kurashov, V.          | 42           |
| Kutovoi, S.           | 57           |
| Kuzin, S. V.          | 38           |
| Kuzmin, V. V.         | 40           |
| Lambert, C.           | 39           |
| Lang, J.              | 123          |
| Latypov, V. A.        | 126, 128     |
| Latypov, R. R.        | 54           |
| Leushin, A. M.        | 126, 128     |
| Likerov, R.           | 57           |
| Likhtenshtein, G. I.  | 106          |
| Lim, H.               | 47           |
| Liodl, A.             | 124          |
| Lisin, V. N.          | 97           |
| Lo, C. C.             | 46, 50       |
| Lozovoi, A.           | 94, 151      |
| Lubitz, W.            | 102          |
| Lukzen, N. N.         | 39, 153      |
| Lvov, D. V.           | 30           |
| Lvov, S.              | 154          |
| Lyon, S. A.           | 50           |
| Madzhidov, T. I.      | 146          |

---

|                   |              |
|-------------------|--------------|
| Maiti, T.         | 170          |
| Majer, J.         | 48           |
| Makarov, M. N.    | 160          |
| Maksutoğlu, M.    | 159          |
| Mamadazizov, S.   | 155          |
| Mamatova, A.      | 158          |
| Mamin, G.         | 118          |
| Maraşlı, A.       | 159          |
| Marque, S.        | 18           |
| Maruyama, K.      | 7            |
| Maryasov, A. G.   | 31           |
| Mattea, C.        | 94, 151      |
| Medvedev, B.      | 168          |
| Melnikova, D. L.  | 160          |
| Mershiev, I. G.   | 90           |
| Meyer, D. C.      | 41           |
| Mingalieva, L. V. | 83, 145, 164 |
| Mironov, V. L.    | 77           |
| Mladenova, B.     | 14           |
| Möbius, K.        | 11, 42       |
| Mølmer, K.        | 46           |
| Moiseev, S. A.    | 54, 60       |
| Mokeev, M.        | 43           |
| Möller, A.        | 82           |
| Mori, N.          | 7            |
| Morita, Y.        | 7            |
| Morozov, V. I.    | 60           |
| Morton, J. J. L.  | 46, 47, 50   |
| Moshkina, E. M.   | 124          |
| Mozzhukhin, G. V. | 88, 90       |
| Münchgesang, W.   | 41           |
| Murzakaev, V.     | 162          |
| Nacher, P.-J.     | 40, 89       |
| Nadtochenko, V.   | 42           |
| Nakagawa, T.      | 7            |
| Nakamura, T.      | 73           |
| Nakazawa, S.      | 7            |
| Nalbandyan, V.    | 168          |
| Nateprov, A. N.   | 138          |
| Nenashev, A. V.   | 80           |
| Nikitina, J.      | 132          |
| Nishida, S.       | 7            |
| Nizov, N. A.      | 51           |
| Nizov, V. A.      | 51           |
| Nuretdinov, I. A. | 148          |
| Nurgaliev, D.     | 162          |

|                          |                        |
|--------------------------|------------------------|
| Nurgazizov, N. I.        | 83                     |
| Nur, S.                  | 47                     |
| <b>Ohmichi</b> , E.      | 10                     |
| Ohta, H.                 | 10                     |
| Okada, K.                | 7                      |
| Okubo, S.                | 10                     |
| Orlinskii, S.            | 118                    |
| Ovcharenko, V. I.        | 190                    |
| Ovchinnikov, I. V.       | 145, 164               |
| Öztürk, Y.               | 159                    |
| <b>Paramonov</b> , N. A. | 38                     |
| Perminov, N. S.          | 54                     |
| Petersen, E. S.          | 50                     |
| Petrenko, O.             | 75                     |
| Petrosyan, A. G.         | 169                    |
| Petrov, S. V.            | 128                    |
| Petrovnin, K. V.         | 54                     |
| Petrov, O. V.            | 165                    |
| Petukhov, V. Yu.         | 99, 114, 136, 140      |
| Pla, J. J.               | 46                     |
| Poddutoori, P. K.        | 96                     |
| Pomogailo, D. A.         | 38                     |
| Popov, I.                | 166                    |
| Porsev, V. E.            | 99                     |
| Powell, A.               | 172                    |
| <b>Raitsimring</b> , A.  | 3, 105                 |
| Rameev, B. Z.            | 88, 90, 159            |
| Rasmussen, K.            | 14                     |
| Rautskii, M. V.          | 124                    |
| Rodionov, A. A.          | 183                    |
| Romanov, N. G.           | 72                     |
| Ross, P.                 | 47                     |
| Rybin, D. S.             | 99, 114, 136           |
| Safullin, G. M.          | 128                    |
| Safullin, K.             | 89                     |
| Sakurai, T.              | 10                     |
| Salikhov, K. M.          | 12, 116, 148, 167, 182 |
| Salikhov, T.             | 168                    |
| Salnikov, V. V.          | 183                    |
| Samarin, N. A.           | 25                     |
| Samarin, A. N.           | 25, 26, 135, 142       |
| Samartsev, V. V.         | 97                     |
| Sapozhnikov, M. V.       | 77                     |
| Sato, K.                 | 7                      |
| Savitsky, A.             | 17, 42                 |
| Savostina, L.            | 158                    |



---

|                       |                        |
|-----------------------|------------------------|
| Sawada, S.            | 7                      |
| Schäpers, M.          | 82                     |
| Schenkel, T.          | 46                     |
| Semenov, A. V.        | 25, 26, 135            |
| Semenov, A.           | 42                     |
| Sergeicheva, E. G.    | 76                     |
| Shagalov, V.          | 162                    |
| Shakurov, G. S.       | 169                    |
| Sharafutdinova, D. R. | 99, 136                |
| Shegeda, A. M.        | 97                     |
| Shelaev, I.           | 42                     |
| Sherstyukov, O. N.    | 54                     |
| Shestakov, A. V.      | 174                    |
| Shibata, T.           | 7                      |
| Shiomi, D.            | 7                      |
| Shipunov, T. V.       | 160                    |
| Shitsevalova, N. Yu.  | 25, 26                 |
| Shukaev, I.           | 168                    |
| Shukla, A. K.         | 170                    |
| Shulgin, D. A.        | 90                     |
| Shustov, V. A.        | 57, 145, 174           |
| Sigillito, A. J.      | 50                     |
| Simmons, M.           | 50                     |
| Sitdikov, I.          | 149                    |
| Skirda, V.            | 162                    |
| Skorohodov, E. V.     | 77, 79                 |
| Sluchanko, N. E.      | 25                     |
| Smirnov, A. I.        | 75                     |
| Sobgayda, D. A.       | 51, 53                 |
| Soldatov, T. A.       | 75                     |
| Solovarov, N.         | 179                    |
| Solovev, P. N.        | 143                    |
| Soltamov, V. A.       | 72                     |
| Sosin, S. S.          | 76                     |
| Spiess, H. W.         | 109                    |
| Spindler, N.          | 34                     |
| Srivastava, M.        | 8                      |
| Stapf, S.             | 94, 151, 165           |
| Steiner, U. E.        | 39                     |
| Sturm, J. C.          | 50                     |
| Sugisaki, K.          | 7                      |
| Sukhanov, A. A.       | 68, 164, 172, 177, 182 |
| Suter, D.             | 52                     |
| Suzuki, S.            | 7                      |
| Takahashi, H.         | 10                     |
| Takata, A.            | 75                     |

|                   |                                  |
|-------------------|----------------------------------|
| Takui, T.         | 7                                |
| Talbot, C.        | 89                               |
| Tarasov, V.       | 68, 179                          |
| Tastevin, G.      | 40                               |
| Tobar, M.         | 49                               |
| Toyota, K.        | 7                                |
| Tsvetkov, Yu. D.  | 107                              |
| Turanov, A.       | 180                              |
| Turanova, O. A.   | 145, 164                         |
| Tyryshkin, A. M.  | 50                               |
| Tyurin, V. S.     | 177                              |
| Ulanov, V. A.     | 92, 186                          |
| Ünver, İ. S.      | 88                               |
| Vashurin, N.      | 166                              |
| Vasil'ev, S. G.   | 59                               |
| Vavilova, E.      | 27, 82, 168                      |
| Vdovichev, S. N.  | 79                               |
| Vion, D.          | 46                               |
| Vogl, M.          | 27                               |
| Volkov, M. Yu.    | 182                              |
| Volkov, V. I.     | 19                               |
| Volodin, A.       | 86                               |
| Vorobiev, A. Kh.  | 38, 66, 121                      |
| Vorobeva, V. E.   | 188, 190                         |
| Voronkova, V.     | 172, 177                         |
| Vyalikh, A.       | 41                               |
| van der Est, A.   | 96                               |
| Weber, R.         | 43                               |
| Weis, C. D.       | 46                               |
| Wolter, A. U. B.  | 82                               |
| Wurmehl, S.       | 27                               |
| Yafarova, G. G.   | 130                              |
| Yamamoto, S.      | 7                                |
| Yamane, T.        | 7                                |
| Yatsyk, I.        | 57, 124, 132, 136, 170, 174, 183 |
| Yurtaeva, S. V.   | 183                              |
| Zagumennyi, A.    | 57                               |
| Zakharchenko, T.  | 41                               |
| Zaliznyak, I. A.  | 76                               |
| Zaripov, R. B.    | 60, 148, 186                     |
| Zavartsev, Yu.    | 57                               |
| Zelensky, I. V.   | 51, 53                           |
| Zharikov, E.      | 68, 179                          |
| Zhiteitsev, E. R. | 186                              |
| Zhitomirsky, M.   | 75                               |
| Zhou, X.          | 46                               |
| Zhou, H.          | 160                              |

|                  |     |
|------------------|-----|
| Ziatdinov, A. M. | 69  |
| Zinovieva, A. F. | 80  |
| Zinovyeu, V. A.  | 80  |
| Zobov, V. E.     | 187 |
| Zong, F.         | 34  |
| Zueva, E. M.     | 190 |
| Zvereva, E.      | 168 |

© Федеральное государственное учреждение науки  
Казанский физико-технический институт имени Е. К. Завойского  
Казанского научного центра Российской академии наук, 2016

---

Ответственный редактор: В. К. Воронкова; редакторы С. М. Ахмин, Л. В. Мосина; технический редактор  
О. Б. Яндуганова. Издательство КФТИ КазНЦ РАН,  
420029, Казань, Сибирский тракт, 10/7, лицензия № 0325 от 07.12.2000.



